

Integrative descriptions of two new species of *Dugesia* from Hainan Island, China (Platyhelminthes, Tricladida, DugesIIDae)

Lei Wang^{1,3}, Zi-mei Dong¹, Guang-wen Chen¹, Ronald Sluys², De-zeng Liu¹

1 College of Life Science, Henan Normal University, Xinxiang, 453007 Henan, China **2** Naturalis Biodiversity Center, Leiden, the Netherlands **3** Medical College, Xinxiang University, Xinxiang 453003, China

Corresponding author: Guang-wen Chen (chengw0183@sina.com)

Academic editor: Y. Mutafovich | Received 17 November 2020 | Accepted 24 February 2021 | Published 05 April 2021

<http://zoobank.org/A5EF1C8A-805B-4AAE-ACEB-C1C6B691FCA>

Citation: Wang L, Dong Z-m, Chen G-w, Sluys R, Liu D-z (2021) Integrative descriptions of two new species of *Dugesia* from Hainan Island, China (Platyhelminthes, Tricladida, DugesIIDae). ZooKeys 1028: 1–28. <https://doi.org/10.3897/zookeys.1028.60838>

Abstract

Two new species of the genus *Dugesia* (Platyhelminthes, Tricladida, DugesIIDae) from Hainan Island of China are described on the basis of morphological, karyological and molecular data. *Dugesia semiglobosa* Chen & Dong, **sp. nov.** is mainly characterized by a hemispherical, asymmetrical penis papilla with ventrally displaced ejaculatory duct opening terminally at tip of penis papilla; vasa deferentia separately opening into mid-dorsal portion of intrabulbar seminal vesicle; two diaphragms in the ejaculatory duct; copulatory bursa formed by expansion of bursal canal, lined with complex stratified epithelium, which projects through opening in bursa towards intestine, without having open communication with the gut; mixoploid chromosome complement diploid ($2n = 16$) and triploid ($3n = 24$), with metacentric chromosomes. *Dugesia majuscula* Chen & Dong, **sp. nov.** is mainly characterized by oviducts opening asymmetrically into female reproductive system; hyperplastic ovaries; expanded posterior section of bursal canal; vasa deferentia separately opening into mid-dorsal portion of seminal vesicle; asymmetrical penis papilla due to ventral course of ejaculatory duct, which has subterminal and dorsal opening at tip papilla; mixoploid chromosome complement diploid ($2n = 16$) and triploid ($3n = 24$); chromosomes metacentric. Apart from their anatomy, separate species status of the two new species is supported also by their genetic distances and by their positions in the phylogenetic tree. The sexualization process may have been induced by the lower temperatures, in comparison with their natural habitat, under which the worms were cultured in the laboratory.

Keywords

Histology, karyology, molecular distance, molecular phylogeny, taxonomy

Introduction

Approximately 94 species of the freshwater planarian genus *Dugesia* Girard, 1850 have been reported from a major portion of the Old World and Australia (Sluys and Riutort 2018; Song et al. 2020). Thus far, 22 species of *Dugesia* are known from the Oriental region (Sluys et al. 1998), while only three species have been recorded from China, viz., *D. japonica* Ichikawa & Kawakatsu, 1964, *D. sinensis* Chen & Wang, 2015, and *D. umbonata* Song & Wang, 2020 (Kawakatsu et al. 1976; Chen et al. 2015; Song et al. 2020). Hainan Island is the largest tropical island of China and forms part of the Indo-Burma biodiversity hotspot (Mittermeier et al. 2005, 2011) and represents an endemic bird area (Stattersfield et al. 1998). Although Liu (1993, map on p. 158) recorded the occurrence of *Dugesia* on Hainan Island from three localities, no information was provided on the taxonomic identity of the species. Therefore, in this paper we describe for the first time two new species of *Dugesia* from Hainan Island, which also form new species to the planarian fauna of China, on the basis of an integrative taxonomic approach, using morphological, karyological, and molecular data.

Materials and methods

Specimen collection and culturing

Specimens were collected during 2016–2018 from under stones in springs with the help of a paint brush (for sampling localities, see Fig. 1). The worms were transferred to plastic bottles filled with spring water, which were placed in a cooler, containing an ice bag, during transportation to the laboratory. In the laboratory, the planarians were cultured in autoclaved tap water at 20 °C and fed with fresh beef liver once per week. The worms were starved for at least one week before being used in karyotype studies, histological studies, or DNA extraction. Images of the external appearance of the worms were obtained by using a digital camera attached to a stereo-microscope.

Histology and karyology

Histological sections were prepared as described by Dong et al. (2017). In brief, worms were killed with 1% nitric acid and thereafter fixed in Bouin's fluid for ~ 24 h, then rinsed in 70% ethanol, and, subsequently, dehydrated in an ascending series of ethanol solutions, after which the animals were cleared in xylene and embedded in synthetic paraffin. Serial sections were made at intervals of 6–8 µm and were stained with haematoxylin-eosin. Images were acquired by a digital camera attached to a compound microscope. Preparations of specimens have been deposited in the Zoological Museum of the College of Life Science of Henan Normal University (ZMHNU), Xinxiang, China.

Karyological preparations were made by means of the air-drying technique, following Dong et al. (2017). Well-spread sets of metaphase plates from five randomly

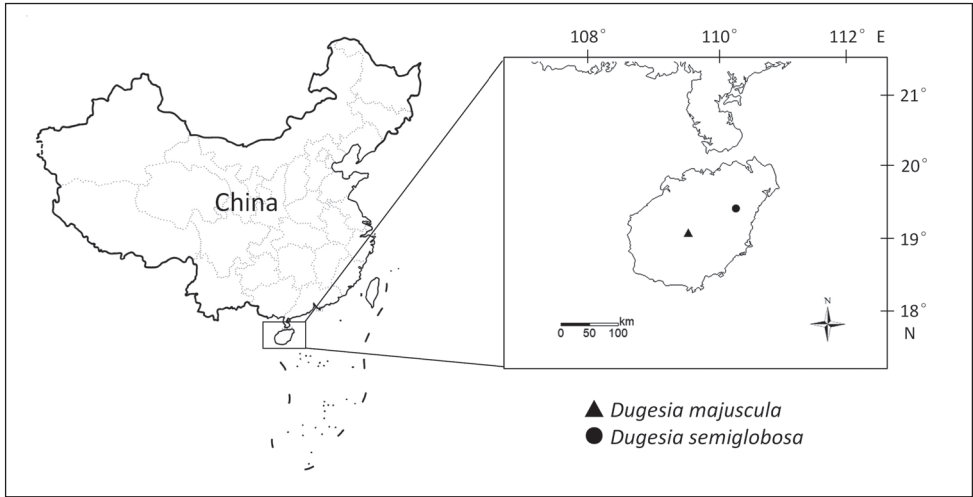


Figure 1. Collection sites of *Dugesia* on Hainan Island.

selected individuals were used for karyotype analysis; karyotype parameter measurements were carried out as described by Chen et al. (2008). Chromosomal nomenclature follows Levan et al. (1964).

DNA extraction, amplification, sequencing, and phylogenetic analysis

Total genomic DNA was extracted by using the QIAamp DNA Mini Tissue Kit (Qiagen, Germany), according to the manufacturer's protocols. Fragments of the Cytochrome C oxidase subunit I (COI) and internal transcribed spacer-1 (ITS-1) were amplified using specific primers (see Suppl. material 2: Table S1 for sequences and annealing temperatures). Premix Ex TaqHot Start Version (TaKaRa, Otsu Japan) was used for the polymerase chain reaction (PCR). Amplifications were conducted in a final volume of 30 μ L under the following conditions: 5 min at 94 $^{\circ}$ C, 35 cycles of 40 s at 94 $^{\circ}$ C, an annealing step for 30 s, and 1 min at 72 $^{\circ}$ C, and 5 min at 72 $^{\circ}$ C as a final extension (for annealing temperatures see Suppl. material 2: Table S1). Purification of PCR products and sequencing were done by GENEWIZ (Tianjin, China). Sequencing reactions were performed with the same primers used to amplify the fragments. All specimens were sequenced for both forward and reverse DNA strands. Chromatograms were visually checked. In the case of *Dugesia majuscula* Chen & Dong, sp. nov., we were able to extract DNA from no less than 12 specimens. With respect to *D. semiglobosa* Chen & Dong, sp. nov., we could only extract DNA from four specimens. For both of the two new species COI and ITS-1 were amplified.

In order to determine whether the presumed new species are molecularly different from other *Dugesia* species, we performed a phylogenetic analysis. In the ingroup we included the two new species as well as 28 other *Dugesia* species from the Oriental, Australasian, Mediterranean, Eastern and Western Palearctic regions; the freshwater

species *Schmidtea mediterranea* Benazzi et al., 1975 was chosen as outgroup taxon, since this genus forms the sister-group of the genus *Dugesia* (Álvarez-Presas et al. 2008; for GenBank accession numbers, see Table 1).

Nuclear ribosomal markers were aligned online with MAFFT (Online Version 7.247) using the G-INS-i algorithm (Katoh and Standley 2013), and checked by using BioEdit v7.2.6.1. For alignments of the protein-coding COI sequences we used the TranslatorX pipeline (<http://translatorx.co.uk>; Abascal et al. 2010). Nucleotide sequences were translated into amino acid sequences (Translation table 9), followed by MAFFT, using the FFT-NS-2 progressive alignment method, and checked by using BioEdit v7.2.6.1, and then back-translated to nucleotide sequences. Since automated removal of gap columns and variable regions had been reported to negatively affect the accuracy of the inferred phylogeny (Dessimoz and Gil 2010; Tan et al. 2015), the Gblocks option (Talavera and Castresana 2007) was disabled. The concatenated sequences for the phylogenetic analysis were in the order ITS-1+ COI and consisted of a total of 1473 bp, including 4.4% missing data. In the concatenated sequences, missing data had been coded as “?”.

MrBayes v3.2 (Ronquist et al. 2012) and RaxML v8.2.10 (Stamatakis 2014) were used to infer phylogenies with the Bayesian Inference (BI) and Maximum-likelihood (ML) methods, respectively. For BI a run of 3 million generations and 25% burn-in was used under the GTR+I+G model. For the ML analysis, 10,000 replicates were performed under the GTR+I+G model. BI and ML trees were visualized and edited using Figtree v1.4.3.

Genetic distances were calculated for COI and ITS-1 with the help of MEGA 6.06 (Tamura et al. 2013) under the Kimura 2-parameter substitution model (Lázaro et al. 2009; Solà et al. 2013).

Results

Molecular phylogeny

We obtained fragments of sequences of COI and ITS-1 from 12 specimens of *D. majuscula* and four specimens of *D. semiglobosa*. The final alignments of these fragments of the nuclear ribosomal internal spacer ITS-1 and the mitochondrial gene COI were 676 and 816 base pairs (bp), respectively. In the two populations of *D. majuscula* and *D. semiglobosa*, there was no variation in COI and ITS-1.

The phylogenetic trees and their supporting values resulting from the analysis of the concatenated dataset are very similar for both ML and BI, differing only in nodes weakly supported in at least one of the methodologies (Fig. 2; Suppl. material 1: Figure S1). The new species *D. majuscula* and *D. semiglobosa* occupy separate branches that are clearly differentiated from their congeners. Interestingly, these two species from Hainan Island are not each other's closest relatives, as *D. semiglobosa* shares a sister-group relationship

Table 1. GenBank accession numbers of COI and ITS-1 sequences used for molecular analysis.

Species	GenBank		Species	GenBank	
	COI	ITS-1		COI	ITS-1
<i>D. aethiopica</i>	KY498845	KY498785	<i>D. improvisa</i>	KC006987	KC007065
<i>D. afromontana</i>	KY498846	KY498786	<i>D. japonica</i>	FJ646990	FJ646904
<i>D. arcadia</i>	KC006971	KC007044	<i>D. liguriensis</i>	FJ646992	FJ646907
<i>D. ariadnae</i>	KC006972	KC007048	<i>D. majuscula</i>	MW533425	MW533591
<i>D. batuensis</i>	KF907818	KF907815	<i>D. malickyi</i>	KC006990	KC007069
<i>D. benazzii</i>	FJ646977 + FJ646933	FJ646890	<i>D. naiadis</i>	KF308756	
<i>D. bengalensis</i>		FJ646897	<i>D. notogaea</i>	FJ646993 + FJ646945	FJ646908
<i>D. bifida</i>	KY498851	KY498791	<i>D. ryukyuensis</i>	AF178311	FJ646910
<i>D. cretica</i>	KC006976	KC007050	<i>D. semiglobosa</i>	MW525210	MW526992
<i>D. damoae</i>	KC006979	KC007057	<i>D. sicula</i>	FJ646994+FJ646947	DSU84356
<i>D. deharvengi</i>	KF907820	KF907817	<i>D. sigmoides</i>	KY498849	KY498789
<i>D. effusa</i>	KC006983	KC007058	<i>D. sinensis</i>	KP401592	
<i>D. elegans</i>	KC006984	KC007063	<i>D. subtentaculata</i>	FJ646995 + FJ646949	DSU84369
<i>D. gibberosa</i>	KY498857	KY498803	<i>D. umbonata</i>	MT176641	MT177211
<i>D. gonocephala</i>	FJ646986 + FJ646941	FJ646901	<i>S. mediterranea</i>	JF837062	AF047854
<i>D. hepta</i>	FJ646988 + FJ646943	FJ646902			

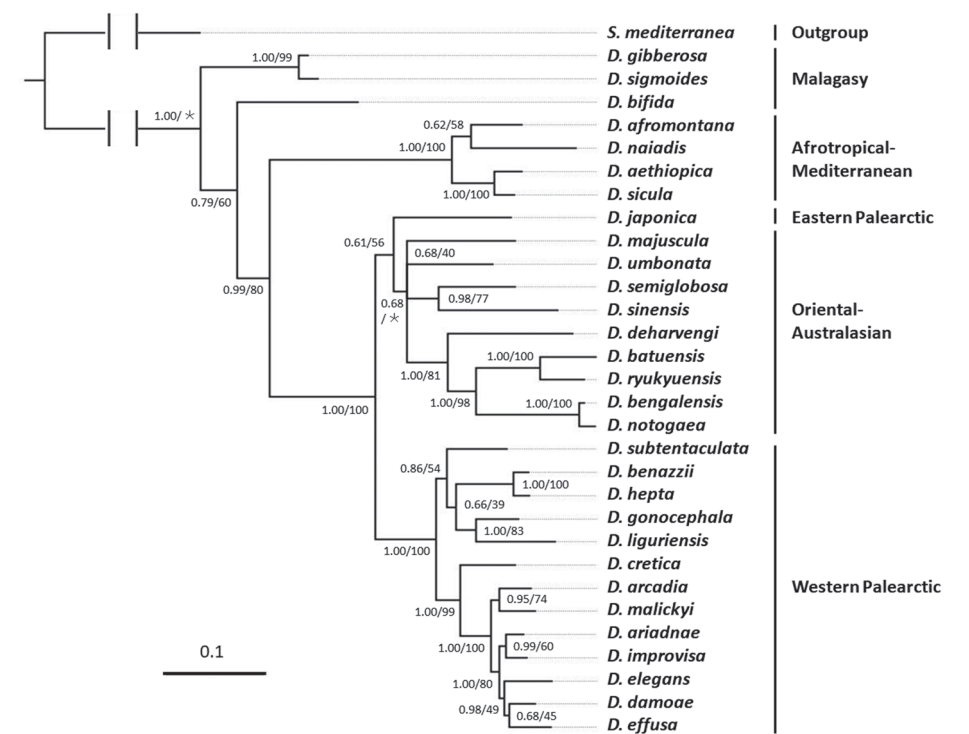


Figure 2. Phylogenetic tree obtained from Bayesian analysis of the concatenated dataset. Numbers at nodes indicate support values (posterior probability/bootstrap). *: Bootstrap value not applicable to the node, because of different topologies of trees obtained by BI and ML methods. Scale bar: substitutions per nucleotide position.

with *D. sinensis*, forming a clade that is part of a polytomy that comprises also three other branches, viz. *D. majuscula*, *D. umbonata*, and a clade comprising five species from the Oriental and Australasian regions (*D. deharvengi* Kawakatsu & Mitchell, 1989, *D. batuensis* Ball, 1970, *D. ryukyuensis* Kawakatsu, 1976, *D. bengalensis* Kawakatsu, 1983, *D. notogaea* Sluys & Kawakatsu, 1998).

In addition to the fact that the new species occupy separate branches in the phylogenetic tree, separate species status of *D. majuscula* and *D. semiglobosa* is supported also by our analysis of the genetic distances among the species included in our study, albeit that both COI and ITS-1 distances vary greatly among species (Suppl. material S2, S3). With respect to COI, the highest distance value between *D. majuscula* and its Oriental-Australasian congeners is 22.02%, while the lowest distance value is 13.68%. The highest distance value between *D. semiglobosa* and the Oriental-Australasian congeners is 21.06%, while the lowest distance value is 10.61%. Furthermore, there is a 19.52% difference between the two new species.

With respect to ITS-1, the highest distance value between *D. majuscula* and its Oriental-Australasian congeners is 12.52%, while the lowest distance value is 5.82%. The highest distance value between *D. semiglobosa* and its Oriental-Australasian congeners is 15.74%, while the lowest distance value is 9.74%. For this marker the distance between the two new species is 5.83% (Suppl. material 4: Table S3).

Systematic account

Order Tricladida Lang, 1884

Suborder Continenticola Carranza, Littlewood, Clough, Ruiz-Trillo, Baguña & Riutort, 1998

Family DugesIIDae Ball, 1974

Genus *Dugesia* Girard, 1850

Dugesia semiglobosa Chen & Dong, sp. nov.

<http://zoobank.org/59911F90-F4AC-4F86-8D54-9551D8ED67DF>

Figures 3–7

Material examined. Holotype: ZMHNU-JWT5, Jiuwentang village (19°23'10"N, 110°19'42"E; alt. 80 m above sea level (a.s.l.), Anding County, Hainan Province, China, 24 February 2018, coll. GW Chen and co-workers, sagittal sections on 17 slides.

Paratypes: ZMHNU-JWT1, *ibid.*, sagittal sections on 17 slides; ZMHNU-JWT2, *ibid.*, sagittal sections on 14 slides; ZMHNU-JWT3, *ibid.*, sagittal sections on 16 slides; ZMHNU-JWT4, *ibid.*, horizontal sections on 7 slides; ZMHNU-JWT6, *ibid.*, transverse sections on 33 slides; ZMHNU-JWT7, *ibid.*, transverse sections on 30 slides; ZMHNU-JWT8, *ibid.*, sagittal sections on 49 slides; ZMHNU-JWT9, *ibid.*, sagittal sections on 30 slides.

Diagnosis. *Dugesia semiglobosa* is characterized by the following features: hemispherical, asymmetrical penis papilla with ventrally displaced ejaculatory duct opening

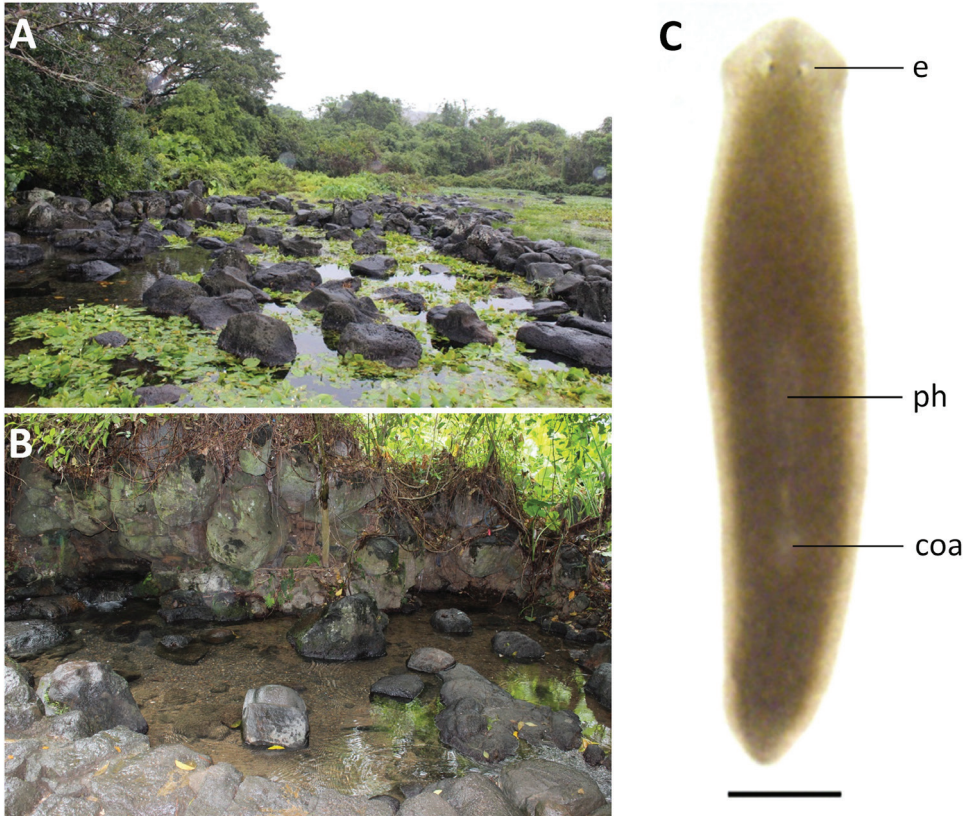


Figure 3. Habitat and external appearance of *Dugesia semiglobosa* **A** sampling site **B** habitat **C** sexually mature, living individual (anterior is to the up). Abbreviations: coa: copulatory apparatus; e: eye; ph: pharynx. Scale bar: 1 mm.

terminally at tip of penis papilla; absence of duct intercalated between seminal vesicle and diaphragm; vasa deferentia separately opening into mid-dorsal portion of intrabulbar seminal vesicle; two diaphragms in the ejaculatory duct; symmetrical openings of oviducts into bursal canal; copulatory bursa formed by expansion of bursal canal, lined with complex stratified epithelium, which projects through opening in bursa towards intestine, without having open communication with the gut; mixoploid chromosome complement diploid ($2n = 16$) and triploid ($3n = 24$); chromosomes metacentric.

Etymology. The specific epithet is derived from the Latin *semis*, half, and *globosus*, spherical, and alludes to the hemispherical penis papilla.

Habitat and reproduction. Specimens were collected from Jiuwentang volcano spring at an altitude of 80 m a.s.l. and with a water temperature of 23 °C. This spring is the third largest volcano spring in China, while it is also its largest selenium-rich spring (Fig. 3A, B). None of the animals was sexually mature at collection. However, after having been kept under laboratory conditions for ~ 150 days, the animals sexualized and laid cocoons. Newly laid cocoons are yellow, but turn dark brown after 2 to

3 days. Cocoons are spherical in shape (1 mm in diameter) and provided with a stalk. Thus far, none of the cocoons hatched, thus, most likely being infertile.

Karyology. Each of the five, randomly selected specimens exhibited mixoploid chromosome complements. In a total of 100 metaphase plates examined, 67 exhibited diploid chromosome portraits of $2n = 2x = 16$, while in 20 plates chromosome complements were triploid with $2n = 3x = 24$ chromosomes (Fig. 4); chromosome complements of the remaining 13 plates could not be determined, due to either lack of well-dispersed chromosomes or over-dispersed sets of chromosomes. All chromosomes were metacentric; karyotype parameters, including relative length, arm ratio, and centromeric index, are given in Table 2. The first pair of chromosomes is clearly larger than others, being 1.8 times larger than the shortest chromosome. Chromosomal plates and idiogram are shown in Fig. 4.

Description. Body of living asexual specimens is 4–6 mm in length and 0.72–0.85 mm in width, while in sexualized animals the body is 8–12 mm in length and 1.25–1.51 mm in width. Two eyes located in the center of the head, being situated in pigment-free patches. Each pigmented eye cup houses numerous photoreceptor cells. Head of low triangular shape and provided with two blunt auricles. Body light brown dorsally, excepting the pale body margin and accumulations of pigment following the outline of the pharynx. Ventral surface is paler than the dorsal one (Fig. 3C).

Pharynx situated in the mid-region of the body, measuring $\sim 1/5^{\text{th}}$ of the body length (Fig. 3C). Mouth opening located at the posterior end of the pharyngeal pocket. Outer pharyngeal musculature composed of a subepidermal layer of longitudinal muscles, followed by a thick layer of circular muscles; extra inner layer of longitudinal muscles is absent (Fig. 5A). The inner pharyngeal musculature consists of a subepithelial layer of circular muscle, followed by a layer of longitudinal muscle, the former being thicker than the latter (Fig. 5A).

In specimen JWT-7 the ventrally placed ovaries are clearly hyperplastic and fused to form a single mass that extends into the lateral regions of the body (Fig. 5B). In other specimens examined (JWT-2, JWT-3, JWT-5, JWT-6, JWT-10), the gonads are generally atypical, in that they are very small (Fig. 5C). Only in specimen JWT-8 the ovaries are more or less of normal size. In general, ovaries are situated at a short distance behind the brain.

From the ovaries the oviducts run ventrally in a caudal direction to the level of the genital pore, after which they curve dorso-medially to open separately and symmetrically into the ventral portion of the bursal canal, close to its communication with the atrium (Figs 5D, 7).

The small, dorsally located testes are well developed and provided with mature spermatozoa (Fig. 5C). Testicular follicles are arranged on either side of the midline of the body in nine or ten longitudinal zones, extending from the posterior level of the ovaries to almost the posterior end of the body. The vasa deferentia, filled with spermatozoa, expand to form spermiducal vesicles at the level of the pharynx that occupy $< 1/3^{\text{rd}}$ of the dorso-ventral space (Fig. 5E). At the level of the penis bulb the vasa deferentia decrease in diameter and bend sharply towards the dorsal body surface

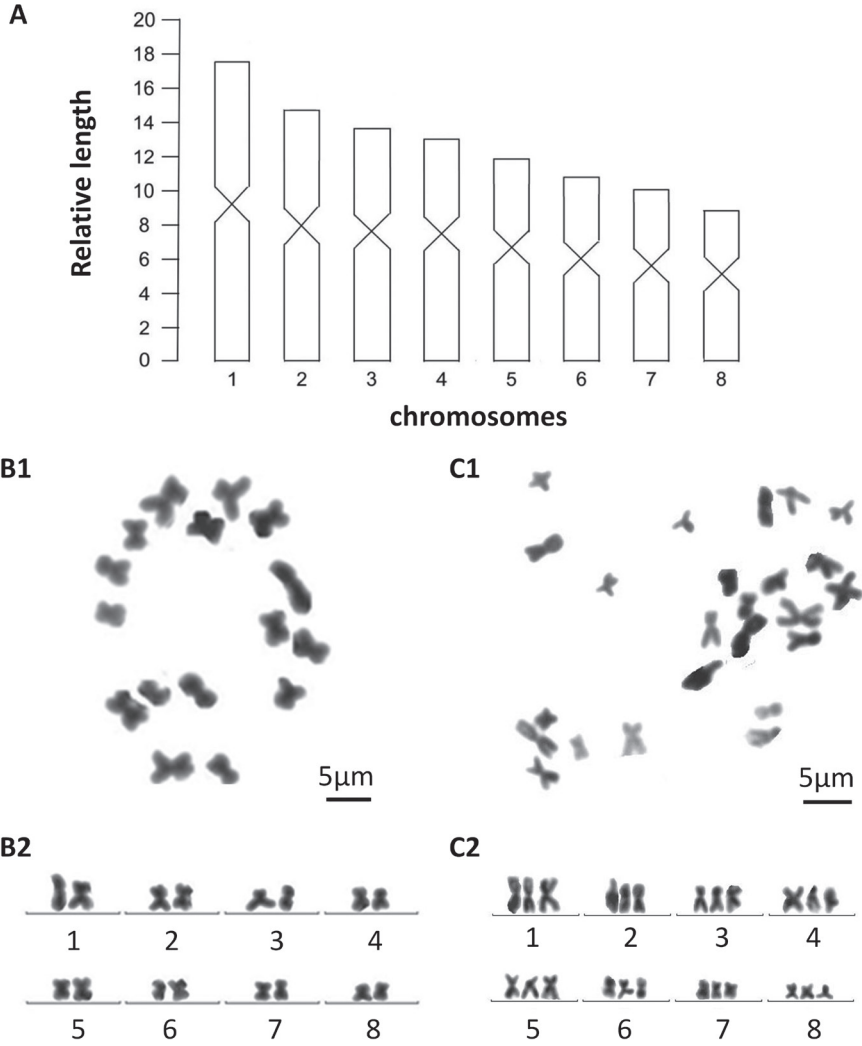


Figure 4. *Dugesia semiglobosa* **A** idiogram **B1** metaphasic plate of diploid cell **B2** karyogram of diploid cell **C1** metaphasic plate of triploid cell **C2** karyogram of triploid cell.

Table 2. Karyotype parameters (mean values and standard deviations) of *Dugesia semiglobosa*; m: meta-centric.

Chromosome	Relative length	Arm ratio	Centromeric index	Chromosome type
1	17.43 ± 0.93	1.12 ± 0.09	47.31 ± 1.83	m
2	14.71 ± 0.46	1.19 ± 0.09	45.88 ± 1.69	m
3	13.69 ± 0.45	1.30 ± 0.18	43.86 ± 3.53	m
4	12.93 ± 0.46	1.34 ± 0.14	43.21 ± 2.54	m
5	11.78 ± 0.26	1.29 ± 0.11	43.82 ± 2.12	m
6	10.80 ± 0.17	1.27 ± 0.06	44.33 ± 1.35	m
7	9.92 ± 0.53	1.28 ± 0.10	44.24 ± 1.97	m
8	8.72 ± 0.64	1.21 ± 0.05	45.40 ± 1.02	m

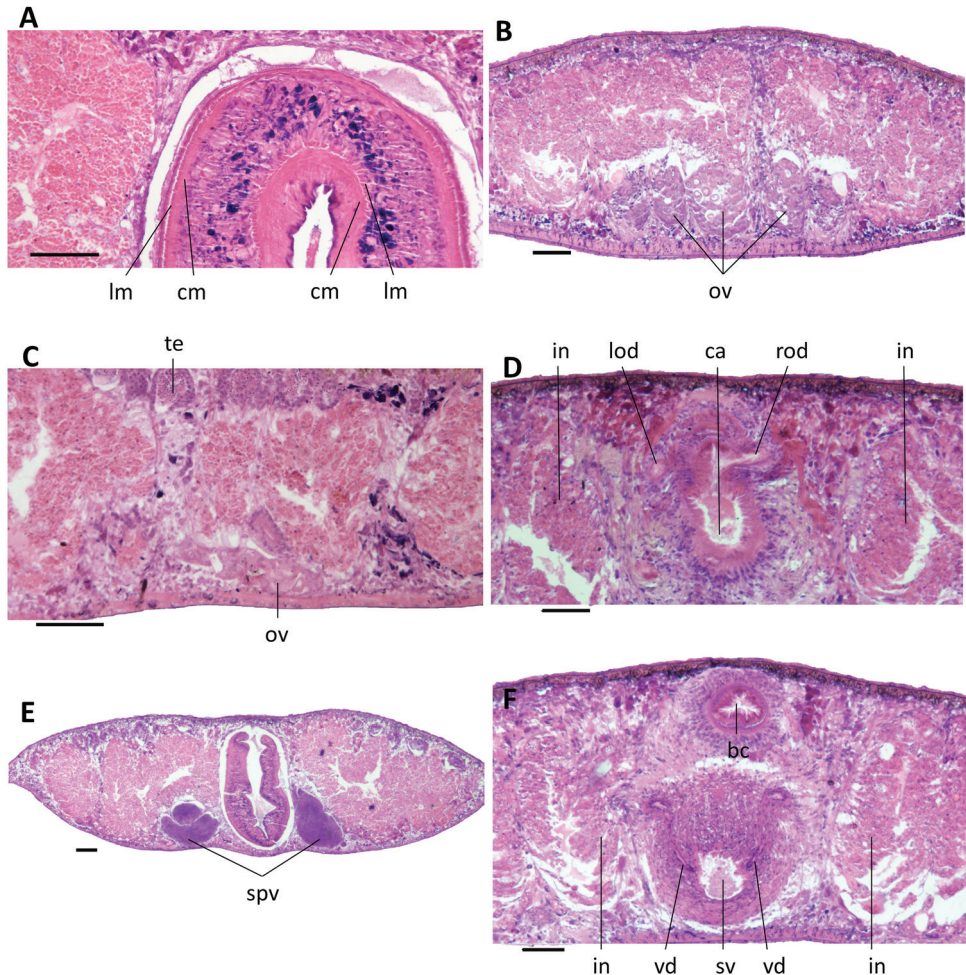


Figure 5. *Dugesia semiglobosa* **A** transverse section of paratype JWT 6, showing longitudinal and circular muscles in outer and inner pharyngeal musculature **B** transverse section of paratype JWT 7, showing hyperplastic ovaries. **C** sagittal section of holotype JWT 5, showing testes and small ovary **D** transverse section of paratype JWT 7, showing symmetrical openings of the oviducts **E** transverse section of paratype JWT 6, showing spermiducal vesicles **F** transverse section of paratype JWT 7, showing openings of the vasa deferentia into the seminal vesicle. The anterior is to the front in **A, B, D, E, F**, and anterior is to the right in **C**. Abbreviations: bc: bursal canal; ca: common atrium; cm: circular muscles; in: intestine; lm: longitudinal muscles; lod: left oviduct; ov: ovary; rod: right oviduct; spv: spermiducal vesicle; sv: seminal vesicle; te: testis; vd: vas deferens. Scale bars: 100 μ m.

and upon recurving ventrad they penetrate the dorso-lateral wall of the penis bulb to open separately and symmetrically into the mid-dorsal portion of the seminal vesicle (Figs 5F, 6A, 7). The sperm ducts are lined with nucleated cells and are surrounded by a layer of circular muscles. The reniform seminal vesicle is lined by a flat, nucleated epithelium and is surrounded by intermingled muscle fibers (Figs 5F, 6A,). The seminal vesicle opens into the ejaculatory duct via a small, pointed diaphragm. A second,

rather large and blunt diaphragm is located in the proximal portion of the ejaculatory duct (Figs 6A, 7). The ejaculatory duct is lined by an infranucleated epithelium; we were unable to discern any musculature around the duct. The ejaculatory duct follows a noncentral, ventrally displaced course through the penis papilla, opening at its tip, thus resulting in an asymmetrical penis papilla in which the dorsal lip is much larger than the ventral one (Figs 6A, 7).

The complete penis, comprising papilla and bulb, is nearly spherical, with the penis papilla being a hemispherical structure that is covered with an infranucleated epithelium, which is underlain by a subepithelial layer of circular muscle, followed by a layer of longitudinal muscle fibres (Fig. 6A). The penis papilla almost completely occupies the male atrium, the latter communicating with the common atrium via a slight constriction (Figs 6E, F, 7). The common atrium opens to the exterior via a gonoduct, which is lined by a columnar epithelium and receives the openings of abundant cement glands.

From its point of communication with the common atrium, the bursal canal gradually expands in diameter, meanwhile curving anteriorly, while running on the left side of the male copulatory apparatus (Figs 6D, 7). The bursal canal is lined with columnar, nucleated, ciliated cells and is surrounded by a subepithelial layer of longitudinal muscles, followed by a layer of circular muscle (Figs 6D, 7). An ectal reinforcement layer of longitudinal muscles runs from the vaginal region to approximately halfway along the bursal canal. Shell glands discharge their erythrophil secretion into the vaginal region of the bursal canal, near the oviducal openings.

More or less dorsally to the penis bulb, the bursal canal first decreases somewhat in diameter but thereafter greatly expands to give rise to a more or less globular structure immediately in front of the male complex. This globular structure may be called a copulatory bursa since it occupies the same position as in other species of *Dugesia*, or freshwater planarians in general. The bursa is lined with a complex type of stratified epithelium. The basal portion of this epithelium consists of more or less cuboidal, nucleated cells and is basically a continuation of the lining epithelium of the rest of the bursal canal, albeit that there the cells are columnar. This basal layer is followed by a thick zone of stratified, non-nucleated squamous epithelium, leaving very little room for any lumen within the bursa. The cells of this squamous layer have an irregular shape, while those in the top zone, near the lumen, are vacuolated and provided with granular, cyanophil inclusions. The bursa is surrounded by a layer of longitudinal muscles (Figs 6C, 7). However, at one point this muscle layer is interrupted because of the presence of an opening in the bursa. This opening is located, more or less, at the antero-dorsal wall of the bursa. A portion of the squamous inner lining of the bursa projects through the opening and approaches and/or touches portions of the gut that are in its proximity. However, in none of the specimens examined we discerned an open connection between bursa and intestine.

Discussion. The curious copulatory bursa of *D. semiglobosa* is unparalleled among species of *Dugesia*, or freshwater planarians in general. Generally, copulatory bursae are lined with an epithelium consisting of tall columnar, vacuolated, and nucleated cells, while they are surrounded by only a very weak musculature. The structure of the bursa of *D. semiglobosa* differs considerably from this ground-plan condition, as it is basically

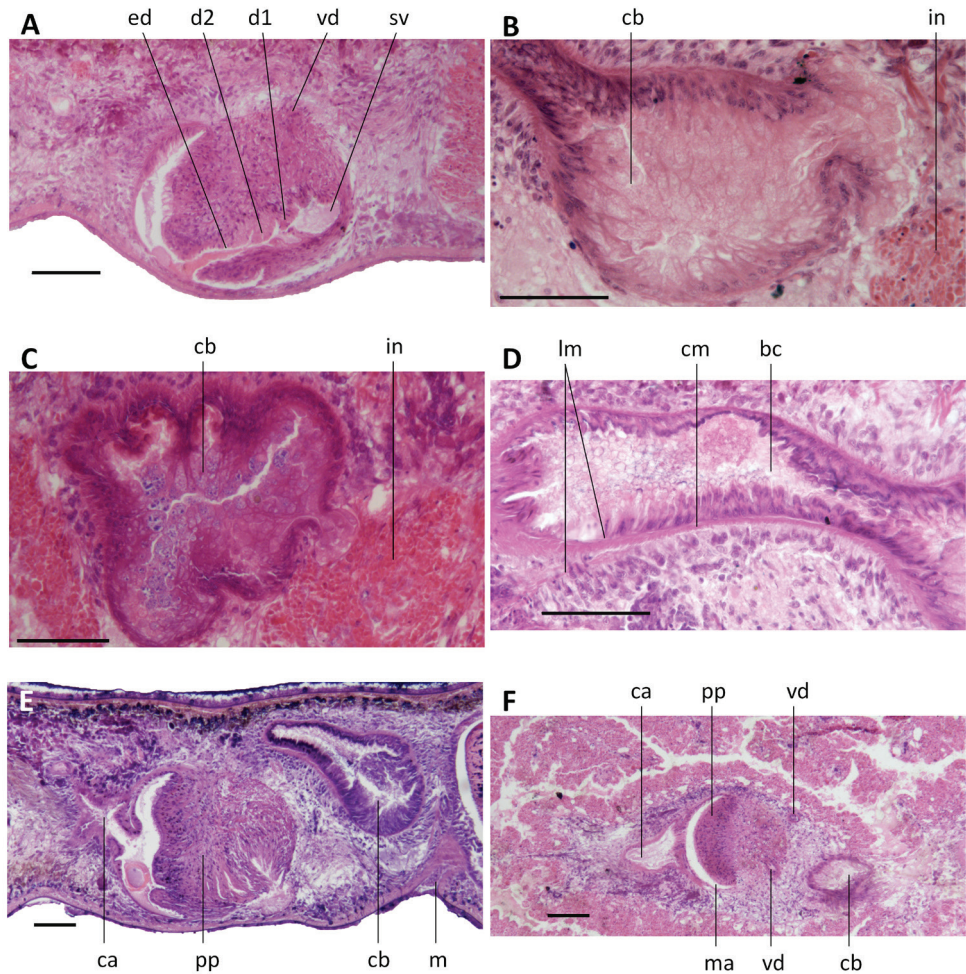


Figure 6. *Dugesia semiglobosa* **A** sagittal section of holotype JWT 5, showing reniform seminal vesicle, two diaphragms in the ejaculatory duct, ventral course of the ejaculatory duct, and hemispherical penis papilla **B** sagittal section of holotype JWT 5, showing copulatory bursa **C** transverse section of paratype JWT 7, showing copulatory bursa **D** sagittal section of holotype JWT 5, showing bursal canal and its surrounding musculature **E** sagittal section of holotype JWT 9, showing small copulatory bursa, and mouth **F** horizontal section of paratype JWT 4, showing hemispherical penis papilla. The anterior is to the right in **A, B, D, E, F** and anterior is to the front in **C**. Abbreviations: bc: bursal canal; ca: common atrium; cb: copulatory bursa; cm: circular muscles; d: diaphragm; ed: ejaculatory duct; in: intestine; lm: longitudinal muscles; m: mouth; ma: male atrium; pp: penis papilla; sv: seminal vesicle; vd: vas deferens. Scale bars: 100 μ m.

an expanded continuation of the bursal canal, albeit with a simpler coat of muscles and a more complex lining epithelium.

Dugesia semiglobosa exhibits a combination of three characteristic features (ventrally displaced ejaculatory duct, absence of duct intercalated between seminal vesicle and dia-

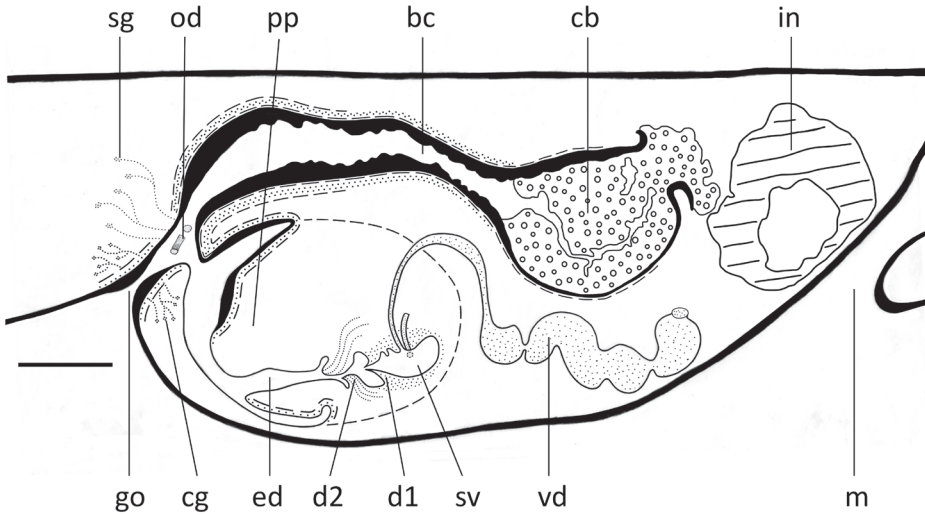


Figure 7. *Dugesia semiglobosa*. Sagittal reconstruction of the copulatory apparatus of the holotype (anterior is to the right). Abbreviations: bc: bursal canal; cb: copulatory bursa; cg: cement glands; d: diaphragm; ed: ejaculatory duct; go: gonopore; in: intestine; m: mouth; od: oviduct; pp: penis papilla; sg: shell glands; sv: seminal vesicle; te: testis; vd: vas deferens. Scale bar: 100 μ m.

phragm, terminal opening of ejaculatory duct) that is found in only nine congeners, viz., *D. annandalei* Kaburaki, 1918, *D. damoae* De Vries, 1984, *D. didiaphragma* De Vries, 1988, *D. elegans* De Vries, 1984, *D. gibberosa* Stocchino & Sluys, 2017, *D. maghrebiana* Stocchino et al. 2009, *D. malickyi* De Vries, 1984, *D. naiadis* Sluys, 2013, and *D. sinensis*. Among these nine species, *D. semiglobosa* most closely resembles *D. didiaphragma* and *D. maghrebiana* in that these species also possess two diaphragms, in contrast to all other species mentioned. Presence of two diaphragms is a rare condition among species of *Dugesia* and is only known from three other species, viz., *D. bijuga* Harrath & Sluys, 2019, *D. machadoi* de Beauchamp, 1952, and *D. mirabilis* De Vries, 1988. However, in these three last-mentioned species the ejaculatory duct runs a central course through the penis papilla, in contrast to the ventral trajectory in *D. semiglobosa*. Further, there are ample other features that preclude assignment of our specimens to either of these Afrotropical species. Neither is it possible to assign our animals to *D. didiaphragma* or *D. maghrebiana* as they lack the large seminal vesicle enclosed by a highly muscularized, elongated penis bulb of the former and the knob-like extension on the penis papilla of the latter.

It is interesting to note that in all species in possession of two diaphragms, the small proximal diaphragm basically is formed by a non-glandular constriction of the seminal vesicle, while the true diaphragm is a larger structure and receives the secretion of penial glands, as usual for the diaphragm of species of *Dugesia*. The same situation applies to the two diaphragms in *D. semiglobosa*. It is noteworthy that in *D. mirabilis* both the proximal and distal diaphragm are glandular (De Vries 1988).

***Dugesia majuscula* Chen & Dong, sp. nov.**

<http://zoobank.org/C4E72273-DA7E-48DE-BFFC-B0F88DE47626>

Figures 8–12

Material examined. Holotype: ZMHNU-YHYQ 4, sagittal sections on 36 slides, Yingge mountain, Qiongzong County, Hainan Province, China (19°3'24"N, 109°33'49"E), 24 February 2018, altitude 584 m a.s.l., coll. GW Chen and co-workers.

Paratypes: ZMHNU-YHYQ1, *ibid.* sagittal sections on 45 slides; ZMHNU-YHYQ2, *ibid.*, sagittal sections on 18 slides; ZMHNU-YHYQ3, *ibid.*, sagittal sections on 24 slides; ZMHNU-YHYQ5, *ibid.*, sagittal sections on 32 slides; ZMHNU-YHYQ 6, horizontal sections on 18 slides; ZMHNU-YHYQ 7, horizontal sections on 12 slides; ZMHNU-YHYQ8, *ibid.*, transverse sections on 24 slides; ZMHNU-YHYQ9, *ibid.*, sagittal sections on 15 slides; ZMHNU-YHYQ10, *ibid.*, sagittal sections on 19 slides.

Diagnosis. *Dugesia majuscula* is characterized by the following features: oviducts opening asymmetrically into female reproductive system; hyperplastic ovaries; expanded posterior section of bursal canal; vasa deferentia separately opening into mid-dorsal portion of seminal vesicle; asymmetrical penis papilla due to ventral course of ejaculatory duct, which has subterminal and dorsal opening at tip papilla; mixoploid chromosome complement diploid ($2n=16$) and triploid ($3n = 24$), with metacentric chromosomes.

Etymology. The specific epithet is derived from the Latin adjective *majusculus*, somewhat larger, and alludes to expanded portion of the bursal canal.

Habitat and reproduction. Animals were collected from a freshwater stream in the Yingge Mountains, at a water temperature of 19 °C and an altitude of 584 m a.s.l. (Fig. 8A, B). Approximately 40 individuals were collected in February 2018, none of which was sexually mature. During the first period of 80–90 days (March to May) in the laboratory culture, worms only showed asexual reproduction by means of fission. However, during the following period of 40–60 days, seven individuals sexualized, while after another 180 days, 1/3 of the animals sexualised, although thus far they have not produced any cocoons.

Karyology. Each of the five, randomly selected specimens exhibited mixoploid chromosome complements. In a total of 100 metaphase plates examined, 75 exhibited diploid chromosome complements of $2n = 2x = 16$, while in 18 plates chromosome complements were triploid with $2n = 3x = 24$ chromosomes (Fig. 9); chromosome complements of the remaining seven plates could not be determined, due to either lack of well-dispersed chromosomes or over-dispersed sets of chromosomes. All chromosomes were metacentric; karyotype parameters, including relative length, arm ratio, and centromeric index, are given in Table 3. The first pair of chromosomes is clearly larger than the others, being 1.86 times larger than the shortest chromosome. Chromosomal plates and idiogram are shown in Fig. 9.

Description. Body size of living asexual specimens is 5–8 mm in length and 0.65–0.78 mm in width, while in sexualized specimens the body measures 10–16 mm in length and 1.05–1.36 mm in width. Head of low triangular shape, provided with two



Figure 8. Habitat and external appearance of *Dugesia majuscula* **A** sampling locality **B** habitat **C** sexually mature, living individual (anterior is to the up). Abbreviations: coa: copulatory apparatus; e: eye; ph: pharynx. Scale bar: 1 mm.

Table 3. Karyotype parameters (mean values and standard deviations) of *Dugesia majuscula*; m: metacentric.

Chromosome	Relative length	Arm ratio	Centromeric index	Chromosome type
1	17.76 ± 0.82	1.20 ± 0.08	45.66 ± 1.69	m
2	14.95 ± 0.72	1.15 ± 0.08	46.61 ± 1.67	m
3	13.30 ± 0.33	1.19 ± 0.04	45.70 ± 0.74	m
4	12.27 ± 0.31	1.25 ± 0.09	44.68 ± 1.81	m
5	11.47 ± 0.46	1.31 ± 0.17	43.58 ± 3.37	m
6	10.77 ± 0.44	1.19 ± 0.10	46.06 ± 2.07	m
7	10.21 ± 0.57	1.20 ± 0.08	45.77 ± 1.50	m
8	9.28 ± 0.34	1.25 ± 0.17	44.73 ± 3.13	m

blunt auricles and two eyes located in pigment-free patches (Fig. 8C). Each pigmented eye cup is provided with numerous retinal cells. Dorsal surface brown with numerous dark spots (Fig. 8C); ventral surface paler than dorsal one and provided with only scattered small, dark spots.

Pharynx positioned in the mid-region of the body and measuring $\sim 1/6^{\text{th}}$ of the body length (Fig. 8C); the mouth opening is situated at the hind end of the pharyngeal pocket. The pharyngeal outer musculature is composed of an outer, subepithelial layer of longitudinal muscles, followed by a layer of circular muscles. An extra longitudinal muscle layer internally to the circular muscles is absent (Fig. 10A). Inner pharyngeal musculature composed of an outer layer of longitudinal muscles and a subepithelial layer of circular muscles, the latter being thicker than the outer layer (Fig. 10A).

Ovaries hyperplastic, with several scattered masses at a short distance behind the brain, extending backwards over a distance of at least 800 μm (Fig. 10B) and occupying the entire dorso-ventral space. In live animals, the hyperplastic ovaries are visible

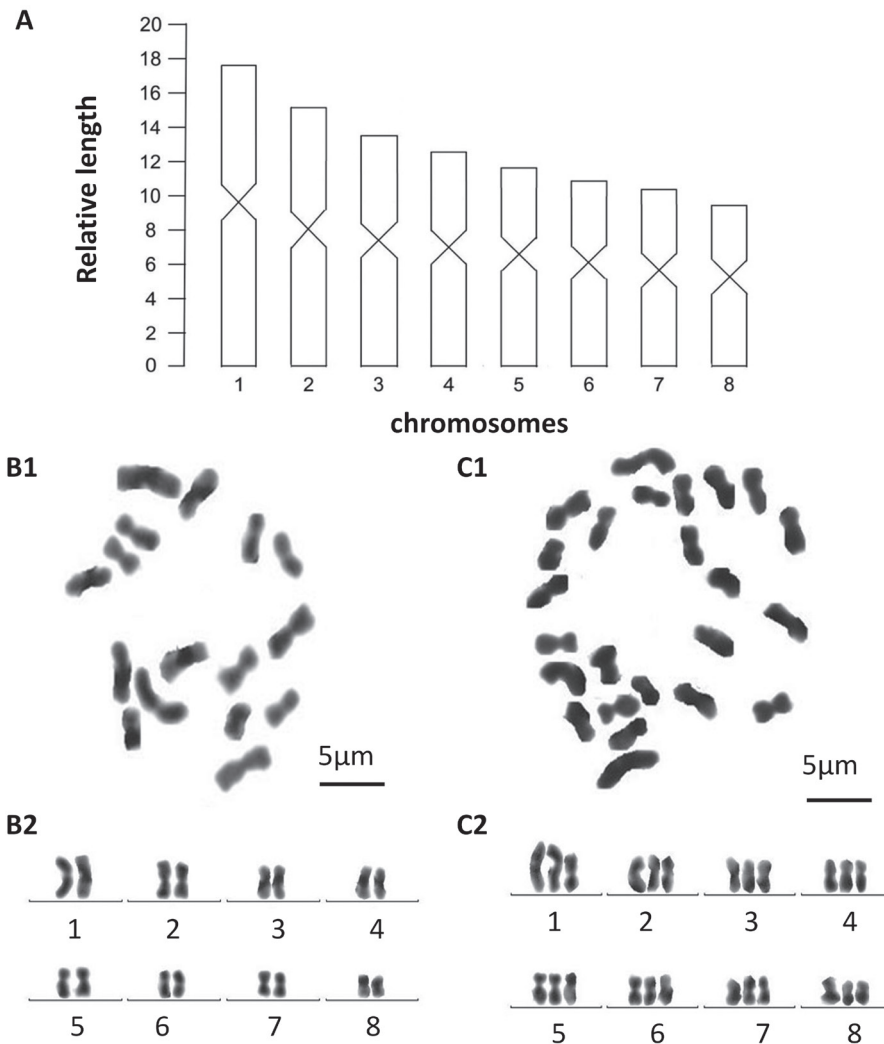


Figure 9. *Dugesia majuscula* **A** idiogram **B1** metaphasic plate of diploid cell **B2** karyogram of diploid cell **C1** metaphasic plate of triploid cell **C2** karyogram of triploid cell.

through the dorsal body surface as two short, transparent stripes (Fig. 8C). From the ovaries, the oviducts run ventrally in a caudal direction to the level of the genital pore where they turn dorso-medially to open separately and asymmetrically into the female reproductive system. In point of fact, the right oviduct opens either into the most postero-ventral part of the expanded portion of the bursal canal or somewhat more ventrally (YHYQ-5), while the left oviduct opens into the common atrium, a distinct female atrium being absent (Figs 10C, 12).

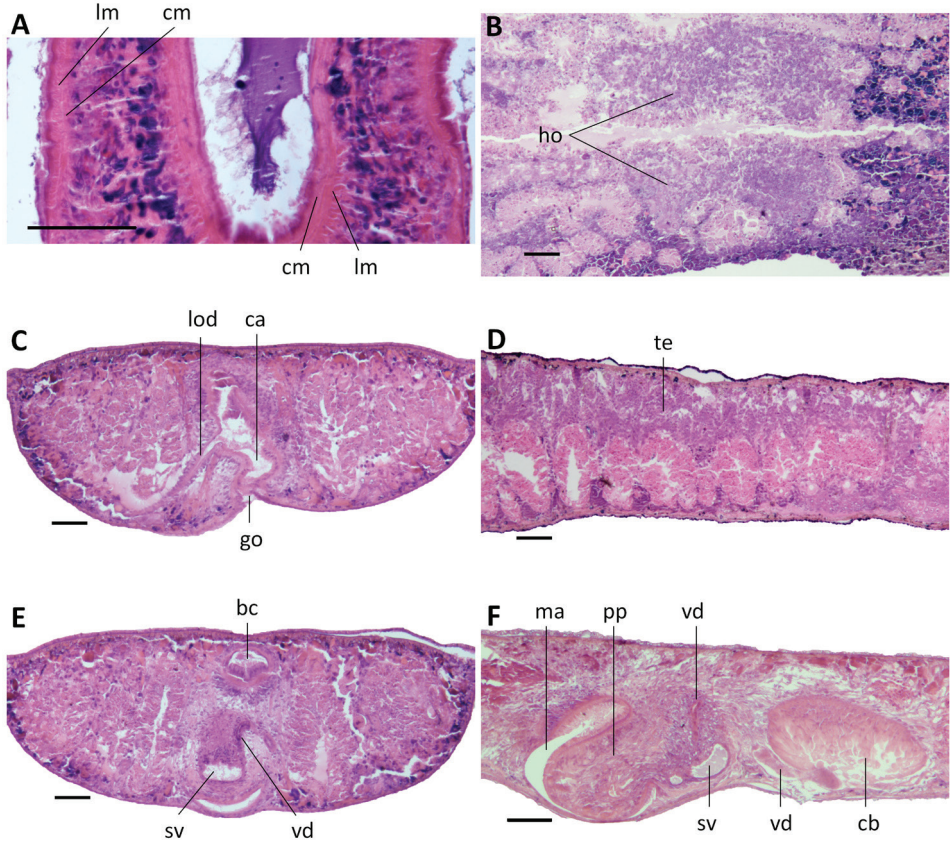


Figure 10. *Dugesia majuscula* **A** transverse section of paratype YHYQ8, showing longitudinal and circular muscles in outer and inner pharyngeal musculature **B** horizontal section of paratype YHYQ7, showing hyperplastic ovaries **C** transverse section of paratype YHYQ8, showing opening of the left oviduct **D** sagittal section of paratype YHYQ10, showing dorsal testes **E** transverse section of paratype YHYQ8, showing course of a vas deferens **F** sagittal section of paratype YHYQ3, showing opening of a vas deferens into seminal vesicle. The anterior is to the front in **A, C, E** and anterior is to the right in **B, D, F**. Abbreviations: bc: bursal canal; ca: common atrium; cb: copulatory bursa; cm: circular muscles; go: gonopore; ho: hyperplastic ovaries; lm: longitudinal muscles; lod: left oviduct; ma: male atrium; pp: penis papilla; sv: seminal vesicle; te: testis; vd: vas deferens. Scale bars: 100 µm.

The well-developed testes are situated dorsally and extend from the level of the ovaries to the posterior end of the body (Fig. 10D). Upon approaching the level of the penis bulb, composed of intermingled muscle fibers, the vasa deferentia curve dorso-mediad and near the postero-dorsal wall of the penis bulb the sperm ducts abruptly bend ventrad to penetrate the wall of the penis bulb. Within the bulb, the sperm ducts open separately and symmetrically into the mid-dorsal portion of a large reniform seminal vesicle (Figs 10E, F, 12). The sperm ducts are lined with nucleated cells and are surrounded by a layer of circular muscles. The seminal vesicle

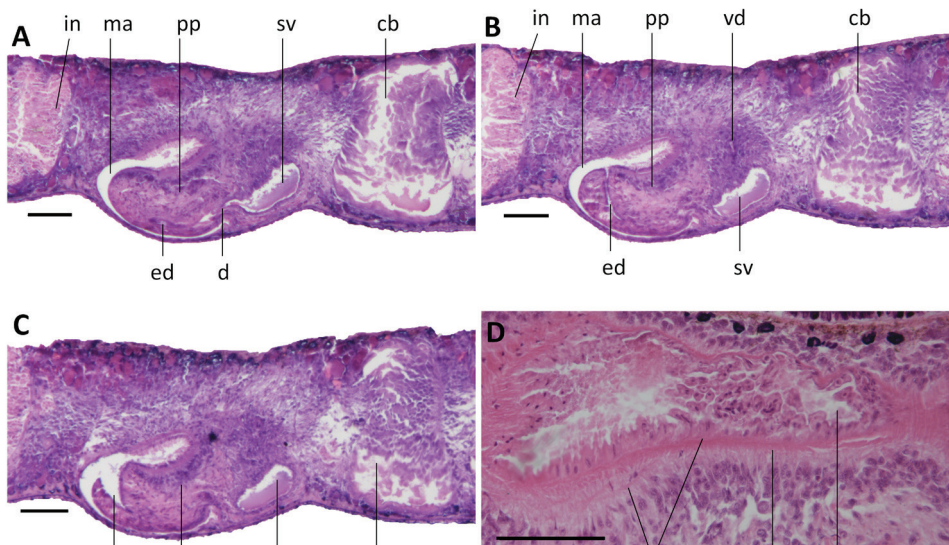


Figure 11. *Dugesia majuscula* **A** sagittal section of holotype YHYQ4, showing seminal vesicle, ejaculatory duct, small diaphragm, penis papilla, and copulatory bursa **B** Sagittal section of holotype YHYQ4, showing seminal vesicle, ejaculatory duct, penis papilla, and copulatory bursa **C** sagittal section of paratype YHYQ5, showing terminal and dorsal opening of ejaculatory duct **D** sagittal section of paratype YHYQ9, showing bursal canal and its musculature. The anterior is to the right in **A, B, C, D**. Abbreviations: bc: bursal canal; cb: copulatory bursa; cm: circular muscles; d: diaphragm; ed: ejaculatory duct; in: intestine; lm: longitudinal muscles; ma: male atrium; pp: penis papilla; sv: seminal vesicle; vd: vas deferens. Scale bars: 100 μ m.

opens into the ejaculatory duct via a very small diaphragm positioned at a level that corresponds with the root of the penis papilla (Figs 11A, 12). The ejaculatory duct runs ventrally through the penial papilla and opens to the exterior by means of sub-terminal dorsal opening at the tip of the papilla (Figs 11A–C, 12). The ejaculatory duct is lined by a cuboidal epithelium; we were unable to discern any musculature around the ejaculatory duct.

The cylindrical penis papilla is covered by an epithelium that is underlain with a subepithelial layer of circular muscle, followed by a layer of longitudinal muscle fibers. As a result of the ventral course of the ejaculatory duct, the penis papilla is asymmetrical, with its dorsal lip being much larger than the ventral one. The basal part of the penis papilla has an oblique, ventro-caudal orientation, after which the penis papilla makes a bend, so that the rest of the papilla has a more or less horizontal orientation (Figs 11A–C, 12). The papilla almost completely occupies the male atrium, which communicates with the common atrium via a more or less pronounced constriction (Fig. 12). In turn, the latter communicates with a gonoduct, lined with a columnar epithelium and receiving the openings of abundant cement glands, which leads to the ventral gonopore.

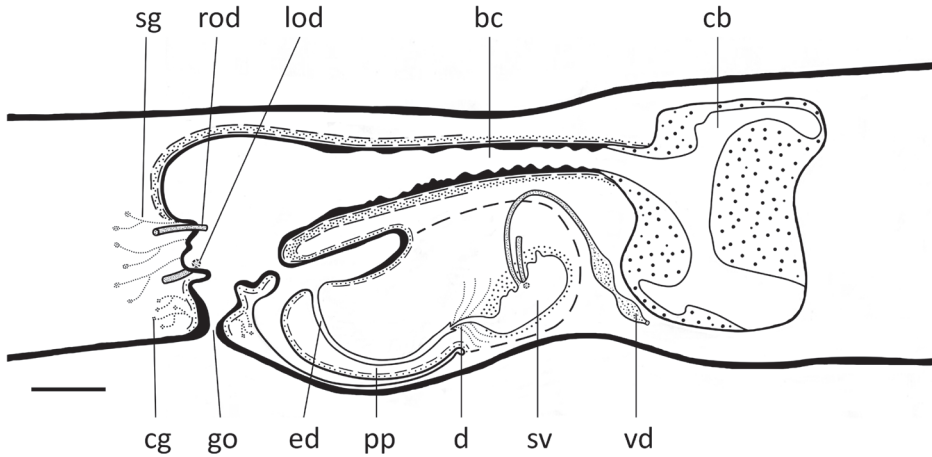


Figure 12. *Dugesia majuscula*. Sagittal reconstruction of the copulatory apparatus of the holotype (anterior is to the right). Abbreviations: bc: bursal canal; cb: copulatory bursa; cg: cement glands; d: diaphragm; ed: ejaculatory duct; go: gonopore; lod: left oviduct; pp: penis papilla; rod: right oviduct; sg: shell glands; sv: seminal vesicle; vd: vas deferens. Scale bar: 100 μ m.

The large sac-shaped copulatory bursa, which occupies the entire dorso-ventral space, is lined by a vacuolated epithelium provided with basal nuclei. There is hardly any musculature surrounding the bursa (Figs 11A–C, 12). From the postero-dorsal wall of the bursa, the bursal canal runs in a caudal direction to the left side of the male copulatory apparatus. Dorsally to the male atrium the bursal canal expands, particularly in dorso-ventral direction, to form a spacious posterior section that communicates with the common atrium. The bursal canal is lined with cylindrical, infranucleated, and ciliated cells and is surrounded by a subepithelial layer of longitudinal muscles, followed by a well-developed layer of circular muscle and a thin layer of longitudinal muscles. The outer longitudinal muscles constitute the ectal reinforcement layer, which extends from the vaginal region to approximately halfway along the bursal canal (Figs 11D, 12). Erythrophil shell glands open into the vaginal region of the bursal canal around the oviducal openings.

Discussion. Our present task of comparing the features of *D. majuscula* with already known species of *Dugesia* is made considerably easier by the fact that it exhibits the unusual character of a subterminal dorsal opening of the ejaculatory duct at the tip of the penis papilla, which thus far has been reported for only one other species, viz., *D. umbonata* from southwest China (Song et al. 2020). In view of the sister-group relationship between these two species (Fig. 2), this subterminal, dorsal opening of the ejaculatory duct may be hypothesized to represent a synapomorphy for *D. umbonata* and *D. majuscula*.

Although *D. umbonata* exhibits also asymmetrical oviducal openings and a ventrally displaced ejaculatory duct, as in *D. majuscula*, it differs from the latter notably in the presence of a large, muscularized hump on its bursal canal, among other differ-

ences. A subterminal opening of the ejaculatory duct is not uncommon among species of *Dugesia*, but in most cases the openings are ventral, in contrast to the dorsal opening in *D. majuscula* and *D. umbonata*. The only exception is *D. hepta* Pala et al., 1981 but in this species the ejaculatory duct exits at the dorso-lateral tip of the penis papilla, while in this species the ejaculatory duct is dorsally displaced, in contrast to the ventral course in *D. majuscula* and *D. umbonata*. Furthermore, in *D. hepta* the oviducts open symmetrically into the bursal canal (Stocchino et al. 2005), whereas in *D. majuscula* and *D. umbonata* the oviducal openings are asymmetrical.

General discussion

Molecular phylogeny and distances

The topology of our phylogenetic tree (Fig. 2) basically accords with results from previous phylogenetic analyses (Lázaro et al. 2009; Solà et al. 2013; Stocchino et al. 2017; Song et al. 2020). Detailed comparison between these results and our tree are complicated since the various studies included different sets of species as well as different molecular markers, while it also serves little purpose as our sole aim was to assess the taxonomic status of the two new Chinese species. Song et al. (2020) already noted that because of the rather low number of *Dugesia* species for which molecular information is available, it is presently not well possible to analyse the historical biogeography of the genus.

For being able to interpret genetic distances between presumably new species in the delimitation of species boundaries, it is necessary to have well-supported information on distances between already well-known species. Presently, our information on genetic distances between species of *Dugesia* is rather limited. Harrath et al. (2019) found that for COI, the lowest distance value between species was 7%, while Stocchino et al. (2017) reported distances usually greater than 10% among species from Madagascar. Furthermore, Lázaro et al. (2009) and Solà et al. (2013) showed, respectively, that the lowest distance value between Mediterranean species generally is greater than 10% or 6%. With respect to the new species *D. majuscula* and *D. semiglobosa*, the lowest genetic distance value between these species and their Oriental-Australasian congeners was 13.68% and 14.26%, respectively, while there is a 19.52% difference between the two new species (Suppl. material 3: Table S2). The lowest distance values reported for ITS-1 were 6% between Malagasy species (Stocchino et al. 2017), and 7% and 1% for Mediterranean species (Lázaro et al. 2009; Solà et al. 2013). With respect to *D. majuscula* and *D. semiglobosa*, the lowest distance values between these species and other Oriental-Australasian congeners were 5.82% and 9.74%, respectively. For this marker, the distance between the two new species was 5.83% (Suppl. material 4: Table S3). Thus, these inter-species genetic distances for COI and ITS-1 support both the molecular phylogenetic and the anatomical results, which already indicated that *D. majuscula* and *D. semiglobosa* are well-separated from their congeners.

Morphology

It is well-known that sexualized specimens from originally fissiparous populations generally develop hyperplastic ovaries (cf. Song et al. 2020 and references therein), excepting *D. benazzii* and *D. etrusca*, in which ex-fissiparous individuals did not develop hyperplastic ovaries (Stocchino et al. 2012; Stocchino and Manconi 2013). Furthermore, in such sexualized specimens with hyperplastic ovaries, testes may be under-developed or even be completely absent. However, such is not the case in *D. semiglobosa* and *D. majuscula*, as in both species the sexualized individuals possessed well-developed testes, while their vasa deferentia contained ample sperm, a condition that was previously observed also in *Dugesia bifida* Stocchino & Sluys, 2014 (Stocchino et al. 2014). Nevertheless, in the two new species cocoons were either not produced or were infertile.

It is noteworthy that in both new species from Hainan Island the vasa deferentia follow a characteristic course by first turning towards the dorsal body surface and then recurving ventrad and, subsequently, opening through the dorsal wall of the seminal vesicle. This specific course of the sperm ducts is uncommon among species of *Dugesia* and thus far had been reported only from *D. bengalensis*. However, in other features *D. bengalensis* is rather different from both *D. semiglobosa* and *D. majuscula*. For example, in *D. bengalensis* the sperm ducts open into the anterior portion of the seminal vesicle, while the ejaculatory duct has a subterminal ventral opening and the oviducal openings are symmetrical (Kawakatsu et al. 1983).

Karyology

Within the genus *Dugesia*, the basic chromosome number is seven, eight, or nine (Stocchino et al. 2004). With respect to karyotypes with a haploid number of $n = 8$, there are species in which all chromosomes are metacentric and species in which some chromosomes are not metacentric. Since in *D. semiglobosa* and *D. majuscula* all chromosomes are metacentric, we shall restrict our discussion to those species that also exhibit chromosome complements with a basic number of eight, metacentric chromosomes. Such a chromosome portrait is present in the following species: *D. gonocephala* (Dugès, 1830), many Sardinian populations of *D. benazzii* Lepori, 1951, *D. etrusca labronica* Lepori, 1950, *D. sagitta* Schmidt, 1861, *D. elegans*, *D. indonesiana* Kawakatsu, 1973, *D. japonica*, and presumably also in *D. colapha* Dahm, 1967 (cf. Dahm 1967; Benazzi and Goubault 1975; Kawakatsu et al. 1976; Ball 1979; De Vries 1984; Deri et al. 1999; Pala et al. 1999; Stocchino 2018). Evidently, none of these species is anatomically similar to *D. semiglobosa* or *D. majuscula*, otherwise we would have included these in our comparative morphological discussions (see above).

In view of the fact that both *D. semiglobosa* and *D. majuscula* exhibited mixoploid chromosome complements, it is interesting to note that such a combination of diploid and triploid metacentric chromosomes in a basic set of eight chromosomes

has been reported also for *D. japonica* Ichikawa & Kawakatsu, 1964 and *D. siamana* Kawakatsu, 1980 (Oki et al. 1981; Stocchino et al. 2004 and references therein). Mixoploid complements have been reported also for other species of *Dugesia* with a different basic number of chromosomes, such as $n=7$ or $n=9$, which we shall here not further discuss.

It has been suggested that polyploidization is adaptive in harsh climatic conditions and extreme environments (Stebbins 1971). In a study on the freshwater planarians *Phagocata vitta* Dugès, 1830, *Polycelis felina* Dalyell, 1814, and *Crenobia alpina* Dana, 1776, Lorch et al. (2016) reported that mean chromosome numbers increased with latitude, with higher latitudes coinciding with harsher climatic conditions. In contrast, mean chromosome numbers decreased with increasing temperature, temperature ranges, precipitation, and net primary production. Furthermore, populations with high chromosome numbers, due to polyploidization, tended to reproduce asexually, whereas populations with relatively low ploidy levels reproduced sexually. Nevertheless, these results and conclusions may not be well applicable to the two new Chinese *Dugesia*'s, since both species are mixoploid and possess hyperplasic ovaries. It is highly likely that the hyperplasic ovaries in the sexualized, ex-fissiparous animals prevented normal reproduction. In such abnormal ovaries the oocytes are also anomalous (Harrath et al. 2014), thus preventing regular oogenesis. That the cause of the infertility lies in the hyperplasic ovaries is supported by the fact that the testes are well-developed and that, thus, spermatogenesis presumably is regular. That gonadic anomalies effectuate infertility is known also from other species of *Dugesia* (cf. Stocchino et al. 2012; Harrath et al. 2017). Nevertheless, it is known that in some species of *Dugesia* ex-fissiparous individuals are able to produce fertile cocoons (Harrath et al. 2013; Stocchino and Manconi 2013 and references therein; Stocchino et al. 2014) but, apparently, *D. semiglobosa* and *D. majuscula* do not have that capacity.

The fact that animals from both species sexualized under laboratory conditions suggests that these conditions induced, or at least were favourable to sexualization. In our laboratory cultures we used a lower temperature than that of their habitat, in that in our cultures water temperature was 20 °C, whereas temperature in the springs was 23 °C and 19 °C. Furthermore, the specimens were collected in the coldest month of the year, viz., February. In Hainan Island, the average temperature during the coldest period usually is 18–22 °C, a situation that lasts for ~ 40 days. However, the temperatures in other months of the year are considerably higher than the temperature at which we collected our specimens. Especially, average temperatures from May to October reach 26–35 °C, with the highest temperature frequently being higher than 39 °C. This means that most of the time the two new species experience a relatively warm environment, in contrast to the relatively cold laboratory cultures. At collection, none of the specimens exhibited any signs of reproductive organs, while in the laboratory they sexualized at a lower temperature than they usually experience in their natural surroundings, with *D. semiglobosa* even producing cocoons, albeit inviable ones. This suggests that the sexualization process was induced by the lower temperatures that the worms experienced in the laboratory.

Acknowledgements

This work was supported by grants from the National Natural Science Foundation of China (nos. 32070427, 31570376, 31471965, and u1604173) and the Program for Innovative Research Team in University of Henan Province (18IRTSTHN022). We are grateful to Dr. G. A. Stocchino (University of Sassari, Italy) for information and discussion on karyology in the genus *Dugesia*. We thank are grateful to Drs F. Carbayo, P. Boll, and two anonymous reviewers for their constructive criticisms, which improved the manuscript.

References

- Abascal F, Zardoya R, Telford MJ (2010) TranslatorX: Multiple alignment of nucleotide sequences guided by amino acid translations. *Nucleic Acids Research* 38: W7–13. <https://doi.org/10.1093/nar/gkq291>
- Álvarez-Presas M, Baguña J, Riutort M (2008) Molecular phylogeny of land and freshwater planarians (Tricladida, Platyhelminthes): From freshwater to land and back. *Molecular Phylogenetics and Evolution* 47(2): 555–568. <https://doi.org/10.1016/j.ympev.2008.01.032>
- Ball IR (1979) The karyotypes of two *Dugesia* species from Corfu, Greece (Platyhelminthes, Turbellaria). *Bijdragen tot de Dierkunde* 48: 187–190. <https://doi.org/10.1163/26660644-04802007>
- Benazzi M, Benazzi Lentati G (1970) *Animal Cytogenetics Vol. 1: Platyhelminthes*. Gebrüder Borntraeger, Berlin, Stuttgart, 182 pp.
- Benazzi M, Goubault N (1975) Cytotaxonomical study of *Dugesia indonesiana* Kawakatsu (Tricladida Paludicola). *Accademia Nazionale dei Lincei, Rendiconti della Classe di Scienze Fisiche, Matematiche e Naturali*, ser. 8, vol. 58, fasc. 2: 237–243.
- Chen GW, Wang YL, Wang HK, Fu RM, Zhang JF, Liu DZ (2008) Chromosome and karyotype analysis of *Polycelis wutaishanica* (Turbellaria, Tricladida) from Shanxi province, China. *Acta Zootaxonomica Sinica* 33(3): 449–452.
- Chen Y-H, Chen X-M, Wu C-C, Wang A-T (2015) A new species of the genus *Dugesia* (Tricladida, Dugesiidae) from China. *Zoological Systematics* 40: 237–249.
- Dahm AG (1967) A new *Dugesia* “microspecies” from Ghana belonging to the *Dugesia gonocephala* group – Turbellaria Tricladida Paludicola. *Arkiv för Zoologi* 19: 309–321.
- Deri P, Colognato R, Rossi L, Salvetti A, Batistoni R (1999) A karyological study on populations of *Dugesia gonocephala* s.l. (Turbellaria, Tricladida). *Italian Journal of Zoology* 66: 245–253. <https://doi.org/10.1080/11250009909356262>
- Dessimoz C, Gil M (2010) Phylogenetic assessment of alignments reveals neglected tree signal in gaps. *Genome Biology* 11: R37. <https://doi.org/10.1186/gb-2010-11-4-r37>
- De Vries EJ (1984) On the karyology of *Dugesia gonocephala* s.l. (Turbellaria, Tricladida) from Montpellier, France. *Hydrobiologia* 132: 251–256. <https://doi.org/10.1007/BF00046257>
- De Vries EJ (1988) A synopsis of the nominal species of the subgenus *Dugesia* (Platyhelminthes: Tricladida: Paludicola) from Africa and Madagascar. *Zoological Journal of the Linnean Society* 92: 345–382. <https://doi.org/10.1111/j.1096-3642.1988.tb01729.x>

- Dong Z-M, Chen G-W, Zhang H-C, Liu D-Z (2017) A new species of *Polycelis* (Platyhelminthes, Tricladida, Planariidae) from China. *Acta Zoologica Academiae Scientiarum Hungaricae* 63(3): 263–276. <https://doi.org/10.17109/AZH.63.3.263.2017>
- Harrath AH, Semlali A, Mansour L, Ahmed M, Sirotkin AV, Al Omar SY, Arfah M, Al Anazi MS, Alhazza IM, Nyengaard JR, Alwasel S (2014) Infertility in the hyperplasic ovary of freshwater planarians: the role of programmed cell death. *Cell and Tissue Research* 358: 607–620. <https://doi.org/10.1007/s00441-014-1971-0>
- Harrath AH, Semlali A, Mansour L, Aldamas W, Al Omar SY, Al Anazi MS, Nyengaard JR, Alwasel S (2017) Dynamics of Cytokine-like activity in the hyperplasic ovary of ex-fissiparous planarians. *Biological Bulletin* 232: 12–18. <https://doi.org/10.1086/691408>
- Harrath AH, Sluys R, Aldahmash W, Al-Razaki A, Alwasel S (2013) Reproductive strategies, karyology, parasites, and taxonomic status of *Dugesia* populations from Yemen (Platyhelminthes, Tricladida, Dugesidae). *Zoological Science* 30: 502–508. <https://doi.org/10.2108/zsj.30.502>
- Harrath AH, Sluys R, Mansour L, Folefack GL, Aldahmash W, Alwasel S, Solà E, Riutort M (2019) Molecular and morphological identification of two new African species of *Dugesia* (Platyhelminthes, Tricladida, Dugesidae) from Cameroon. *Journal of Natural History* 53: 253–271. <https://doi.org/10.1080/00222933.2019.1577508>
- Katoh K, Standley DM (2013) MAFFT multiple sequence alignment software version 7: Improvements in performance and usability. *Molecular Biology and Evolution* 30: 772–780. <https://doi.org/10.1093/molbev/mst010>
- Kawakatsu M, Oki I, Tamura S, Sugino H (1976) Studies on the morphology, karyology and taxonomy of the Japanese freshwater planarian *Dugesia japonica* Ichikawa et Kawakatsu, with a description of a new subspecies, *Dugesia japonica ryukyuensis* subsp. nov. *The Bulletin of Fuji Women's College* 14, ser. II: 81–126.
- Kawakatsu M, Tamura S, Yamayoshi T, Oki I (1980) The freshwater planarians from Thailand and South India. *Annotationes Zoologicae Japonenses* 53: 254–268.
- Kawakatsu M, Oki I, Tamura S, Yamayoshi T (1985) Reexamination of freshwater planarians found in tanks of tropical fishes in Japan, with a description of a new species, *Dugesia austroasiatica* sp. nov. (Turbellaria; Tricladida; Paludicola). *Bulletin of the Biogeographical Society of Japan* 40: 1–19.
- Kawakatsu M, Oki I, Tamura S, Yamayoshi T, Aditya AK (1983) A new freshwater planarian from West Bengal, India (Turbellaria: Tricladida: Paludicola). *Bulletin of the Biogeographical Society of Japan* 38: 3–10.
- Lázaro EM, Sluys R, Pala M, Stocchino GA, Baguña J, Riutort M (2009) Molecular barcoding and phylogeography of sexual and asexual freshwater planarians of the genus *Dugesia* in the Western Mediterranean (Platyhelminthes, Tricladida, Dugesidae). *Molecular Phylogenetics and Evolution* 52: 835–845. <https://doi.org/10.1016/j.ympev.2009.04.022>
- Levan A, Fredga K, Sandberg AA (1964) Nomenclature for centromeric position on chromosomes. *Hereditas* 52: 201–220. <https://doi.org/10.1111/j.1601-5223.1964.tb01953.x>
- Lepori NG (1948) Descrizione di *Dugesia sicula*, nuova specie di Triclade d'acqua dolce dei dintorni di Catania. *Archivio Zoologico Italiano* 33: 461–472.
- Liu DZ (1993) Chinese freshwater turbellarians. Beijing Normal University Publishing House, Beijing, 184 pp. [In Chinese]

- Lorch S, Zeuss D, Brandl R, Brändle M (2016) Chromosome numbers in three species groups of freshwater flatworms increase with increasing latitude. *Ecology and Evolution* 6(5): 1420–1429. <https://doi.org/10.1002/ece3.1969>
- Mittermeier RA, Robles GP, Hoffmann M, Pilgrim J, Brooks T, Mittermeier CG, Lamoreux J, da Fonseca GAB (2005) Hotspots revisited: Earth's biologically richest and most endangered ecoregions. CEMEX, Mexico City, Mexico, 392 pp.
- Mittermeier RA, Turner WR, Larsen FW, Brooks TM, Gascon C (2011) Global biodiversity conservation: the critical role of hotspots. In: Zachos FE, Habel JC (Eds) *Biodiversity Hotspots*, Springer, Heidelberg, 3–22. https://doi.org/10.1007/978-3-642-20992-5_1
- Oki I, Tamura S, Yamayoshi T, Kawakatsu M (1981) Karyological and taxonomic studies of *Dugesia japonica* Ichikawa et Kawakatsu in the Far East. *Hydrobiologia* 84: 53–68. <https://doi.org/10.1007/BF00026163>
- Pala M, Vacca RA, Casu S, Stocchino GA (1995) The freshwater planarian *Dugesia sicula* Lepori from Sardinia (Platyhelminthes, Tricladida). *Hydrobiologia* 310: 151–156. <https://doi.org/10.1007/BF00015533>
- Pala M, Casu S, Stocchino G (1999) Karyology and karyotype analysis of diploid freshwater planarian populations of the *Dugesia gonocephala* group (Platyhelminthes, Tricladida) found in Sardinia. *Hydrobiologia* 392: 113–119. <https://doi.org/10.1023/A:1003534507632>
- Ronquist F, Teslenko M, van der Mark P, Ayres DL, Darling A, Höhna S, Larget B, Liu L, Suchard MA, Huelsenbeck JP (2012) MrBayes 3.2: efficient Bayesian phylogenetic inference and model choice across a large model space. *Systematic Biology* 61: 539–542. <https://doi.org/10.1093/sysbio/sys029>
- Sluys R, Kawakatsu M, Winsor L (1998) The genus *Dugesia* in Australia, with its phylogenetic analysis and historical biogeography (Platyhelminthes, Tricladida, Dugesidae). *Zoologica Scripta* 27: 273–289. <https://doi.org/10.1111/j.1463-6409.1998.tb00461.x>
- Sluys R, Riutort M (2018) Planarian diversity and phylogeny. In: Rink JC (Ed.) *Planarian Regeneration: Methods and Protocols*. Methods in Molecular Biology, vol. 1774. Humana Press, Springer Science+Business Media, New York, 1–56. https://doi.org/10.1007/978-1-4939-7802-1_1
- Solà E, Sluys R, Gritsalis K, Riutort M (2013) Fluvial basin history in the northeastern Mediterranean region underlies dispersal and speciation patterns in the genus *Dugesia* (Platyhelminthes, Tricladida, Dugesidae). *Molecular Phylogenetics and Evolution* 66: 877–888. <https://doi.org/10.1016/j.ympev.2012.11.010>
- Song X-Y, Li W-X, Sluys R, Huang S-X, Wang A-T (2020) A new species of *Dugesia* (Platyhelminthes, Tricladida, Dugesidae) from China, with an account on the histochemical structure of its major nervous system. *Zoosystematics and Evolution* 96: 431–447. <https://doi.org/10.3897/zse.96.52484>
- Stamatakis A (2014) RAxML version 8: a tool for phylogenetic analysis and post-analysis of large phylogenies. *Bioinformatics* (Oxford, England) 30: 1312–1313. <https://doi.org/10.1093/bioinformatics/btu033>
- Stattersfield, AJ, Crosby MJ, Long AJ, Wege DC (1998) *Endemic bird areas of the world. Priorities for biodiversity conservation*. Bird Life International, Cambridge, 815 pp.
- Stebbins GL (1971) *Chromosomal evolution in higher plants*. Edward Arnold, London.

- Stocchino GA (2018) 80 years of research on planarians (Platyhelminthes, Tricladida) from Sardinia, Italy: an annotated checklist. *Zootaxa* 4532: 539–552. <https://doi.org/10.11646/zootaxa.4532.4.5>
- Stocchino GA, Corso G, Manconi R, Pala M (2005) Endemic freshwater planarians of Sardinia: Redescription of *Dugesia hepta* (Platyhelminthes, Tricladida) with a comparison of the Mediterranean species of the genus. *Journal of Natural History* 39: 1947–1960. <https://doi.org/10.1080/00222930500060025>
- Stocchino GA, Manconi R (2013) Overview of life cycles in model species of the genus *Dugesia* (Platyhelminthes Tricladida). *Italian Journal of Zoology* 80(3): 319–328. <https://doi.org/10.1080/11250003.2013.822025>
- Stocchino GA, Manconi R, Corso G, Pala M (2004) Karyology and karyometric analysis of an Afrotropical freshwater planarian (Platyhelminthes, Tricladida). *Italian Journal of Zoology* 71: 89–93. <https://doi.org/10.1080/11250000409356557>
- Stocchino GA, Manconi R, Corso G, Sluys R, Casu S, Pala M (2009) African planarians: Morphology and karyology of *Dugesia maghrebiana* sp. n. (Platyhelminthes, Tricladida) from Tunisia. *Italian Journal of Zoology* 76: 83–91. <https://doi.org/10.1080/11250000802141683>
- Stocchino GA, Sluys R, Manconi R (2012) A new species of *Dugesia* (Platyhelminthes, Tricladida, Dugesiidae) from the Afromontane forest in South Africa, with an overview of freshwater planarians from the African continent. *Zootaxa* 3551: 43–58. <https://doi.org/10.11646/zootaxa.3551.1.3>
- Stocchino GA, Sluys R, Deri P, Manconi R (2013) Integrative taxonomy of a new species of planarian from the Lake Ohrid basin, including an analysis of biogeographical patterns in freshwater triclads from the Ohrid region (Platyhelminthes, Tricladida, Dugesiidae). *ZooKeys* 313: 25–43. <https://doi.org/10.3897/zookeys.313.5363>
- Stocchino GA, Sluys R, Manconi R (2014) A new and aberrant species of *Dugesia* (Platyhelminthes, Tricladida) from Madagascar. *ZooKeys* 425: 71–88. <https://doi.org/10.3897/zookeys.425.7811>
- Stocchino GA, Sluys R, Riutort M, Solà E, Manconi R (2017) Freshwater planarian diversity (Platyhelminthes: Tricladida: Dugesiidae) in Madagascar: new species, cryptic species, with a redefinition of character states. *Zoological Journal of the Linnean Society* 181: 727–756. <https://doi.org/10.1093/zoolinnean/zlx017>
- Tamura K, Stecher G, Peterson D, Filipski A, Kumar S (2013) MEGA6: Molecular Evolutionary Genetics Analysis version 6.0. *Molecular Biology and Evolution* 30: 2725–2729. <https://doi.org/10.1093/molbev/mst197>
- Talavera G, Castresana J (2007) Improvement of phylogenies after removing divergent and ambiguously aligned blocks from protein sequence alignments. *Systematic Biology* 56: 564–577. <https://doi.org/10.1080/10635150701472164>
- Tan G, Muffato M, Ledergerber C, Herrero J, Goldman N, Gil M, Dessimoz C (2015) Current methods for automated filtering of multiple sequence alignments frequently worsen single-gene phylogenetic inference. *Systematic Biology* 64: 778–791. <https://doi.org/10.1093/sysbio/syv033>

Supplementary material 1

Figure S1. Phylogenetic tree obtained from ML analysis of the concatenated dataset

Authors: Lei Wang, Zi-mei Dong, Guang-wen Chen, Ronald Sluys, De-zeng Liu

Data type: phylogenetic tree

Explanation note: Numbers at nodes indicate support values (bootstrap). Scale bar: substitutions per site.

Copyright notice: This dataset is made available under the Open Database License (<http://opendatacommons.org/licenses/odbl/1.0/>). The Open Database License (ODbL) is a license agreement intended to allow users to freely share, modify, and use this Dataset while maintaining this same freedom for others, provided that the original source and author(s) are credited.

Link: <https://doi.org/10.3897/zookeys.1028.60838.suppl1>

Supplementary material 2

Table S1. Primers used for amplification, with their annealing temperatures

Authors: Lei Wang, Zi-mei Dong, Guang-wen Chen, Ronald Sluys, De-zeng Liu

Data type: molecular data

Copyright notice: This dataset is made available under the Open Database License (<http://opendatacommons.org/licenses/odbl/1.0/>). The Open Database License (ODbL) is a license agreement intended to allow users to freely share, modify, and use this Dataset while maintaining this same freedom for others, provided that the original source and author(s) are credited.

Link: <https://doi.org/10.3897/zookeys.1028.60838.suppl2>

Supplementary material 3

Table S2. Genetic distances for COI

Authors: Lei Wang, Zi-mei Dong, Guang-wen Chen, Ronald Sluys, De-zeng Liu

Data type: molecular data

Explanation note: Highest and lowest distance values between the two new Chinese species and Oriental-Australasian congeners indicated in blue and red, respectively. Purple: distance value between the two new species.

Copyright notice: This dataset is made available under the Open Database License (<http://opendatacommons.org/licenses/odbl/1.0/>). The Open Database License (ODbL) is a license agreement intended to allow users to freely share, modify, and use this Dataset while maintaining this same freedom for others, provided that the original source and author(s) are credited.

Link: <https://doi.org/10.3897/zookeys.1028.60838.suppl3>

Supplementary material 4

Table S3. Genetic distances for ITS-1

Authors: Lei Wang, Zi-mei Dong, Guang-wen Chen, Ronald Sluys, De-zeng Liu

Data type: molecular data

Explanation note: Highest and lowest distance values between the two new Chinese species and Oriental-Australasian congeners indicated in blue and red, respectively. Purple: distance value between the two new species.

Copyright notice: This dataset is made available under the Open Database License (<http://opendatacommons.org/licenses/odbl/1.0/>). The Open Database License (ODbL) is a license agreement intended to allow users to freely share, modify, and use this Dataset while maintaining this same freedom for others, provided that the original source and author(s) are credited.

Link: <https://doi.org/10.3897/zookeys.1028.60838.suppl4>

Integrative taxonomy uncovers a new stygobiotic *Caridina* species (Decapoda, Caridea, Atyidae) from Guizhou Province, China

Shuo Feng^{1*}, Qing-Hua Chen^{2*}, Zhao-Liang Guo¹

1 Department of Animal Science, School of Life Science and Engineering, Foshan University, Nanhai 528231, Guangdong Province, China **2** South China Institute of Environmental Sciences, Ministry of Ecology and Environment, Guangzhou 510520, Guangdong Province, China

Corresponding author: Zhao-Liang Guo (zlguo@fosu.edu.cn)

Academic editor: C. Magalhães | Received 1 February 2021 | Accepted 6 March 2021 | Published 5 April 2021

<http://zoobank.org/F71826D1-E5F6-49BD-94EC-4DBBA76D40EC>

Citation: Feng S, Chen Q-H, Guo Z-L (2021) Integrative taxonomy uncovers a new stygobiotic *Caridina* species (Decapoda, Caridea, Atyidae) from Guizhou Province, China. ZooKeys 1028: 29–47. <https://doi.org/10.3897/zookeys.1028.63822>

Abstract

Collecting much-needed information on the taxonomy, distribution, and ecology of cave-dwelling shrimp is vital for addressing the urgent challenges in conservation biodiversity in fragile cave ecosystems. *Caridina incolor* **sp. nov.**, a new atyid shrimp from an underground stream of Yaoshui Cave, Daqikong scenic area, Libo County, Guizhou Province, southwestern China is described based on morphology and DNA analysis (mitochondrial COI). *Caridina incolor* **sp. nov.** differs from epigean congeners by its smaller eyes which range from reduced to completely blind; colorless body and appendages; long stylocerite and sixth abdominal segment; and relatively large eggs. In comparison to other cave species, *Caridina incolor* **sp. nov.** presents a long rostrum and stylocerite; slender sixth abdominal segment; and unique shape of the appendix masculina. Data on the habitat, ecology, and levels of threat are provided and suggest that it should be categorized as Critically Endangered (CR) under the current IUCN criteria.

Keywords

Caridina, COI, conservation biodiversity, freshwater biodiversity, southwestern China, speleology, taxonomy

* Contributed equally as the first authors.

Introduction

China is rich in subterranean environments, with more than 500,000 documented caves, most of which are located in the southwest karst region, such as Guangxi, Guizhou, and Yunnan Province (Chen 2006; Ran and Yang 2015). This underground setting has a unique ecological habitat characterized by permanent darkness, relatively constant air and water temperature, and scarcity of food supply (Rétaux and Casane 2013; Culver and Pipan 2019; Mammola et al. 2019). They may have served as faunal refuges and indeed are known to harbor an impressive array of shrimp species (Holthuis 1974, 1977; Hobbs et al. 1977; Hart and Manning 1981; Liang and Yan 1981; Mejía-Ortíz and Hartnoll 2006; Li 2007; Cai and Ng 2009, 2018; Pan et al. 2010; Zhu et al. 2020). Though the stygobiont shrimps are prone to geographic and genetic isolation, they exhibit a suite of convergent characteristics under natural selection, including reduction or loss of eyes, loss of pigment, elongated antennae and ambulatory appendages. Non-visual sensory structures are enhanced with the loss of vision, which ultimately leads to speciation (Barr 1968; Holthuis 1986; Peck 1986; Christiansen 2005; Mejía-Ortíz et al. 2006). They serve an important underground ecological role and have a position near the base of the food chain. By consuming organic matter such as leaves and twigs that get flushed into caves, they are the primary decomposers and make nutrients available to other organisms in the ecosystem, such as fish and crabs (Botosaneanu 1985).

In China, most cave systems have not been adequately surveyed because of the difficulty in sample collection. To date, 24 described species of four genera of atyids are presently known as inhabitants of the subterranean aquatic realm, some of which are completely adapted to subterranean life, and the majority from the genus *Caridina* H. Milne Edwards, 1837 (Liang and Yan 1981; Guo et al. 1992, 1996; Liang and Zhou 1993; Cai 1995; Cai and Li 1997; Cai and Liang 1999; Cai and Ng 1999, 2018; Liang et al. 1999, 2005; Li and Li 2010; Xu et al. 2020).

Guizhou Province is the central area of karst landforms in southwest China, with 73% of the land covered with carbonate rocks (He and Li 2016; Zhou et al. 2017). The karstic nature of this area promotes the formation of submerged cave systems, with more than 700 large cave systems documented (Zhang and Zhu 2012). Although Guizhou presents great biospeological potential, most submerged cave systems have not been adequately surveyed or studied. The research concerning the cave-dwelling atyids in Guizhou started with a study by Cai and Li (1997), who described *Caridina demenica* Cai & Li, 1997 with pigmented reduced eyes from Libo County. Liang et al. (2005), subsequently revealed another three new atyids: *Caridina caverna* Liang, Chen & Li, 2005 which is blind and depigmented; *C. acuta* Liang, Chen & Li, 2005 which has slightly reduced eyes and pigmentation; and *Neocaridina brevidactyla* Liang, Chen & Li, 2005 which apparently does not show any adaptation to subterranean life. Cai and Ng (2018) reported a new cave-dwelling atyid *Caridina jiangkou* Cai & Ng, 2018 from Jiangkou County, which is also of the typical epigean form. More recently, Xu et

al. (2020) reported *Caridina sinanensis* Xu, Li, Zheng & Guo, 2020 from Sinan County, which is unpigmented, and the cornea is vestigial with only a small pigment spot.

During our biospeleological surveys in Guizhou Province, stygobiont atyid shrimps belonging to the genus *Caridina* were collected from Yaoshui Cave, Daqikong scenic area, Libo County. The specimens collected could not be assigned to any known species of this genus based on a combination of morphological and molecular features (COI). *Caridina incolor* sp. nov. is rare and has a restricted distribution; its taxonomic uniqueness also suggests that it may be relictual. The impact of anthropogenic activities on the new species are also noted and suggests it is in need of urgent conservation intervention.

Materials and methods

Study cave and ecological data

Daqikong scenic area is named after a seven span bridge on the Dagou River near Mengtang Village, Wangmeng Township. It is situated about 25 km southwest of Libo County, at the border region of Guizhou and Guangxi in southwestern China. Yaoshui Cave is near the Mengtang scenic spot of Daqikong scenic area, at 25°17'1"N, 107°45'8"E and an altitude of 520 m. The entrance is about 120 m away from the tour plank road, located halfway up a limestone hill. The opening of the cave is arched and 2 m wide and 4 m high. There is naked shale above the entrance, with some ferns, bryophytes and vines present in the surrounding areas (Fig. 5A). Beyond the entrance is a rocky horizontal passage which is 2 m wide. Shrimps were observed in a pool (2 m², 0.8 m deep, and in the weak light zone) situated 2 m from the entrance. The weak light zone channel is rugged and can only be entered along the tunnel wall. Another 4 m in is the underground river (in total darkness). In some areas, it is shallow (0.1–0.5 m) with a muddy bottom. However, in the deeper parts (1.3–2.5 m), the bottom becomes rocky and slopes precipitously to unknown depths. A number of shrimps were taken in the shallows. This cave was inhabited by bats and a thick layer of bat guano was also found on the ground.

During the November collection trip, the water was clear and the water parameters of the river were: temperature 21 °C, pH 7.5, and dissolved oxygen 8.8 mg l⁻¹. Water levels of Yaoshui Cave fluctuate dramatically throughout the year. During spring and summer, heavy precipitation inundates the passage and blocks access to the entrance. Also, an outflowing stream snakes down into Dagou River (Fig. 5B). During autumn and winter, due to lower water levels, some pools may become dry, but the underground river does not dry up. The outline of the Yaoshui Cave is shown in Figure 1. The cave was visited by Deng et al. in 2011. Twenty-six cavefish specimens were collected and a new species, *Oreonectes daqikongensis* Deng, Wen, Xiao & Zhou, 2016 was described. They mention that only the blind fish was found in the underground river, and no other fish, shrimp, or aquatic animal were found (Deng et al. 2016). This blind fish was collected in the deeper parts of the river during this survey (Fig. 1C).

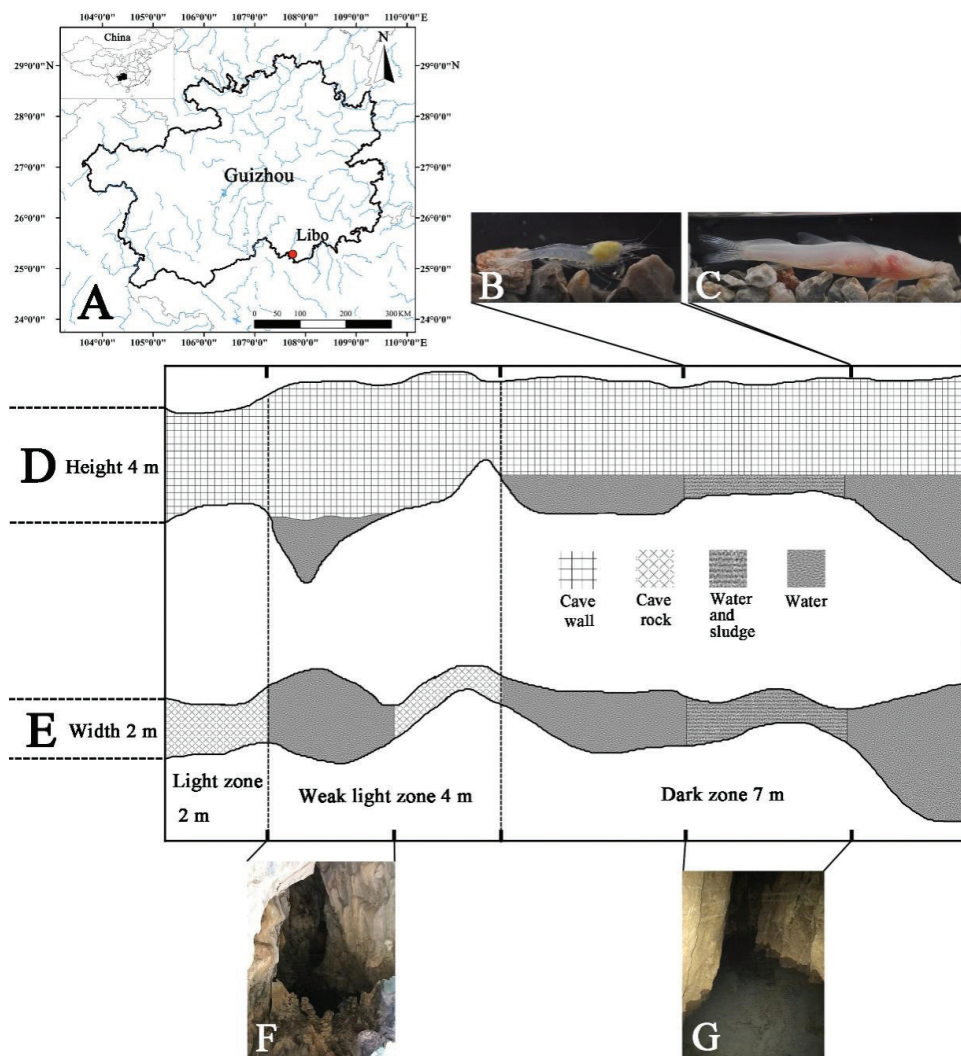


Figure 1. Type locality and schematic diagram of the cave of *Caridina incolor* sp. nov. **A** Yaoshui Cave is located near Libo County and is marked by the red dot **B** the sampling point of shrimp **C** the sampling point of fish **D** side view of the cave **E** plan view of the cave **F** a pool in a weak light zone **G** river in the dark zone.

Sample collection

On August 3, the cave gallery was inundated due to the rain. Sample collectors managed to wade in, but only a juvenile female was collected. On November 27, the water level was lower, sample collectors successfully entered the cave. Under the light of our headlights, a school of translucent white shrimps were observed swimming or clinging to the cave wall of the river. Forty-two individuals were collected in the shallow muddy areas. Samples were collected with a hand net (mesh size 0.6 mm). The sampling scene was recorded with photographs and video-recordings. Specimens

were placed in oxygenated polythene bags, anaesthetized with ice, then transported back to the hotel. The shrimps were fixed in 95% ethanol after they were photographed. The ethanol was changed after 24 h with fresh 75% ethanol. The blind fish (*Oreonectes daqikongensis*) was also collected. Basic hydrological and physico-chemical parameters of the cave were measured by the following instruments: Bosch GLM-30 Laser rangefinder, eTrex Venture GPS locator, JWSA2-2 temperature and hygrometer, BDO820 Portable dissolved oxygen determining meter, and BPH-220 pH measuring apparatus.

Morphological analysis

Specimens were examined using a dissecting microscope (Olympus SZX7). Morphometric measurements on selected characters and illustrations were made using a digital camera (DP22) mounted on a stereomicroscope (Olympus SZX7) with Olympus CellSens Entry v1.18 software. The measuring method of morphometric characters follows that of von Rintelen and Cai (2009). The following abbreviations are used throughout the text: alt (altitude), cl (carapace length), rl (rostral length), and tl (total length). All measurements are in millimeters. Specimens were deposited in the Department of Animal Science, School of Life Science and Engineering, Foshan University (FU).

Molecular data and analysis

Genomic DNA was extracted from abdominal muscle tissue using the Universal Genomic DNA Kit (Beijing, China), following manufacturer instructions. Segments of the mitochondrial cytochrome oxidase I (COI) were amplified by using the primers LCO1490 and HCO2198 (Folmer et al. 1994). PCRs were run in 50 µl volume reactions. COI cycling conditions were: 94 °C for 3 min followed by 35 × (94 °C for 30 s/46±1 °C for 60 s/72 °C for 60 s), with a final elongation step of 5 min at 72 °C. PCR products were forwardly sequenced using primers with an Applied Biosystems 3730 Analyzer (Applied Biosystems, Foster City, CA, USA).

For the phylogenetic analyses, we included species similar in morphology to the new species and also other *Caridina* species that are known to occur in the neighboring areas. A total of 47 nucleotide sequences of 13 *Caridina* and 3 *Neocaridina* species and an outgroup (Table 1) were incorporated and analyzed with MAFFT v7.313 (Katoh and Standley 2013). All the COI sequences were obtained by PCR. The new sequencing results are corrected for 617-bp (COI) for subsequent analysis. All the sequences were aligned with Mega 7.0 (Kumar et al. 2016) software using the muscle alignment module. Genetic distances were calculated using Maximum Composite Likelihood. The best partitioning strategy was selected according to ModelFinder (Kalyaanamoorthy et al. 2017) Bayesian information criterion (BIC) and default parameters. MrBayes v.3.2.6 (Ronquist et al. 2012) was performed using PhyloSuite v1.2.2 (Zhang et al. 2020). Maximum likelihood (ML) was performed using IQ-TREE 1.6.12 (Nguyen et al. 2015). According to the Bayes information criterion (ModelFinder default

Species	Sampling locality	GenBank numbers
<i>Caridina incolor</i> sp. nov.	Libo, Guizhou	MW237749–MW237753
<i>Caridina sinanensis</i>	Sinan, Guizhou	MT433962–MT433964
<i>Caridina zhongshanica</i>	Zhongshan, Guangdong	MN701597–MN701598
<i>Palaemon modestus</i>	Dongting lake, Hunan	MK412768–MK412769
<i>Neocaridina denticulata</i>	Hulun lake, Inner Mongolia	MW222157–MW222159
<i>Neocaridina palmata</i>	Hong Kong, China	MW226891–MW226893
<i>Caridina mariae</i>	Nankun Mountain, Huizhou	MN701601–MN701602
<i>Caridina serrata</i>	Dong'ao Island, Zhuhai	MN701599–MN701600
<i>Caridina tetrazona</i>	Zhuhai, Guangdong	MN701593–MN701594
<i>Caridina cantonensis</i>	Qingyuan, China	MN701589–MN701590
<i>Caridina</i> sp. 2	Huanjiang, Guangxi	MW237763–MW237764
<i>Caridina huananensis</i>	Yingde, Qingyuan	MN701607–MN701608
<i>Caridina lanceifrons</i>	Dongfang, Hainan	MN701605–MN701606
<i>Caridina zhujiangensis</i>	Dong'ao Island, Zhuhai	MN701603–MN701604
<i>Caridina carvernicola</i>	Mashan, Guangxi	MW237867
<i>Neocaridina heteropoda</i>	Guilin, Guangxi	MW221964–MW221966 MW222154–MW222156
<i>Caridina</i> sp. 1	Mashan, Guangxi	MW237861–MW237866

recommendation), the best model for Bayesian inference (BI) and maximum likelihood method (ML) are GTR+I+G and TIM2+G+I, respectively. Markov chain Monte Carlo (MCMC) analysis was performed with two simultaneous runs starting with random trees to approximate the posterior probabilities of trees. Each run consisted of four chains, with default heating parameters and ran for 4×10^6 generations, discarding the first 25% as burnin.

Table 2. Pairwise genetic distance among 17 species based on COI (below diagonal) gene.

	Species	1	2	3	4	5	6	7	8	9	10	11	12	13	14	15	16	17
1	<i>Caridina incolor</i> sp. nov.																	
2	<i>Caridina sinanensis</i>	0.13																
3	<i>Caridina zhongshanica</i>	0.17	0.14															
4	<i>Palaeomon modestus</i>	0.24	0.20	0.19														
5	<i>Neocaridina denticulata</i>	0.18	0.14	0.15	0.20													
6	<i>Neocaridina palmata</i>	0.18	0.14	0.16	0.21	0.05												
7	<i>Caridina mariae</i>	0.17	0.15	0.08	0.21	0.16	0.17											
8	<i>Caridina serrata</i>	0.16	0.12	0.11	0.21	0.14	0.16	0.12										
9	<i>Caridina tetrazona</i>	0.17	0.14	0.12	0.21	0.17	0.17	0.13	0.09									
10	<i>Caridina cantonensis</i>	0.16	0.14	0.01	0.19	0.15	0.16	0.08	0.11	0.12								
11	<i>Caridina</i> sp. 2	0.15	0.11	0.14	0.21	0.15	0.15	0.15	0.13	0.14	0.15							
12	<i>Caridina huananensis</i>	0.16	0.12	0.14	0.21	0.15	0.17	0.14	0.13	0.14	0.14	0.14						
13	<i>Caridina lanceifrons</i>	0.19	0.18	0.18	0.22	0.20	0.18	0.19	0.18	0.18	0.18	0.19	0.19					
14	<i>Caridina zhuijiangensis</i>	0.18	0.16	0.17	0.20	0.18	0.18	0.19	0.18	0.19	0.17	0.16	0.18	0.17				
15	<i>Caridina carvernicola</i>	0.16	0.12	0.14	0.21	0.14	0.15	0.14	0.13	0.13	0.14	0.02	0.13	0.20	0.15			
16	<i>Neocaridina heteropoda</i>	0.18	0.14	0.16	0.20	0.13	0.15	0.16	0.15	0.15	0.16	0.16	0.16	0.18	0.20	0.15		
17	<i>Caridina</i> sp. 1	0.16	0.11	0.14	0.21	0.15	0.15	0.14	0.14	0.14	0.14	0.05	0.14	0.19	0.15	0.03	0.15	

Taxonomic account

Family Atyidae De Haan, 1849

Subfamily Atyinae De Haan, 1849

Genus *Caridina* H. Milne Edwards, 1837

Caridina incolor sp. nov.

<http://zoobank.org/FF693EA8-140F-49F5-8B85-A59080737670>

Figures 3–5

Material examined. *Holotype*: Adult male (FU, 2018-11-27-01), tl 21.8 mm, cl 5.1 mm, rl 3.0 mm; Yaoshui Cave, Mengtang Village, Wangmeng Township, Daqikong scenic area, Libo County, Guizhou Province, China (25°17'1"N, 107°45'8"E, alt. 520.0 m), November 27, 2018.

Paratypes: 1 male (FU, 2018-11-27-02) tl 25.9 mm, cl 6.1 mm, rl 3.1 mm; 16 males (FU, 2018-11-27-03) tl 17.4–25.9 mm, cl 4.2–6.0 mm, rl 2.4–3.4 mm; 10 females (FU, 2018-11-27-04), tl 17.8–25.2 mm, cl 4.5–6.1 mm, rl 2.4–3.4 mm; cl 4.9–6.6 mm, same data as for holotype. *Paratypes*: 6 males (FU, 2018-11-27-05) tl 18.4–25.1 mm, cl 4.4–5.9 mm, rl 2.5–3.0 mm; 9 females (3 ovigerous) (FU, 2018-11-27-06), tl 17.5–25.0 mm, cl 4.5–6.0 mm, rl 2.4–3.1 mm; cl 5.0–6.3 mm, same data as for holotype. Two samples from (FU, 2018-11-27-05) and three samples from (FU, 2018-11-27-06) were sequenced.

Comparative material examined. *Caridina sinanensis* Xu, Li, Zhang and Guo 2020. *Holotype*: Adult male (FU, 2019-01-25-01), tl 16.7 mm, cl 4.8 mm, rl 1.5 mm; a cave river at Pengjiaao, Tangtou Town, Sinan County, Guizhou Province, southwestern, China (27°44'10"N, 108°11'58"E, alt. 294.7 m), January 25, 2019. *Paratypes*: 1 male (FU, 2019-01-25-02) cl 5.4 mm; 1 male (FU, 2019-01-25-03) cl 6.8 mm; 1 male (FU, 2019-01-25-04) cl 4.8 mm; 2 males (FU, 2019-01-25-05), cl 4.2–6.2 mm; 20 females (9 ovigerous) (FU, 2019-01-25-05), cl 4.9–6.6 mm.

Diagnosis. Body and appendages without coloration, translucent. Rostrum slender, slightly elevated at base, reaching to base of 3rd segment of antennular peduncle to end of scaphocerite; straight, slightly sloping downwards, sometimes with tip turned upwards; rostral formula 6–10+11–27/4–15. First pereopod carpus 0.83–0.91 × as long as chela, 2.3–2.7 × as long as high; chela 2.2–2.5 × as long as broad; fingers 1.1–1.4 × as long as palm. Second pereopod carpus 1.3–1.4 × as long as chela, 5.4–5.6 × as long as high; chela 2.4–2.6 × as long as broad; fingers 1.6–1.8 × as long as palm. Third pereopod propodus 3.8–4.0 × as long as dactylus, 13.6–14.4 × breadth, with 8–11 thin spines on the posterior and lateral margins. Fifth pereopod propodus 4.0–4.7 × as long as dactylus, 17.6–20.5 × breadth, with 17–20 thin spines on the posterior and lateral margins, dactylus terminating in one claw, with 50–55 spinules on flexor margin. Endopod of male subrectangular, slightly wider proximally, length 0.39–0.46 × exopod length, 2.0–2.2 × proximal breadth, ending broadly rounded; inner margin slightly concave, bearing spine-like setae, outer margin slightly convex, proximally 1/3 bearing nearly equal length short spine-like setae, distally 2/3 bearing nearly equal

length long spine-like setae, and top bearing nearly equal length stout spine-like setae; appendix interna well developed, arising from distal 1/3 of endopod, beyond the end of endopod, distally with cincinulli. Appendix masculina rod-shaped and gradually tapering into a triangular tip, reaching about $0.48\text{--}0.51 \times$ length of endopod, with numerous long spined setae on proximal and distal regions; endopod reaching about $0.76\text{--}0.79 \times$ length of exopod; appendix interna well developed, reaching about $0.58\text{--}0.78 \times$ length of appendix masculina, with cincinulli distally. Uropodal diaeresis with 10–12 movable spinules. Females carry 10–15 eggs, size of undeveloped eggs (without eyespots) $0.83\text{--}0.88 \times 1.18\text{--}1.26$ mm.

Description. *Body* (Figs 3A, 5C–F): Slender, smooth, colorless, translucent, sub-cylindrical, and medium-sized, males up to 25.9 mm tl, females up to 25.2 mm tl.

Rostrum (Figs 3A, 4A, 5C–F): $0.47\text{--}0.77$ of cl, slender, slightly elevated at base, reaching to base of 3rd segment of antennular peduncle to end of scaphocerite; straight, slightly sloping downwards (55.8%, $N = 43$), tip sometimes turned upward (44.2%); armed dorsally with 17–27 teeth, including 6–10 (usually 5–8) on the carapace, with 4–15 (usually 5–8) ventral teeth; lateral carina dividing rostrum into two unequal parts, continuing posteriorly to the orbital margin.

Eyes (Figs 3A, 4A, 5C–F) small, bullet-like, reduced, with a short stalk, lacking facets, cornea pigmentation has great variability in the eye phenotype, with the smaller pigmented cornea (79%, $N = 43$), or totally pigmentless and blind (21%).

Carapace (Figs 3A, 4A): Smooth, swollen; antennal spine acute, fused with inferior orbital angle; pterygostomial angle angular, produced forward; pterygostomial spine absent.

Antennule (Fig. 3B): Reaching slightly short of scaphocerite; stylocerite long, reaching end of the basal segment, basal segment robust, anterolateral angle with broadly produced sharp projection, reaching 0.25 length of 2nd segment; about $0.72\text{--}0.76 \times$ of combined length of 2nd and 3rd segments, 2nd segment as long as $0.76\text{--}0.82 \times$ of basal segment, $1.2\text{--}1.3 \times$ of 3rd segment; all segments with sub-marginal plumose setae.

Antenna (Fig. 3C): Peduncle about $0.44\text{--}0.58 \times$ as long as scaphocerite; scaphocerite $3.1\text{--}3.8 \times$ as long as wide, outer margin straight, asetose, ending in a strong sub-apical spine, inner and anterior margins with long plumose setae.

Mouthparts characteristic of the genus. Mandible with well-developed incisor and molar processes; left incisor process with a single short sharp outer tooth, two long stout inner teeth, 7 curving setae followed by a patch of long setae; molar process stout and with triturative surface (Fig. 3D). Maxillula with broadly rounded lower lacinia, with several rows of marginal and submarginal plumose setae; upper lacinia elongate, medial edge straight, with 25–35 strong spinules and simple setae; palp simple, longer than wide, slightly expanded distally, with 4 simple setae at basal part and 6 at distal part (Fig. 3E). Maxilla with well-developed scaphognathite, tapers posteriorly, with a regular row of long plumose setae and short marginal plumose setae continuing down the proximal triangular process distally, furnished with numerous long plumose setae; upper and middle endite with marginal, simple, denticulate setae, with plumose setae distally; lower endite with long simple marginal setae; palp shorter than the cleft of upper endite, wider than distal setose proximally (Fig. 3F). First maxilliped palp

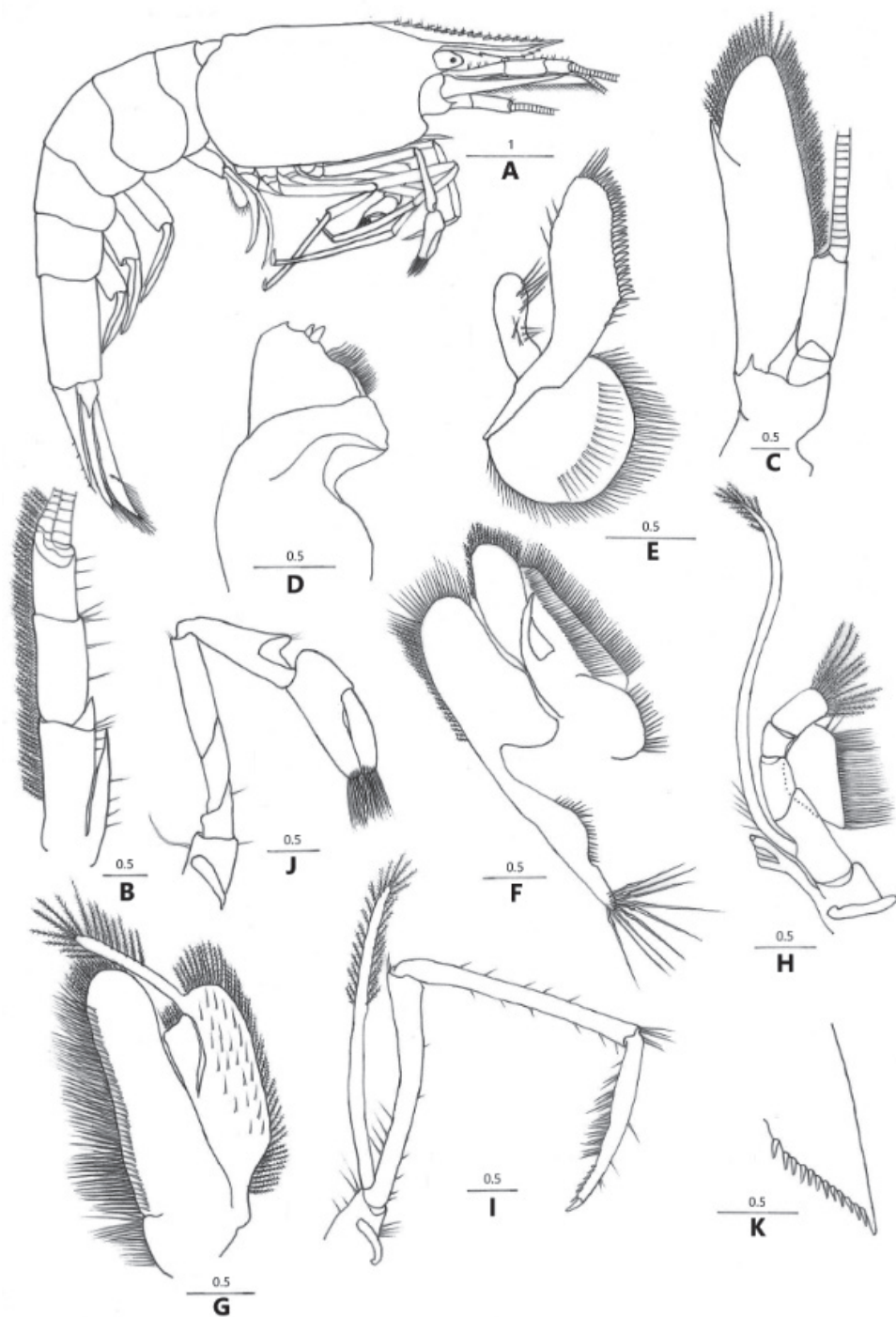


Figure 3. *Caridina incolor* sp. nov. **A** entire animal, lateral view **B** antennule **C** antenna **D** mandible **E** maxillula **F** maxilla **G** first maxilliped **H** second maxilliped **I** third maxilliped **J** first pereopod **K** diaeresis of uropodal exopod **A** holotype **B–K** paratype (FU, 2018-11-27-02).

broad, with terminal plumose setae; caridean lobe broad, with marginal plumose setae; exopodal flagellum well developed, with marginal plumose setae distally; ultimate and penultimate segments of endopod indistinctly divided; medial and distal margins of an ultimate segment with marginal and sub-marginal rows of simple, denticulate and plumose setae; penultimate segments with marginal long plumose setae (Fig. 3G). The second maxilliped with endopodite ultimate and penultimate antennomeres fused, slightly concave, reflected against basal antennomeres, inner margin of ultimate, penultimate, and basal segments with long setae of various types; exopod flagellum long, slender with marginal plumose setae distally. Podobranchium comb-like (Fig. 3H). Third maxilliped with three-segmented endopod, reaching slightly beyond scaphocerite; penultimate segment $0.89\text{--}0.96 \times$ of the basal segment; distal segment $0.75\text{--}0.91 \times$ of the penultimate segment, ending in a large claw-like spine surrounded by simple setae, preceded by about 7–9 spines on the distal third of the posterior margin, with a clump of long and short simple, serrate setae proximally; exopod flagellum well developed, about $0.25\text{--}0.34 \times$ of the penultimate segment of endopod, distal margin with long plumose setae (Fig. 3I).

First pereopod (Fig. 3J): Short, reaches the end of eyes; chela length $2.2\text{--}2.5 \times$ breadth, $1.1\text{--}1.2 \times$ length of the carpus; movable finger length $3.1\text{--}3.4 \times$ breadth, $1.1\text{--}1.4 \times$ length of the palm, setal brushes well developed; carpus excavated distodorsally, length $2.3\text{--}2.7 \times$ breadth, about the same length of merus.

Second pereopod (Fig. 4B): Reaches about the end of 3rd antennular peduncle segment, slenderer and longer than the first pereopod; chela length $2.4\text{--}2.6 \times$ breadth, $0.73\text{--}0.77 \times$ length of the carpus; movable finger length $4.5\text{--}4.8 \times$ breadth, and $1.6\text{--}1.8 \times$ length of the palm, setal brushes well developed; carpus length $5.4\text{--}5.6 \times$ breadth, slightly excavated distally, $1.0\text{--}1.1 \times$ length of merus.

Third pereopod (Fig. 4C, D): Reaches beyond the end of scaphocerite; dactylus length $4.4\text{--}4.7 \times$ breadth, ending in prominent claw-like spine surrounded by simple setae, behind which bears 6–7 spines; propodus length $3.8\text{--}4.0 \times$ of the dactylus, bearing 8–11 spinules on posterior margin, $13.6\text{--}14.4 \times$ breadth; carpus length $0.65\text{--}0.72 \times$ of the propodus; merus length $1.9\text{--}2.1 \times$ of the carpus, with about 3 strong spines on the posterior margin.

Fourth pereopod (Fig. 4E, F): Reaches end of 3rd segment of antennular peduncle; dactylus length $4.2\text{--}5.0 \times$ breadth, ending in prominent claw-like spine surrounded by simple setae, behind which bears 7–8 spines; propodus length $3.8\text{--}4.6 \times$ of the dactylus, bearing 12–15 spinules on posterior margin, $14.6\text{--}17.4 \times$ breadth; carpus length $0.58\text{--}0.73 \times$ of the propodus; merus length $1.9 \times$ of the carpus, with about 3 strong spines on the posterior margin.

Fifth pereopod (Fig. 4G, H): Reaches end of 3rd segment of antennular peduncle; dactylus length $4.2\text{--}5.6 \times$ breadth, ending in prominent claw-like spine surrounded by simple setae, behind which bears comb-like row 50–55 spines; propodus length $4.0\text{--}4.7 \times$ of the dactylus, bearing 17–20 spinules on posterior margin, $17.6\text{--}20.5 \times$ breadth; carpus length $0.55\text{--}0.60 \times$ of the propodus; merus length $1.5\text{--}1.6 \times$ of the carpus, with about 3 strong spines on the posterior margin.

First four pereopods with epipod. Branchial formula typical for the genus.

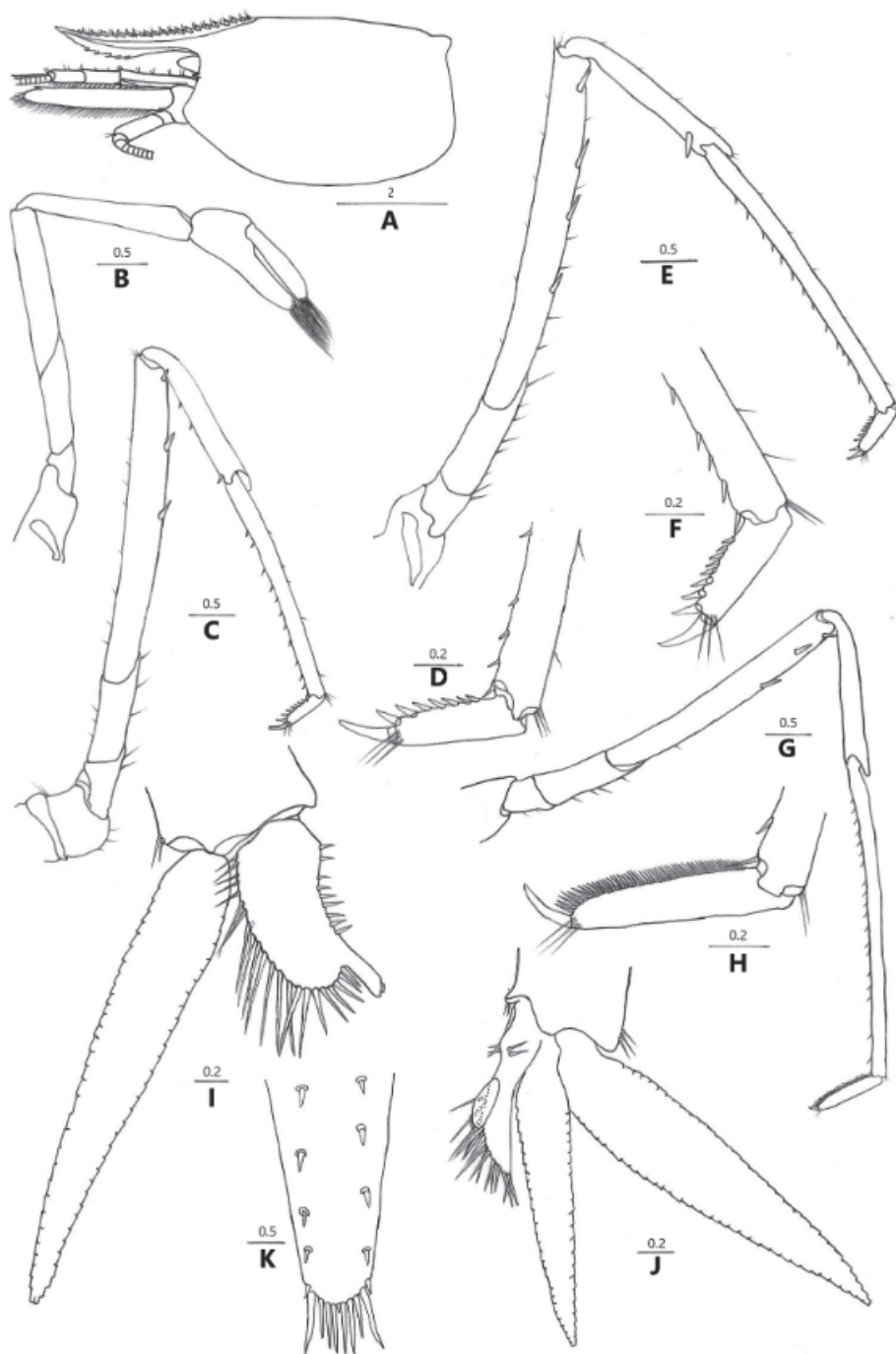


Figure 4. *Caridina incolor* sp. nov. **A** carapace and cephalic appendages, lateral view **B** second pereopod **C** third pereopod **D** dactylus of third pereopod **E** fourth pereopod **F** dactylus of fourth pereopod **G** fifth pereopod **H** dactylus of fifth pereopod **I** first male pleopod **J** second male pleopod **K** distal margin of telson **A–K** paratype (FU, 2018-11-27-02).

First pleopod (Fig. 4I): Endopod of male subrectangular, slightly wider proximally, length $0.39\text{--}0.46 \times$ exopod length, $2.0\text{--}2.2 \times$ proximal breadth, ending broadly rounded; inner margin slightly concave, bearing spine-like setae, outer margin slightly convex, proximally $1/3$ bearing nearly equal length short spine-like setae, distally $2/3$ bearing nearly equal length long spine-like setae, and top bearing nearly equal length stout spine-like setae; appendix interna well developed, arising from distal $1/3$ of endopod, reaching beyond the end of endopod, with cincinulli distally.

Second pleopod (Fig. 4J): Appendix masculina rod-shaped and gradually tapering into a triangular tip, reaching about $0.48\text{--}0.51 \times$ length of endopod, with numerous long spine setae on proximal and distal margins; endopod reaching about $0.76\text{--}0.79 \times$ length of exopod; appendix interna well developed, reaching about $0.58\text{--}0.78 \times$ length of appendix masculina, with cincinulli distally.

Telson (Fig. 4K): $0.40\text{--}0.55 \times$ of cl, shorter than sixth abdominal segment, $0.67\text{--}0.96 \times$ length of the sixth abdominal segment, posteriorly tapering, with median projection, dorsal surface with 5 pairs of stout movable spine setae including the pair at posterolateral angles; posterior margin with 4 pairs of intermedial strong spiniform setae, sublateral pair shorter than lateral and inner pairs. Exopodite of the uropod bears a series of 10–12 movable spinules along the diaresis, the last one shorter than the lateral process (Fig. 3K).

Females carry 10–15 eggs, size of undeveloped eggs (without eyespots) $0.83\text{--}0.88 \times 1.18\text{--}1.26$ mm.

Coloration (Fig. 5C–F): Body and appendages are colorless and translucent; vestigial pigment present at the center of the cornea or without pigment; internal organs (gonads and hepatopancreas) are yellow; eggs in females brown.

Etymology. *Caridina incolor* sp. nov. is named after the colorless and transparent body color.

Remarks. *Caridina incolor* sp. nov. might be more closely related to the epigeal species than to its supposed cave congeners. It is morphologically similar to *C. guiyangensis* Liang, 2002, from Guiyang, Guizhou Province in the long rostrum and indentation, the shape of endopod of the male first pleopod and appendix masculina. Although no molecular comparison with *C. guiyangensis* could be accomplished, *C. incolor* sp. nov. can easily be distinguished from the latter by the reduced eyes, colorless body and appendages (versus developed eyes and pigmentation in *C. guiyangensis*); the long stylocerite, reaching to the end of the antennule basal segment (versus reaching $0.85 \times$ of basal segment in *C. guiyangensis*); the long penultimate segment of the 3rd maxilliped, which is distinctly longer than the basal segment and distal segment (versus penultimate segment as long as basal segment and distinctly shorter than distal segment in *C. guiyangensis*); absence of a projection on the base of the inner margin of male first pleopod endopod (vs. with projection in *C. guiyangensis*); and relatively large eggs, size of undeveloped eggs $0.83\text{--}0.88 \times 1.18\text{--}1.26$ mm (versus $0.63\text{--}0.75 \times 1.05\text{--}1.13$ in *C. guiyangensis*). In comparison to other cave species within *Caridina*, *C. sinanensis* Xu, Li, Zhang & Guo, 2020, is most similar in sharing the long 6th abdominal segment, and the variably pigmented cornea. However, the new species differs from the latter by possessing a relatively long and slender rostrum which reaches beyond the end of

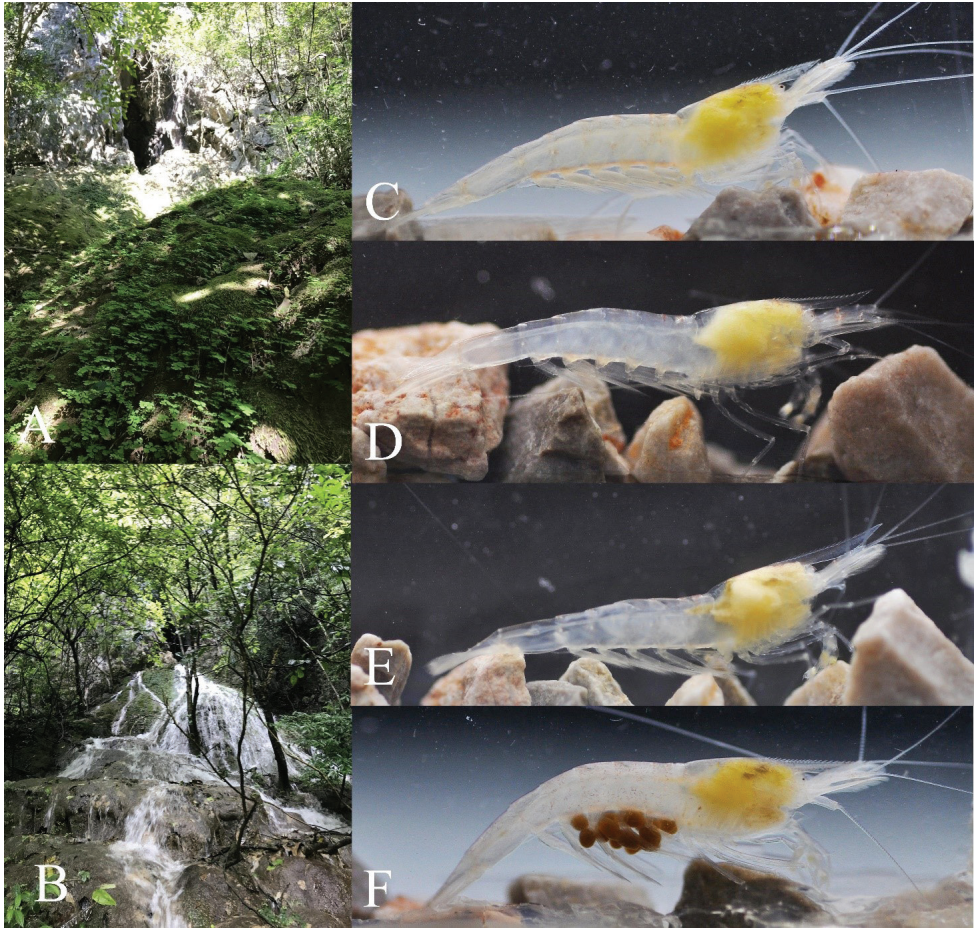


Figure 5. Habitats, variable features, and live coloration of *Caridina incolor* sp. nov. **A** surrounding environment of Yaoshui Cave during the dry season **B** same site during the rainy season **C–E** variable rostrum and eye size in life **F** ovigerous female in life.

the 3rd antennular peduncle segment (versus stouter, reaching to the end of the 2nd segment in *C. sinanensis*); the long stylocerite, reaching to the end of the basal segment of the antennule (versus reaching 0.75–0.88 × of basal segment in *C. sinanensis*); and completely different shape of the endopod of the 1st pleopod and appendix masculina of the 2nd pleopod in males (Fig. 4I, J, versus Fig. 4H, J, K in Xu et al. 2020).). There are another six atyids, *Caridina acuta*, *C. caverna*, *C. demenica*, *C. jiangkou*, *C. sinanensis*, and *Neocaridina brevidactyla*, that have been reported from nearby caves from Guizhou Province. *Caridina incolor* sp. nov. differs from *N. brevidactyla* in the completely different shape of the endopod of 1st pleopod and appendix masculina of the 2nd pleopod in males; lack of a hook-like projection on the posterior part of coxa of the 2nd pereopod and a pterygostomial spine. *C. incolor* sp. nov. differs from all other cave species in having a long rostrum and stylocerite (with the longest rostrum and stylocerite amongst all

known seven cave atyids); slender sixth abdominal segment which is distinctly longer than the telson (only *C. sinanensis* has a slender sixth abdominal segment that is slightly longer than the telson, other cave species have a stout sixth abdominal segment which is distinctly shorter than the telson); and an appendix masculina that is unique in shape and gradually tapers into a triangular tip. These taxa can be separated from each other by morphological differences as discussed in Xu et al. (2020).

Molecular phylogenetic results. We analyzed 47 COI sequences in total. Five specimens of *Caridina incolor* sp. nov. were used in the molecular phylogenetic analysis shown in Figure 2. Specimens assigned to *Caridina incolor* sp. nov. formed a clade distinct from other species. *Caridina incolor* sp. nov. is well distinguished from the other 16 atyids with a sequence divergence of 13.7% – 24.5% (COI). The sequence divergence between *Caridina incolor* sp. nov. and *C. sinanensis* is the closest. The topology of the Bayesian (BI) trees and the ML tree are basically similar. Phylogenetic trees revealed the relationship between *Caridina incolor* sp. nov. and 16 other species of atyids, with the posterior probability and bootstrap values from the BI and ML analysis shown in Figures 2. According to Hebert, Ratnasingham and de Waard 2003, the genetic distances supports *Caridina incolor* sp. nov. as a new species.

Conservation. Threats to cave shrimp are of concern due to the uniqueness of the habitat and increasing anthropogenic activities. Based on the information available, the Yaoshui Cave and its faunas are potentially at risk from excessive levels of external disturbance. Daqikong scenic area is famous for its marvelous primeval forests, steep canyons, spectacular caves, and underground rivers. Over the years, tourism to the region has improved the welfare of local residents and has become a major industry in this area. Moreover, new recreational trails and amusement facilities have been built in the scenic area. It is almost inevitable that these new projects will put great pressure and impact on caves and their faunas. In addition, land development and agriculture lead to habitat degradation and groundwater pollution, which also has a negative impact on the survival of this species.

So far, no freshwater shrimps are protected by the national legislation. The Announcement of the Ministry of Agriculture and Rural Areas of China has failed to categorize the strictly endemic cave species as Endangered (CITES Appendix aquatic wild species of China, no. 69, 2018). *Caridina incolor* sp. nov. is new to science and the conservation status remains unassessed. Using the criteria provided by the IUCN (2019) Red List Categories and Criteria (version 14) (IUCN 2019), the new species should be considered as a critically endangered (CR) species on account for its exceptional rarity, restricted distribution, and exposure to serious anthropogenic impacts.

The Yaoshui Cave, which is home to two unique and range-restricted species (atyid shrimp, *Caridina incolor* sp. nov., and loach fish, *Oreonectes daqikongensis*) is biologically significant without question. These strictly-adapted cave species must be considered as important units for conservation, and devising an effective conservation strategy is clearly an urgent priority. It has also become obvious that there is a need to collect more baseline data, such as the exact population size, structure, natality, and mortality rates. Regular monitoring may be necessary to ensure populations are sustained in

the face of further anthropogenic disturbances. Equally important, a captive breeding program of these cave species should be developed. In addition, we propose that non-invasive and non-destructive projects, such as eco-tourism, should be promoted. Last but not least, we also appeal to local farmers to lower the usage of agricultural pesticides, herbicides, and fertilizers to help reduce the amount of hazardous chemicals that are leached into the groundwater.

Acknowledgements

This study was supported by the Special Fund for Central Public Welfare Research Institutes (grant no. PM-zx097-201904-134), the Running Cost for Key Laboratory of Utilization and Breeding of Aquatic Resources in Tropical and Subtropical Areas, Ministry of Agriculture and Rural Affairs (grant no. 9020190008) and the Investigation on Crustaceans in Priority Area of Mangrove Diversity Protection in Guangxi Zhuang Autonomous Region (grant no. kh19051). We thank Wenjian Chen and Xiaozhuang Zheng for their assistance in collecting samples. We also appreciate Dr. Chao Huang (Independent researcher) and Erdong Xia (Stevens Institute of Technology/Chinese Academy of Forestry) for improving the manuscript. Thanks are also due to subject editor Célio Magalhães and two reviewers Werner Klotz and Valentin de Mazancourt (Muséum national d'Histoire naturelle) for providing their valuable suggestions, which greatly improved the manuscript.

References

- Barr TC (1968) Cave ecology and the evolution of troglobites. *Evolutionary Biology* 2: 35–102. https://doi.org/10.1007/978-1-4684-8094-8_2
- Botosaneanu L, Gordon I (1985) On a Cave-Dwelling Mysid from Cuba, of the Genus *Speleomysis* Caroli (Mysidacea, Lepidomysidae). *Crustaceana* 49(2): 139–149. <https://doi.org/10.1163/156854085X00378>
- Cai YX (1995) A new troglobitic shrimp from China. *Acta Zootaxon Sinica* 20(2): 157–160. [In Chinese with English abstract]
- Cai YX, Li SQ (1997) *Caridina demenica*, a new species of troglobitic shrimp (Crustacea: Decapoda: Atyidae) from Guizhou, China. *Raffles Bulletin of Zoology* 45(2): 315–318.
- Cai YX, Liang XQ (1999) Descriptions of three new species of freshwater shrimps (Crustacea: Decapoda: Atyidae) from Yunnan, Southern China. *Raffles Bulletin of Zoology* 47(1): 73–80.
- Cai YX, Ng NK (1999) A revision of the *Caridina serrata* species group, with descriptions of five new species (Crustacea: Decapoda: Caridea: Atyidae). *Journal of Natural History* 33: 1603–1638. <https://doi.org/10.1080/002229399299789>
- Cai YX, Ng PKL (2018) Freshwater shrimps from karst caves of southern China, with descriptions of seven new species and the identity of *Typhlocaridina linyunensis* Li and Luo, 2001 (Crustacea: Decapoda: Caridea). *Zoological Studies* 57(27): 1–33.

- Cai YX, Ng NK, PKL (2009) The freshwater shrimps of the genera *Caridina* and *Parisia* from karst caves of Sulawesi Selatan, Indonesia, with descriptions of three new species (Crustacea: Decapoda: Caridea: Atyidae), Journal of Natural History 43(17–18): 1093–1114. <https://doi.org/10.1080/00222930902767482>
- Chen QH, Chen WJ, Zheng XZ, Guo ZL (2020) Two freshwater shrimp species of the genus *Caridina* (Decapoda, Caridea, Atyidae) from Dawanshan Island, Guangdong, China, with the description of a new species. ZooKeys 923: 15–32. <https://doi.org/10.3897/zookeys.923.48593>
- Christiansen K (2005) Morphological adaptations. In: Culver DC, White WB (Eds) Encyclopedia of caves. Elsevier, Amsterdam, 386–397.
- Culver DC, Pipan T (2019) The biology of caves and other subterranean habitats (2nd edn.). Oxford University Press, New York. <https://doi.org/10.1093/oso/9780198820765.001.0001>
- Deng H, Xiao N, Hou X, Zhou J (2016) A new species of the genus *Oreonectes* (Cypriniformes: Nemacheilidae) from Guizhou, China. Zootaxa (4132): 143–150. <https://doi.org/10.11646/zootaxa.4132.1.13>
- Folmer O, Black M, Hoeh W, Lutz R, Vrijenhoek R (1994) DNA primers for amplification of mitochondrial cytochrome c oxidase subunit i from diverse metazoan invertebrates. Molecular Marine Biology and Biotechnology 3(5): 294–299.
- Guo ZL, Choy SC, Gui QM (1996) *Caridina semiblepsia*, a new species of troglonic shrimp (Crustacea: Decapoda: Atyidae) from Hunan Province, China. Raffles Bulletin of Zoology 44(1): 65–75.
- Guo ZL, Jiang H, Zhang MC (1992) A new species of *Caridina* from Hunan, China (Decapoda: Atyidae). Sichuan Journal of Zoology 11(2): 4–6. [In Chinese with English abstract]
- Hart CW, Manning RB (1981) The cavernicolous caridean shrimps of Bermuda (Alpheidae, Hippolytidae, and Atyidae). Journal of Crustacean Biology 1(3): 441–456. <https://doi.org/10.2307/1547975>
- He W, Li P (2016) Characteristics and exploitation of karst cave resources in Guizhou. Journal of Guizhou Normal University (Natural Science Edition) 34(3): 1–6. [In Chinese with English abstract]
- Hebert PDN, Ratnasingham S, de Waard JR (2003) Barcoding animal life: cytochrome c oxidase subunit 1 divergences among closely related species. Proceedings of the Royal Society B—Biological Sciences 270 (suppl.1): s96–s99. <https://doi.org/10.1098/rsbl.2003.0025>
- Hobbs Jr HH, Hobbs III HH, Daniel MA (1977) A review of the troglobitic decapod crustaceans of the Americas. Smithsonian Contributions to Zoology 244: 1–183. <https://doi.org/10.5479/si.00810282.244>
- Holthuis LB (1974) Subterranea Crustacea Decapoda Macrura collected by Mr. Botosaneanu during the 1973 Cuban–Roumanian Biospeological Expedition to Cuba. International Journal of Speleology 6: 231–242. <https://doi.org/10.5038/1827-806X.6.3.4>
- Holthuis LB (1977) Cave shrimps (Crustacea, Decapoda, Natantia) from Mexico. In: Subterranean fauna of Mexico. Part III, Quaderni Accademia Nazionale dei Lincei 171: 173–195.
- Holthuis LB (1986) Decapoda. In: Botosaneanu L (Ed.) Stygofauna Mundi. A faunistic, distributional, and ecological synthesis of the world fauna inhabiting subterranean waters (including the marine interstitial). E.J. Brill/Dr. W. Backhuys, Leiden, 589–615.

- IUCN (2019) Guidelines for Using the IUCN Red List Categories and Criteria. Version 14. Prepared by the Standards and Petitions Committee. <http://www.iucnredlist.org/documents/RedListGuidelines.pdf>
- Kalyaanamoorthy S, Minh BQ, Wong TKF, Haeseler AV, Jermini LS (2017) ModelFinder: fast model selection for accurate phylogenetic estimates. *Nature Methods* 14(6): 587–591. <https://doi.org/10.1038/nmeth.4285>
- Katoh K, Standley DM (2013) MAFFT multiple sequence alignment software Version 7: improvements in performance and usability. *Molecular Biology and Evolution* 30(4): 772–780. <https://doi.org/10.1093/molbev/mst010>
- Kumar S, Stecher G, Tamura K (2016) MEGA7: molecular evolutionary genetics analysis version 7.0 for bigger datasets. *Molecular Biology and Evolution* 33(7): 1870–1874. <https://doi.org/10.1093/molbev/msw054>
- Li J, Li S (2010) Description of *Caridina alba*, a new species of blind atyid shrimp from Tenglongdong Cave, Hubei Province, China (Decapoda, Atyidae). *Crustaceana* 83: 17–27. <https://doi.org/10.1163/001121609X12530988607399>
- Li Ran, Chen (2006) Zhanjiang. *Paracobitis maolanensis*. *Journal of Ocean University* 26(4): 1–1. [A cave in Maolan Reserve, Guizhou Province] [In Chinese with English abstract]
- Li XZ, Liu RY, Liang XQ, Chen GX (2007) Fauna Sinica. Invertebrata (Vol. 44). Crustacea Decapoda Palaemonoidea. Science Press Beijing, 381 pp. [in Chinese with English abstract]
- Liang XQ, Yan SL (1981) A new genus and two new species of freshwater prawns (Crustacea Decapoda) from Guangxi, China. *Acta Zootaxonomica Sinica* 6(1): 31–35. [In Chinese with English abstract]
- Liang XQ, Zhou J (1993) Study on new atyid shrimps (Decapoda, Caridea) from Guangxi, China. *Acta Hydrobiologica Sinica* 17(3): 231–239. [In Chinese with English abstract]
- Liang XQ, Chen HM, Li WX (2005) Three new species of atyid shrimps (Decapoda, Caridea) from caves of Guizhou, China. *Acta Zootaxonomica Sinica* 30(3): 529–534. [In Chinese with English abstract]
- Liang XQ, Guo ZL, Tang KE (1999) On new genus and species of atyid shrimps (Decapoda, Caridea) from Hunan, China. *Journal of Fisheries of China* 23(S1): 69–73. [In Chinese with English abstract]
- Mammola S, Cardoso P, Culver DC, Deharveng L, Ferreira RL, Fišer C, Galassi DMP, Griebler C, Halse S, Humphreys WF, Isaia M, Malard F, Martinez A, Moldovan OT, Niemiller ML, Pavlek M, Reboleira ASPS, Souza-Silva M, Teeling EC, Wynne JJ, Zagamajster M (2019) Scientists' Warning on the Conservation of Subterranean Ecosystems. *BioScience* 69(8): 641–650. <https://doi.org/10.1093/biosci/biz064>
- Mejía-Ortíz LM, Hartnoll RG (2006) A new use for useless eyes in cave crustaceans. *Crustaceans* 79(5): 593–600. <https://doi.org/10.1163/156854006777584313>
- Mejía-Ortíz LM, Hartnoll RG, López-Mejía M (2006) Progressive troglomorphy of ambulatory and sensory appendages in three Mexican cave decapods. *Journal of Natural History* 40(5–6): 255–264. <https://doi.org/10.1080/00222930600628382>
- Nguyen LT, Schmidt HA, von Haeseler A, Minh BQ (2015) IQ-TREE: a fast and effective stochastic algorithm for estimating maximum-likelihood phylogenies. *Molecular Biology and Evolution* 32(1): 268–274. <https://doi.org/10.1093/molbev/msu300>

- Pan YT, Hou Z, Li, SQ (2010) Description of a new *Macrobrachium* species (Crustacea: Decapoda: Caridea: Palaemonidae) from a cave in Guangxi, with a synopsis of the stygobiotic Decapoda in China. *Journal of Cave and Karst Studies* 72(2): 86–93. <https://doi.org/10.4311/jcks2009lsc0087>
- Peck L, Morris D, Clarke A (1986) The caeca of punctate brachiopods: a respiring tissue not a respiratory organ. *Lethaia* 19(3): 232–232. <https://doi.org/10.1111/j.1502-3931.1986.tb00736.x>
- Ran JC, Yang WC (2015) A review of progress in China troglafauna research. *Journal of Resources and Ecology* 6(4): 237–246. <https://doi.org/10.5814/j.issn.1674-764x.2015.04.007>
- Rétaux S, Casane D (2013) Evolution of eye development in the darkness of caves: Adaptation, drift, or both? *EvoDevo* 4: 1–12. <https://doi.org/10.1186/2041-9139-4-26>
- Ronquist F, Teslenko M, van der Mark P, Ayres DL, Darling A, Höhna S, Larget B, Liu L, Suchard A, Huelsenbeck JP (2012) MrBayes 3.2: efficient Bayesian phylogenetic inference and model choice across a large model space. *Systematic Biology* 61(3): 539–542. <https://doi.org/10.1093/sysbio/sys029>
- von Rintelen K, Cai Y (2009) Radiation of endemic species flocks in ancient lakes: systematic revision of the freshwater shrimp *Caridina* H. Milne Edwards, 1837 (Crustacea: Decapoda: Atyidae) from the ancient lakes of Sula wesi, Indonesia, with the description of eight new species. *The Raffles Bulletin of Zoology* 57(2): 343–452.
- von Rintelen K, von Rintelen T, von Meixner M, Lüter C, Cai Y, Glaubrecht M (2007) Freshwater shrimp-sponge association from an ancient lake. *Biology Letters* 3: 262–264. <https://doi.org/10.1098/rsbl.2006.0613>
- Xu DJ, Li DX, Zheng XZ, Guo ZL (2020) *Caridina sinanensis*, a new species of stygobiotic atyid shrimp (Decapoda, Caridea, Atyidae) from a karst cave in the Guizhou Province, southwestern China. *ZooKeys* 1008: 17–35. <https://doi.org/10.3897/zookeys.1008.54190>
- Zhang D, Gao F, Jakovlić I, Zou H, Zhang J, Li WX, Wang GT (2020) PhyloSuite: An integrated and scalable desktop platform for streamlined molecular sequence data management and evolutionary phylogenetics studies. *Molecular Ecology Resources* 20(1): 348–355. <https://doi.org/10.1111/1755-0998.13096>
- Zhang YH, Zhu DH (2012) Large Karst Caves Distribution and Development in China. *Journal of Guilin University of Technology* 32(1): 20–28. <https://doi.org/10.3969/j.issn.1674-9057.2012.01.003> [In Chinese with English abstract]
- Zheng XZ, Chen WJ, Guo ZL (2019) The genus *Macrobrachium* (Crustacea, Caridea, Palaemonidae) with the description of a new species from the Zaomu Mountain Forest Park, Guangdong Province, China. *ZooKeys* 866: 65–83. <https://doi.org/10.3897/zookeys.866.32708>
- Zhou ZF, Zhang SY, Xiong KN, Li B, Tian ZH, Chen Q, Yan LH, Xiao SZ (2017) The spatial distribution and factors affecting karst cave development in Guizhou Province. *Journal of Geographical Sciences* 27(8): 1011–1024. <https://doi.org/10.1007/s11442-017-1418-0>
- Zhu XP, Chen QH, Zheng XZ, Chen WJ, Guo ZL (2020) *Macrobrachium tenuipes*, a new stygophile freshwater prawn specie (Crustacea: Caridea: Palaemonidae) from a karst cave of Guangxi, southwestern China. *PeerJ* 4759(4): 511–529. <https://doi.org/10.11646/zootaxa.4759.4.3>

First record of the genus *Arria* (Mantodea, Haaniidae, Arriini) from Thailand, with the description of a new species of moss-dwelling praying mantis

Thornthan Unnahachote¹, Evgeny Shcherbakov², Nantasak Pinkaew¹

1 Department of Entomology, Faculty of Agriculture at Kamphaeng Saen, Kasetsart University, Nakhon Pathom, 73140 Thailand **2** Department of Entomology, Faculty of Biology, Lomonosov Moscow State University, Leninskie Gory st. 1 bldg 12, Moscow 119991, Russia

Corresponding author: Nantasak Pinkaew (agrnsnp@ku.ac.th)

Academic editor: Fred Legendre | Received 22 December 2020 | Accepted 19 March 2021 | Published 5 April 2021

<http://zoobank.org/A23086C9-1000-4E80-AC95-FF1990D6042A>

Citation: Unnahachote T, Shcherbakov E, Pinkaew N (2021) First record of the genus *Arria* (Mantodea, Haaniidae, Arriini) from Thailand, with the description of a new species of moss-dwelling praying mantis. ZooKeys 1028: 49–60. <https://doi.org/10.3897/zookeys.1028.62347>

Abstract

Arria muscoamicta Unnahachote & Shcherbakov, **sp. nov.** is described based on a male from central Thailand. This is the first record of *Arria* Stål, 1877 from the country. The new species is closely allied to *A. leigongshanensis* (Ge & Shen, 2008) from China, differing by the absence of prozonal tubercles, the elongated pronotum, nine tibial anteroventral spines, and the truncated hindwings. The new species is a moss-camouflaging mantis living at high altitude. The taxonomic problems of the genus are briefly discussed.

Keywords

Camouflage, predatory insect, Southeast Asia, taxonomy

Introduction

There are many genera of praying mantises from both the Old and the New World, and some members are camouflaged as moss, such as the following genera: *Astape* Stål, 1877, *Haania* Saussure, 1871, *Majangella* Giglio-Tos, 1915, and *Pseudopogonogaster* Beier, 1942. These, as well as others, are colloquially referred to as “moss mantises”. Almost all of them have evolved special morphology, such as spines, lobes,

and tubercles on their bodies, which aid in their camouflage on moss beds (Beier 1952; Rivera et al. 2011; Svenson and Vollmer 2014). Among the least studied of the genera that include moss-camouflaging species is the genus *Arria*, which was described by Stål (1877) with *Arria cinctipes* Stål, 1877 as its type species (type locality “India orientalis”). Species of *Arria* exhibit a strong sexual dimorphism: the male has well-developed wings reaching beyond the tip of the abdomen, while the female is completely apterous. In addition, they live at high elevations, and the ootheca has a small number of eggs, making it difficult to obtain specimens from field surveys (Ge and Chen 2008; Zhu et al. 2012). After the most recent taxonomic changes (Schwarz and Roy 2018; Wang et al. 2021), there are currently eight species belonging to the genus: *Arria cinctipes* and *Arria meghalayensis* (Mukherjee, 1995) from India: “India orientalis” and Meghalaya, respectively; and *Arria oreophilus* (Tinkham, 1937), *Arria pallida* (Zhang, 1987), *Arria brevifrons* (Wang & Bi, 1991), *Arria sticta* (Zhou & Shen, 1992), *Arria leigongshanensis* (Ge & Chen, 2008), and *Arria pura* Wang & Chen, 2021 from China: Sichuan, Yunnan, Zhejiang, Hainan, and Guizhou, respectively. However, only one species, *A. leigongshanensis*, was known as being a moss-camouflaging species. Here we describe a new species closely related to *A. leigongshanensis* from high-elevation, mossy forests in central Thailand, Nakhon Nayok province, representing the first report of the genus from the country.

Materials and methods

The male holotype was collected at a light trap and preserved in a freezer before being pinned on a mounting block and dried. Five nymphs were found on separate occasions by visual inspection in the moss close to where the holotype was collected. The holotype is deposited at the Thailand Natural History Museum (THNHM). The nymphs could not be preserved.

For genitalia preparations, the tip of abdomen was separated from the specimen and macerated in 10% potassium hydroxide (KOH) solution, then rinsed with demineralised water and placed in glycerine for dissection. Afterwards it was placed in a genital vial with glycerine for long-term preservation and pinned together with the holotype.

Observation of the external structures and male genitalia were made with an Optika microscope (Optika Microscopes, Italy). Live photographs of the adult were taken by W. Pathomwattananuruk with a Nikon AF-S Micro Nikkor 60 mm lens attached to a Nikon D7000 camera. Live photograph of the nymph was taken by W. Khaikaew with an AF-S Micro 60 mm f/2.8G lens attached to a Nikon D610. Male genitalia photographs were taken with a Leica S8 APO stereomicroscope equipped with a Leica MC170 HD camera module. The classification system is according to Schwarz and Roy (2019). The morphological nomenclature and standards of measurement follow Brannoch et al. (2017), Schwarz and Roy (2019), and Vermeersch (2018).

Abbreviations

AL	Ala length	PCL	Procoxa length
AvS	Anteroventral spine	PFL	Profemur length
CfW	Costal field width of tegmen	PL	Pronotum length
DS	Discoidal spine	PnW	Pronotum narrow width
F	Femur	PtL	Protarsus length
HW	Head width	PTL	Protibia length
MsFL	Mesofemur length	PvS	Posteroventral spine
MstL	Mesotarsus length	PW	Pronotum width
MsTL	Mesotibia length	PzL	Prozone length
MtFL	Metafemur length	T	Tibia
MttL	Metatarsus length	TgL	Tegmen length
MtTL	Metatibia length	TL	Total length
MzL	Metazone length		

Depositories

GUGC	Institute of Entomology Guizhou University, Guiyang, China;
SMNK	Staatliches Museum für Naturkunde, Karlsruhe, Germany;
THNHM	Thailand Natural History Museum, Pathum Thani, Thailand.

Systematic accounts

Order Mantodea Burmeister, 1838

Family Haaniidae Giglio-Tos, 1915

Subfamily Haaniinae Giglio-Tos, 1915

Tribe Arriini Giglio-Tos, 1919

Genus *Arria* Stål, 1877

***Arria muscoamicta* Unnahachote & Shcherbakov, sp. nov.**

<http://zoobank.org/212326E3-D5A6-445A-AC4F-9A2722B9B48C>

Figures 1–4

Type material. *Holotype*. THAILAND – Nakhon Nayok Province • 1 ♂; Mueang district, Hin Tung subdistrict; 14°21'56"N, 101°24'1"E; 01.IX.2018; alt. 1,240 m; W. Pathomwattananuruk leg.; THNHM-I-23353.

Comparative material. *Arria* sp. LAOS – Bokeo • 1 ♂; Van Pak Len, an Brücke Goldenes Dreieck; 20°12'36"N, 100°3'36"E; 01.IX.2018, IV.1979; H. Lehmannsen leg. (SMNK).

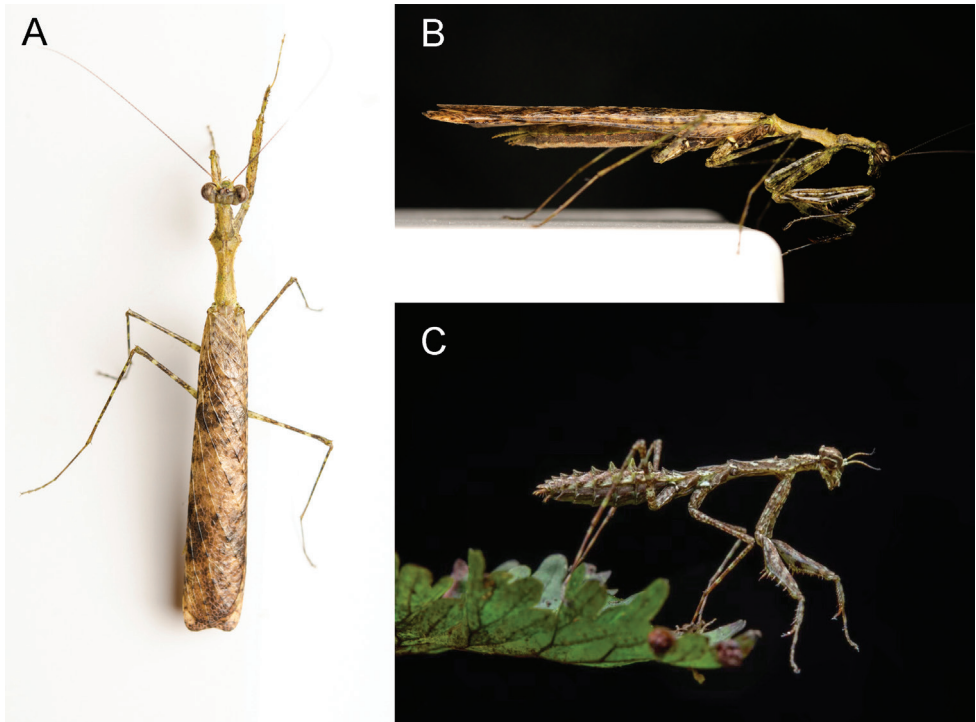


Figure 1. *Arria muscoamicta* sp. nov. in life aspect **A** adult male (the holotype), dorsal view **B** adult male (the holotype), lateral view **C** male nymph. **A, B** W. Pathomwattananuruk, published with permission **C** W. Khaikaew, published with permission.

Comparative photographic material. *Arria leigongshanensis* (Ge & Chen, 2008). Holotype; CHINA – Guizhou • 1 ♂; Leishan, Leigongshan; 13.IX.2005; Song Qiong-Zhang leg. (GUGC).

Differential diagnosis. *A. muscoamicta* sp. nov. is similar to the type species of *Arria*, *A. cinctipes*, in foreleg armament and shape of the prothorax and wings; it fits the current concept of the genus *Arria* (but see Discussion).

Arria muscoamicta sp. nov. can be distinguished from the most similar species, *A. leigongshanensis*, by the following characters: 1) pronotum distinctly longer; $MzL/PzL = 1.97$ [vs $MzL/PzL = 1.24$], 2) prozone without distinct pair of conical spines posteriorly [vs with distinct pair of conical spines posteriorly, anterior of supracoxal sulcus], 3) foretibia have nine anteroventral spines [vs 11–13 anteroventral spines], 4) apical lobe of hindwing almost truncated [vs more or less parabolic].



Arria muscoamicta sp. nov. can also be easily distinguished from *A. cinctipes* by the following characters: 1) six tibial posteroventral spines [vs seven tibial posteroventral spines], 2) lack of a pair of small conical tubercles in prozone posteriorly [presence of a pair of small conical tubercles in prozone posteriorly]; from *A. meghalayensis* by six tibial posteroventral spines [vs seven tibial posteroventral spines]; from *A. oreophilus* by following characters: 1) present of conical tubercles on dorsal surface of pronotum [vs

lack of conical tubercles, relatively smooth in male], 2) forewing not narrows distally [vs forewing narrows distally]; from *A. sticta* and *A. pallida* by the apex of hindwing more or less truncate [vs pointed apex].

Etymology. The name of the species means “clothed by moss” in Latin and refers to the moss-like colouration and morphology of the adults and especially the nymphs.

Description. Adult male. Head (Fig. 3A). Wider than long, compound eyes strongly protruded antero-laterally, rounded. Ocellar tubercle elevated. Ocelli large. Lateral lobes of vertex elevated higher than median lobe. Antenna filiform with fine setae, longer than pronotum length, almost entirely dark except pedicel and proximal segments, which are pale green (discolouration in dried specimen). Lower frons (frontal shield) transverse, surface smooth, anterior margin and posterior margin relatively arched. Postfrontal sulcus noticeably elevated. Juxtaocular bulges distinctly protruded, higher than vertical dorsal line. Clypeus with short medial ridge and labrum entirely smooth.

Pronotum (Fig. 2C, D). More or less slender, longer than forecoxa length, ratio of MzL/PzL = 1.97. Supracoxal dilation very prominent. Lateral margin with denticles strongly present at supracoxal dilation and the prozone, less prominent at metazone, with setae along the margin. Dorsal line of prozone concave in the middle. Dorsal surface more or less tuberculate, with two pairs of strong conical tubercles on metazone, anterior pair a little bit larger than posterior pair, and with a small tubercle laterad of each conical tubercle, while only small tubercles present in the prozone. Pair of small depressions present at anterior half of metazone posteriorly of supracoxal sulcus. Cervicalia complete. Anterior and posterior ventral cervical sclerites similar in size and shape, non-interrupted. Intercervical sclerites connected to those on opposite side, transverse, margin elevated, distinctly concave at the middle, anterior margin more or less angulated. Lateral cervical sclerites large, longer than wide, strongly concave along the side which close to ventral cervical sclerites.

Prothoracic leg (Figs 2B, 3B). Coxa shorter than femur, internal surface somewhat smooth. Dorsal margin with a few short spines, with larger spines present in the proximal half, while very small or nearly absent at the middle and in the distal half. Ventral margin with small irregular denticles. Coxal lobes divergent, dorsal lobe a bit longer than ventral one. Femur with dorsal margin slightly S-shaped. Femoral brush ellipse-shaped. Tibial spine groove present near the middle of femur's length. Anterior genicular lobe with a spine; posterior genicular lobe with a spine (absent on right side). Anterior side with distinctly two infusate patches presents at middle of femur length and in the femoral brush area, respectively. Eleven or 12 AvS arranged as  (11 small vertical bars followed by 1 large vertical bar on the right side), all AvS infusate. Four DS, 3rd largest, 1st and 4th somewhat equal in length. Four PvS equal in length. Ventral side with small blunt tubercles in the posterior half before 1st DS, row of smaller tubercles starting from 2nd DS to the distal half along anteroventral side, and a group of small acute tubercles present at medioventral to posteroventral area between 2nd and 3rd PvS (Fig. 3B). Tibia with nine AvS elongating distally, 1st smallest and 9th longest respectively. Six PvS arranged as  with gap between 1st PvS and base of tibia largest. First tarsomere of protarsus

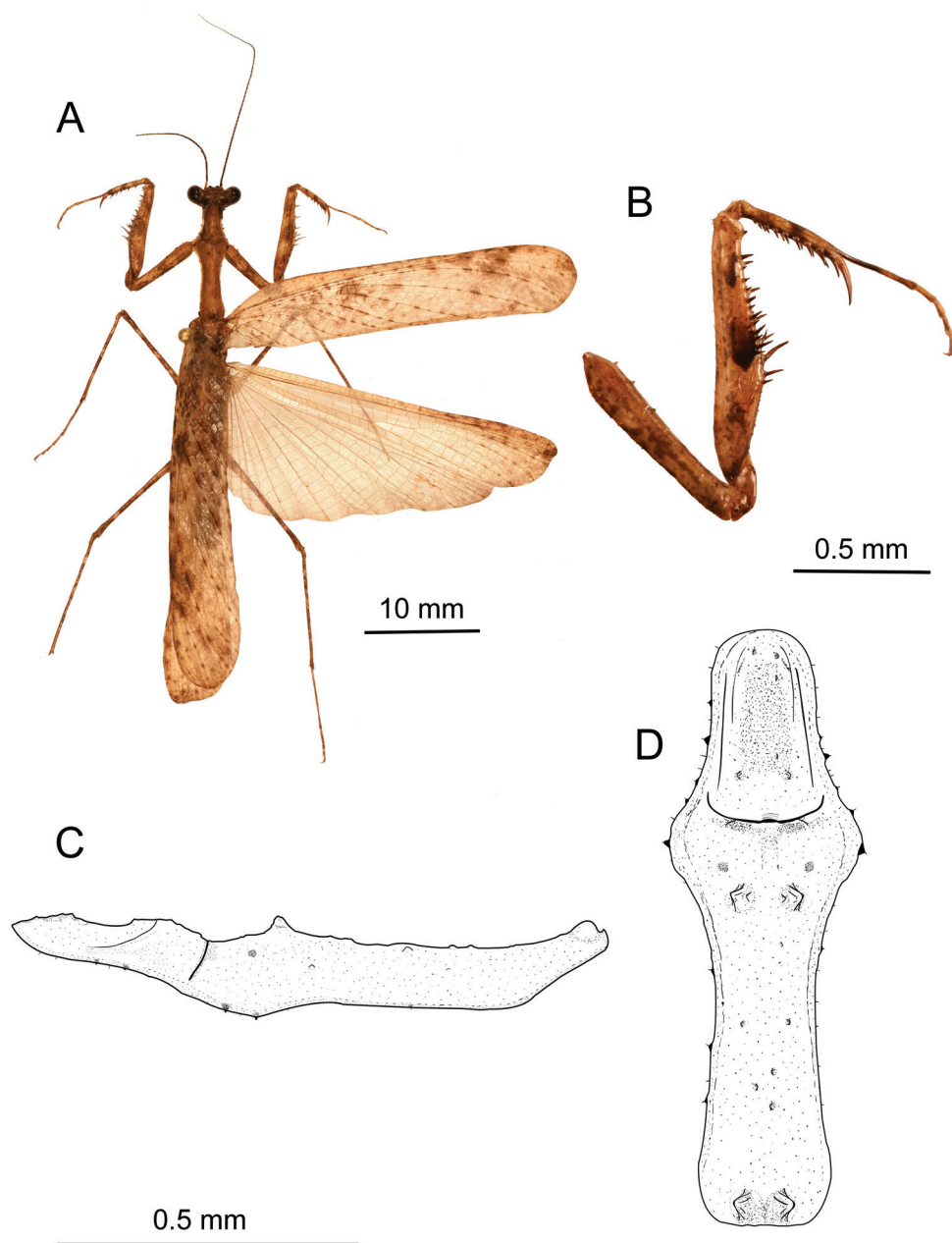


Figure 2. *Arria muscoamicta* sp. nov. **A** dorsal habitus **B** anterior side of prothoracic leg **C, D** pronotum in lateral and dorsal views, respectively.

longer than remaining segments combined. Spinal formula: F = 4DS/11–12AvS/4PvS; T = 9AvS/6PvS.

Meso- and metathoracic legs. Long and slender with fine setae, without dilations or projections. Femora with rounded genicular lobes each bearing a single short api-

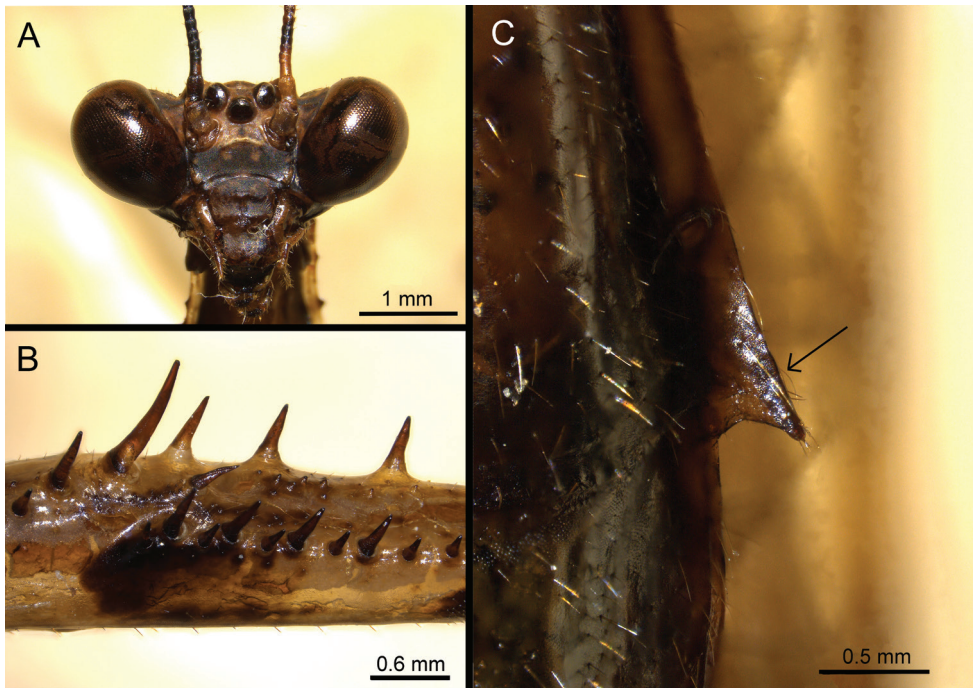


Figure 3. *Arria muscoamicta* sp. nov. **A** head in frontal view **B** ventral view of prothoracic femur **C** lateral lobe of abdominal tergite.

cal spine. Tibiae with two apical spines. First tarsomere of mesotarsus slightly longer than remaining segments combined. First tarsomere of metatarsus much longer than remaining segments combined.

Flight organs. Forewing long, narrow, with rounded apex and covered by small setae. Costal area relatively narrow. Hindwing with almost truncated apex bearing small lobe anteriorly, protruding a little beyond forewing in resting position.

Abdomen. Narrow, with small but distinct, acute lateral lobes on each abdominal tergite (Fig. 3C). Cerci cylindrical with numerous setae, last cercomere conical. Tergite X (supra-anal plate) transverse, covered by setae, posterior margin more or less rounded with small projection at the middle. Coxosternite IX (subgenital plate) longer than wide, two posterolateral ridges present on ventral side and forming base of styli ventrally. Posterior margin truncated. Ventral side with fine setae, much denser in posterior half and on styli.

Genitalia (Fig. 4). Ventral phallomere oval, moderately wide, sclerotised by sclerite L4A. Lobe bl small, oval. Strip of L4A sclerotising bl even smaller than bl as a whole, but very distinct, curved ventro-dorsad across right edge of the phallomere and narrows towards the apex. Only one process sdg present, its base wide and distal half curved almost at right angle, being directed to the right and slightly posteriad in dorsal perspective and also slightly dorsad in lateral perspective. Posterior edge of sdg convex on the left, then concave, then convex again on the right. Distal half of sdg approximately the same length as sdg base's width, but three times narrower than long. This

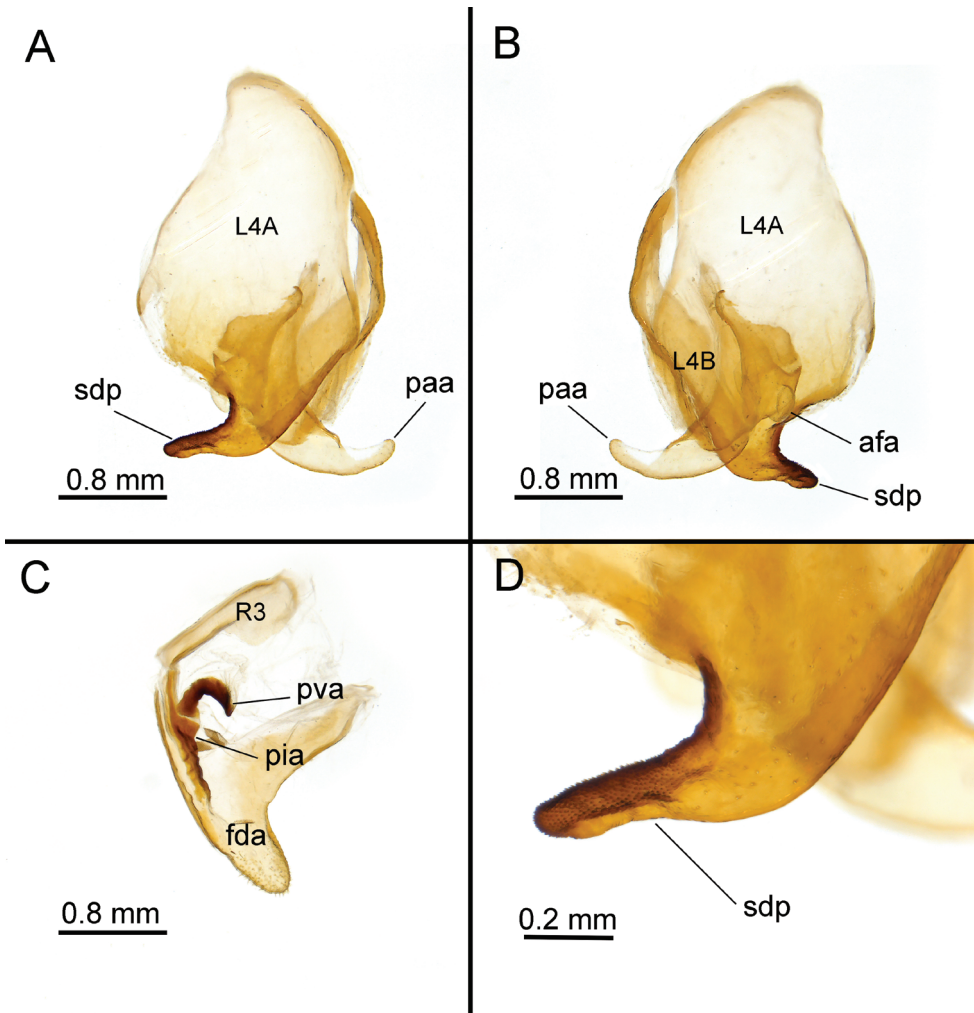


Figure 4. *Arria muscoamicta* sp. nov., male genitalia **A, B** left complex in ventral and dorsal perspectives, respectively **C** right phallomere in ventral perspective **D** close up of sdp.

distal part strongly sclerotised, slightly flattened in antero-posterior direction and its surface sharply divided in the same direction into posterior smooth area and anterior densely spinulated area including rounded apex. Field of spinules reaches the turning point and continues antieriad as simply strongly sclerotised right edge of sdp. Dorsal sclerotisation of sdp by L4A not covering whole sdp, but with medial membranous evagination almost up to turning point. However, along the right edge it extends even beyond base of sdp, and along left edge of ventral phallomere it reaches process pda as narrow band. Pda expressed only as a lobe, with surface between it and articulation A1 gently concave. A1 simple. Apophysis swe moderately wide and very distinct. Sclerite L4B convex, undulated, and relatively narrow.

Process paa simple, moderately long, directed to the left, but gently curving anteriorly. Edge pba with only one process, presumed to be afa. Afa membranous, moderately sized, bulbous. Pouch pne narrow and gently S-shaped in its anterior part, its posterior and ventral walls sclerotised by sclerite L1. L1 roughly triangular, widened in its right part and sclerotising area of pba immediately anterior of afa as well as area to the left of afa (on pne plane) but not afa itself. Articulation A2 very wide, articulation A4 absent. Sclerite L2 elongated, with narrow left arm, approximately square right arm and slightly twists along posterior wall of paa leaving dorsal surface of paa weakly sclerotised.

Right phallomere triangular, with strongly concave left edge. Lobe fda covered by short, not very sparse setae within depressions at apex, and sclerotised by sclerite R1A dorsally and along the edges. Arm bm simple, flat. Gap between sclerites R1A and R1B apparent, narrow. Apophysis pia long, partially sclerotised by R1A and in the sclerotised part with slightly uneven edge on macroscale, tuberculate on microscale. Apophysis pva claw-shaped, sclerotised by sclerite R1D. Groove lge very long and narrow, sclerotised by R1B. Sclerite R3 relatively short, axe-shaped, groove age very wide.

Female. Unknown.

Measurements (mm). TL = 42.7, HW = 4.3, PL = 9.2, PW = 3.0, PnW = 1.4, PzL = 3.1, MzL = 6.1, TgL = 29.3, CfW = 1.1, AL = 26.9, PCL = 6.3, PFL = 8.5, PTL = 4.6, PtL = 5.5, MsFL = 9.1, MsTL = 7.8, MstL = 6.3, MtFL = 10.5, MtTL = 10.0, MttL = 8.5

Colouration. Body pale greenish to brownish with irregular, brownish patches scattered across its surface. Pronotum lighter and more monochrome, with two barely contrasting lateral bands anterior of supracoxal sulcus. Posterior surfaces of prothoracic coxa, femur, and tibia each with two or three darkened bands with highly irregular edges. Meso- and metathoracic legs also with two or three indistinct darkened bands, but only on femur and tibia. Forewing beige with large and small, irregular, brown patches across its surface and interrupted darkened areas along the main veins. Hindwing subhyaline, with darker patches present on apical lobe. Abdomen with longitudinal median stripe paler than lateral ones.

Discussion

Arria muscoamicta sp. nov. lives in evergreen mossy forests at high elevations of approximately 1,200 m above sea level in Thailand. The dominant trees of the region include oaks and chestnuts such as *Lithocarpus*, *Quercus*, and *Castanopsis*, which are covered by bryophytes and epiphytes (Smitinand 1968). The climate of the region (data recorded at the Khao Kheow Weather Observing Station) includes relatively low and consistent air temperatures throughout the year. For example, the annual average temperature between 2017–2020 was 20.35 °C, December (average between 2017–2020) was the coldest month (18.15 °C), while the hottest month was May (average between 2017–2020) with a temperature of 21.77 °C. The relative air humidity is high but fluctuates between 67% and 99%; the lower humidity levels are

observed during November and March, which was when the holotype and the male nymph were collected, respectively. It would seem that nymphs of *A. muscoamicta* sp. nov. require a relatively low temperature for their development, as all of our nymphs died after being relocated to a laboratory room with ambient temperature of approximately 30 °C and without air conditioning. The male nymph was collected by searching mossy trees in the vicinity of the holotype collection point, and it is at this stage especially that the mossy-camouflaging morphological peculiarities are apparent (Fig. 1C). In addition to even more patchy colouration than in adult male, all abdominal tergites possess posteromedial lobe similar to those in nymphs and females of *A. leigongshanensis*.

Schwarz and Roy (2018) synonymised *Palaeothespis* Tinkham, 1937 and *Pseudothespis* Mukherjee et al., 1995 with *Arria*, noting that, with respect to the number of foreleg spines, shape, and tuberculation of the head and pronotum, and the shape of male tegmina and of the abdominal lobes in females, *Arria* and *Pseudothespis* fall into the range described for *Palaeothespis*. While this statement is true, there are significant morphological differences between different species of *Arria* (sensu Schwarz and Roy 2018), involving presence/absence of the pronotal tubercles, shape of the pronotum, shape of the apical lobe of the hind wing, and number of various foreleg spines. In addition, the species composition of and distinction between *Arria* and the closely allied genus *Sinomiapteryx* Tinkham, 1937, are currently somewhat ambiguous. For example, *A. sticta* and *A. pallida* are significantly more similar in morphology to *S. brevifrons* and *S. yunnanensis* Xu, 2007 than to the other *Arria* species, in being united by the gently oval edges of the supracoxal dilatation, narrow tegmina, and pointed, lancet-shaped apical lobe of the hindwing. A specimen from Thailand investigated by Schwarz and Roy (2019), whose genitalia are depicted in their work as “*Sinomiapteryx* sp.”, also belongs to the latter group. Another specimen from that group from Laos (in the collection of SMNK) with almost identical genitalia was examined by the second author. The genitalia of these specimens are strikingly different from those of *A. muscoamicta* sp. nov. At the same time, the abovementioned species do not share with *S. grahami* Tinkham, 1937, the type species of *Sinomiapteryx*, some of its most prominent characters, such as very wide forewings with strongly curved main veins and large space between R and ScP, truncated apex of hindwings and somewhat more defined supracoxal dilatation.

While this work was in peer review, another paper has been published (Wang et al. 2021) which has clarified some of the abovementioned issues, specifically by synonymizing *S. yunnanensis* with *A. pallida* and by transferring *S. brevifrons* to *Arria*. Wang et al. (2021) also suggested that species with the terminal lobe near the distal process of the ventral phallomere (as in the abovementioned group that includes *A. sticta*, *A. pallida*, etc.) should belong to *Arria*, while those without it (including *A. muscoamicta* sp. nov.) should be assigned to *Sinomiapteryx*. Unfortunately, the authors were not able to study the type species of both genera to justify this diagnostic character, and the other characters listed by them are inconsistent within the suggested groupings, leaving the problem still unresolved.

Arria muscoamicta sp. nov. is similar to the type species of *Arria*, *A. cinctipes*, in so many respects (e.g., the shape of pronotum and the presence of metazonal tubercles) that we consider our combination to remain a valid one. However, as shown above, the taxonomy of the tribe Arriini as a whole needs revision. This would require genital preparation of all holotypes, currently deposited in the museums of USA (1 species), Sweden (1 species), India (1 species), and China (the remainder). Molecular and ecological data might also provide important insights. The discovery of additional new species in this enigmatic and poorly known group of mantodeans is also highly likely.

Acknowledgements

We wish to express our gratitude to Prof. Dr Jichun Xing (Guizhou University) who provided photographs of the *Arria leigongshanensis* holotype and Gunvi Lindberg (Naturhistoriska Riksmuseet) who provided photographs of the *A. cinctipes* holotype for comparison with the new species. TU also thanks Wuttipon Pathomwattanaru-ruk and Wuttikrai Khaikaew for their support in collecting material and taking the photographs. ES would like to express sincere gratitude to Alexander Riedel (SMNK) and Christian J. Schwarz (Ruhr Universität Bochum) for the opportunity and full assistance in studying specimens from SMNK collection.

This research is funded by Kasetsart University through the Graduate School Fellowship Program.

References

- Beier M (1952) Die Mantiden der Subtribus Haaniées (Thespinae – Oligonychini) (Orth.). *Treubia* 21: 199–210.
- Brannoch SK, Wieland F, Rivera J, Klass KD, Bethoux O, Svenson GJ (2017) Manual of praying mantis morphology, nomenclature, and practices (Insecta: Mantodea). *ZooKeys* 696: 1–100. <https://doi.org/10.3897/zookeys.696.12542>
- Ge D-Y, Chen X-S (2008) Review of the genus *Palaeothespis* Tinkham (Mantodea: Thespidae), with description of one new species. *Zootaxa* 1716: 53–58. <https://doi.org/10.11646/zootaxa.1716.1.5>
- Mukherjee TK, Ghosh AK, Hazra AK (1995) The mantid fauna of India (Insecta: Mantodea). *Oriental Insects* 29: 185–358. <https://doi.org/10.1080/00305316.1995.10433744>
- Rivera J, Yagui H, Ehrmann R (2011) Mantids in the mist—taxonomy of the Andean genus *Pseudopogonogaster* Beier, 1942, a cloud forest specialist, with notes on its biogeography and ecology (Mantodea: Thespidae: Miopteryginae). *Insect Systematics & Evolution* 42: 313–335. <https://doi.org/10.1163/187631211X595056>
- Schwarz CJ, Roy R (2018) Some taxonomic and nomenclatural changes in Mantodea (Diconotoptera). *Bulletin de la Société entomologique de France* 123(4): 451–460. <https://doi.org/10.32475/bsef>

- Schwarz CJ, Roy R (2019) The systematics of Mantodea revisited: an updated classification incorporating multiple data sources (Insecta: Dictyoptera). *Annales de la Société entomologique de France* (NS) 55: 101–196. <https://doi.org/10.1080/00379271.2018.1556567>
- Smitinand T (1968) Vegetation of Khao Yai National park. *Natural History Bulletin of the Siam Society* 22: 289–305.
- Stål C (1877) *Systema Mantodeorum*, Essai d'une systematization nouvelle des mantodées. Bihang till Konglika Svenska Vetenskaps-akademiens Handlingar 4(10): 1–91.
- Svenson GJ, Vollmer W (2014) A case of the higher-level classification of praying mantises (Mantodea) obscuring the synonymy of *Majangella* Giglio-Tos, 1915 (Liturgusidae, Liturgusinae) and *Ephippiomantis* Werner, 1922 (Hymenopodidae, Acromantinae). *Zootaxa* 3797(1): 103–119. <https://doi.org/10.11646/zootaxa.3797.1.10>
- Tinkham ER (1937) Studies in Chinese Mantidae (Orthoptera). *Lingnan Science Journal* 16(3): 481–499.
- Vermeersch XHC (2018) *Phasmomantella* gen. nov., a spectacular new genus of praying mantis from southern Central Vietnam (Mantodea, Mantidae, Deroplatyinae, Euchomenellini). *European Journal of Taxonomy* 442: 1–17. <https://doi.org/10.5852/ejt.2018.442>
- Wang Y, Yang L, Ye F, Chen X (2021) A new species of the genus *Arria* Stål, 1877 (Mantodea, Haaniidae) from China with notes on the tribe Arriini Giglio-Tos, 1919. *ZooKeys* 1025: 1–19. <https://doi.org/10.3897/zookeys.1025.56780>
- Zhang G-Z (1987) A new species of the genus *Palaeothespis* Tinkham From China (Mantidae: Thespinae). *Entomotaxonomia* 9(3): 239–241.
- Zhou W-B, Chen S-G (1992) Study on fauna of Mantodea from Zhejiang and Yunnan province with description of two new species. *Journal of Shanghai Normal University (Natural Sciences)* 21(1): 62–67.
- Zhu X, Wu C, Yuan Q (2012) *Mantodea in China*. Xiyuan Publishing House, Beijing, 331 pp.

A new genus and species of Mileewini leafhoppers (Hemiptera, Cicadellidae, Mileewinae) from China, with a key to genera

Bin Yan¹, Hong-Li He¹, Mao-Fa Yang^{1,2}, Mick D. Webb³

1 Institute of Entomology, Guizhou University; The Provincial Key Laboratory for Agricultural Pest Management of the Mountainous Region, Guiyang, Guizhou 550025, China **2** College of Tobacco Science, Guizhou University; Guizhou Provincial Key Laboratory of Tobacco Quality Research, Guizhou University, Guiyang, Guizhou 550025, China **3** Department of Life Sciences (Entomology), The Natural History Museum, London SW7 5BD, UK

Corresponding author: Mao-Fa Yang (gdgdly@126.com; mdwebb04@gmail.com)

Academic editor: Mike Wilson | Received 28 January 2021 | Accepted 2 March 2021 | Published 5 April 2021

<http://zoobank.org/52895BB4-C53D-4AA9-A6E8-66BF953CF872>

Citation: Yan B, He H-L, Yang M-F, Webb MD (2021) A new genus and species of Mileewini leafhoppers (Hemiptera, Cicadellidae, Mileewinae) from China, with a key to genera. ZooKeys 1028: 61–67. <https://doi.org/10.3897/zookeys.1028.63727>

Abstract

A new leafhopper genus and species, *Anzihelus bistriatus* Yan & Yang, **gen. nov. sp. nov.** (Cicadellidae, Mileewinae, Mileewini) is described from Sichuan Province, China. Habitus images and figures of the male and female genitalia are provided together with a key to the genera of Mileewini from China.

Keywords

Auchenorrhyncha, Homoptera, identification, morphology, Old World, taxonomy

Introduction

Mileewinae (Hemiptera, Cicadellidae) is a relatively small leafhopper subfamily comprising eight genera in four tribes distributed mainly in the Oriental and Ethiopian regions with a few species in the Neotropical and Palaearctic regions (Dietrich 2011; Krishnankutty and Dietrich 2011). At present, three genera with 69 species are recorded from China (He et al. 2021), all in the tribe Mileewini, a tribe distinguished in

the Old World by the radial posterior hind wing vein (RP) extending to the anterior margin of the wing subapically (Fig. 1h) rather than apically. Due to the relatively small number of genera in the tribe it is of some interest that a new genus was discovered in China. In this article the new genus is described together with its type species and a key provided to the genera of Mileewini from China. The new genus is distinguished by its elevated head above the pronotum (Fig. 1b) and an unusual feature of the male Xth segment, i.e., with a single medial ventral process from its posterior margin (Fig. 2a, c); processes of the Xth segment are absent in other Mileewini but when present in other leafhoppers they are usually paired, caudally or anteriorly. Type specimens of the new species are deposited in the Institute of Entomology, Guizhou University, Guiyang, China (GUGC) and a single male paratype in the Natural History Museum, London, UK.

Material and methods

The length of the body reported in the descriptions includes the forewings at rest. Morphological terminology follows Dietrich (2011). Male specimens were dissected under a Leica M125 microscope, then transferred to glycerine for further observation. Male genitalia were drawn using an Olympus CX41 microscope and drawings were enhanced using Adobe Illustrator CS6. Habitus photographs were taken with a Keyence VHX-6000 digital camera. All specimens studied are deposited in the Institute of Entomology, Guizhou University, Guiyang, China (GUGC).

Taxonomy

Key to the genera of Mileewini from China

- 1 Forewing with apex truncate or emarginate and sometimes distinctly expanded from base to apex ***Mileewa***
- Forewing with apex rounded, similar in width from base to apex (Fig. 1g) **2**
- 2 Head equal in width to pronotum or slightly wider (Fig. 1a); male style apical process elongate, without setae at apex (Fig. 2e); female second valvulae evenly tapered to apex (Fig. 1l) **3**
- Head narrower than pronotum; male style apical process reduced with setae at apex; female second valvulae abruptly constricted subapically, beak-like (see He et al. 2018, fig. 33) ***Processina***
- 3 Head in profile level with pronotum, brown with yellow marking; male Xth segment (basal anal tube segment) without caudal process ***Ujna***
- Head in profile elevated above level of pronotum (Fig. 1b), uniformly pale; male Xth segment (basal anal tube segment) with single caudal process (Fig. 2a, c) ***Anzihelus* gen. nov.**

Anzihelus gen. nov.

<http://zoobank.org/37327FC6-BDF4-4516-A74F-5DDBDEF76292>

Type species. *Anzihelus bistriatus* sp. nov.

Description. Small pale and slender leafhoppers. Head slightly wider than pronotum, shagreen; crown with anterior margin broadly rounded in dorsal view, median length almost equal to interocular width; shallowly concave at ocelli, the latter located slightly anterior to a line between anterior eye angles; laterofrontal sutures extending onto crown and attaining ocelli; coronal suture three-fifths median length. Face with frontoclypeus shallowly convex; anteclypeus slightly elevated in midline and slightly tapered to broadly rounded apex. Pronotum laterally carinate. Forewing with two open subapical cells; membrane equal in length to clavus. Hind wing with vein RP extending to anterior margin of wing subapically (Fig. 1h). Fore femur with two stout AV setae and several finer IC setae (Fig. 1i). Hindleg femoral setal formula 2:1:1.

Male genitalia. Pygofer lobe in lateral view triangular with a weakly sclerotized band between lobe and dorsal bridge; ventroposterior margin with few spine-like setae; with short process arising at midlength of ventral margin, not attaining end of pygofer, apex pointed. Anal tube as long as pygofer, a medial lamellar process arising caudally from ventral surface, aligned vertically and bifurcate apically. Valve fused to pygofer. Subgenital plates long, narrow, apices exceeding posterior margin of pygofer; with uniseriate row of macrosetae from ventral margin in lateral view and some short and long microsetae on lateral surface. Connective Y-shaped, arms and stem short with a basomedial lobe. Style elongate apex foot-like with inner heel, with few fine setae on inner margin slightly distad of midlength. Aedeagus laterally compressed with distal processes on shaft, gonopore apical; basal apodeme short.

Female valvulae I in lateral view (Fig. 1j, k), with dorsal and ventral margins of shaft distinctly convex; apex acute; with diagonal strigate sculpture dorsally and apically; basal ventral striae present. Valvulae II in lateral view (Fig. 1l, m) leaf-shaped distally, apex subacute; blade dorsally with small and closely spaced crenulate sculpture and numerous irregular fine marginal teeth.

Remarks. The new genus is similar to other Old World Mileewini genera (*Mileewa*, *Ujna* and *Processina*) in having vein RP in the hind wing extending to the anterior margin subapically (Fig. 1h) rather than the more usual apical margin and the marginal vein reaching the wing margin between Pcu and A1. It also has the basal ventral striae of the first valvulae found in the above genera (Fig. 1j). The latter feature, of unknown function, has been referred to as the ventral interlocking device but this function is performed by the rami of the first and second valvulae. The new genus can be distinguished from other Mileewini by its elevated vertex above the pronotum and from most other cicadellids by the male Xth segment (basal anal tube segment) with an unusual single caudal medial process (see also key to genera).

Etymology. The genus takes its name from the locality of the type species, Anzihe Nature Reserve.

Distribution. China (Sichuan).

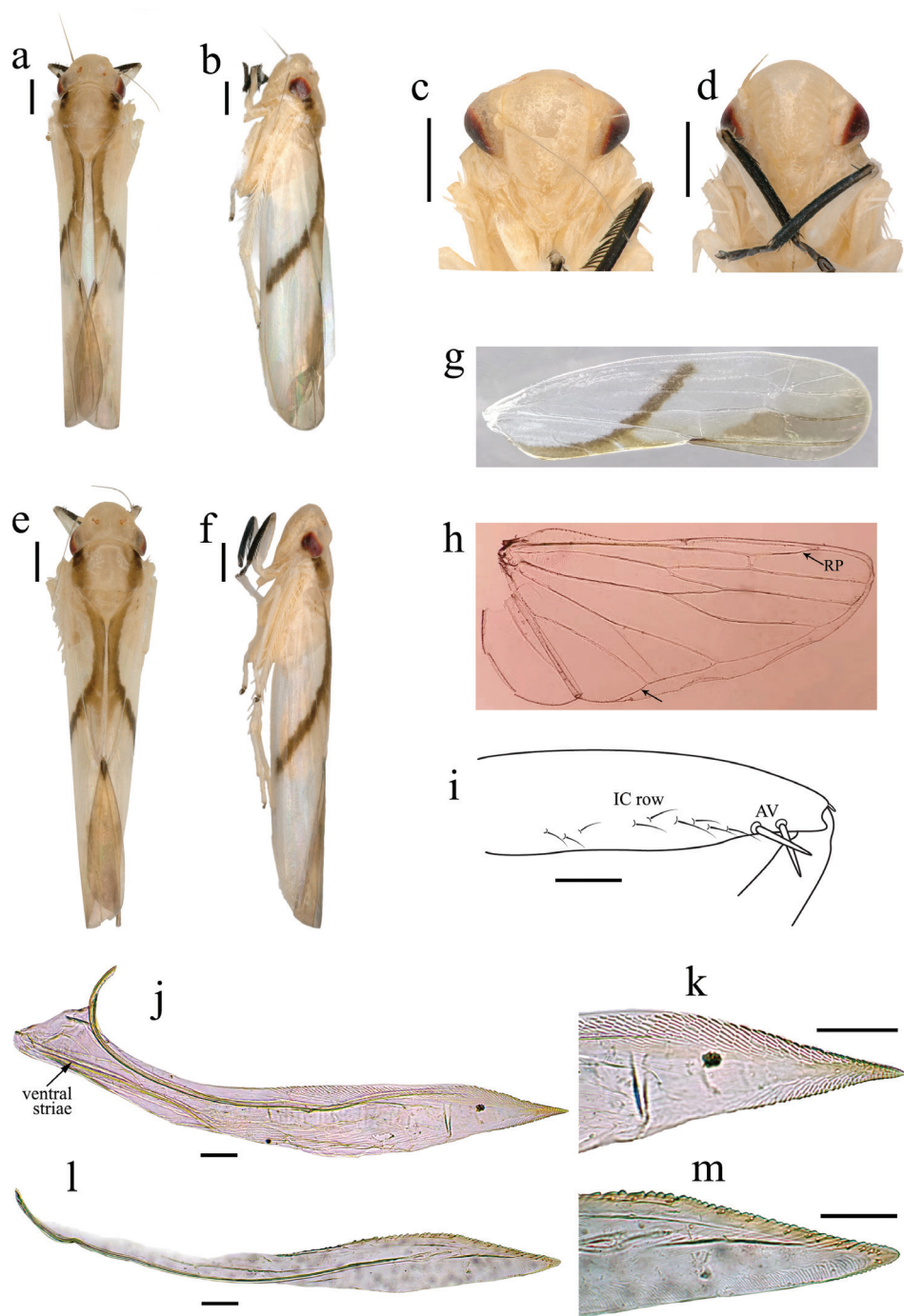


Figure 1. *Anzihelus bistriatus* sp. nov. **a–c** (male) **a** habitus, dorsal view **b** habitus, lateral view **c** face **d–f** (female) **d** face **e** habitus, dorsal view **f** habitus, lateral view **g–h** wings **g** forewing **h** hind wing **i** fore femur, anterior surface **j–m** valvulae **j, k** first valvulae, lateral view **l, m** second valvulae, lateral view (**l** damaged basally). Scale bars: 500µm (**a–f**); 0.1 mm (**i–m**).

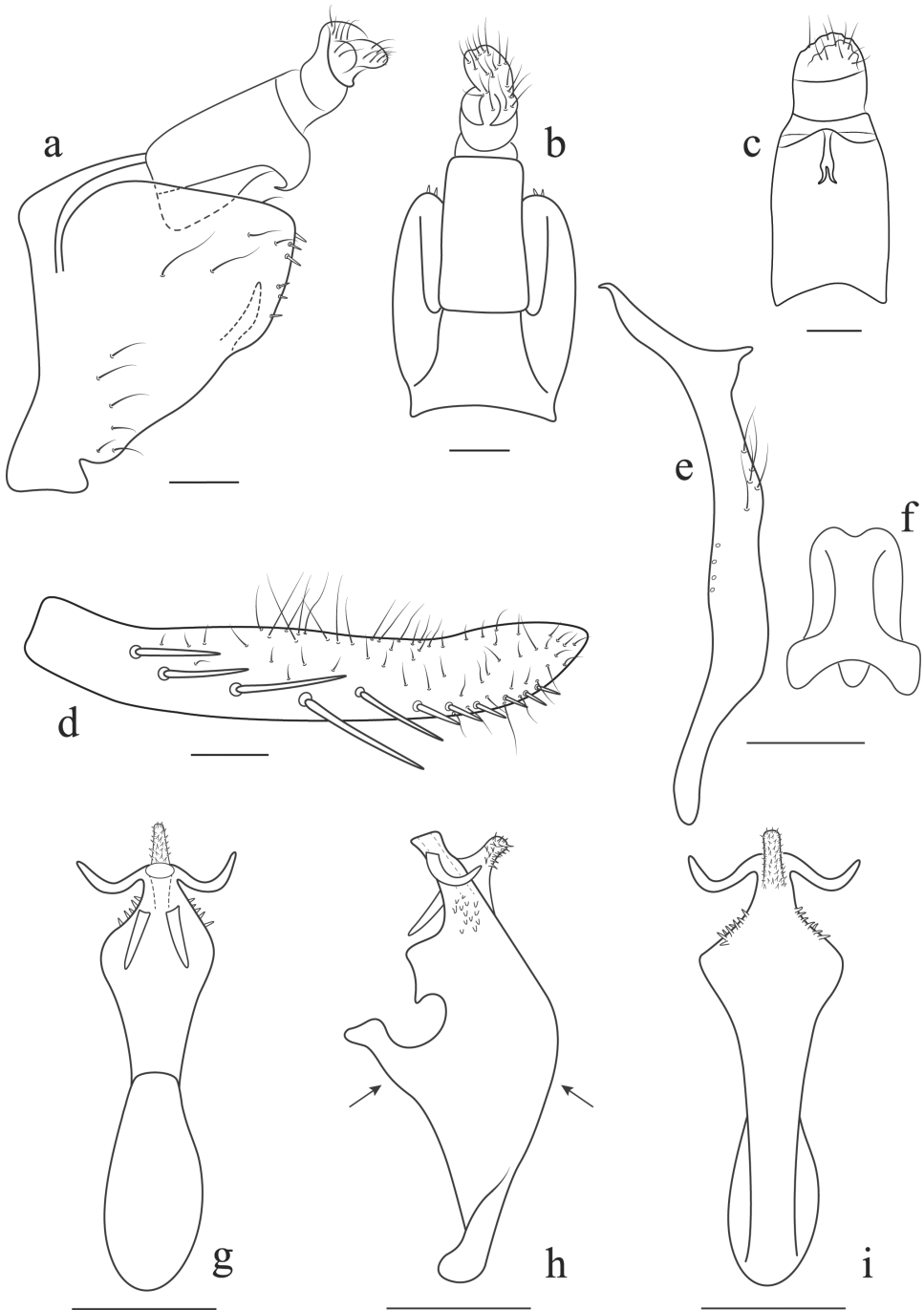


Figure 2. *Anzibelus bistriatus* sp. nov. **a, b** male genitalia **a** lateral view **b** dorsal view **c** anal tube, ventral view **d** subgenital plate, ventrolateral view **e** style, lateral view **f** connective, dorsal view **g–i** aedeagus **g** dorsal view (viewed from left-hand arrow in Fig. 2h) **h** lateral view **i** ventral view (viewed from right-hand arrow in Fig. 2h). Scale bars: 0.1 mm.

***Anzihelus bistriatus* sp. nov.**

<http://zoobank.org/AE1ED0A1-00E8-4384-8113-63C44FF41BB2>

Figs 1, 2

Material examined. *Holotype*: ♂, China, Sichuan Province, Chongzhou City, Anzihe Nature Reserve, 1595 m, 30 July 2016, coll. Bin Yan. *Paratypes*: 6♂♂4♀♀, same data as holotype; 1♂, same data as holotype except, 1687 m, 31 July 2016, at light. All type species deposited in Institute of Entomology, Guizhou University, Guiyang, China (GUGC) and one male paratype in BMNH.

Description. *Length*. Male: 5.5–6.0 mm; female: 5.6–6.0 mm.

Color pale yellow. Ocelli red or orange-yellow; eyes reddish brown laterally. Thorax with a brown band extending from behind each eye on pronotum, onto mesonotum and continued onto inner margin of clavus and diagonally across wing to costal margin. Forewing brownish hyaline distally. Legs with fore tibiae and tarsi black.

Male genitalia. Genitalia as in generic description with aedeagus (Fig. 2g-i) broad in lateral view with shaft constricted and narrowed distally, with a short ventral process arising medially from ventral surface and a pair of short slightly more elongate processes arising subapically from dorsal surface and apically, all densely covered with micro-spines, lamellate medial lobe from dorsal surface basally.

Female genitalia. Sternite VII, in ventral view, with length approximately equal to width; posterior margin convex medially.

Etymology. The specific name refers to the two dark longitudinal stripes dorsally.

Remarks. This new species can be easily recognized by its pale colour with a brown diagonal stripe across the forewings.

Distribution. China (Sichuan).

Acknowledgements

We wish to thank Chandra Viraktamath for his helpful corrections to the manuscript. This work was supported by the National Science Foundation of China (31672335); the Program of Excellent Innovation Talents, Guizhou Province, China ([2016]-4022); and International cooperation base for insect evolutionary biology and pest control ([2016]-5802).

References

Dietrich CH (2011) Tungurahualini, a new tribe of Neotropical leafhoppers, with notes on the subfamily Mileewinae (Hemiptera, Cicadellidae). ZooKeys 124: 19–39. <https://doi.org/10.3897/zookeys.124.1561>

- He H, Yang M, Yu X (2018) Three new species of the leafhopper genus *Processina* (Hemiptera: Cicadellidae: Mileewinae) from Thailand. *Zootaxa* 4531: 279–287. <https://doi.org/10.11646/zootaxa.4531.2.9>
- He H, Yan B, Yang M, Webb MD (2021) Four new species of *Mileewini* leafhoppers (Hemiptera: Cicadellidae: Mileewinae) from China, with a checklist to Chinese species. *Zootaxa* 4949(3): 521–540. <https://doi.org/10.11646/zootaxa.4949.3.5>
- Krishnankutty SM, Dietrich CH (2011) Review of mileewine leafhoppers (Hemiptera: Cicadellidae: Mileewinae) in Madagascar, with description of seven new species. *Annals of the Entomological Society of America* 104(4): 636–648. <https://doi.org/10.1603/AN11022>

A new species, a new combination, and a new record of *Crossotarsus* Chapuis, 1865 (Coleoptera, Curculionidae, Platypodinae) from China

Shengchang Lai¹, Ling Zhang², You Li³, Jianguo Wang²

1 College of Forestry, Nanjing Forestry University, Nanjing, Jiangsu 210037, China **2** College of Agricultural Sciences, Jiangxi Agricultural University, Nanchang, Jiangxi 330045, China **3** School of Forest Resources and Conservation, University of Florida, Gainesville, FL, 32611, USA

Corresponding author: Jianguo Wang (jgwang@jxau.edu.cn)

Academic editor: M. Alonso-Zarazaga | Received 22 November 2020 | Accepted 22 February 2021 | Published 6 April 2021

<http://zoobank.org/3279FAE9-E002-4142-930F-96DF49B9E959>

Citation: Lai S, Zhang L, Li Y, Wang J (2021) A new species, a new combination, and a new record of *Crossotarsus* Chapuis, 1865 (Coleoptera, Curculionidae, Platypodinae) from China. ZooKeys 1028: 69–83. <https://doi.org/10.3897/zookeys.1028.61018>

Abstract

This study describes a new species, *Crossotarsus beaveri* Lai & Wang, **sp. nov.**, designates a new combination, *C. brevis* (Browne, 1975, **comb. nov.** from *Platypus* Herbst, 1793), and notes a new record, *C. emorus* Beeson, 1937, from China. Genetic data from four genes indicate that the new species and *C. brevis* form a clade clustered with other *Crossotarsus* species. Molecular phylogeny and morphological characters support their taxonomic placement.

Keywords

Ambrosia beetle, Fujian, Jiangxi, molecular phylogeny, pinhole borer, taxonomy

Introduction

The genus *Crossotarsus* Chapuis 1865 was erected for 29 species of pinhole borers. *Crossotarsus wallacei* (Thomson, 1857) was designated as the type species of the genus (Hopkins 1914). Wood (1993) revised the genera of Platypodidae and placed *Crossotarsus* in the subfamily Platypodinae, tribe Platypodini. *Crossotarsus* is distinguished from

other Platypodine genera primarily by the following combination of characters (Browne 1961; Wood 1993; Beaver and Sanguansub 2015): 1. Labial palps two-segmented, with basal segments fused in the midline; 2. Sexually dimorphic protibiae, the outer face of the protibia transversely carinate in the male and finely granulate in the female; 3. Pronotum without specialized mycangial pores in either sex; 4. Femoral grooves angulate at the anterior extremity and gently rounded behind; 5. Metacoxa strongly projecting with a deep vertical posterior face. But Wood's (1993) generalisation that the female pronotum of *Crossotarsus* species has numerous mycangial pores is incorrect (Beaver 2004).

The catalog of Wood and Bright (1992) includes 118 species of *Crossotarsus*. As a result of taxonomic changes since that time, 116 species are currently recognised. Most species of *Crossotarsus* occur in the Oriental region, extending from India across Southeast Asia and Indonesia to Australia and the Pacific islands, and northward to Taiwan and Japan (Wood 1993). *Crossotarsus externedentatus* (Fairmaire 1849) is also widespread in the Afrotropical forests.

The Platypodinae have been almost entirely neglected in China. Only a few papers include original records of *Crossotarsus* from the country. Yin and Huang (1987) recorded three species: *C. coniferae* Stebbing, 1906, *C. squamulatus* Chapuis, 1865, and *C. wallacei* from Yunnan. Yin et al. (2002) added two species: *C. externedentatus* and *C. terminatus* Chapuis, 1865 from Hainan island, and Zhang et al. (2008) cited 13 species from China. After taxonomic changes (Beaver 2004; 2005; 2016; Bright 2014), the following 13 species are currently known from China: *C. coniferae* (Yunnan, Sichuan, Xizang); *C. emancipatus* Murayama, 1934 (Taiwan); *C. externedentatus* (Hainan, Taiwan); *C. flavomaculatus* Strohmeier, 1912 (Taiwan); *C. formosanus* Strohmeier, 1912 (Taiwan); *C. niponicus* Blandford, 1894 (Taiwan); *C. piceus* Chapuis, 1865 (Taiwan); *C. saltatorinus* (Schedl, 1954) (Fujian); *C. sauteri* (Strohmeier, 1913) (Taiwan); *C. simplex* Murayama, 1925 (Taiwan); *C. squamulatus* (Yunnan); *C. terminatus* (Hainan, Yunnan, Xizang); *C. wallacei* (Hainan, Taiwan).

In this study, we describe a new species of *Crossotarsus* from China, give a new distribution record, transfer a previously described species to the genus, and provide molecular data of Chinese species for molecular phylogenetic analyses.

Materials and methods

Abbreviations used for collections

BMNH The Natural History Museum, London, United Kingdom.

JXAU College of Agricultural Sciences, Jiangxi Agricultural University, Nanchang, China.

KIZCAS Kunming Institute of Zoology, Chinese Academy of Sciences, Kunming, China.

NIAES National Institute of Agro-Environmental Sciences (ITLJ), Tsukuba, Ibaraki, Japan.

- NMNS** National Museum of Natural Science, Taichung, Taiwan.
NZMC National Zoological Museum of China, Institute of Zoology, Chinese Academy of Science, Beijing, China.
RAB Private collection of Roger A. Beaver, Chiang Mai, Thailand.
RIFID Research Institute of Forest Insect Diversity, Namyangju, South Korea.
SYU Museum of Biology, Sun Yat-sen University, Guangzhou, China.
USNM National Museum of Natural History, Washington D.C., USA.
ZIN Zoological Institute. Russian Academy of Sciences, St. Petersburg, Russia.

Adults of the new species were collected by log dissection. The samples were immediately preserved in tubes containing 99.9% ethyl alcohol, which were stored at -20°C for DNA extraction and examination. Specimens were examined using an Olympus SZX160 stereoscopic zoom microscope. Photographs were taken with a KEYENCE VHX-6000 Digital Microscope System. All photos were further adjusted and assembled with Adobe Photoshop CS6. Body length was measured between the anterior margin of the pronotum and the elytral apex (head not included).

Genomic DNA was extracted from the adult head. The total genomic DNA was extracted from each individual using the Ezup Column Animal Genomic DNA Purification Kit (Sangon Biotech Co. Ltd). Amplification of four gene fragments (COI, EF-1 α , CAD, 28S) was made by PCR, using primers (Table 1) and cycling conditions previously described (Jordal et al. 2011). The PCR products were sent to Sangon Biotech Co. Ltd (Shanghai, China) for sequencing, and the sequences were analyzed using the software DNASTar. Additional information on *Crossotarsus* material was collected by the authors in China or downloaded from NCBI (The National Center for Biotechnology Information) (Table 2). Concatenated DNA sequence data from Jordal (2013) were analysed in MrBayes v. 3.2.6 (Ronquist et al. 2012). Partitions and models were estimated by PartitionFinder 2 (Lanfear et al. 2017) and ModelFinder (Kalyaana-moorthy et al. 2017) respectively in PhyloSuite (Zhang et al. 2020), GTR+G+I were selected for each partition. 10 million generations were run, with 25% of the generations as burn-in. PSRF close to 1.0 and standard deviation of split frequencies below 0.01 were accepted.

Table 1. Gene fragments targeted for PCR and the primers used. Sequencing primers were identical to those used in PCR.

Gene	Primer name	Annealing	Primer sequence	Reference
COI	S1718	46	5'-GGAGGATTTGGAAATTGATTAGTTCC-3'	Jordal et al. 2011
	A2411		5'-GCTAATCATCTAAAACTTTAATTCWGTWG-3'	
28S	S3690	55	5'-GAGAGTTMAASAGTACGTGAAAC-3'	Jordal et al. 2011
	A4394		5'-TCGGAAGGAACCAGCTACTA-3'	
EF-1 α	S149	52	5'-ATCGAGAAGTTCGAGAAGGAGGCYCARGAAATGGG-3'	Jordal et al. 2011
	A1043		5'-GTATATCCATTGGAAATTTGACCNNGRTGRTT-3'	
CAD	CAD for4	50	5'-TGGAARGARTBGARTACGARGTGGTYCG-3'	Jordal et al. 2011
	CAD rev1mod		5'-GCCATYRCYTCBCCYACRCTYTTTCAT-3'	

Table 2. Material used for phylogenetic analyses, including their GenBank accession numbers.

No.	Taxon	Country	CAD	COI	EF-1 α	28S	Reference
1	<i>C. beaveri</i> sp. nov.	China: Jiangxi	LC616080	LC613149	–	LC613157	This study
2	<i>C. brevis</i> (Browne, 1975)	China: Yunnan	LC616086	LC613154	LC616520	LC613163	This study
3	<i>C. chalcographus</i> Schedl, 1972	Papua New Guinea	KR261163	KR261313	–	–	Jordal 2015
4	<i>C. emorsus</i> Beeson, 1937	China: Yunnan	LC616087	LC613155	–	LC613164	This study
5	<i>C. externedentatus</i> (Fairmaire, 1849)	China: Yunnan	LC616083	LC613152	LC616518	LC613160	This study
6	<i>C. externedentatus</i> (Fairmaire, 1849)	Tanzania	KR261162	KR261312	–	KR261216	Jordal 2015
7	<i>C. externedentatus</i> (Fairmaire, 1849)	Madagascar	KR261166	KR261316	KR261275	KR261218	Jordal 2015
8	<i>C. fractus</i> Sampson, 1912	Papua New Guinea	KR261165	KR261315	KR261274	–	Jordal 2015
9	<i>C. minusculus</i> Chapuis, 1865	Papua New Guinea	HQ883809	HQ883669	HQ883739	HQ883579	Jordal 2015
10	<i>C. niponicus</i> Blandford, 1894	China: Sichuan	–	LC613156	–	LC613165	This study
11	<i>C. nitescens</i> Schedl, 1979	Australia	KR261161	KR261311	KR261272	–	Jordal 2015
12	<i>C. sauteri</i> (Strohmeyer, 1913)	China: Jiangxi	LC616081	LC613150	LC616516	LC613158	This study
13	<i>C. squamulatus</i> Chapuis, 1865	China: Yunnan	LC616084	LC613153	–	LC613161	This study
14	<i>C. terminatus</i> Chapuis, 1865	China: Jiangxi	LC616082	LC613151	LC616517	LC613159	This study
15	<i>C. wallacei</i> (Thomson, 1857)	China: Yunnan	LC616085	–	LC616519	LC613162	This study
16	<i>P. contaminatus</i> (Blandford, 1894)	China: Jiangxi	LC387560	LC383433	LC387562	LC386151	Lai et al. 2019

Results

Crossotarsus beaveri Lai & Wang, sp. nov.

<http://zoobank.org/B8D65F2C-90C7-4B5B-84D0-AA714D42A565>

Figures 1, 2

Type material. Holotype. Male, CHINA: Jiangxi Province, Ganzhou City, Longnan County, Jiulianshan national nature reserve of Jiangxi, Hualu Village, 24°37'19"N, 114°29'57"E, 2.VII.2020, log dissection, host *Paulownia fortunei*, Shengchang Lai leg. (deposited in NZMC IOZ(E)225775).

Allotype. Female, same data as holotype (deposited in NZMC IOZ(E)225776).

Paratypes. 6 males, 6 females, same data as holotype, but host *Phoebe zhennan* and *Liquidambar formosana* (5 males, 5 females JXAU; 1 male, 1 female NZMC); 11 male, 6 females, as holotype except: Xunwu County, Xiangshan Town, Congkeng Village, 24°54'20"N, 115°52'44"E, ca 650m, 15.IX.2017, log dissection, host *Castanopsis fargesii* and *Vernicia montana*, Shengchang Lai leg. (10 males, 5 females JXAU; 1 male, 1 female RAB); 6 males, 6 females, as holotype except: Xunwu County, Liuche Town, Luanluozhang, 24°40'41"N, 115°44'9"E, ca 640 m, 22.VIII.2017, log dissection, host *Castanopsis carlesii*, Shengchang Lai leg. (5 males, 5 females JXAU; 1 male, 1 female RAB); 38 males, 38 females, China: Fujian Province, Zhangzhou City, Yunxiao County, Xiahe Town, Qigaoqi Village, 24°1'31"N, 117°10'36"E, 8.VII.2019, log dissection, host *C. carlesii*, Ling Zhang leg. (2 males, 2 females BMNH; 2 males, 2 females KIZCAS [KIZ0121459–0121462]; 2 males, 2 females NIAES; 2 males, 2 females NMNS; 2 males, 2 females RAB; 2 males, 2 fe-

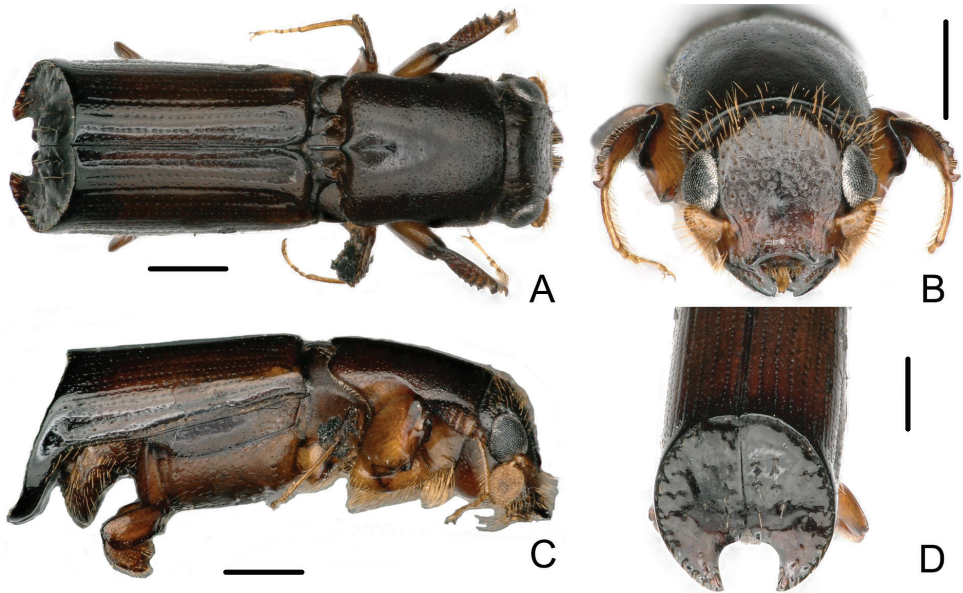


Figure 1. Male of *Crossotarsus beaveri* sp. nov. **A** dorsal view **B** head **C** lateral view **D** declivity. Scale bars: 0.5 mm.

males RIFID; 2 males, 2 females SYU; 2 males, 2 females USNM; 2 males, 2 females ZIN; 20 males, 20 females JXAU).

Description. Male. 3.58–4.01 mm long (mean = 3.78; $n = 20$); 2.75–2.95 times as long as wide. Head and pronotum dark brown, disc of elytra reddish brown becoming dark brown, declivity of elytra nearly black.

Head. Frons flat, slightly shining, with irregular large punctures; finely, sparsely punctured above the epistoma, bearing bristly, erect, long setae, weakly concave, smooth around short median line, upper part of frons with scattered, coarse punctures, the punctures with moderate, semierect, dorsally directed setae. Antennal scape clavate with scattered, forwardly directed hairs on apical half; club oval, flattened, evenly covered with short setae. Labial palps two-segmented, with basal segments fused along the midline.

Pronotum. About 1.2 times longer than wide, shining, no mycangial pores, the lateral femoral grooves angulate anteriorly, pronotum widest in front of the grooves, with finely, scattered, irregular punctures, a few semierect backwardly pointed hairs close to anterior margin, median line extending about 1/4 from base.

Scutellum. Depressed below level of elytra, with a median longitudinal groove between lateral carinae.

Elytra. About 2.0 times as long as wide, about 1.4 times as long as pronotum. Surface of disc smooth, shining, striae distinctly impressed for almost their entire length, except striae 6 and 7, other striae with circular, distinct, shallow punctures, the bases of striae 1 and 2, striae 3 and 4, respectively, conjoint, more impressed; interstriae slightly raised on disc, interstriae 1, 3 and 5 distinctly raised and conjoint at base,

interstriae 8 and 9 fused at apex of disc, forming ventral, rounded angle; cylindrical declivity obliquely truncate, acutely margined all around except at sutural apex, strongly concave, forming a cup-like structure, surface shining, with 4 rows of longitudinal granules bearing erect, long, golden setae, a row of sparse, medially directed, erect golden setae at the inner margin of declivity, elytral apex broadly emarginate, the main emargination approximately U-shaped, about as wide as deep, extending about 1/3 of the height of the declivity, at its inner end a much smaller, V-shaped second emargination (Fig. 1A, D).

Protibia. Five transverse carinae at tibial apex, transverse rugae at base.

Abdomen. Abdominal ventrites 1–4 moderately finely punctured, with irregular rows of erect, short hairs at both sides posteriorly, ventrite 5 strongly concave at middle, with dense, large, circular punctures.

Female. 3.64–4.42 mm long (mean = 3.96 mm; $n = 20$); 2.79–2.93 times as long as wide. Head and pronotum brown, disc of elytra reddish brown becoming dark brown to apex.

Head. Similar to male, but frons flatter, very shining, smooth, with shallow, small punctures; finely, sparsely punctured above the epistoma, bearing bristly, erect, long setae; very shallowly concave in median line, upper part of frons with scattered, shallow, small punctures, the punctures with moderate, semierect, dorsally directed setae.

Pronotum. Similar to male.

Elytra. About 1.8 times as long as wide, about 1.5 times as long as pronotum, sides subparallel. Similar to male, but disc of elytra shining, with dense, longitudinal, semierect, backwardly pointed hairs at apex and declivity, striae weakly impressed, interstriae smoother, declivity vertical, a few irregularly granules, sparsely hairy.

Protibia. Three transverse carinae at tibial apex, fine, confused granules at base.

Abdomen. Surface of abdominal ventrites smooth, rounded, sparsely hairy, ventrite 5 without concavity, punctures shallow.

Etymology. The species is named for Roger A. Beaver to honor his contributions to the study of platypodines and scolytines.

Host plants. *Castanopsis carlesii* (Hemsl.) Hayata, *C. fargesii* Franch. (Fagaceae), *Liquidambar formosana* Hance (Altingiaceae), *Phoebe zhennan* S.K.Lee & F.N.Wei (Lauraceae), *Paulownia fortunei* (Seem.) Hemsl. (Paulowniaceae), *Vernicia montana* Lour. (Euphorbiaceae).

Distribution. China (Jiangxi, Fujian).

Diagnosis. The species is placed in *Crossotarsus* because it possesses a combination of characters similar to that cited in the introduction.

Crossotarsus beaveri is very similar to *Crossotarsus brevis* (Browne, 1975) (new combination, see below) and *Crossotarsus platypoides* (Browne, 1955). They can be easily distinguished from other *Crossotarsus* species by the male elytral apex truncate with a large, circular, concave declivity. The elytral apex of male of *C. beaveri* and that of *C. brevis* possess a deep, acutely margined declivity, with a broad, almost circular, apical emargination.

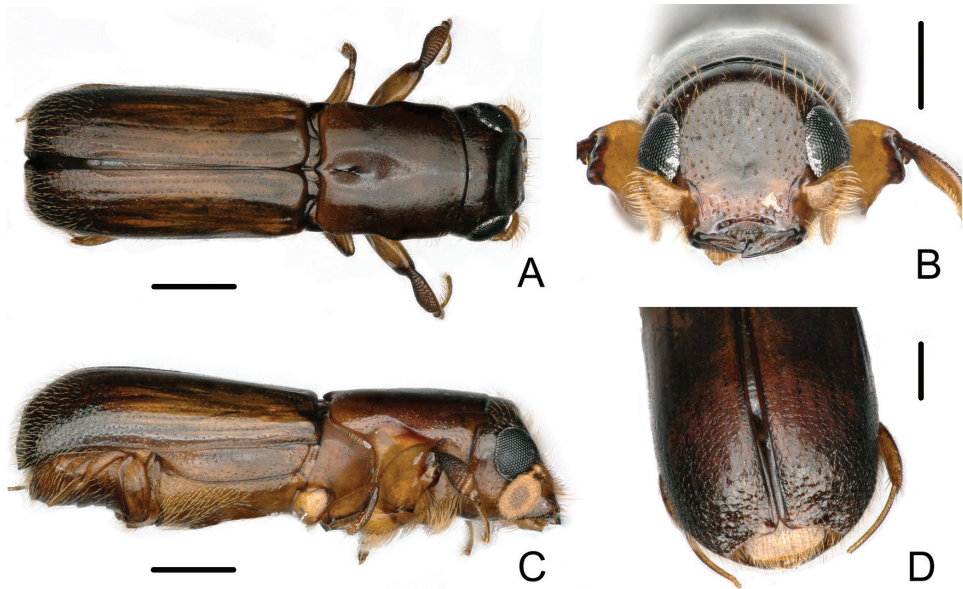


Figure 2. Female of *Crossotarsus beaveri* sp. nov. **A** dorsal view **B** head **C** lateral view **D** declivity. Scale bars: 0.5 mm.

Key to the species of *Crossotarsus* with a circular, truncate elytral declivity

- 1 Male elytral apex truncate, with a circular, shallow, concave, bluntly margined declivity; sutural apex of declivity slightly dehiscent without apical emargination. Female smaller and stouter, 2.60–2.70 mm long, 2.70–2.75 times as long as wide ***C. platypoides* Browne**
- Male elytral apex truncate, with a circular, deep, concave, acutely margined declivity, with a broad, almost circular, apical emargination. Female larger and more elongate, 3.00–3.90 mm long, 2.79–3.44 times as long as wide **2**
- 2 Male striae weakly impressed on disc of elytra (Fig. 1A); declivity gradually, obliquely truncate, its face shining, cylindrical, apex rounded with a double sutural emargination, borders of inner emargination weakly elevated, outer emargination forming pointed angles; surface of declivity with 4 longitudinal rows of granules, bearing erect, long golden setae (Fig. 1D). Female frons flat, more shining, smoother, very shallowly concave in median line; dense, shallow, small punctures bearing semierect hairs on upper part; almost flat above the epistoma below median line (Fig. 2B); striae weakly impressed on disc of elytra (Fig. 2A). 3.64–3.90 mm long ***C. beaveri* sp. nov.**
- Male striae moderately impressed on disc of elytra (Fig. 3A); declivity abruptly, vertically truncate, its face subnitid, cylindrical, apex rounded with a double sutural emargination, borders of inner emargination distinctly elevated and dilated, outer emargination forming obtuse angles; surface of declivity with

sparse, obscure granules, bearing erect, long golden setae (Fig. 3D). Female frons slightly shining, reticulate, very distinctly concave, smooth around median line; dense, deep, large punctures bearing semierect hairs on upper part; weakly, irregularly impressed above the epistoma below median line (Fig. 4B); striae moderately impressed on disc of elytra (Fig. 4A). 2.96–3.44 mm long..

..... *C. brevis* (Browne)

***Crossotarsus brevis* (Browne, 1975), comb. nov.**

Figures 3, 4

Platypus brevis Browne: Beaver and Browne 1975: 306.

Dinoplatypus brevis Browne: Beaver 1998:184.

Material examined. 7 males, 5 females (JXAU); 1 male, 1 female (RAB): CHINA: Yunnan Province, Xishuangbanna Dai Autonomous Prefecture, Jinghong City, Damanmi Village, 22°02'50"N, 100°48'27"E, ca 580 m, 20.I.2018, log dissection, host unknown, Shengchang Lai leg.

Taxonomy. The specimens in the RAB were identified by comparison to a paratype *C. brevis*, which is also in the RAB. Browne put this species in *Platypus* Herbst, noting that the apical emargination of the elytra was rather similar to that of *Platypus caliculus* Chapuis 1865 (Beaver and Browne 1975). In fact, *C. brevis* has the typical characters of *Crossotarsus*: labial palps two-segmented, with basal segments fused in the midline, whereas *Platypus* has the labial palps three-segmented, with separate basal segments. Beaver (1998) transferred the species from *Platypus* to *Dinoplatypus* Wood following Wood's (1993) attempt to split the genus *Platypus*. Wood diagnosed *Dinoplatypus* largely on the basis of the circular, truncate, elytral declivity of the male, with the sutural apex emarginate. However, this is an adaptive character of the declivity which has evolved independently more than once in the Platypodinae, as it has in the Scolytinae (Hulcr et al. 2015). Molecular phylogenetic study also shows that the few morphological characters used by Wood (1993) to erect several groups of Neotropical and Indo-Malayan/Australasian species in Platypodini to new genera are not sufficiently diagnosable for all those groups (Jordal 2015).

Browne (1961) and Beaver and Sanguansub (2015) suggested that the adult generic characters of primary value in *Crossotarsus* included the structure of the labial and maxillary palps, the form of the pronotum, the sexual dimorphism of the protibia, and various modifications of the abdominal sternites in the male. Based on the two-segmented labial palps, the lateral pronotal emarginations angulate anteriorly, the pronotum without mycangial pores, and the sexual dimorphism of the protibiae, *Platypus brevis* belongs in the genus *Crossotarsus*, and is here transferred to that genus.

Distribution. Thailand (Beaver and Liu 2013). New to China (Yunnan).

Host. *Castanopsis* sp. (Fagaceae) (Beaver and Liu 2013).

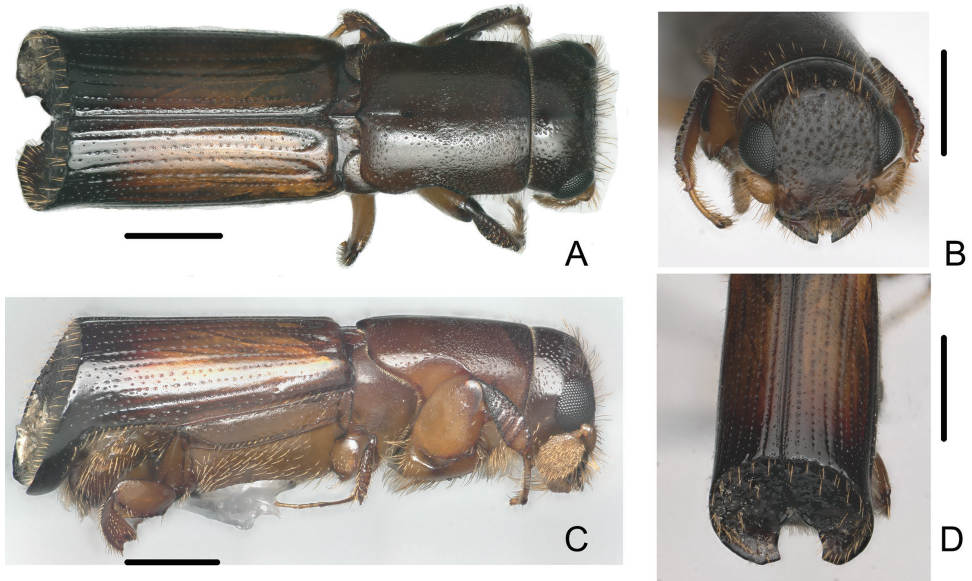


Figure 3. Male of *Crossotarsus brevis* (Browne) **A** dorsal view **B** head **C** lateral view **D** declivity. Scale bars: 0.5 mm.

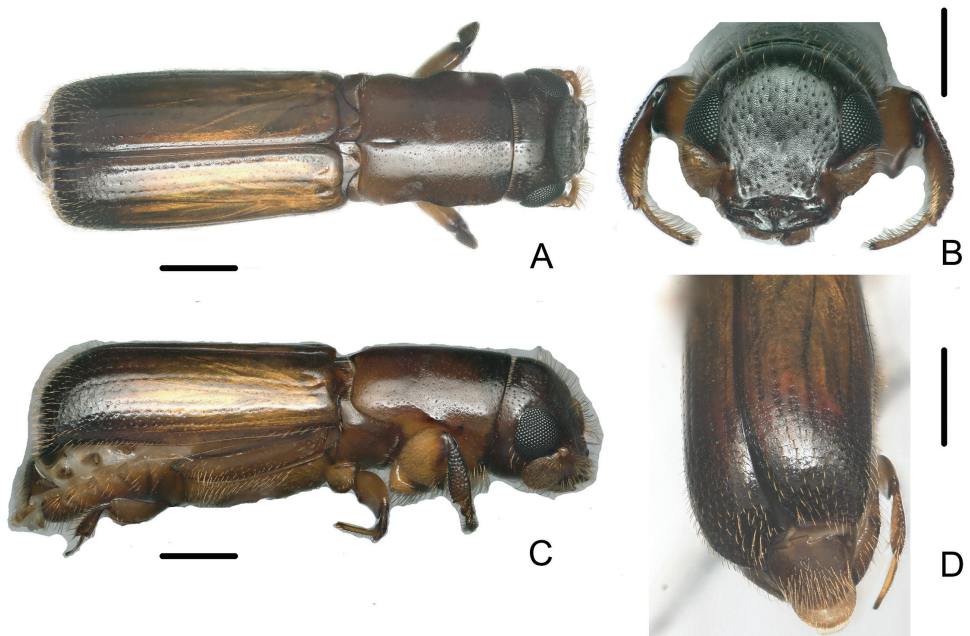


Figure 4. Female of *Crossotarsus brevis* (Browne) **A** dorsal view **B** head **C** lateral view **D** declivity. Scale bars: 0.5 mm.

New record

Crossotarsus emorsus Beeson, 1937

Figures 5, 6

Crossotarsus emorsus Beeson, 1937: 87.

Material examined. 4 males, 1 female (JXAU) CHINA: Yunnan Province, Xishuangbanna Dai Autonomous Prefecture, Jinghong City, Nabanhe River Watershed National Nature Reserve, Guomenshan, ca 1030 m, 22°14'46"N, 100°36'10"E, 27.I.2018, log dissection, host *Dalbergia assamica*, Shengchang Lai leg.; 1 male, 1 female (RAB); 1 male (JXAU) China: Yunnan Province, Xishuangbanna Dai Autonomous Prefecture, Jinghong City, Damanmi Village, ca 580 m, 22°02'50"N, 100°48'27"E, 20.I.2018, log dissection, host *Cassia siamea*, Shengchang Lai leg.

Diagnosis. *C. emorsus* is similar to *C. terminatus* but can be distinguished using the characters given in Table 3.

Distribution. Myanmar, Thailand, Laos (Beaver and Liu 2013; Beaver 2016). New to China (Yunnan).

Host. The species is recorded from trees in the families Lecythidaceae, Fabaceae, Sterculiaceae and Verbenaceae (Beeson 1937), and is presumably polyphagous (Beaver 2016). Host plants recorded here are: *Senna siamea* (Lam.) H.S.Irwin & Barneby and *Dalbergia assamica* Benth. (Fabaceae).

Molecular data. The phylogenetic tree for analyzing the evolutionary relationships of 13 taxa including the ingroups (*Crossotarsus* species) and the outgroups (*P. contaminatus*) was constructed based on four genes (Fig. 7). The BI tree shows the new species (*C. beaveri*) and the new combination (*C. brevis*) forming a clade, with high node support. These group with Schedl's (1972a) '*Crossotarsi coleoptrati*' (*C. fractus* Sampson, 1912, *C. squamulatus* and *C. terminatus*) and cluster with all remaining *Crossotarsus* species. It confirms that the taxonomic changes and the relationship of *C. brevis* and *C. brevis* are correct. It also indicates that *C. emorsus*, *C. fractus*, *C. squamulatus* and *C. terminatus* should be considered distinct species (as by Beaver and Liu 2013), and not considered synonyms or subspecies (Schedl 1972a).

Discussion

Crossotarsus beaveri is clearly related to *C. brevis*. They are the sister lineage to the *Crossotarsi coleoptrati* group, not the genus *Dinoplatypus*. This is a good example that declivity in males usually is an adaptive character and not of generic significance. We consider that the morphologically diagnosable characters of the genus *Crossotarsus* should refer to the summary by Browne (1961) and Beaver and Sanguansub (2015, 2020), as introduction.

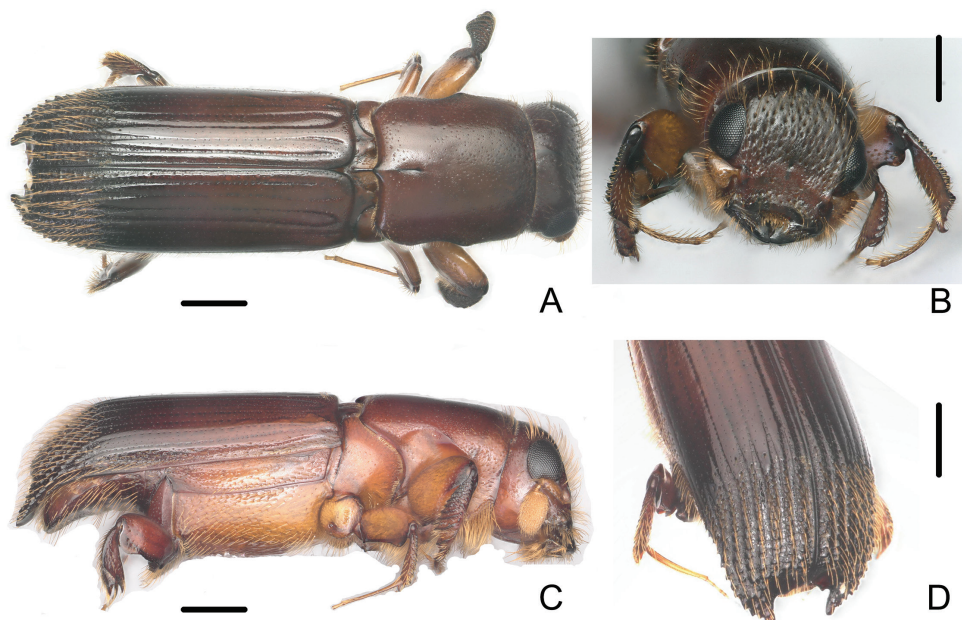


Figure 5. Male of *Crossotarsus emorsus* Beeson **A** dorsal view **B** head **C** lateral view **D** declivity. Scale bars: 0.5 mm.

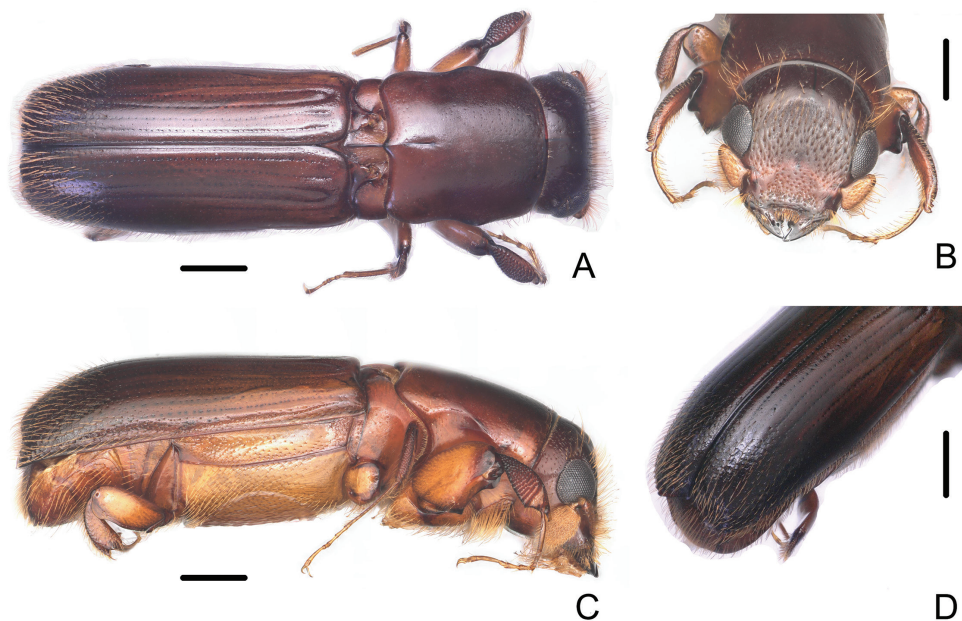


Figure 6. Female of *Crossotarsus emorsus* Beeson **A** dorsal view **B** head **C** lateral view **D** declivity. Scale bars: 0.5 mm.

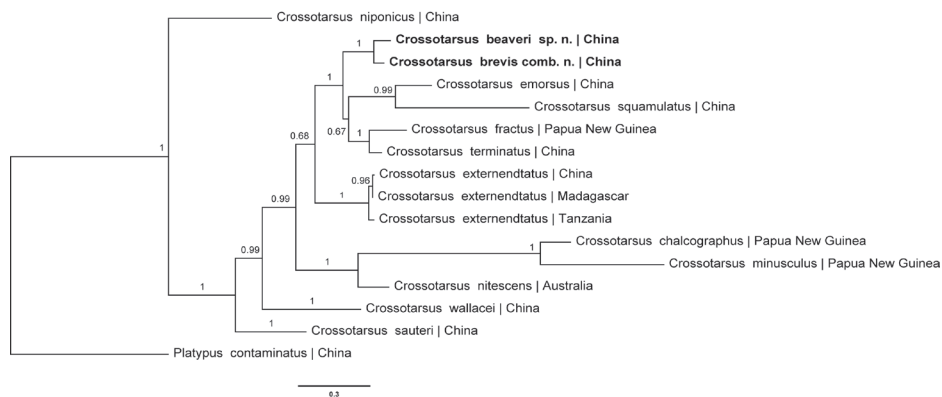


Figure 7. Tree topology resulting from Bayesian analysis of four genes. Posterior probabilities are given on the nodes. New species and new combination in boldface.

Table 3. Diagnostic characters separating *Crossotarsus emorsus* and *Crossotarsus terminatus*.

	<i>C. emorsus</i>	<i>C. terminatus</i>
Body size	Male size 4.56–4.80 mm long, 3.20–3.42 times as long as wide; Female size 4.8–5.34 mm long, 3.38–3.43 times as long as wide.	Male size 3.32–3.40 mm long, 2.78–3.00 times as long as wide; Female size 3.44–3.58 mm long, 2.87–2.93 times as long as wide.
Frons	Male frons almost flat, with shallower, irregularly placed punctures; circularly concave in median line. Female frons almost flat, without concave around median line.	Male frons coarser, with deeper, irregularly placed punctures; linearly concave in median line. Female frons concave forming a big, circular impression around concave median line.
Elytra	Male without lateral emargination at declivity base, semicircular lateral borders with serrated, lateral tubercles.	Male with lateral emargination at declivity base, semicircular lateral borders rounded, without distinct serrated, lateral tubercles.

The genus *Crossotarsus* is one of the largest genera of Platypodinae, with more than 100 species. Although there are 13 previously recorded species of Chinese *Crossotarsus* (Yin and Huang 1987; Yin et al. 2002; Zhang et al. 2008), many additional species have been reported from countries neighboring China (Beaver and Shih 2003; Goto 2009; Beaver and Liu 2013; Beaver 2016) which still have not been found in China. This strongly indicates that many more species remain to be discovered, especially on the Chinese mainland. *Crossotarsus* is monophyletic in the latest molecular phylogeny (Jordal 2015). There are few molecular data for the genus in GenBank, less than 10% of the whole. More taxonomic samples are needed.

Acknowledgements

We thank Roger Beaver for reviewing earlier manuscript drafts and kindly commenting on the status of the new species. We also appreciate the help provided by Jiaxin Liao and Yufeng Cao in our fieldwork. This research was funded by grant CARS-33-BC2-JX01 from Survey of Bark Beetles on the Rubber Tree in China Project and the National Natural Science Foundation of China (no. 31160380, 31360457, 31760543).

References

- Beaver RA (1998) New synonymy, new combinations and taxonomic notes on Scolytidae and Platypodidae (Insecta: Coleoptera). *Annalen des Naturhistorischen Museums in Wien. Serie B für Botanik und Zoologie* 100: 179–192.
- Beaver RA (2004) The genus *Crossotarsinus* Schedl (Coleoptera: Platypodidae). *Entomologist's Monthly Magazine* 140: 243–245.
- Beaver RA (2005) New synonymy in Taiwanese ambrosia beetles (Coleoptera: Curculionidae: Platypodinae). *Plant Protection Bulletin* 47: 195–200.
- Beaver RA (2016) The platypodine ambrosia beetles of Laos (Coleoptera: Curculionidae: Platypodinae). *Entomologica Basiliensia et Collectionis Frey* 35: 487–504.
- Beaver RA, Browne FG (1975) The Scolytidae and Platypodidae (Coleoptera) of Thailand: a checklist with biological and zoogeographical notes. *Oriental Insects* 9(3): 283–211. <https://doi.org/10.1080/00305316.1975.10434499>
- Beaver RA, Liu LY (2013) A synopsis of the pin-hole borers of Thailand (Coleoptera: Curculionidae: Platypodinae). *Zootaxa* 3646(4): 447–486. <https://doi.org/10.11646/zootaxa.3646.4.7>
- Beaver RA, Sanguansub S (2015) A review of the genus *Carchesiopygus* Schedl (Coleoptera: Curculionidae: Platypodinae), with keys to species. *Zootaxa* 3931(1): 401–412. <https://doi.org/10.11646/zootaxa.3931.3.4>
- Beaver RA, Sanguansub S (2020) New synonymy and taxonomic changes in Australian and oriental pin-hole borers (Coleoptera: Curculionidae, Platypodinae). *Entomologist's Monthly Magazine* 156(2): 79–86. <https://doi.org/10.31184/M00138908.1562.4024>
- Beaver RA, Shih HT (2003) Checklist of Platypodidae (Coleoptera: Curculionoidea) from Taiwan. *Plant Protection Bulletin* 44: 75–90.
- Beeson CFC (1937) New *Crossotarsus* (Platypodidae, Col.). *The Indian Forest Records* 3: 47–103.
- Bright DE (2014) A catalog of Scolytidae and Platypodidae (Coleoptera), Supplement 3 (2000–2010), with notes on subfamily and tribal reclassifications. *Insecta Mundi* 0356: 1–336.
- Blandford WFH (1894) The rhynchophorous Coleoptera of Japan. Part III. Scolytidae. *Transactions of the Entomological Society of London*, 53–141.
- Browne FG (1961) Taxonomic notes on Platypodidae (Coleoptera). *Annals and Magazine of Natural History, Series 13*, 4(47): 641–656. <https://doi.org/10.1080/00222936108651189>
- Chapuis F (1865) *Monographie des Platypides*. H. Dessain, Liège, 344 pp.
- Fairmaire L (1849) *Essai sur les coléoptères de la Polynésie*. *Revue et Magasin de Zoologie Pure et Appliquée, Série 2*, 2: 1–102.
- Goto H (2009) Taxonomic history of Japanese bark and ambrosia beetles with a check list of them. *Journal of Japanese Forest Society* 91: 479–485. <https://doi.org/10.4005/jjfs.91.479>
- Hopkins AD (1914) List of generic names and their type-species in the coleopterous superfamily Scolytoidea. *Proceedings of the United States National Museum* 48(2066): 115–136. <https://doi.org/10.5479/si.00963801.2066.115>
- Hulcr J, Atkinson TH, Cognato AI, Jordal BH, Mckenna DD (2015) Morphology, taxonomy, and phylogenetics of bark beetles. In: Vega FE, Hofstetter RW (Eds) *Bark Beetles. Biology and Ecology of Native and Invasive Species*. Academic Press, London, 41–84. <https://doi.org/10.1016/B978-0-12-417156-5.00002-2>

- Jordal BH (2013) Deep phylogenetic divergence between *Scolytoplatypus* and *Remansus*, a new genus of Scolytoplatypodini from Madagascar (Coleoptera, Curculionidae, Scolytinae). *ZooKeys* 352: 9–33. <https://doi.org/10.3897/zookeys.352.6212>
- Jordal BH (2015) Molecular phylogeny and biogeography of the weevil subfamily Platypodinae reveals evolutionarily conserved range patterns. *Molecular Phylogenetics and Evolution* 92: 294–307. <https://doi.org/10.1016/j.ympev.2015.05.028>
- Jordal BH, Sequeira AS, Cognato AI (2011) The age and phylogeny of wood boring weevils and the origin of subsociality. *Molecular Phylogenetics and Evolution* 59: 708–724. <https://doi.org/10.1016/j.ympev.2011.03.016>
- Kalyaanamoorthy S, Minh BQ, Wong TK, von Haeseler A, Jermiin LS (2017) ModelFinder: fast model selection for accurate phylogenetic estimates. *Nature Methods* 14(6): 587–589. <https://doi.org/10.1038/nmeth.4285>
- Lai SC, Liao JX, Dai XH, Wang YX, Wang JG (2019) Identification of hawthorn trunk borer (*Platypus contaminatus*), an important insect pest on hawthorn. *Plant Quarantine* 33(1): 48–51. [in Chinese with English summary]
- Lanfear R, Frandsen PB, Wright AM, Senfeld T, Calcott B (2017) PartitionFinder 2: new methods for selecting partitioned models of evolution for molecular and morphological phylogenetic analyses. *Molecular Biology and Evolution* 34(3): 772–773. <https://doi.org/10.1093/molbev/msw260>
- Murayama J (1925) Supplementary notes on the Platypodidae of Formosa. *Journal of the College of Agriculture, Hokkaido Imperial University* 15: 229–235.
- Murayama J (1934) Supplementary notes on the platypodidae of Formosa IV. *Journal of the Faculty of Agriculture, Hokkaido Imperial University* 35(3): 133–149.
- Ronquist F, Teslenko M, van der Mark P, Ayres DL, Darling A, Höhna S, Larget B, Liu L, Suchard MA, Huelsenbeck JP (2012) MrBayes 3.2: efficient Bayesian phylogenetic inference and model choice across a large model space. *Systematic Biology* 61: 539–542. <https://doi.org/10.1093/sysbio/sys029>
- Sampson FW (1912) Some new species of Ipidae and Platypodidae in the British Museum. *Annals and Magazine of Natural History, Series 8*, 10: 245–250. <https://doi.org/10.1080/00222931208693228>
- Schedl KE (1954) Fauna Indomalayensis IV. *Philippine Journal of Science* 83: 137–159.
- Schedl KE (1972a) Monographie der Familie Platypodidae Coleoptera. W. Junk, Den Haag, 322 pp.
- Schedl KE (1972b) Scheld K E. Scolytidae and Platypodidae from the Papuan subregion and Australia. 279. Contribution to the morphology and taxonomy of the Scolytidae. *Papua New Guinea Agricultural Journal* 23(3/4): 61–72.
- Schedl KE (1979) Bark and timber beetles from Australia. 326. Contribution to the morphology and taxonomy of the Scolytoidea. *Entomologische Arbeiten aus dem Museum G. Frey* 28: 157–163.
- Stebbing EP (1906) Departmental notes on insects that affect forestry. No. 3. Office of Superintendent of Government Printing, Calcutta, 335–469.
- Strohmeyer H (1912) H. Sauter's Formosa-ausbeute, Ipidae und Platypodidae (Col.). *Entomologische Mitteilungen* 1: 38–42. <https://doi.org/10.5962/bhl.part.25902>

- Strohmeyer H (1913) Neue Platypodiden. Entomologische Blätter 9: 161–165.
- Thomson J (1857) Description de trois espèces de coléoptères. Archives Entomologiques 1: 341–344.
- Wood SL (1993) Revision of the genera of Platypodidae (Coleoptera). Great Basin Naturalist 53(3): 259–281. <https://doi.org/10.5962/bhl.part.16605>
- Wood SL, Bright DE (1992) A catalog of Scolytidae and Platypodidae (Coleoptera), Part 2: taxonomic index. Great Basin Naturalist Memoirs 13: 1–1553.
- Yin HF, Huang FS, (1987) Platypodidae. In: Huang FS, Zheng LY (Eds) Forest Insects of Yunnan. Yunnan Science and Technology Press, Kunming, 854–858. [in Chinese]
- Yin HF, Huang FS, Zeng R, Li H (2002) Coleoptera: Platypodidae. In: Huang FS (Eds) Forest Insects of Hainan. Science Press, Beijing, 472–473. [in Chinese]
- Zhang D, Gao F, Jakovlić I, Zou H, Zhang J, Li WX, Wang GT (2020) PhyloSuite: an integrated and scalable desktop platform for streamlined molecular sequence data management and evolutionary phylogenetics studies. Molecular Ecology Resources 20(1): 348–355. <https://doi.org/10.1111/1755-0998.13096>
- Zhang Y, Du YZ, Zhu HB, Gu J, Zhang YZ (2008) Species record of Chinese *Crossotarsus*. Entomological Journal of East China 17(3): 205–212. [in Chinese with English summary]

Carpophiline-ID: an interactive matrix-based key to the carpophiline sap beetles (Coleoptera, Nitidulidae) of Eastern North America

Courtney L. DiLorenzo¹, Gareth S. Powell²,
Andrew R. Cline³, Joseph V. McHugh¹

1 Department of Entomology, University of Georgia, 455 Biological Sciences Building Athens, GA 30602, USA

2 Department of Biology, Brigham Young University, Provo, UT 84602, USA **3** Plant Pest Diagnostics Center, Department of Food & Agriculture, 3294 Meadowview Rd Sacramento, CA 95832, USA

Corresponding author: Courtney L. DiLorenzo (clbris14@gmail.com)

Academic editor: A. Smith | Received 8 October 2020 | Accepted 12 February 2021 | Published 6 April 2021

<http://zoobank.org/83C4652D-542C-4914-9A0B-0DD14EE4FF76>

Citation: DiLorenzo CL, Powell GS, Cline AR, McHugh JV (2021) Carpophiline-ID: an interactive matrix-based key to the carpophiline sap beetles (Coleoptera, Nitidulidae) of Eastern North America. ZooKeys 1028: 85–93. <https://doi.org/10.3897/zookeys.1028.59467>

Abstract

Carpophiline-ID is presented, a matrix-based Lucid™ key, for the adult stage of the known species of Carpophilinae (Coleoptera: Nitidulidae) of North America, east of the Mississippi River. An overview of the features and technical specifications used to build the key is provided. The list of terminal taxa used in the key represents the most current regional account for Carpophilinae, a beetle subfamily of agricultural and ecological importance. The value of matrix-based, free access keys for the identification of difficult taxa is discussed.

Keywords

Anatomy, characters, determinations, identification key, interactive key, matrix key, morphology, multi-entry key, taxonomy

Introduction

Matrix-based keys, such as Lucid keys, are often superior to traditional dichotomous keys. They allow users to follow different paths to a determination, use particular subsets of characters, use multi-state and non-traditional characters (e.g., biological, geographical, phenological, and genetic data), and allow creators to incorporate extensive supporting graphics to aid in identification (Penev et al. 2009, 2012; Cerretti et al. 2012). Lucid keys are structured around a data matrix of diagnostic characters scored for each taxon in the key. Identifications proceed by users selecting any character in the key and indicating the state observed for the specimen. The software eliminates taxa that do not match the selected criterion. This format makes the key “undirected”, allowing users to take multiple paths, skipping difficult, missing, or inapplicable characters to identify specimens. Since undirected keys work by eliminating taxa that do not match the character states observed for the subject, users may choose more than one “observed” state option if uncertain. Lucid provides a web hosting service, making these keys widely accessible for free to the scientific community and the general public. These advantages make Lucid™ keys superior to traditional dichotomous keys, especially when dealing with difficult to identify specimens.

Sap beetles are represented by ~ 4,500 species in ~ 350 genera worldwide (Ślipiński et al. 2011). Of those, ~ 165 species in ~ 30 genera are known to occur in North America (Habeck 2002). East of the Mississippi River, the subfamily Carpophilinae is represented by four genera and 21 species, most of which are widely distributed. Carpophilinae are distinguished from other Nitidulidae in the Nearctic Region by the following combination of characters: Elytra short and apically truncate, not covering pygidium and one or two preceding tergites; terminal segment of labial palpi somewhat enlarged, shorter to slightly longer than wide, widely truncate at apex; antennal grooves often elongate, convergent posteriorly; elytra lacking sutural striae, elongate marginal setae present laterally, longitudinal carinae and longitudinal rows of setae, or punctures present (Habeck 2002).

Several species of Carpophilinae, especially those in *Nitops* Murray, feed on pollen as adults. Ongoing research continues to determine pollination efficacy by these beetles, especially for plants in the genus *Annona* L. (Magnoliales: Annonaceae) (George et al. 1989; Tsukada et al. 2008; Higuchi et al. 2014). Most carpophiline taxa are associated with ripe, rotting, or dried fruits and vegetables; however, some species have demonstrated the ability to damage healthy fruit and transmit bacterial pathogens, making them pests of agricultural commodity production (Leschen and Marris 2005). Currently, best management practices for Carpophilinae in stone fruits are field sanitation, harvesting fruits before fully ripe, and using trap and kill bait stations to reduce populations levels (Hossain et al. 2006; Bartelt and Hossain 2006). Trap and kill bait stations use lures containing pheromones to capture beetles. To be successful, it is important to correctly identify the species involved so the correct pheromones can be deployed. Due to the association with ripe and stored crops, many species are spread through international food

trade. The ability for port and border inspectors to correctly identify detected carpophilines is paramount in preventing the entry of invasive exotic species at ports of entry.

Historical dichotomous keys to Carpophilinae of the USA are available (e.g., Parsons 1943; Connell 1977; Connell 1991). However, these keys exclude several eastern species and rely on difficult characters, limiting usefulness and applicability. In addition, high quality graphics illustrating each species and difficult characters are lacking from those works. To aid in accurate identification of this difficult and important group, a web-based Lucid key was developed for the Carpophilinae genera and species in eastern North America.

Project description

Taxonomic coverage

This key covers all Carpophilinae known to occur east of the Mississippi River in the USA and east of 90° longitude in Canada, including all four genera and 21 of the 34 species currently known to occur in America north of Mexico.

List of the terminal taxa included in the current version of the identification key (last update September 2020)

Caplothorax lugubris (Murray, 1864); *Caplothorax melanopterus* (Erichson, 1843); *Caplothorax sayi* (Parsons, 1943); *Carpophilus antiquus* Melsheimer, 1844; *Carpophilus brachypterus* (Say, 1825); *Carpophilus corticinus* Erichson, 1843; *Carpophilus dimidiatus* (Fabricius, 1792); *Carpophilus discoideus* (LeConte, 1858); *Carpophilus fumatus* Boheman, 1851; *Carpophilus hemipterus* (Linnaeus, 1758); *Carpophilus marginatus* Erichson, 1843; *Carpophilus marginellus* Motschulsky, 1858; *Carpophilus mutilatus* Erichson, 1843; *Carpophilus nepos* Murray, 1864; *Carpophilus pilosellus* Motschulsky, 1858; *Carpophilus tempestivus* Erichson, 1843; *Nitops craigheadi* (Dobson, 1972); *Nitops floralis* (Erichson, 1843); *Nitops ophthalmicus* (Murray, 1864); *Nitops pallipennis* (Say, 1823); *Urophorus humeralis* (Fabricius, 1798).

Images of terminal taxa

For each species represented in the key, there is a minimum of one male dorsal and one male ventral habitus photograph. All specimens imaged were determined by the second and third authors (GSP & ARC). Photographs illustrating each character and all of the various states are provided in the key. All species-specific character images are included in the appropriate Species Fact Sheet, along with corresponding dorsal and ventral habitus images. These Species Fact Sheets can be accessed by hyperlinks provided for each species in the Entities section of the key.

Characters used in the key

General features

Diagnostic characters in the key were derived from existing literature (Parsons 1943; Connell 1977; Connell 1991), study of specimens, and from museum specimen collection data. Published attributes of species were confirmed using specimens in the Smithsonian Institution National Museum of Natural History (NMNH), Illinois Natural History Survey Insect Collection (INHS-INHSIC), Florida State Collection of Arthropods (FSCA), and University of Georgia Collection of Arthropods (UGCA). Morphological terms used here follow those of Parsons (1943) and Connell (1977). An anatomical atlas is included in the Features section to aid non-specialists in interpreting characters used in the key.

The data matrix includes 41 anatomical, distributional, and ecological characters. These characters appear in the Features section, each with two to five possible character states. All features refer to either external adult anatomical structures that can be easily seen with a stereomicroscope, ecological details, or the locality where the specimen was collected. For length and ratio features, numeric ranges were derived from the literature (Parsons 1943; Connell 1977, 1991) and measurements taken from museum specimens. Morphological features are grouped by the following structures/regions: antenna, eye, pronotum, prothorax, mesothorax, elytra, metathorax, pygidium, and abdominal ventrites. This approach allows the user to quickly find characters of interest. Characters based on the distribution, ecology, and overall specimen appearance are grouped under the heading “general features.” Since some morphological features are only present in either the male or female, characters not relevant for a particular specimen can be excluded from consideration quickly by indicating the sex of the specimen. The key is intended for non-experts and is strongly image-based. For relative diagnostic characters (e.g., “dense” vs. “sparse”), users are expected to select the image of the character state that most closely matches what they observe on their specimen. As a result, they do not need to know the range of variation of that character within this taxon and do not need any special equipment other than a microscope to use the key.

List of characters used in the key

GENERAL: sex (male/female); length (mm); host association (cactus flowers/other hosts or habitats); geographic distribution (Northeast/Mid-Atlantic/Great Lakes Region/Mississippi Valley/Southeast); body convexity in lateral view (flattened/convex); body surface overall appearance (glossy/dull).

ANTENNA: antennal club shape (round/oval); antennomere coloration (abruptly darker at club/gradually darker towards club/unicolorous throughout).

EYE: ratio of eye width at widest point: intraocular distance at narrowest point (1:3 or less/between 1:4 and 1:9/1:10 or more).

PRONOTUM: pronotal disc setation length (long/not distinctly long); pronotal disc punctation density (dense/sparse/not conspicuously dense or sparse); pronotum coloration (black/dark brown/medium brown, light brown, or orange); pronotum posterior angles (broadly rounded, no distinct 'corner' created/squared due to extra anterior deflexion of lateral margin/nearly forming a 90-degree angle, not broadly rounded or squared off).

ELYTRA: elytral coloration (bearing pattern or markings/unicolorous); elytral color pattern (conspicuous yellowish humeral and apical patches/light humeral patches only/darker coloration near scutellum and apex/darker coloration near scutellum only/dark coloration near apex only); elytral coloration unicolorous (unicolorous and distinctly darker than pronotum and tergites/unicolorous and distinctly lighter than pronotum and tergites/unicolorous, similar to pronotum and tergites); shape of elytra apex (straight, squarely truncate/rounded, arching posteriorly).

PROTHORAX: ratio of prosternal process width at narrowest point between coxae to width at widest point posterior to coxae (less than 1:2/greater than 1:2); median longitudinal carina on prosternal process (present/absent).

MESOTHORAX: posterior rim of mesocoxal cavities (crenulate, not forming axillary space/smooth, not forming axillary space/smooth, forming small axillary space extending $\sim \frac{1}{4}$ posteriad along metepisternal suture/smooth, forming large axillary space extending $\frac{1}{2}$ posteriad along metepisternal suture); mesosternal median longitudinal ridge (present/absent); mesosternal anterior impunctate edge along median longitudinal ridge (present/absent, bearing longitudinal ridge only); mesosternal impunctate area near center (present/absent, punctate throughout).

METATHORAX: male metathoracic tibial shape (abruptly dilated apically/gradually dilated apically); male metathoracic femur (bearing small toothlike projection on inner margin near trochanter/lacking a tooth-like projection near trochanter); metathoracic tibial spines along posterior margin (present, distinct/absent, not distinct).

PYGIDIUM: male pygidial lateral margin shape (visibly constricted/not constricted); male supplementary segment visibility in dorsal view (visible/not visible); female pygidium bearing large oval depression with vague anterior margin at apex (present/absent); female pygidium apical flexion (deflexed ventrally/upturned medially/not flexed upward or downward); female pygidium bearing weak median longitudinal ridge (present/absent); female pygidium bearing grooves along lateral margins (present/absent); female pygidium lateral margin shape (visibly constricted/not constricted, straight); female pygidium apical margin shape (pointed, acute/broadly rounded or truncated); female pygidial disc setation length (short, at most just able to reach base of nearest seta/medium to long, clearly able to overlap adjacent setae); female pygidial disc setal density (dense/sparse); female hypopygidium setation length (apical setae longer than other setae/apical setae not distinctly different in length from other setae).

ABDOMINAL VENTRITES: male 4th ventrite setation (bearing many distinctly elongate setae medially at posterior margin/without any distinctly elongate setae); male 5th ventrite setation compared to density anterior to supplementary segment (less dense or absent/not distinctly different density); male 5th ventrite depression, shape and loca-

tion (single undivided median circular depression with coarse punctation anterior to supplementary segment/single undivided median circular depression anterior to supplementary segment/single median rounded depression divided by horizontal ridge anterior to supplementary segment/pair of elongate oval depressions lateral and anterior to supplementary segment/without any depressed area anterior to supplementary segment); male setation on supplementary segment (setose with two distinctly longer setae/etae of approximately equal length); female hypopygidium setation length (apical setae longer than other setae/apical setae not distinctly different in length from other setae).

Software technical specifications

Application: Lucid Builder 3.5 (<https://www.lucidcentral.org>, website provides technical specifications and features list)

Key Version: 1.0

Requirements for use: Java-enabled browser and internet connection

License for use of the key: Creative Commons Attribution License 4.0 (CC-BY), which permits unrestricted use, distribution, reproduction, and editing, provided the original author and source are credited.

Web location: <https://site.caes.uga.edu/carpophiline-id/>

Data resources

The data underpinning the Lucid Key (Lucid Key files) reported in this paper are deposited in the Dryad Data Repository at <https://doi.org/10.5061/dryad.h44j0zphq>

Website features

Species fact sheets

<https://site.caes.uga.edu/carpophiline-id/taxon-fact-sheets/>

All 21 species represented as entities in the key are figured with dorsal habitus, ventral habitus, and diagnostic character images. Each species fact sheet includes a diagnosis and summaries of the known biology and distribution, as well as references. Within the interactive key, these pages can be accessed through hyperlinks provided within each species entry.

Resources

<https://site.caes.uga.edu/carpophiline-id/resources/>

This section provides an anatomical atlas (also available within the key), a glossary of terminology, and diagnoses for the beetle family Nitidulidae and the subfamily

Carpophilinae. The anatomical atlas illustrates all of the structures mentioned in the key on a dorsal and/or ventral habitus image of a male specimen of *Carpophilus marginellus*. The glossary provides definitions of terms used in the key. Definitions were derived from Nichols (1989), Parsons (1943), and Connell (1977). The diagnostic pages provide lists of anatomical characters used to recognize beetles belonging to Nitidulidae and the subfamily Carpophilinae.

References

<https://site.caes.uga.edu/carpophiline-id/references/>

This section provides a list of useful references about Carpophilinae, building interactive keys, and making species fact sheets.

Conclusions and future work

Since multi-access keys enable users to skip sex-specific, hard-to-view, and rarely available characters, additional, more difficult diagnostic features (e.g., male genitalic anatomy, features on immature stages, genetic markers, etc.) will be added as they become available. A comprehensive taxonomic revision of the Carpophilinae of North America is currently being conducted (by GSP). Upon completion, newly published information may be incorporated into the data matrix and species fact sheets to update the interactive key.

This key provides a user-friendly tool that will make species-level identifications of Carpophilinae possible for specialists and non-specialists. Additions and updates will be possible as new characters become available and taxonomic changes occur within the group. The key may also be expanded to include newly discovered species, or to extend geographic distributions to create a more inclusive tool.

Acknowledgements

This work was completed in partial fulfillment of M.Sc. degree requirements at the University of Georgia for author CLB. The senior author thanks the Department of Entomology, her Advisory Committee members (W.G. Hudson, B.R. Blaauw, and J.V. McHugh), and members of the McHugh lab (B. Hounkpati, T. McElrath, C. Fair, K. Murray, B. Clark, and T. Sheehan) for their support and feedback. We thank E.R. Hoebeke (UGCA) and students from the University of Georgia Department of Entomology (C. Fair, B. Hounkpati, and C. Higashi) for beta testing the Carpophilinae-ID key. We would like to thank M. Greenland (UGA College of Agricultural and Environmental Sciences Office of Information Technology) for website technical support and M. Taylor (lucidcentral.org) for assistance with key deployment. The work was partially supported by a grant from the H.H. Ross Fund, a grant from the Georgia Peach Council, and by USDA National

Institute of Food and Agriculture, Hatch project GEO00886 (to JVM). GSP thanks the following individuals who facilitated the study of primary type material which was vital to this study: M. Barclay and M. Geiser (NHM), B. Jaeger and J. Frisch (MNHUB), P. Perkins (MCZ), F.W. Shockley (USNM), and A. Taghavian (MNHN). We also thank F.W. Shockley of the Smithsonian Institution National Museum of Natural History (NMNH), T.C. McElrath of the Illinois Natural History Survey Insect Collection (INHS-INHSIC), and P.E. Skelley and K.E. Schnepf of the Florida State Collection of Arthropods (FSCA) for loans of authoritatively determined specimens.

References

- Bartelt RJ, Hossain MS (2006) Development of synthetic food-related attractant for *Carpophilus davidsoni* and its effectiveness in the stone fruit orchards in southern Australia. *Journal of Chemical Ecology* 32(10): 2145–2162. <https://doi.org/10.1007/s10886-006-9135-7>
- Cerretti P, Tschorsnig H, Lopresti M, Di Giovanni F (2012) MOSCHweb – a matrix-based interactive key to the genera of the Palearctic Tachinidae (Insecta, Diptera). *ZooKeys* 205: 5–18. <https://doi.org/10.3897/zookeys.205.3409>
- Connell WA (1977) A key to *Carpophilus* sap beetles associated with stored foods in the United States (Coleoptera: Nitidulidae). *Cooperative Plant Pest Report* 2(23): 398–404.
- Connell WA (1991) Sap beetles (Nitidulidae, Coleoptera). In: Gorham JR (Ed.) *Insect and Mite Pests in Food. Agriculture Handbook No. 655*. United States Government Printing Office, Washington, 151–174.
- George AP, Nissen RJ, Ironside DA, Anderson P (1989) Effects of Nitidulid beetles on pollination and fruit set of *Annona* spp. hybrids. *Scientific Horticulture* 39: 289–299. [https://doi.org/10.1016/0304-4238\(89\)90122-2](https://doi.org/10.1016/0304-4238(89)90122-2)
- Habeck DH (2002) 77 – Nitidulidae Latreille, 1802. In: Arnett RH, Thomas MC, Skelley PE, Frank JH (Eds) *American Beetles (Vol. 2) – Polyphaga: Scarabaeoidea through Curculionoidea*. CRC Press, Florida, 319–321.
- Higuchi H, Tsukada M, Ninomiya T, Furukawa T, Yoshida A, Kuriyama M (2014) Pollination of cherimoya (*Annona cherimola* Mill.) by the mass-propagated beetles *Haptoncus ocularis*, *Mimemodes monstrosus*, and *Carpophilus marginellus*. *Tropical Agriculture and Development* 58(1): 18–25.
- Hossain MS, Williams DG, Mansfield C, Bartelt RJ, Callinan L, Il'ichev AL (2006) An attract-and-kill system to control *Carpophilus* spp. in Australian stone fruit orchards. *Entomologia Experimentalis et Applicata* 118(1): 11–19. <https://doi.org/10.1111/j.1570-7458.2006.00354.x>
- Leschen RAB, Marris JWM (2005) *Carpophilus* (Nitidulidae) of New Zealand and notes on Australian species. *MAF Technical Report FMA 121*.
- Nichols SW (1989) *The Torre-Bueno glossary of entomology*. Revised edition of a glossary of entomology by J.R. de la Torre-Bueno including Supplement A by George S. Tulloch. New York Entomological Society, New York, 840 pp.
- Parsons CT (1943) A revision of Nearctic Nitidulidae (Coleoptera). *Bulletin of the Museum of Comparative Zoology* 92(3): 121–278.

- Penev L, Sharkey M, Erwin T, van Noort S, Buffington M, Seltsmann K, Johnson N, Taylor M, Thompson F, Dallwitz M (2009) Data publication and dissemination of interactive keys under the open access model. *Zookeys* 21: 1–17. <https://doi.org/10.3897/zookeys.21.274>
- Penev L, Cerretti P, Tschorsnig HP, Lopresti M, Di Giovanni F, Georgiev T, Stoev P, Erwin T (2012) Publishing online identification keys in the form of scholarly papers. *ZooKeys* 205: 1–3. <https://doi.org/10.3897/zookeys.205.3581>
- Ślipiński SA, Leschen RAB, Lawrence JF (2011) Order Coleoptera Linnaeus, 1758. *Animal Biodiversity: An Outline of Higher-level Classification and Survey of Taxonomic Richness*. *Zootaxa* 3148(237): 203–208. <https://doi.org/10.11646/zootaxa.3148.1.39>
- Tsukada M, Tanaka D, Higuchi H (2008) Thermal requirement for development of *Carpophilus marginellus* (Coleoptera: Nitidulidae), a potential pollinator of cherimoya and atemoya trees (Magnoliales: Annonaceae). *Applied Entomology and Zoology* 43(2): 281–285. <https://doi.org/10.1303/aez.2008.281>

The genus *Syntozyga* Lower (Lepidoptera, Tortricidae) in China, with descriptions of two new species

Wenxu Yang¹, Ruiqin Dong¹, Xueling Song¹, Haili Yu^{1,2}

1 Shaanxi Key Laboratory for Animal Conservation, Northwest University, Xi'an, Shaanxi Province, 710069, China **2** Key Laboratory of Resource Biology and Biotechnology in Western China (Northwest University), Ministry of Education, Xi'an, Shaanxi Province, 710069, China

Corresponding author: Haili Yu (yuhaili@nwu.edu.cn)

Academic editor: E. van Nieuwerkerken | Received 3 November 2020 | Accepted 3 March 2021 | Published 6 April 2021

<http://zoobank.org/8A81FD9B-57B2-4F8D-9D53-50EAF8B429BA>

Citation: Yang W, Dong R, Song X, Yu H (2021) The genus *Syntozyga* Lower (Lepidoptera, Tortricidae) in China, with descriptions of two new species. ZooKeys 1028: 95–111. <https://doi.org/10.3897/zookeys.1028.60297>

Abstract

Species of the genus *Syntozyga* Lower, 1901 (Lepidoptera, Tortricidae, Olethreutinae) from China are studied. *Syntozyga apicispinata* **sp. nov.** and *S. similispirographa* **sp. nov.** are described, *S. pedias* (Meyrick, 1920) is recorded for the first time from China, and *S. spirographa* (Diakonoff, 1968) is newly recorded from the Chinese mainland. Adults and genitalia are illustrated, and a distribution map of the Chinese species is given. Keys to identify the Chinese species of *Syntozyga* are provided. Species of the genus are well clustered in a neighbor-joining tree based on the sequence data of the COI gene. COI sequences corresponding to the new species and *S. spirographa* (Diakonoff, 1968) are submitted to BOLD.

Keywords

Barcodes, new species, Olethreutinae

Introduction

The genus *Syntozyga*, a member of the subfamily Olethreutinae, was established by Lower (1901) with *S. psammetalla* Lower, 1901 as the type species. Diakonoff (1973) redescribed and figured *Syntozyga* species from south Asia, synonymized *Eleuthodema* Bradley, 1957 with *Syntozyga*, and placed *Syntozyga* together with five other related genera (*Bactra* Stephens, 1834, *Parabactra* Meyrick, 1910, *Henioloba* Diakonoff, 1973, *Bubonoxena* Diakonoff, 1968, and *Cyclacanthina* Diakonoff, 1973) in Bactrae, one

of his newly proposed 12 subtribes of the tribe Olethreutini. The taxonomic status of this genus group has been in dispute (Kuznetsov and Stekolnikov 1977; Razowski 1989; Dang 1990; Horak and Brown 1991; Horak 2006; Sofonkin 2007; Gilligan et al. 2018). Horak (2006) synonymized *Bubonoxena* and *Cyclacanthina* with *Syntozyga*, provided extensive descriptions, references, and pictures of *Syntozyga* adults, and discussed its relationships and taxonomy. Up to now, *Syntozyga* has contained 19 species with representatives in the Oriental, African, and Australian faunas (Lower 1901; Meyrick 1907, 1911, 1920, 1921; Turner 1916, 1945, 1946; Diakonoff 1968, 1971, 1973; Kuznetsov 1988a, b; Horak 2006; Aarvik 2008; Razowski and Trematerra 2010; Razowski and Wojtusiak 2012; Razowski 2014; Gilligan et al. 2018; Razowski and Bassi 2018). The ecology and host plants of *Syntozyga* are poorly known. Fletcher (1932) reported from India that the larvae of *S. ephippias* (Meyrick, 1907) are borers in stems of *Commelina benghalensis* (Commelinaceae). *Syntozyga sedifera* (Meyrick, 1911) was reared from *Glochidion* sp. (Phyllanthaceae) in Australia (Brown et al. 2008).

Seven full-length barcodes (COI gene, 658 bp) representing three species of *Syntozyga* are available through GenBank (accessed 20 October 2020); these are given in Suppl. material 1: Table S1.

Up to now, no species of *Syntozyga* has been known from the Chinese Mainland, but *Syntozyga spirographa* (Diakonoff, 1968) has been recorded from Taiwan (Heppner and Inoue 1992). The purpose of this paper is to provide faunistic data on the *Syntozyga* species in China. Herein, we add three species of *Syntozyga* to the reported Chinese fauna, including two new species, *S. apicispinata* sp. nov. from Tibet and Yunnan and *S. similispirographa* sp. nov. from Yunnan, and one species newly recorded for China, *S. pedias* (Meyrick, 1920) from Hainan Island, in addition to numerous records for *S. spirographa* from the Chinese mainland. Eleven COI sequences (658 bp) representing three species (*S. apicispinata* sp. nov., *S. similispirographa* sp. nov., and *S. spirographa*) were obtained (Suppl. material 1: Table S1).

Material and methods

The material examined in this study was collected by using light traps. Terminology for forewing pattern follows Brown and Powell (1991), as refined by Baixeras (2002). Methods for genitalia dissection follow Li (2002). The abdomen and genitalia were slide-mounted using Canada balsam. The specimens were examined with an Olympus SZX71 stereomicroscope. All images were captured with a digital microscope (VHX-5000).

Total genomic DNA was extracted with the Genomic DNA Extraction Kit (Tiangen Biotech., Beijing, China) from legs removed from dried adult specimens according to the manufacturer's instructions. Genomic DNA was eluted into 50 µL TE buffer and stored in a freezer (–20 °C). The target fragments of COI were amplified as described by Hebert et al. (2004). The sequences were aligned using ClustalW in MEGA 7 (Kumar et al. 2016) and the genetic distance was analyzed using the Kimura 2-Parameter model. The sequence data obtained in this study have been deposited in GenBank (Accession

numbers: MW187146–MW1871556) and in the BOLD database (Ratnasingham and Hebert 2007) (Voucher numbers: TORTR001-20–TORTR011-20).

The types of the new species are deposited in the Insect Collection of the Northwest University, Xi'an, China (NWU).

Results

Syntozyga Lower, 1901

Syntozyga Lower, 1901: 70. Type species: *Syntozyga psammetalla* Lower, 1901.

Eleuthodema Bradley, 1957: 95. Type species: *Polychrosis pedias* Meyrick, 1920.

Bubonoxena Diakonoff, [1968]: 40. Type species: *Bubonoxena spirographa* Diakonoff, [1968].

Cyclacanthina Diakonoff, 1973: 337. Type species: *Cyclacanthina episema* Diakonoff, 1973.

Remarks. Superficially, adults of *Syntozyga* are similar to many species of Olethreutini, especially members of the subtribe Olethreutae, but they lack secondary sexual structures on the wing and legs in the male, that makes it easy to identify them from Olethreutae. In the male genitalia, *Syntozyga* is readily separated from most genera of Olethreutini by the absence of an uncus and by strongly reduced socii. In the Olethreutinae, reduction of the appendages of the tegumen is also found in the tribe Grapholitini, but their valvae are extremely simple in structure and evenly spined. In contrast, *Syntozyga* is characterized by a valva with a broad sacculus projecting distally and carrying varied vestiture such as spine clusters and strong bristles or thorns; sometimes a naked lobe (or two) is present between the cucullus and the apex of sacculus (*S. cerchnograptia* Razowski, 2014, *S. triangulana* Aarvik, 2008, *S. spirographa*, *S. similispirographa* sp. nov., and *S. apicispinata* sp. nov.). Detailed descriptions of the morphology of *Syntozyga* were provided by Diakonoff (1968, 1973) and Horak (2006).

Key to Chinese species of *Syntozyga* based on habitus

- 1 Forewing with apex rounded, markings dark blackish brown, sparsely dusted with pale yellow, media fascia not interrupted medially.....***S. pedias***
- Forewing with apex projecting, or nearly square, markings dark brown, densely suffused with pale yellow, media fascia interrupted medially.....**2**
- 2 Forewing with indistinct silvery striae between markings on distal part; hindwing brown..... ***S. apicispinata* sp. nov.**
- Forewing with distinct leaden striae between markings on distal part; hindwing grayish brown.....**3**
- 3 Hindwing with termen nearly straight, not concave.....***S. similispirographa* sp. nov.**
- Hindwing with termen concave at M_2 ***S. spirographa***

Key to Chinese species of *Syntozyga* based on male genitalia

- 1 Valva without spine clusters or strong thorns from ventral edge, distal part broadly rounded, broader than basal half *S. apicispinata* sp. nov.
- Valva with a cluster of long spines or a strong thorn from ventral edge, distal part narrower than basal half 2
- 2 Valva bearing a strong thorn on apical margin of sacculus with any associated spines shorter than thorn *S. pedias*
- Valva with a cluster of long spines on apical margin of sacculus 3
- 3 Valva with median part more than 2 times apical part in width; basal excavation short, distal edge reaching middle of sacculus; a naked triangular lobe adjacent to the spine patch of cucullus ventrally, with its base distant from the cluster of long spines on sacculus *S. similispirographa* sp. nov.
- Valva with median part less than 1.5 times apical part in width; basal excavation broad, distal edge reaching 2/3 of sacculus; a naked triangular lobe between the spine patch of cucullus and the cluster of long spines on sacculus, its base adjacent to the spine cluster *S. spirographa*

Syntozyga pedias (Meyrick, 1920)

(Figs 1, 5, 9)

Polychrosis pedias Meyrick, 1920: 347 (♀, Bengal).

Eucosma familiaris Meyrick, 1921: 153 (♂♀, Java).

Lobesia pedias: Clarke, 1958: 472 (fig. 2b of holotype).

Syntozyga pedias Diakonoff, 1973: 341 (Cheng [sic] Mai, Kuala Lumpur, Borneo, Bali, Celebes, Western New Guinea) (figs 515, 531–533, 537, 546).

Material examined. CHINA, Hainan Prov.: 1♂, Datian Reserve, 19°06'N, 108°47'E, alt. 25 m, 1 Jul. 2009, leg. Zhaohui Du and Linlin Yang.

Distribution. India, Indonesia, Thailand, Malaysia, China (Hainan).

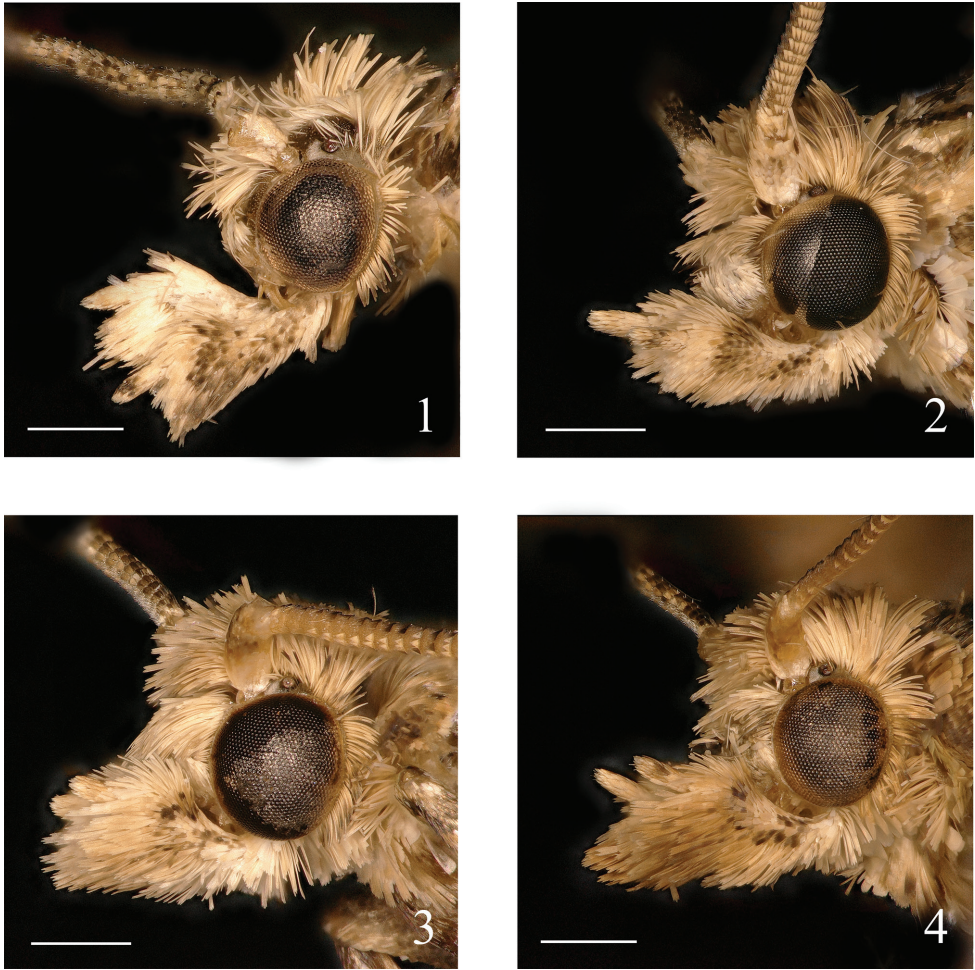
Note. This species is newly recorded for China. The male genitalia accord well with those of the lectotype of *Eucosma familiaris* from Java figured by Diakonoff (1973).

Syntozyga apicispinata Yang & Yu, sp. nov.

<http://zoobank.org/31C77B40-5FA3-4633-B34C-3E3C6E01EB87>

(Figs 2, 6, 10b)

Type material. *Holotype*: CHINA, Tibet: Motuo County, Bengbeixiang, 29°24'N, 95°17'E, alt. 990 m, 12 Aug. 2017, leg. Mujie Qi and Xiaofei Yang, genitalia slide no. YWX18246. *Paratypes*: CHINA, Tibet: 6♂, same data as holotype; 2♂, same data as holotype except 29°25'N, 95°18'E, alt. 810 m, 15 Aug. 2017; 3♂; same data as



Figures 1–4. Heads of *Syntozyga* **1** *S. pedias*, Hainan (male) **2** *S. apicispinata* sp. nov., Tibet (male holotype) **3** *S. spirographa*, Hainan (male) **4** *S. similispirographa* sp. nov., Yunnan (male holotype). Scale bars: 0.5 mm.

holotype except alt. 750 m, 31 Jul.–1 Aug. 2018, leg. Mujie Qi; **Yunnan Prov.:** 1♂, Xishuangbanna, Guanping, 22°46'N, 100°59'E, alt. 1200 m, 18 Aug. 2005, leg. Yingdang Ren; 1♂, Xishuangbanna, Yexianggu, 22°10'N, 100°52'E, alt. 760 m, 11 Jul. 2015, leg. Kaijian Teng and Xia Bai; 1♂, Mengla, Bubeng, 21°36'N, 101°35'E, alt. 650 m, 31 Jul. 2020, leg. Yongyan Li and Wenxu Yang.

BOLD voucher no. TORTR001-20, TORTR008-20, TORTR009-20, TORTR010-20, TORTR011-20.

Diagnosis. Externally, *S. apicispinata* is similar to *S. spirographa* (Diakonoff, 1968) and *S. similispirographa*, but the relatively paler striae derived from the costal strigulae and the brown or pale brown hindwing can be used to separate it from the latter two species. The male genitalia of *S. apicispinata* are very different from those of *S. spirographa* and *S. similispirographa*. It can be best distinguished by a distally broad, ovate valva,

a finger-like prominence on costa, the absence of a cluster of long spines on apex of sacculus, the presence of a cluster of short spines below apex of cucullus and a stout phallus with minute cornuti apically. Within the genus, this species resembles *S. episema* (Diakonoff, 1973) from Java and Sumba in the male genitalia, but it can be separated from *S. episema* by the valva with its ventral edge not concave in the middle and without long thorns, a sacculus with a sharp, triangular prominence on ventral margin of basal excavation, and a cucullus bearing a cluster of short spines below apex. In *S. episema*, the ventral edge of the valva is concave medially and is densely set with several long thorns, there is no prominence on the ventral margin of the basal excavation and the apical part of cucullus has no prominent spine clusters. *Syntozyga apicispinata* also resembles *S. negligens* (Diakonoff, 1973) from Java and Sulawesi in the male genitalia, but it can be distinguished from the latter species by the valva with its apical part broader than its basal part and having a sharp triangular prominence on the ventral margin of the basal excavation. In *S. negligens*, the apical part of the valva is narrower than its basal part, and there is no projection from the ventral margin of the basal excavation.

Description. Male (Fig. 6). Forewing length 5.5–6.5 mm. **Head** (Fig. 2): ocellus well developed; chaetosemata present. Frons smooth, creamy white; vertex roughly scaled, creamy. Antenna with scape creamy, flagellum dark brown, dusted with pale brown distally. Labial palpus porrect, creamy suffused with pale brown, median segment expanded slightly, terminal segment 1/2 times of median segment in length, brown apically.

Thorax: creamy, dusted with brown and dark brown medially; posterior crest distinct. Collar creamy. Tegula dark brown basally and creamy suffused pale brownish yellow distally. Hind tibia not expanded, without hair pencil in male. Forewing elongate subrectangular, costa evenly arched, apex blunt, termen oblique; upperside general ground color creamy, with markings dark brown and dusted with pale brownish yellow; costal strigulae creamy white, the fifth and sixth pairs suffused with gray brown; basal fascia broken into two parts, a small blotch on costa and an obliquely arched streak extending to inner margin of wing; subbasal fascia consisting of three parts, an oblique blotch on costa, an irregular blotch between upper edge of cell and $1A+2A$, and an indistinct spot or shadow on base of dorsum; a discontinuous pale streak present between pairs of strigulae three and four, extending to dorsum; media fascia broken medially, anterior half fused with costal part of postmedian fascia forming a conspicuous subtriangular patch on costa, extending to midwing, lower part present between midwing and distal half of dorsum, indistinct and intricate, confluent with the surrounding spots and pretornal patch; postmedian fascia obliquely arched, indistinct between $2/3$ length of R_2 and midlength of R_3 , lower part elongate, extending to termen between M_2 and CuA_1 ; a short line present on costa between strigulae seven and eight; preterminal fascia and terminal fascia as two elongate streaks confluent to termen; cilia pale brown fixed with dark brown and creamy; underside yellowish brown to brown. Hindwing subtriangular, brown; cilia pale brown; underside pale brown.

Abdomen: male genitalia (Fig. 10): tegumen low, with ear-like shoulders laterally and a moderately broad, rounded triangular top with some hairs; vinculum a scler-

rotized band, strong, somewhat W-shaped; uncus absent; socii strongly vestigial, indicated by a narrow patch of sparse spines on ventrodistal margin of tegumen; gnathos a weakly sclerotized band; valva broad, oval, costa with a folded ridge from the base to the apex, a short finger-like prominence protruding from the middle of the ridge bearing long thorns basally and apically, basal excavation large, sacculus narrow with three sclerotized, naked lobes (Fig. 10a): one small subtriangular sitting on the ventral margin of the basal excavation medially, the other two large, rounded, occupying the distal half of the sacculus, positioned right next to each other, the inner one with its edge smooth, the outer one with its edge serrated; a patch of thin, short bristles present beyond the basal excavation; cucullus membranous, roughly as long as basal part of valva, broadly rounded, with bristles along margin, a short conspicuous lobe proximal to apical margin, carrying a dense cluster of spines; phallus short and stout, with tiny spiny cornuti apically (Fig. 10b).

Female unknown.

Etymology. The specific name is derived from the Latin prefix *apici-* (= apical) and the adjective *spinatus* (= spiny), indicating the apical spine cluster of the valva.

Syntozyga spirographa (Diakonoff, 1968)

(Figs 3, 7a, 11, 13)

Bubonoxena spirographa Diakonoff, 1968: 66 (♂, Luzon) (figs 82, 103–104, 540).

Syntozyga spirographa: Diakonoff, 1973: 346 (North Celebes, West Sumatra) (figs 516, 547).

Material examined. **CHINA, Chongqing:** 2♂, Mt. Jinfo, 29°02'N, 107°11'E, alt. 1100 m, 5 May 2013, leg. Xiaofei Yang; **Fujian Prov.:** 1♀, Xiamen, 24°35'N, 117°55'E, alt. 40 m, 11 Jul. 2010, leg. Bingbing Hu and Jing Zhang; 1♀, same data except 28 Jun. 2012, leg. Zhibo Wang; **Guangxi Prov.:** 4♂, Yizhou, Pingxin village, 24°40'N, 108°21'E, alt. 150 m, 16 Aug. 2011, leg. Shulian Hao and Yinghui Sun; 8♂, 1♀, Pingxiang, 22°01'N, 106°51'E, alt. 190 m, 300 m, 550 m, 26 Jun.–2 Aug. 2011, leg. Bingbing Hu; 1♂, same data except alt. 280 m, 15 May 2012, leg. Xiaofei Yang; 1♂, same data except 23 Mar. 2013; **Guizhou Prov.:** 1♂, Libo, Banzhai village, 25°13'N, 108°10'E, alt. 530 m, 9 Aug. 2018, leg. Meiling Zheng, Jiaqi Deng and Xiaojun Zhu; 1♂, same data except alt. 510 m, 24 Jul 2019, leg. Mengran Xing, Baixue Zhao and Hao Sun; **Hainan Prov.:** 1♂, Lingao County, Mt. Duowenling, 19°47'N, 109°45'E, alt. 120 m, 9 May 2009, leg. Bingbing Hu and Qing Jin; 2♂, Lingshui, Mt. Diaoluo, 18°39'N, 109°56'E, alt. 80 m, 21–22 Apr. 2013, leg. Yinghui Sun, Wei Guan and Tengting Liu; 1♂, Changjiang County, Qichazhen, 19°6'N, 109°4'E, alt. 130 m, 4 May 2013, leg. Yinghui Sun, Wei Guan and Tengting Liu; 1♂, Baisha County, Hongxin village, 19°40'N, 109°31'E, alt. 460 m, 1 Jul. 2014, leg. Peixin Cong, Linjie Liu and Sha Hu; 1♂, Ledong, Jianfengzhen, 18°41'N, 108°46'E, alt. 50 m, 12 Jul. 2014, leg. Peixin Cong, Linjie Liu and Sha Hu; 1♂, Dongfang, Datian village, 19°3'N,

108°50'E, alt. 120 m, 2 Jan. 2018, leg. Mujie Qi and Shuai Yu; 1♂, Dongfang, Lemei village, 19°8'N, 108°84'E, alt. 80 m, 3 Jan. 2018, leg. Mujie Qi and Shuai Yu; **Yunnan Prov.:** 3♂, 1♀, Mengla, River Nanla, 21°59'N, 101°58'E, alt. 650 m, 12–14 Jul. 2013, leg. Shurong Liu, Yuqi Wang and Kaijian Teng.

BOLD voucher no. TORTR003-20, TORTR004-20, TORTR005-20, TORTR006-20.

Distribution. Philippines, Indonesia, China (Chongqing, Fujian, Guangxi, Guizhou, Hainan, Yunnan, Taiwan).

Notes. In China, previously Taiwan was the only area where *S. spirographa* had been collected (Heppner and Inoue 1992). In the present study, we identified this species from six provinces of the Chinese mainland for the first time, with a distribution to the south of latitude 30°N and between longitudes 100°E and 118°E.

***Syntozyga similispirographa* Yang & Yu, sp. nov.**

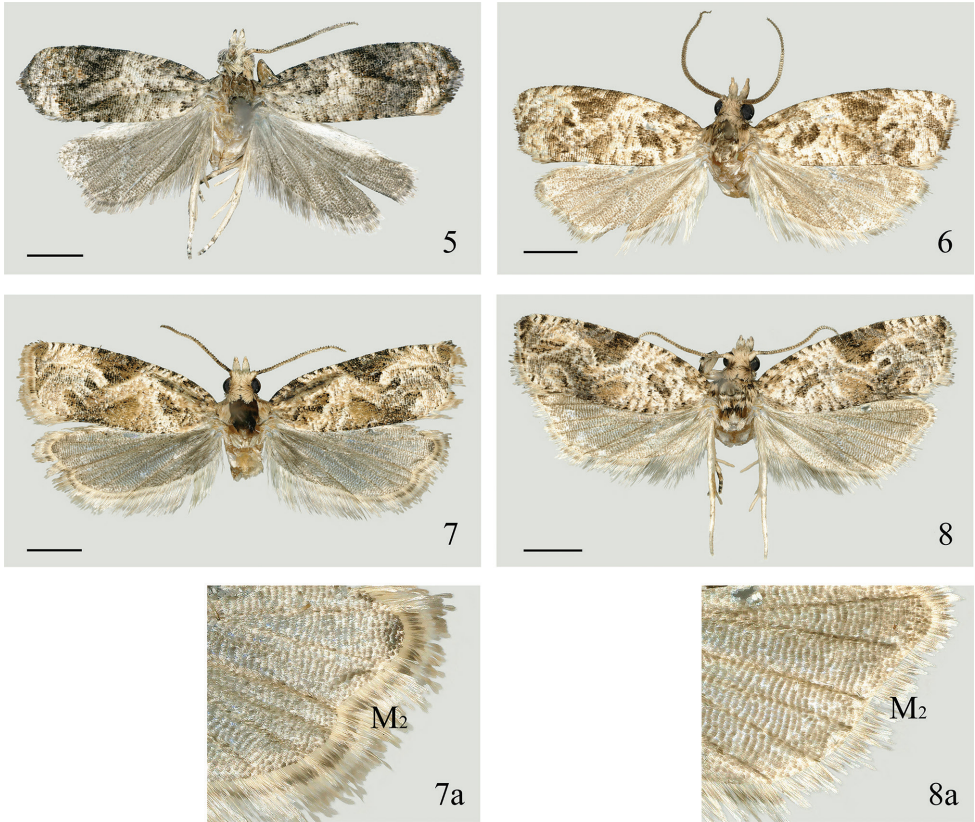
<http://zoobank.org/DC2336BD-4545-47A5-ADE7-E0A24270AEE3>

(Figs 4, 8a, 12a, 14)

Type material. *Holotype:* CHINA, **Yunnan Prov.:** 1♂, Longling, Xiaoheishan Reserve, 24°52'N, 98°84'E, alt. 1970 m, 30 Jul. 2015, leg. Kaijian Teng and Baixia, genitalia slide no. YWX18337. *Paratypes:* CHINA, **Yunnan Prov.:** 3♂, same data as holotype except 17–19 Jul. 2013, leg. Shurong Liu, Yuqi Wang and Kaijian Teng; 1♂, Pu'er, Mt. Yunpan, 22°41'N, 100°39'E, alt. 1400 m, 9 Jul. 2013, leg. Zhenguo Zhang; 1♂, same data except alt. 1620 m, 6 Aug. 2020, leg. Wenxu Yang; 1♂, Pu'er, Sun River Reserve, 22°35'N, 101°06'E, alt. 1600 m, 11 Jul. 2013, leg. Zhenguo Zhang; 16♂, same data except alt. 1450 m, 13 May–3 Jun. 2014; 8♂, 2♀, Pu'er, Sun River Reserve, 22°60'N, 101°11'E, alt. 1630 m, 6–7 Jul. 2013, leg. Shurong Liu, Yuqi Wang and Kaijian Teng; 1♂, Pu'er, Sun River Reserve, 22°68'N, 101°03'E, alt. 1450 m, 6 Jul. 2015, leg. Kaijian Teng; 1♀, Jingdong, 22°60'N, 101°11'E, 18 Aug. 2009, leg. Xicui Du.

BOLD voucher no. TORTR002-20, TORTR007-20.

Diagnosis. *Syntozyga similispirographa* is very similar to *S. spirographa* in external appearance. The shape of the hindwing termen is the only stable superficial character to identify the two species, it is concave at M_2 in *S. similispirographa* and straight in *S. spirographa*. However, the genitalia in both sexes are distinct. In *S. similispirographa*, the apical part of the cucullus is obviously narrow, less than half the width of the median part of the valva; the basal excavation is short, reaching only to mid length of sacculus; the naked triangular lobe is adjacent to the spine patch of cucullus, its base is distant from the cluster of long spines of sacculus; the phallus is moderately wide, with its width at middle about 1/5 its length. In *S. spirographa*, the apical part of cucullus is rounded, more than 2/3 the width of the median part of the valva; the long basal excavation is extending to 2/3 length of sacculus; the naked, triangular lobe is situated between the spine patch of cucullus and the cluster of long spines on sacculus, its base is adjacent to the spine cluster; the phallus is slender, its width in middle is about 1/8 its length. In the female

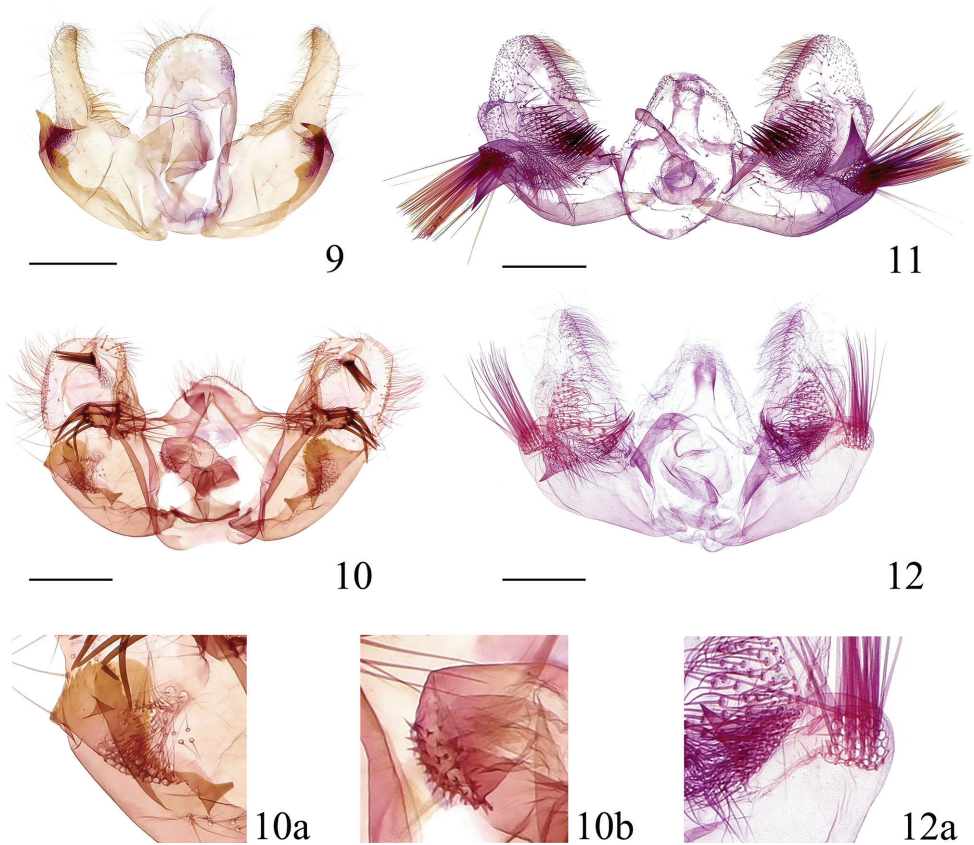


Figures 5–8. Adults of *Syntozyga* **5** *S. pedias*, Hainan (male) **6** *S. apicispinata* sp. nov., Tibet (male holotype) **7** *S. spirographa*, Hainan (male) **7a** termen of hindwing **8** *S. similispirographa* sp. nov., Yunnan (male holotype) **8a** termen of hindwing. Scale bars: 1.5 mm.

genitalia of *S. similispirographa* the sterigma is complex and not flat, including the anteriorly raised, spinulose lamella antevaginalis and two naked, concave lateral extensions. In *S. spirographa*, the sterigma is relatively uniform structure, indicated by the large, wholly spinulose lamella antevaginalis which is extending posteriorly and laterally. Externally *S. similispirographa* also resembles *S. apicispinata*, but the leaden striae on the forewing and the relatively darker, more grayish hindwing separate it from the latter species.

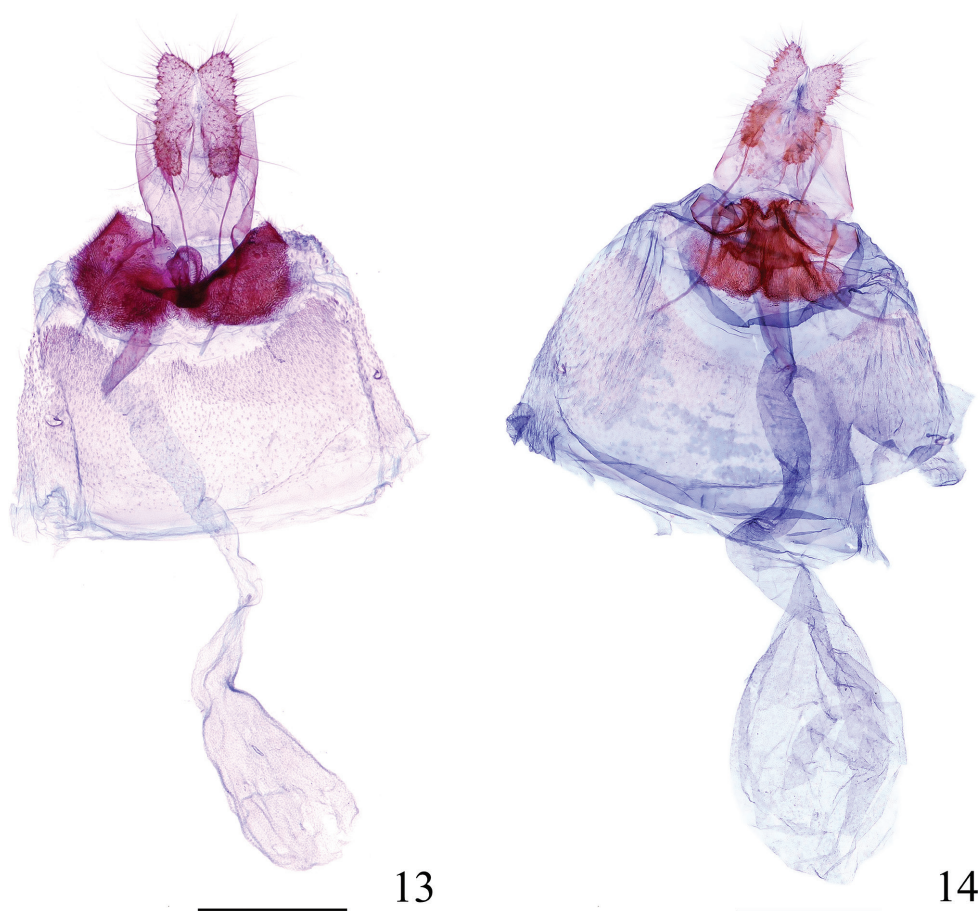
Description. Adult (Fig. 8). Forewing length 5.0–7.0 mm in male, 5.5–7.0 mm in female. **Head** (Fig. 4): ocellus well developed; chaetosemata present. Frons smooth, white; vertex roughly scaled, creamy. Antenna with scape creamy, flagellum brown. Labial palpus porrect to ascending, pale creamy, median segment widened in distal half, dusted with brown and dark brown laterally, terminal segment slender, about half length of median segment, sparsely or slightly dusted with brown.

Thorax: creamy, dusted with brown medially; posterior crest distinct. Collar creamy. Tegula dark brown basally and creamy suffused with yellow and pale brown distally. Hind tibia not expanded, without hair pencil in male. Forewing elongate subrectangular,



Figures 9–12. Male genitalia of *Syntozyga* **9** *S. pedias*, Hainan, slide no. YHL07156 **10** *S. apicispinata* sp. nov. (holotype), Tibet, slide no. LYY18320 **10a** naked lobes **10b** cornuti **11** *S. spirographa*, Hainan, slide no. LKL15037 **12** *S. similispirographa* sp. nov. (paratype), Yunnan, slide no. YWX18337 **12a** naked lobe. Scale bars: 0.5 mm.

costa lightly curved throughout, apex rounded-rectangular, termen oblique; upperside ground color creamy white, markings dark brown dusted densely with yellow; costal strigulae creamy white, basal two pairs suffused with yellow; basal fascia broken, indicated by a small blotch below base of costa and a short streak on inner margin of wing; subbasal fascia represented by a darker brown spot on costa, an oblique blotch between 2/5 length of cell and 1/3 length of 1A+2A, and several faint ripples above the basal part of dorsum; leaden striae from strigulae three and four distinct on disc of cell and extending obliquely to 2/3 length of dorsum and confluent with significant leaden striae from strigulae five and six below distal part of lower edge of cell, thus separating media fascia; upper part of media fascia fused with costal part of postmedian fascia, forming a large, somewhat inverted triangular patch, lower part of media fascia between distal part of cell and dorsum, oblique triangular; a darker brown dot on outer edge of cell often present; pretornal patch distinguishable, oblique elongate; lower part of postmedian fascia oblique, present between midlength of R_4 and 2/3 length of M_2 , surrounded by leaden



Figures 13, 14. Female genitalia of *Syntozyga* **13** *S. spirographa*, Fujian, slide no. YWX18338 **14** *S. similispirographa* sp. n. (paratype), Yunnan, slide no. YWX18342. Scale bars: 0.5 mm.

striae from distal five pairs of costal strigulae, which broadly extend to tornus; preterminal fascia indistinguishable; terminal fascia a narrow streak, extending along termen to M_2 ; cilia pale brown mixed dark brown and creamy; underside yellowish brown to brown. Hindwing subtriangular, termen nearly straight (Fig. 8a); pale gray-brown to pale brown; cilia gray to pale brown; underside pale gray to pale brown.

Abdomen: male genitalia (Fig. 12): tegumen low, with a rounded or triangular top; vinculum a narrow band; socii indicated by a narrow spine patch, below margin of tegument apex; gnathos a weakly sclerotized band; valva somewhat triangular, basal half gradually widening, medially about twice as wide as distal part of cucullus; basal excavation short, distal edge reaching about 1/2 length of sacculus; sacculus broad, almost naked except for prominent and rounded apex bearing a cluster of very long spines; cucullus triangular, gradually narrowed to apex, apex rounded-acute, disc area with an elongate semicircular patch of spines, an acute triangular lobe proximate to this spine patch ventrally, naked, with its base distant from the cluster of long spine on

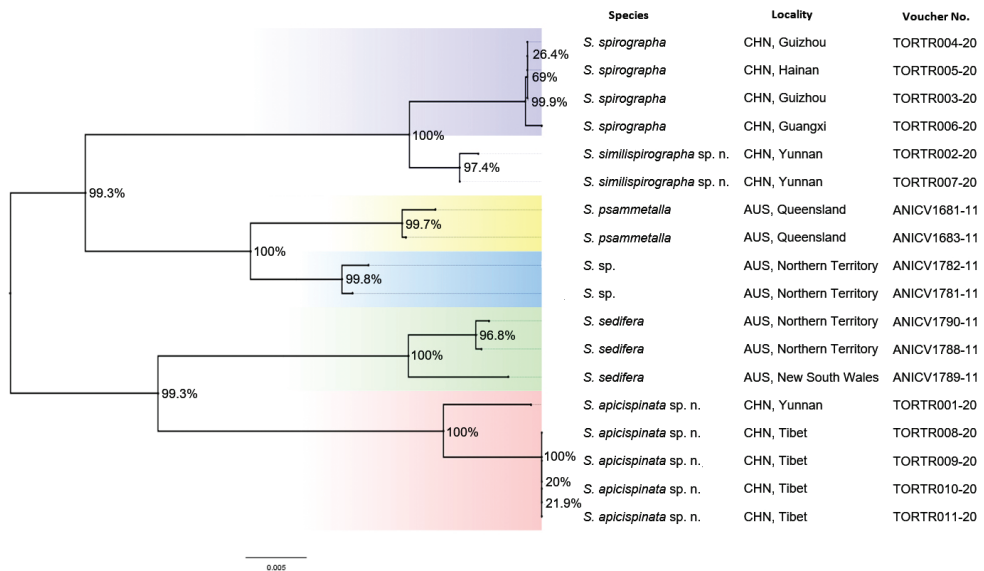


Figure 15. Neighbor-joining Tree, based on DNA barcodes of *Syntozyga* species. Numbers above/below branches refer to bootstrap proportions.

sacculus (Fig. 12a); a rounded lobe projecting along basal half of ventral margin, short, sparsely set with fine spines; apex with dense spines dorsally; phallus moderately long and wide, tapering towards apex, without cornuti. Female genitalia (Fig. 14): papilla analis narrow and elongate. Sternum 7 weakly sclerotized and with a concave hind margin. Sterigma an irregularly shaped complex structure, lamella antevaginalis broad, spinulose, raised medially and with a longitudinal groove anteriorly, ostium flanked by two concave, naked and petal-shaped pockets. Ductus bursae membranous and smooth, with weakly sclerotized and ill-defined colliculum, faintly widening towards corpus bursae. Corpus bursae ovate, weakly granular, without signa.

Etymology. This specific name is derived from the Latin prefix *simil-* (= similar) and the taxon name *spirographa*, referring to the similarity of this new species to *S. spirographa* (Diakonoff).

Molecular data analyses

All results are based on 18 COI gene sequences belonging to the six species listed in Suppl. material 1: Table S1. Of these, 11 sequences were newly obtained, and seven sequences were taken from GenBank. All sequences are 658 bp in length, and the genetic distances are presented in Suppl. material 1: Table S2. The interspecific genetic distances within the six species varied from 1.4% (*S. spirographa* to *S. similispirographa*) to 8.9% (*S. apicispinata* to *S. spirographa*), and the average divergence is 6.5%. The intraspecific divergence in the six species (including the unidentified species, *Syntozyga* sp.) varied from 0 to 1.5% (*S. sedifera*, individual of *S. apicispinata* from Yunnan to those from Tibet) and the average divergence is 0.4%. A neighbor-joining (NJ) tree

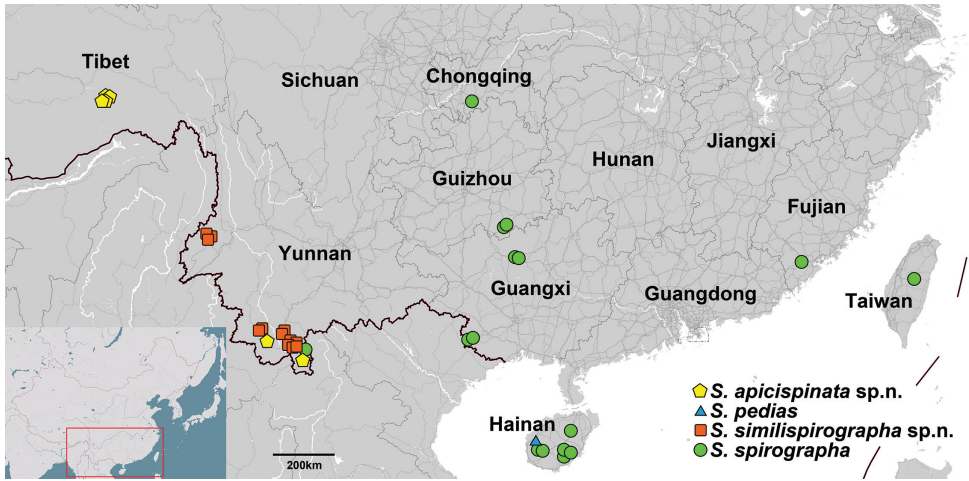


Figure 16. Distribution of *Syntozyga* species in China.

(Fig. 15) covering the above six species was generated for facilitating species delimitation. Six well-supported clades of *Syntozyga* sequences are revealed by the NJ tree, each clade of which represents one species.

Discussion

In Lepidoptera, barcode divergence of approximately 2% is often congruent with morphology-based species-level identifications (Hajibabaei et al. 2006; Zahiri et al. 2014). In this present study, we found that *S. similispirographa*, with a similar appearance to *S. spirographa*, shows a low divergence (1.4%) in their COI barcodes. However, distinct and consistent differences between genital structures in both sexes of the two species can be observed, such as shape and size of basal excavation, width of cucullus, location of the naked, triangular lobe near the cluster of long spines in the male, and sterigma shape in the female (Figs 11–14). Low interspecific genetic divergence of congeneric species pairs may mean recent origin or mitochondrial introgression (Muñoz et al. 2011; Zahiri et al. 2014), and it is risky to draw conclusions about species identification from mtDNA sequence alone (Ritter et al. 2013; Lukhtanov et al. 2015). Therefore, based on significant morphological difference between the two populations in China, in contrast to the consistent genitalia morphology of *S. spirographa* across its wide range, we described individuals from Sun River Reserve and Xiaoheishan Reserve, Yunnan Province, as a distinct species, *S. similispirographa* sp. nov.

Compared to other members of Olethreutini, the Chinese species of *Syntozyga* have a rather long and slender terminal segment of their labial palpus, which is clearly projected, especially in the two new species.

Three species, *S. spirographa*, *S. similispirographa*, and *S. apicispinata*, are distributed in an area 200 km across in southern Yunnan (Fig. 16). They share the forewing pattern

characterized by complicated markings of sinuate pattern elements, with a large, dark-brown, inverted triangle over the central 1/4 of the costa. But while they are difficult to distinguish externally, they have two distinct configurations of the male genitalia. *Syntozyga apicispinata* is characterized by a well-sclerotized sacculus with strongly sclerotized edge, a wide, rounded cucullus with a spined process from its costa and a stout phallus, and has a close relationship with three species described by Diakonoff (1973) (*S. episema*, *S. negligens* and *S. monosema*) from Indonesia and Sri Lanka. In *S. spirographa* and *S. similispirographa*, the male has an expanded sacculus bearing a cluster of very long spines distally, a distally narrowing cucullus with a central spine patch basally and a slender phallus, similar to the south Asian species, *S. ephippias*, and the African *S. tryphera* Razowski & Wojtusiak, 2012 and *S. cerchnograptus*. Accordingly, there is high genetic divergences between *S. apicispinata* and the other two Chinese species, 8.3% to *S. spirographa* and 8.9% to *S. similispirographa*.

The distribution of the four species of *Syntozyga* in China is shown in Fig. 16. *Syntozyga spirographa* has a relatively broad distribution in southern China, but specimens from different localities agree in appearance and genital structure. There is a slight genetic difference (0.2%) between material from Yizhou (Guangxi Prov.) and the other two localities, Libo (Guizhou Prov.) and Dongfang (Hainan Prov.). This is somewhat puzzling as Yizhou is near Libo and located between Libo and Dongfang. Knowledge of host plant association might provide an answer, so further examination is desirable. High intraspecific divergence was observed in the discontinuously distributed *S. apicispinata* (1.5%), collected in southern Tibet and southern Yunnan, respectively, separated by 900–1000 km. However, no obvious genital variation was found between the two populations. *Syntozyga similispirographa* has a narrow distribution in two locations of southwest Yunnan, the Sun river and the Xiaoheishan reserves, separated by approximately 400–500 km. The genetic divergence between two male specimens collected in these two localities is 0.2%. Although *S. pedias* is distributed widely in south-east Asia (India, Thailand, Indonesia), it is only known from Hainan Island in China.

Acknowledgements

We give our cordial thanks to Prof. Houhun Li (Nankai University, Tianjin) for providing the specimens used in this study. We also express our sincere thanks to those who participated in the fieldwork. Special thanks are due to the editor and two reviewers for their critical reviews and linguistic assistance. This research was supported by the National Natural Science Foundation of China (grant no. 31000972) and the Foundation of the Shaanxi Educational Committee of China (grant no. 18JS107).

References

- Aarvik L (2008) New data on Bactrini (Lepidoptera, Tortricidae) from Africa. *Norwegian Journal of Entomology* 55: 7–13.

- Baixeras J (2002) An overview of genus-level taxonomic problems surrounding *Argyroplote* Hübner (Lepidoptera: Tortricidae), with description of a new species. *Annals of the Entomological Society of America* 95(4): 422–431. [https://doi.org/10.1603/0013-8746\(2002\)095\[0422:AOOGLT\]2.0.CO;2](https://doi.org/10.1603/0013-8746(2002)095[0422:AOOGLT]2.0.CO;2)
- Brown RL, Powell J (1991) Description of a new species of *Epiblema* (Lepidoptera: Tortricidae: Olethreutinae) from coastal redwood forests in California with an analysis of the forewing pattern. *Pan-Pacific Entomologist* 67(2): 107–114.
- Brown JW, Robinson G, Powell JA (2008) Food plant database of the leafrollers of the world (Lepidoptera: Tortricidae) (Version 1.0). <http://www.tortricid.net/foodplants.asp>
- Dang PT (1990) Redefinition of the tribe Bactrini Falkovitsh and revised status of genera *Taniva* Heinrich and *Hulda* Heinrich (Tortricidae: Olethreutinae). *Journal of the Lepidopterists' Society* 44: 77–87.
- Diakonoff A (1968) Microlepidoptera of the Philippine Islands. *US National Museum Bulletin* 257: 1–484. <https://doi.org/10.5479/si.03629236.257.1>
- Diakonoff A (1971) South Asiatic Tortricidae from the Zoological Collection of the Bavarian State (Lepidoptera). *Veröffentlichungen der Zoologischen Staatssammlung München* 15: 167–202.
- Diakonoff A (1973) The south Asiatic Olethreutini (Lepidoptera, Tortricidae). *Zoologische Monographiën van het Rijksmuseum van Natuurlijke Historie* 1, [i–xxii,] 700 pp.
- Fletcher TB (1932) Life-Histories of Indian Microlepidoptera (Second Series). Alucitidae (Pterophoridae), Tortricina and Gelechiadae. Government of India Central Publication Branch, Calcutta, 58 pp.
- Gilligan TM, Baixeras J, Brown JW (2018) T@RTS: Online World Catalogue of the Tortricidae (Ver. 4.0). <http://www.tortricid.net/catalogue.asp> [accessed 20 January 2020]
- Hajibabaei M, Janzen DH, Burns JM, Hallwachs W, Hebert PD (2006) DNA barcodes distinguish species of tropical Lepidoptera. *Proceedings of the National Academy of Sciences* 103(4): 968–971. <https://doi.org/10.1073/pnas.0510466103>
- Hebert PD, Penton EH, Burns JM, Janzen DH, Hallwachs W (2004) Ten species in one: DNA barcoding reveals cryptic species in the neotropical skipper butterfly *Astraptes fulgerator*. *Proceedings of the National Academy of Sciences of the United States of America* 101(41): 14812–14817. <https://doi.org/10.1073/pnas.0406166101>
- Hebert PD, Dewaard JR, Zakharov EV, Prosser SW, Sones JE, McKeown JT, Mantle B, La Salle JA (2013) DNA ‘barcode blitz’: rapid digitization and sequencing of a natural history collection. *PLoS ONE* 8(7): e68535. <https://doi.org/10.1371/journal.pone.0068535>
- Heppner JB, Inoue H (1992) Lepidoptera of Taiwan. Vol 1. Introduction and Faunal Synopsis, Part 2: Checklist. Scientific Publishers, Gainesville, 63 pp.
- Horak M (2006) Monograph on Australia Lepidoptera, Vol 10: Olethreutine Moths of Australia (Lepidoptera: Tortricidae). CSIRO Publishing, Collingwood, 528 pp. <https://doi.org/10.1071/9780643094086>
- Horak M, Brown RL (1991) Taxonomy and phylogeny. In: van der Geest LPS, Evenhuis HH (Eds) *Tortricid Pests*. Elsevier Science Publishers, Amsterdam, 23–48.
- Kumar S, Stecher G, Tamura K (2016) MEGA7: Molecular Evolutionary Genetics Analysis version 7.0 for bigger datasets. *Molecular Biology and Evolution* 33(7): 1870–1874. [msw054] <https://doi.org/10.1093/molbev/msw054>

- Kuznetsov VI (1988a) New species of tortricid moths of the subfamily Olethreutinae (Lepidoptera, Tortricidae) of the fauna of North Vietnam. *Entomologicheskoe Obozrenie* 67(30): 615–631. [In Russian]
- Kuznetsov VI (1988b) Review of the moths of supertribes Gatesclarkeanidii and Olethreutidii from the fauna of North Vietnam. *Entomologicheskoe Obozrenie* 70: 165–181. [In Russian]
- Kuznetsov VI, Stekolnikov AA (1977) Functional morphology of the male genitalia and phylogenetic relationships of some tribes in the family Tortricidae (Lepidoptera) of the fauna of the Far East. *Trudy Zoologicheskogo Instituta Leningrad* 70: 65–97. [In Russian]
- Li HH (2002) The Gelechiidae of China (I). Nankai University Press, Tianjin, 538 pp. [In Chinese]
- Lower OB (1901) Descriptions of new genera and species of Australian Lepidoptera. *Transactions of the Royal Society of South Australia* 25: 63–98. <https://doi.org/10.5962/bhl.part.12145>
- Lukhtanov VA, Dantchenko AV, Vishnevskaya MS, Saifitdinova AF (2015) Detecting cryptic species in sympatry and allopatry: analysis of hidden diversity in *Polyommatus (Agrodiaetus)* butterflies (Lepidoptera: Lycaenidae). *Biological Journal of the Linnean Society* 116: 468–485. <https://doi.org/10.1111/bij.12596>
- Meyrick E (1907) Descriptions of Indian Micro-Lepidoptera III. *Journal of the Bombay Natural History Society* 17: 730–754.
- Meyrick E (1911) Revision of Australian Tortricina. *Proceedings of the Linnean Society of New South Wales* 36: 224–303. <https://doi.org/10.5962/bhl.part.21898>
- Meyrick E (1920) Exotic Microlepidoptera 2(11): 321–352.
- Meyrick E (1921) New Micro-Lepidoptera. *Zoologische Mededelingen* 6: 145–202.
- Muñoz AG, Baxter SW, Linares M, Jiggins CD (2011) Deep mitochondrial divergence within a *Heliconius* butterfly species is not explained by cryptic speciation or endosymbiotic bacteria. *BMC Evolutionary Biology* 11: e358. <https://doi.org/10.1186/1471-2148-11-358>
- Ratnasingham S, Hebert PDN (2007) BOLD: the Barcode of Life Data System (www.barcodinglife.org). *Molecular Ecology Notes* 7(3): 355–364. <https://doi.org/10.1111/j.1471-8286.2007.01678.x>
- Razowski J (1989) The genera of Tortricidae (Lepidoptera) Part II: Palaearctic Olethreutinae. *Acta Zoologica Cracoviensia* 32(7): 107–328.
- Razowski J (2014) Systematic and Distributional Data on Leafrollers from the Graziano Bassi Expedition to Tropical Africa (Lepidoptera: Tortricidae). *SHILAP Revista de Lepidopterologia* 42(168): 517–529. <http://www.redalyc.org/articulo.oa?id=45540983002>
- Razowski J, Trematerra P (2010) Tortricidae (Lepidoptera) from Ethiopia. *Journal of Entomological and Acarological Research, Series II* 42(2): 47–79. <https://doi.org/10.4081/jear.2010.47>
- Razowski J, Wojtusiak J (2012) Tortricidae (Lepidoptera) from Nigeria. *Acta Zoologica Cracoviensia* 55(2): 59–130. https://doi.org/10.3409/azc.55_2.59
- Razowski J, Bassi G (2018) Tortricidae (Lepidoptera) from Gabon. *Acta Zoologica Cracoviensia* 61(1–2): 1–30. <https://doi.org/10.3409/azc.61.01>
- Ritter S, Michalski SG, Settele J, Wiemers M, Fric ZF, Sielezniew M, Sasic M, Rozier Y, Durka W (2013) *Wolbachia* infections mimic cryptic speciation in two parasitic butterfly species, *Phengaris teleius* and *P. nausithous* (Lepidoptera: Lycaenidae). *PLoS ONE* 8(11): e78107. <https://doi.org/10.1371/journal.pone.0078107>

- Safonkin AF (2007) Pheromones and phylogenetic relations of leafrollers (Lepidoptera, Tortricidae). Entomological Review 87(9): 1238–1241. <https://doi.org/10.1134/S0013873807090138>
- Turner AJ (1916) New Australian Lepidoptera of the family Tortricidae. Transactions of the Royal Society of South Australia (40): 498–536.
- Turner AJ (1945) Contributions to our knowledge of the Australian Tortricidae (Lepidoptera). Transactions of the Royal Society of South Australia 69: 50–72.
- Turner AJ (1946) Contributions to our knowledge of the Australian Tortricidae (Lepidoptera). Part II. Transactions of the Royal Society of South Australia 70: 189–220.
- Zahiri R, Lafontaine JD, Schmidt BC, deWaard JR, Zakharov EV, Hebert PD (2014) A trans-continental challenge – a test of DNA barcode performance for 1,541 species of Canadian Noctuoidea (Lepidoptera). PLoS ONE 9(3): e92797. <https://doi.org/10.1371/journal.pone.0092797>

Supplementary material I

Tables S1, S2

Authors: Haili Yu

Data type: table

Explanation note: Table S1. Species sampled for the molecular analysis. Table S2. Pair-wise distances calculated within and between *Syntozyga* species resulting from COI gene dataset.

Copyright notice: This dataset is made available under the Open Database License (<http://opendatacommons.org/licenses/odbl/1.0/>). The Open Database License (ODbL) is a license agreement intended to allow users to freely share, modify, and use this Dataset while maintaining this same freedom for others, provided that the original source and author(s) are credited.

Link: <https://doi.org/10.3897/zookeys.1028.60297.suppl1>

A new Andean genus, *Lafontaineana*, with descriptions of four new species and two new Neotropical species of *Panthea* (Noctuidae, Pantheinae)

Jose I. Martinez^{1,3}, B. Christian Schmidt², Jacqueline Y. Miller³

1 Entomology and Nematology Department, University of Florida, Gainesville, 32611, FL, USA **2** Agriculture and Agri-food Canada, Canadian National Collection of Insects, Arachnids and Nematodes, K.W. Neatby Bldg., 960 Carling Ave., K1A 0C6, Ottawa, ON, Canada **3** Florida Museum of Natural History, McGuire Center for Lepidoptera and Biodiversity, University of Florida, Gainesville, 32611, FL, USA

Corresponding author: Jose I. Martinez (joemartinez@ufl.edu)

Academic editor: E.J. van Nieukerken | Received 21 July 2020 | Accepted 3 March 2021 | Published 6 April 2021

<http://zoobank.org/E8106BAE-1F85-44AA-9297-51392D7BC7DA>

Citation: Martinez JI, Schmidt BC, Miller JY (2021) A new Andean genus, *Lafontaineana*, with descriptions of four new species and two new Neotropical species of *Panthea* (Noctuidae, Pantheinae). ZooKeys 1028: 113–134. <https://doi.org/10.3897/zookeys.1028.56784>

Abstract

Lafontaineana Martinez, **gen. nov.** is proposed as a new Neotropical genus of Pantheinae, forming a sister group to *Gaujonia* Dognin, 1891 based on a phylogenetic analysis. In addition, one new combination and four new species are proposed: *Lafontaineana marmorifera* (Walker, 1865), **comb. nov.** (Colombia), *Lafontaineana alexandrae* Martinez, **sp. nov.** (Ecuador), *Lafontaineana imama* Martinez, **sp. nov.** (Colombia), *Lafontaineana puma* Martinez, **sp. nov.** (Ecuador), and *Lafontaineana thuta* Martinez, **sp. nov.** (Ecuador). Two new Neotropical species of *Panthea* are described, *Panthea hondurensis* Martinez, **sp. nov.** and *Panthea taina* Martinez, **sp. nov.**

Keywords

Andes Mountains, cloud forest, *Lichnoptera*, Neotropics, South America, Systematics

Introduction

Lichnoptera Herrich-Schäffer, 1856, is currently the most diverse genus of neotropical pantheines and, like other neotropical Noctuidae, it has been poorly studied. Literature citations of the type species *L. gulo* Herrich-Schäffer, 1856 are largely limited to historical accounts (e.g., Walker 1862; Prittwitz 1871; Kirby 1892; Hampson 1913; Seitz 1919; Nye 1975; Poole 1989). Taxonomic research on the genus *Lichnoptera* by the senior author and Schmidt and Anweiler (2020) has revealed that *Lichnoptera* is a morphologically and genetically heterogeneous group requiring the establishment of new genera. Here, we erect *Lafontaineana* gen. nov. based on the type species *Diphthera marmorifera* (Walker, 1865), and add descriptions of four new species: *Lafontaineana alexandrae* sp. nov., *Lafontaineana imama* sp. nov., *Lafontaineana puma* sp. nov., and *Lafontaineana thuta* sp. nov. *Lafontaineana marmorifera* (Walker) comb. nov. is re-described.

Surprisingly, *Lafontaineana* is restricted to a small area, high elevation (~ 3,000 m) region of the Andes Mountains of Colombia and Ecuador. No records are known from other Andean countries, and the species are rarely collected; life histories and larval host plants remain completely unknown. *Lafontaineana* forms part of the *Lichnoptera* clade or “Jaguar Moths,” a clade which includes approximately 38 species of Neotropical Pantheinae in the genera *Bathyra* Walker, 1865, *Cicadoforma* Martinez, 2020, *Cicadomorphus* Martinez, 2020, *Gaujonia* Dognin, 1891, *Gaujoptera* Martinez, 2020, *Lichnoptera* Herrich-Schäffer, 1856, *Millerana* Martinez, 2020, and *Oculicattus* Martinez, 2020. Jaguar Moths are thought to mimic tiger moths (Erebidae: Arctiinae) (Martinez 2020). We also describe two new Neotropical pantheine species of the genus *Panthea*: *Panthea hondurensis* sp. nov. and *Panthea taina* sp. nov.

Methods and materials

Terminology and specimen preparation techniques follow standard protocols for Noctuidae (Lafontaine 1987, 2004; Schmidt and Anweiler 2020). Genitalia were stained with 1% chlorazol black and examined in 30% ethanol, and subsequently stored in pure glycerin. Type specimen preparations were mounted in Euparal. Photographs of pinned adults were taken using a Canon EOS Rebel T5i camera and Canon EF 100mm f/2.8 USM Macro lens, and the genitalia with a StackShot automated focus stacking macro rail with a Canon EOS 6D and an Infinity long-distance microscope Model K2 DistaMax.

We performed the molecular diagnosis by DNA barcoding four out of six new species mentioned in this study (with the exception of *Panthea taina* sp. nov. and *Lafontaineana puma* sp. nov.), implementing a segment from the mitochondrial cytochrome oxidase (COI) gene. The DNA barcodes of outgroups were taken from the Barcode of Life Data System V4 (<http://barcodinglife.com>). DNA was extracted from dried specimens, typically of a single leg. Sequencing was carried out by the Canadian Centre for DNA Barcoding, Guelph, Ontario (<http://ccdb.ca>) following the protocols of Ratnasingham and Hebert (2013). Concatenation and alignment of sequences was performed

using Geneious 9.1.3 (<http://www.geneious.com>). The gene tree construction was performed using a maximum-likelihood (ML) analysis in IQ-TREE v. 2 following Nguyen et al. (2015), Hoang et al. (2018), and Minh et al. (2020). We estimated branch support by running 1000 replicates of ultrafast bootstraps (UFBoot) ('-bb' command) and 1000 replicates of the Shimodaira-Hasegawa approximate likelihood ratio test (SH-aLRT) ('-alrt' command); values of UFBoot ≥ 95 and SH-aLRT ≥ 80 for nodes were considered highly supported. The divergence among species was obtained by using the identification engine of Barcode of Life Data System V4 (http://www.boldsystems.org/index.php/IDS_OpenIdEngine) and the nucleotide BLAST (<https://blast.ncbi.nlm.nih.gov/Blast.cgi>). Photographs and files including molecular data for voucher specimens are available at Barcode of Life Data System V4 [dataset: Jaguar Moths; code: DS-JAGM (<https://www.dx.doi.org/10.5883/DS-JAGM>)]. Sequence data are available on GenBank (www.ncbi.nlm.nih.gov/Genbank) (Suppl. material 3: Table S1).

The following institutional collections were reviewed to obtain the specimens:

- CNC** Canadian National Collection of Insects, Arachnids and Nematodes, Ottawa, Ontario, Canada;
FSU Friedrich Schiller University of Jena, Jena, Germany;
MGCL McGuire Center for Lepidoptera and Biodiversity, Florida Museum of Natural History, Gainesville, Florida, USA;
NHMUK The Natural History Museum (formerly British Museum [Natural History]), London, United Kingdom.

Systematics

Lafontaineana Martinez, gen. nov.

<http://zoobank.org/9E7D99A1-D567-48DC-B6EA-EBB95FDD11A6>

Gender. Feminine.

Type species. *Diphtera marmorifera* Walker, 1865 by present designation.

Etymology. *Lafontaineana* is proposed in honor of our colleague J. Donald Lafontaine, who has worked with Lepidoptera, especially Noctuoidea, for more than 40 years; his work has been an inspiration to many in the world of noctuid research.

Included species. *Lafontaineana marmorifera* (Walker,) comb. nov. and the four new species described herein: *L. alexandrae* sp. nov., *L. imama* sp. nov., *L. puma* sp. nov., and *L. thuta* sp. nov.

Diagnosis. The external and internal morphologies of *Lafontaineana* and *Lichnoptera* are dissimilar (Figs 6, 7, 21, 29). In *Lafontaineana*, the thorax is white with black patches, which form large black polygons; these patches are smaller in *Lichnoptera*. The black markings of the forewing are wider and more sharply defined. The hindwing has a discal spot and dark lunate mark on the tornus, both of which are absent in *Lichnoptera*. In the male genitalia of *Lafontaineana*, the valva lacks the clasper (present in *Lichnoptera*), and there are sclerotized spines on the vesica (absent

in *Lichnoptera*). In the female genitalia of *Lichnoptera*, the corpus bursae is remarkably smaller than the appendix bursae, while in *Lafontaineana* the opposite is true.

Description. *Lafontaineana* species are sexually dimorphic in size as well as in coloration, and the female is larger and paler than male. Both sexes have filiform antennae; eyes densely covered by short and fine interfacetal setae; haustellum short, dark brown; palpus short with the terminal segment 5× shorter than second segment, divided in black and yellow, but differing in the terminal segment, which is mostly marbled with black, white, and yellow scales. Thoracic dorsal vestiture concolorous except in forewing, of which ground color is white to yellowish white, with prominent black polygons in collar, tegula, and patagium centrally, while ventrally the thorax is gray; thorax with orange hair-like tuft laterally beneath forewing; forewing pattern well-developed with ground color darker in the median field; orbicular spot round and prominent, reniform spot trapezoidal. Hindwing white, semi-hyaline (dark gray in *L. alexandrae*); female with barely visible discal, medial and postmedial lines; dark spots covering costa and Sc+R1 cells; discal spot fused with discal line; lunate marking on tornus, which is longer in female. Abdomen dull orange with dark brown dorsal stripe and brown dorsal tuft on segments A1–A7. Male genitalia with tegumen relatively narrow; long simple valva lacking clasper; cucullar region slightly squared, but narrow and reasonably short; costal and posterior margins with a curved extension on each; juxta mostly shield-like; uncus sinuous; aedeagus short; vesica longer than the aedeagus with a medial diverticulum and a row of sclerotized spines. Female genitalia with sterigma and appendix bursae lightly sclerotized; ductus bursae sclerotized; corpus bursae transparent without signa; anterior and posterior apophysis remarkably short, except in *L. alexandrae* which has large posterior apophysis.

Genetic characterization. DNA barcodes of *Lafontaineana* species are distinguishable from their sister clade, the *Gaujonia* genus group, by $\geq 7\%$ divergence (Fig. 1).

Immature stages. Immature stages as well as the host plants are unknown.

Key to the genus of *Lafontaineana* based on male and female morphology

- 1 Hindwings white with conspicuous lines (Figs 4, 8–15).....2
- Hindwings dark gray with inconspicuous lines (Fig. 16)*L. alexandrae*
- 2 Forewing with rounded orbicular spot (Figs 4, 8, 9, 14, 15)3
- Forewing with squared orbicular spot (Figs 10–13).....4
- 3 Orbicular spot small with a dot in the middle; thorax with small polygons and a wide sulfur-yellow line on metanotum; abdomen with orange bands fused on A1; male genitalia with a small swollen protuberance on the costal margin of valva (Figs 14, 15, 24).....*L. thuta*
- Orbicular spot wide; large polygons on thorax; abdomen with wide orange bands and long white hairy scales covering the genitalia; male genitalia with valva widely swollen on the costal margin (Figs 4, 5, 8, 9).... *L. marmorifera*
- 4 Medial field brown or dark brown (Figs 12, 30)..... *L. puma*
- Medial field slightly suffused brownish yellow; band in the fold of the forewing in pale-yellow (Figs 10, 11) *L. imama*

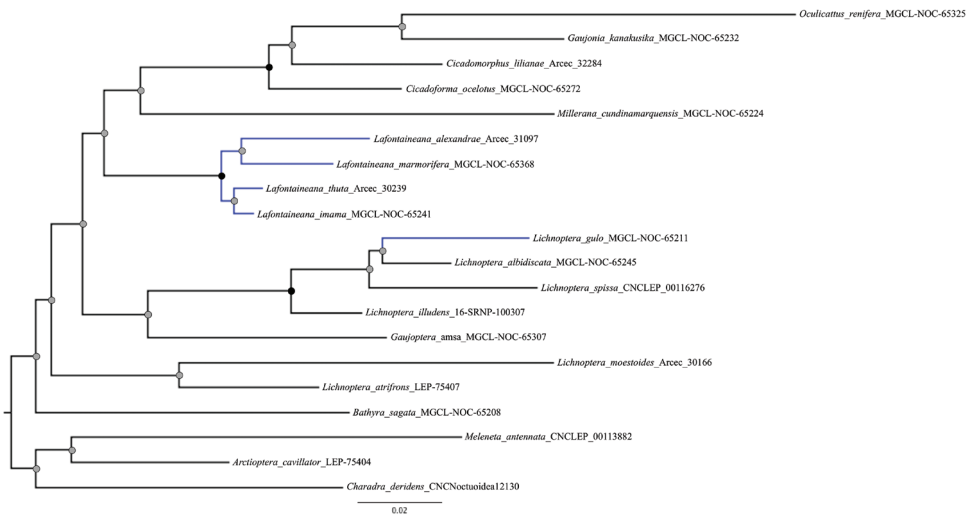


Figure 1. Relationships between the species of the genus *Lafontaineana* and other genera in the *Lichnoptera* clade employing a Maximum Likelihood analysis based on the cytochrome c oxidase I gene (COI). Nodes with black circles represent high support (UFBoot ≥ 95 and SH-aLRT ≥ 80). Nodes with gray circles represent low support (UFBoot < 95 and SH-aLRT < 80). Black branches represent the outgroups.

Descriptions

Lafontaineana alexandrae Martinez, sp. nov.

<http://zoobank.org/0403C48D-C4E9-489F-9F22-8B3AD0830B16>

Figures 16, 30

Type material. Holotype: ♀, ECUADOR, Zamora-Chinchipe, Reserva Biologica San Francisco, Montane Rainforest, Blacklight 2×15W, 30 Jan. 2013, 19.00–21.30 h, 03°58.94'S, 79°04.84'W, 2212 m, coll. Gunnar Brehm & Yoko Matsumura / DNA Barcode run 2013, COI-5P marker, University of Guelph / Arcec 30166 / leg sampled in ethanol G. Brehm, Green vial caps. deposited in FSU.

Etymology. This species is named after the senior authors' sister, Alejandra Martinez, who has supported JIM's work since the beginning of his career.

Diagnosis. *Lafontaineana alexandrae* is the only species in the genus that has a dark hindwing. The female genitalia differ from the rest of the *Lafontaineana* by the presence of the small projections; small papillae anales-like on the A8 membrane.

Description. Head. Palpus marbled in yellow, white, and black; frons covered by a mixture of yellow and black scales. **Thorax.** Polygons small, outlined by wide yellow lines; setal tuft pale orange; ventrally brown with some dark gray scales. **Wing.** Forewing length 22–24 mm; yellow with blurry black lines; basal and medial lines absent, and space between antemedial and subterminal lines brown; crescent-shaped orbicular spot; reniform spot arrow tip-shaped, curving inwards on outer margin with lunate marking near inner margin; hindwing completely covered by gray scales; fringe black with some spots in yellow; pattern lines barely visible. **Legs.** Black with white joints

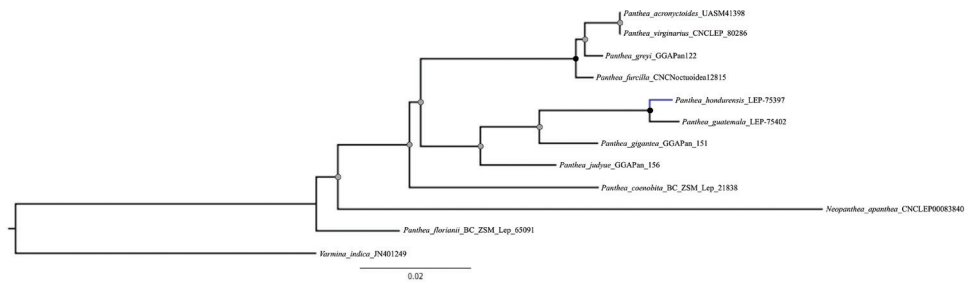
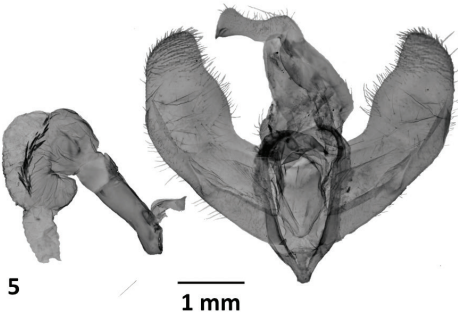
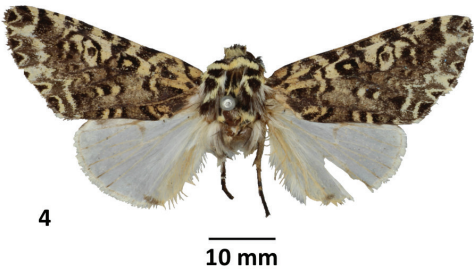
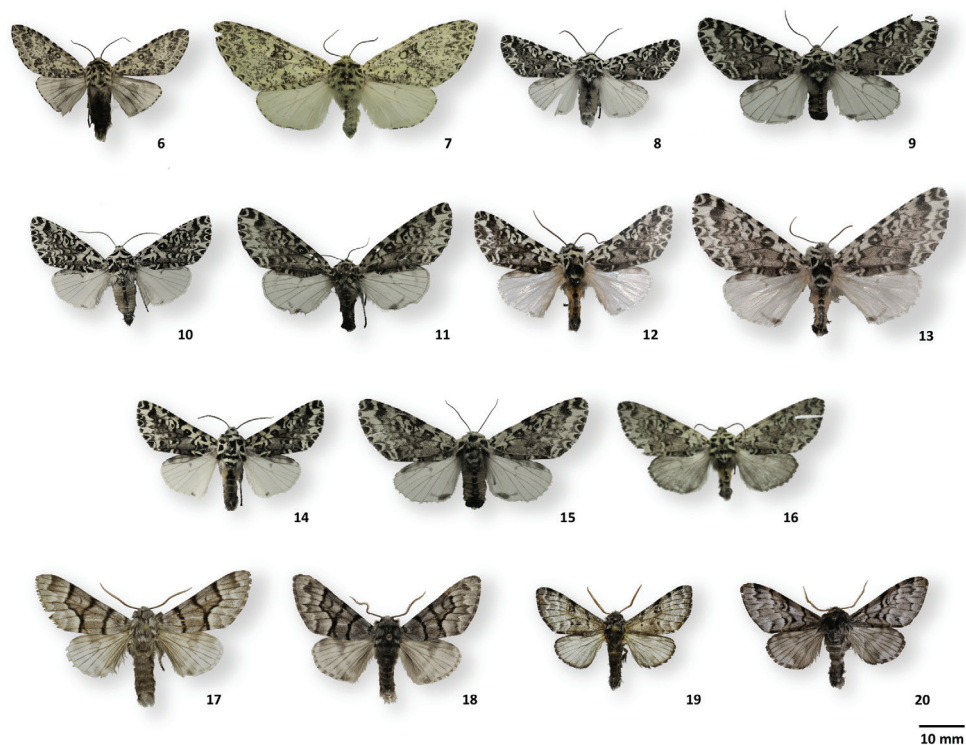


Figure 2. Relationships between the species *Panthea hondurensis* and other *Panthea* species employing a Maximum Likelihood analysis based on the cytochrome c oxidase I gene (COI). Nodes with black circles represent high support (UFBoot ≥ 95 and SH-aLRT ≥ 80). Nodes with gray circles represent low support (UFBoot < 95 and SH-aLRT < 80). Black branches represent the outgroups.



Figures 3–5. *Lafontaineana marmorifera* **3** head, ♂, Cundinamarca, Colombia MGCL **4** holotype ♂, New Grenada (Colombia), NHMUK **5** holotype genitalia ♂, New Grenada (Colombia), NHMUK.



Figures 6–20. Adult habitus of *Lichnoptera*, *Lafontaineana*, and *Panthea* **6** *Lichnoptera gulo*, ♂, MGCL, Cundinamarca, Colombia **7** *L. gulo*, ♀, MGCL, Cundinamarca, Colombia **8** *Lafontaineana marmorifera*, ♂, MGCL, Cundinamarca, Colombia **9** *L. marmorifera*, ♀, MGCL, Cundinamarca, Colombia **10** *L. imama*, ♂, MGCL, holotype, Tolima, Colombia **11** *L. imama*, ♀, MGCL, paratype, Tolima, Colombia **12** *L. puma*, ♂, CNC, holotype, La Alegria, Ecuador **13** *L. puma*, ♀, CNC, paratype, La Alegria, Ecuador **14** *L. thuta*, ♂, MGCL, holotype, Loja, Ecuador **15** *L. thuta*, ♀, MGCL, paratype, Sucumbios, Ecuador **16** *L. alexandrae*, ♀, FSU, holotype, Zamora-Chinchipe, Ecuador **17** *Panthea guatemala*, ♂, CNC, San Lorenzo, Guatemala **18** *P. hondurensis*, ♂, MGCL, holotype, Francisco Morazán, Honduras **19** *P. reducta*, CNC, ♂, Pedernales, Dominican Republic **20** *P. taina*, ♂, La Vega, MGCL, holotype, Dominican Republic.

and yellow tufts. *Abdomen*. Black with yellow interstitial membrane ventrally; dorsally with huge black line of tufts with some scales in white; anal papilla covered by yellow scales. *Female genitalia*. Anal papilla remarkably short; sterigma considerably wide; posterior apophysis round, 2× larger than anal papilla; appendix bursae sclerotized, 1/3× shorter than the corpus bursae; A8 membrane with a projection resembling small anal papilla.

Genetic characterization. The minimum DNA barcode divergence is 4.28% compared to *L. marmorifera*.

Distribution. The holotype, the only known specimen, was found in the cloud forest of southern Ecuador (Fig. 35).

Remarks. Known only from the holotype, which has the tornus of the left forewing broken (Fig. 16), and the right forewing broken at cell R5. The DNA voucher label (Arcec 30166) is different from the voucher published at <http://barcodinglife.com> (Arcec 31097) probably by a confusion.

***Lafontaineana imama* Martinez, sp. nov.**

<http://zoobank.org/8909E464-D6FF-4197-B5A1-4416E3B3F1FA>

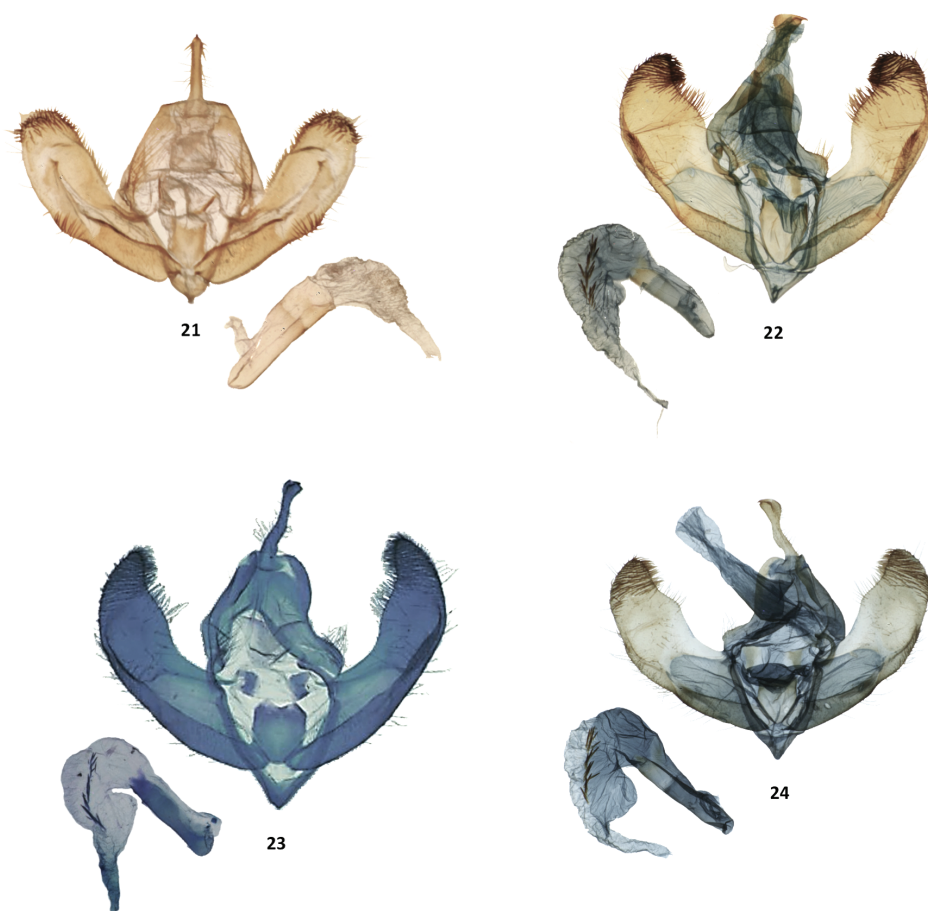
Figures 10, 11, 22, 31

Type material. Holotype: ♂, COLUMBIA, Tolima, Nevado del Tolima, 4°36'02"N, 75°19'51"W, 2600 m, 5–7 Dec. 2013, legit Victor Sinyaev & Mildred Márquez / UF, FLMNH, MGCL 1049058. [DNA voucher MGCL-NOC-65241] deposited in MGCL. **Paratype** (1 ♀ MGCL): COLOMBIA, Tolima, Cerro Bravo, La Libia, 5°06'21"N, 75°16'22"W, 15.–18. Dec. 2015, 3000 m, leg Sinyaev & Machado coll. Dr. Ron Brechlin / UF, FLMNH, MGCL 1049056.

Etymology. *Imama* is the common name of the jaguar *Panthera onca* (Linnaeus) in the Embera language. The name is a noun in apposition.

Diagnosis. *Lafontaineana imama* and *L. puma* resemble each other; however, *L. imama* has a more squared forewing shape. Also, the forewing is paler and shorter, the copper color standing out over the black and brown patterns barely visible. In addition, in *L. imama* the polygons on the thorax are clearly separated, while in *L. puma* some polygons are fused in the middle of the thorax. In the male genitalia the valva is noticeably wider than in *L. puma*, but the apex is much shorter; the vesica has a smaller diverticulum and a shorter row of spines. In the female, the corpus bursae and appendix bursae are narrower than in *L. puma*, and the papillae anales are also wider in *L. puma*.

Description. Head. Palpus with the last segment pale yellow with some spots in black, female with longer spots; frons divided into black and yellow. **Thorax.** The black polygons are separated from each other by pale-yellow lines; grayish blue ventrally. **Wing.** Forewing length, male 19–21 mm; female 23–25 mm; forewing pale yellow with black lines and brownish yellow scales in median field; a pale-yellow band in the fold; black orbicular spot square with a yellow dot on the middle; rectangular reniform spot with the outer margin slightly concave and a black lunate marking inside close to the upper area, while female with presenting only a small dot; hindwing with brown veins; fringe same yellow color with some black spots extending through costal and Sc+R1 cells; tornal lunate marking relatively large; female costal and Sc+R1 cells with large black and pale-yellow spots with the black lines extending and forming discal, medial, and postmedial lines; female tornal lunate marking fused with the postmedial line expanding through 2A and CuA2 cells; black line on the outer margin between 2A and CuA2 vein ends in both sexes. **Legs.** black with some patches in pale yellow on the joints and yellow tufts on the back area of the legs. **Abdomen.** Brown covered by white scales except for A8, which is brown in male ventrally; upper side complete orange with



1 mm

Figures 21–24. Male genitalia of *Lichnoptera* and *Lafontaineana* **21** *Lichnoptera gulo*, MGCL, Cundinamarca, Colombia **22** *L. imama*, MGCL, holotype, Tolima, Colombia **23** *L. puma*, CNC, holotype, La Alegria, Ecuador **24** *L. thuta*, MGCL, holotype, Loja, Ecuador.

a small line of tufts except on A8; female brown with the intersternal membrane white and the last segment yellow ventrally but dorsally similar to male with the A7 and A8 brown, line of tufts with some white scales dorsally. **Male genitalia.** Very wide cucular region, square apex with rounded edges, densely clothed by setae; costal margin with remarkably swollen protuberance; saccular region narrow and its process narrower; juxta spoon-like and quite concave on the upper side; aedeagus short and narrow; diverticulum is not very prominent; line of spines short. **Female genitalia.** Anal papilla small; sterigma sclerotized, thin and elongated; posterior apophysis reduced and almost imperceptible; appendix bursae sclerotized, $\frac{1}{8} \times$ shorter than the corpus bursae.

Genetic characterization. Although *Lafontaineana imama* looks externally most similar to *L. puma*, the DNA barcode of *L. imama* is closer to that of *L. thuta*, differing by only 1.07%. Unfortunately, the DNA of *L. puma* was not available for comparison.

Distribution. The two known specimens were found in deciduous forests of west-central Colombia (Fig. 35).

Remarks. Holotype and paratype are in perfect condition (Figs 10, 11).

***Lafontaineana marmorifera* (Walker, 1865), comb. nov.**

Figures 3–5, 8, 9, 32

Diphtera marmorifera Walker, 1865: (32): 612.

Lichnoptera marmorifera Hampson, 1913: 13: 385, 396–397, pl. 235, fig. 20.

Type material. Holotype: ♂, New Grenada (COLOMBIA), coll. Mr. Marks, labeled “*Diphtera marmorifera*” / [Red labeled] deposited in NHMUK. **Additional examined specimens** (3 ♂, 1 ♀ MGCL): COLOMBIA, Cundinamarca, Guasca, El Chochal de Siecha, 3120 m, 28 Nov. 2019, coll. Jose I. Martinez / UF, FLMNH, MGCL 1049165. [DNA voucher MGCL-NOC-65368]. Colombia, Cundinamarca dept., Vereda La Concepción, Bosque La Guajira, 4°47'34"N, 75°46'60"W, 9–12 IV 2014, 2910 m, coll. M. Márquez & J. Machado (2 ♂). Colombia, Cundinamarca dept., Vereda La Concepción, Bosque La Guajira, 4°47'34"N, 75°46'60"W, 10–13 I 2015, 2910 m coll. Dr. Ron Brechlin / UF, FLMNH, MGCL 1049167 (1 ♀).

Etymology. The name *marmorifera* is probably derived from the marbled coloration of the forewings of this species.

Diagnosis. *Lafontaineana marmorifera* is relatively easy to distinguish from other species because of its pale sulfur yellow color, with brown and black patterns on the lightly squared forewing. Forewing with a large squared orbicular spot and semi-rhomboid-shaped reniform spot, which are totally different from other species. Hindwing with black lines at the end of each vein, a white fringe, and a long discal spot. Forewing length male 18–20 mm, female 24–26 mm. Palp pale sulfur-yellow with black patches on the second segment; antenna black; male thorax is pale sulfur-yellow, paler than the forewings on the dorsal surface, with black polygons outlined with white scales, the ventral area is dark gray. Abdomen dark brown with the two wide stripes and very narrow line of tufts. Male genitalia valva considerably wide; apex rounded; an extension present on the costal margin; sacculus wide with the process same size as sacculus; aedeagus $4\frac{1}{3} \times$ longer than wide; vesica short and broad with medial diverticulum equal in size to the base of the vesica; vesica with dense line of spines.

Genetic characterization. The DNA barcode of *Lafontaineana marmorifera* is close to that of *L. alexandrae* (see *L. alexandrae* genetic characterization).

Distribution. The type specimen was labeled as coming from New Grenada, which was a territory that comprised the four countries Panama, Venezuela, Colom-

bia, and Ecuador. However, curators at the NHMUK in the early 20th century added a label that says Colombia (Fig. 35).

Remarks. Holotype with both antennae broken, the right hindwing is also broken on the CuA2 cell (Fig. 4). However, the other examined specimens are in very good condition.

***Lafontaineana puma* Martínez, sp. nov.**

<http://zoobank.org/829B6BC6-569A-4493-AADD-0E2DBC366689>

Figures 12, 13, 23, 33

Type material. Holotype: ♂, ECUADOR, La Alegria, 2700 m, 14–15 Sep. 1977, coll. Luis E. Peña / LACM ENT 332567 deposited in CNC. **Paratype** (1 ♀ CNC): Same collecting data as holotype / LACM ENT 332566.

Etymology. Since the name “Jaguar Moth” makes reference to wild cats in general, the word *puma* was chosen in reference to the cougar (*Puma concolor* Linnaeus, 1771), which also means powerful in the Quechua language. The specific name is a noun in apposition.

Diagnosis. The only species that looks very similar to *Lafontaineana puma* is *L. imama* (see diagnosis of *L. imama*). However, the main external morphological character is the dorsal fusion of polygons in the middle of the thorax; internally the vesica has a remarkably reduced medial diverticulum.

Description. *Head.* Last segment of the palpus in white with scattered black scales, male darker than female; frons covered by black and yellow scales in male, while grey and yellow in female. *Thorax.* Whitish yellow; polygon on the middle and those on each side of the posterior area from the mesothorax are fused, while the two lateral polygons remain separated; ventrally clothed by white and black scales. *Wing.* Forewing length male 23–25 mm; female 28–30 mm; forewing same yellow color as the thorax; black linear patterns and the space in median field coppery; orbicular spot with the upper and lower sides flattened and large yellow spot in the middle; reniform spot D-shaped outlined with black rectangle; relatively large lunate marking within the reniform spot; hindwing with pale-orange veins and some small black dots; silvery white fringe on the outer margin, while the posterior margin has some brown scales; three well-developed black spots on costal and Sc+R1 cells, narrower in female; small discal spot; discal, medial, and postmedial lines absent in both sexes; tornal lunate marking very small in male and normally expanded through 2A and CuA2 cells in female. *Legs.* black with a small yellow line in each joint; yellow tufts, darker in male. *Abdomen.* The orange lines and the brown line in the middle almost the same size; male with completely brown tufts, female with yellow ends; genitalia covered with orange scales; brownish gray ventrally in male and brown with some brownish gray scales and yellow intersternal membrane in female. *Male genitalia.* Narrow and pointed cucullus; apex rounded and covered by setae; costal margin slightly swollen; sacculus wide with a lightly narrow process; juxta shield-shaped with the upper edges flattened; aedeagus

slightly long; diverticulum relatively prominent; line of spines long and curved along on upper side of vesica. *Female genitalia*. Anal papilla wide; sterigma with long and wide opening; posterior apophysis length $1\frac{1}{4} \times$ anal papilla; appendix bursae and corpus bursae similar in size.

Genetic characterization. Unknown.

Distribution. Both specimens were found in deciduous forests in western Ecuador (Fig. 35).

Remarks. Attempts to extract DNA from these specimens were unsuccessful.

***Lafontaineana thuta* Martinez, sp. nov.**

<http://zoobank.org/D1D69219-8D05-4D90-AFAB-FB831A5104B1>

Figures 14, 15, 24, 34

Type material. *Holotype*: ♂, ECUADOR 8 km SE of Loja, Parque Nacional Podocarpus Cajanuma, mont. rainforest, Blacklight 2 × 15W, 2897 m, 26 iii. 2011, 04°06.86'S, 79°10.47'W, coll. Lisa Lehner & Marc Adams / DNA Barcode run 2013, COI-5P marker, University of Guelph / Arcec 32455. deposited in FSU. *Paratypes* (1 ♂ FSU): ECUADOR Zamora-Chinchipe, Cerro Toledo, Elfin forest, Parque Nacional Podocarpus Cajanuma, mont. rainforest, Blacklight 2 × 15W, 2938 m, 6 Feb. 2013, coll. Gunnar Brehm (1 ♂). (1 ♂, 1 ♀ MGCL): ECUADOR, Pichincha, Quito/ Chiriboga Km 33, 2650 m, 25 Apr. 1976, coll. N. Venedictoff (1 ♂). ECUADOR, Sucumbios, El Playon, 2 km to Minas, 0°37'24"N, 77°39'51"W, 18.-19. II 2013, 3320m, leg. Sinjaev & Romanov / UF, FLMNH, MGCL 1049166 (1 ♀).

Etymology. The name *thuta* means moth in the Quechua language. The specific name is a noun in apposition.

Diagnosis. *Lafontaineana thuta* can be differentiated externally from the other species of genus *Lafontaineana* by the minute yellow dot on the orbicular spot. Internally, *L. thuta* possesses a prominent diverticulum on vesica similar to *L. marmorifera* and *L. puma*, but the line of spines is narrower than *L. marmorifera* and shorter than *L. puma*.

Description. *Head*. Black palpus with some scattered yellow scales on last segment; frons yellow with few black scales. *Thorax*. Sulfur-yellow with a horizontal line on the metathorax with the end near to the abdomen black; polygons small and separated by sulfur-yellow lines; abdominal side gray; dark orange setal tufts. *Wing*. Forewing length male 19–21 mm; female 25–27 mm; sulfur-yellow with black and dark brown patterns; forewing same yellow as thorax; median field dark brown; orbicular spot with a minute yellow dot; reniform spot bean-like with a large dot close to inner margin; hindwing white with orange veins; fringe sulfur-yellow, paler than the forewing; costal margin with black fringe and some yellow scales; posterior margin with white scales; costal and Sc+R1 cells with large black and white patches; small discal spot and tornal lunate marking. *Legs*. Black with large sulfur-yellow and white patches. *Abdomen*. Brown dorsally with a huge black line of tufts from A2 extend-

ing and expanding through the subsequent tergites making the orange lines narrower; white scales at the ends of the tufts; yellowish white with brown scales on the intersternal membrane ventrally. **Male genitalia.** Tegumen short; wide cucullus with a square-shaped apex, clothed by setae; costal margin lightly expanded; sacculus wide and process with a small projection on posterior margin; juxta broadly spoon-shaped with slightly concavity on upper area; aedeagus with huge diverticulum; wide line of spines, long spines. **Female genitalia.** Anal papilla short and squared; sterigma semi-sclerotized, large and widely opened; posterior apophysis 3 × longer than anal papilla; appendix bursae $\frac{1}{6}$ × longer than the corpus bursae.

Genetic characterization. DNA barcoding of *Lafontaineana thuta* showed it to be closer to *L. imama* (see *L. imama* genetic characterization).

Distribution. This species has been found only in high elevations of deciduous forests of Ecuador (Fig. 35).

Remarks. Both holotype and paratype are in perfect condition (Figs 14, 15). As in *L. alexandrae*, the voucher number (Arcec 32455) is different from that published at <http://barcodinglife.com> confusion (Arcec 30239).

***Panthea* Hübner, 1820**

Panthea is a small genus comprising 14 species worldwide, distributed mainly in the Nearctic and Palearctic regions (Anweiler 2009; Behounek et al. 2013; Schmidt and Anweiler 2020). Only three species are known in the Neotropical region (*Panthea furcilla* (Packard, 1864), *P. reducta* Anweiler, 2009, and *P. guatemala* Anweiler, 2009) and we describe two additional species from the Neotropics: *Panthea hondurensis* sp. nov. and *Panthea taina* sp. nov.

The genus *Panthea* is characterized externally by bipectinate antennae, small eyes with dense interfacetal setae, a short haustellum, and the forewings presenting five well-defined transverse lines and poorly developed reniform and orbicular spots (sometimes absent). Internally, male genitalia presenting heavily sclerotized valves, well-developed uncus compressed at the tip, and the vesica without diverticula and armed with wide cornuti. Female genitalia with well-developed sterigma and simple corpus bursae lacking appendix bursae.

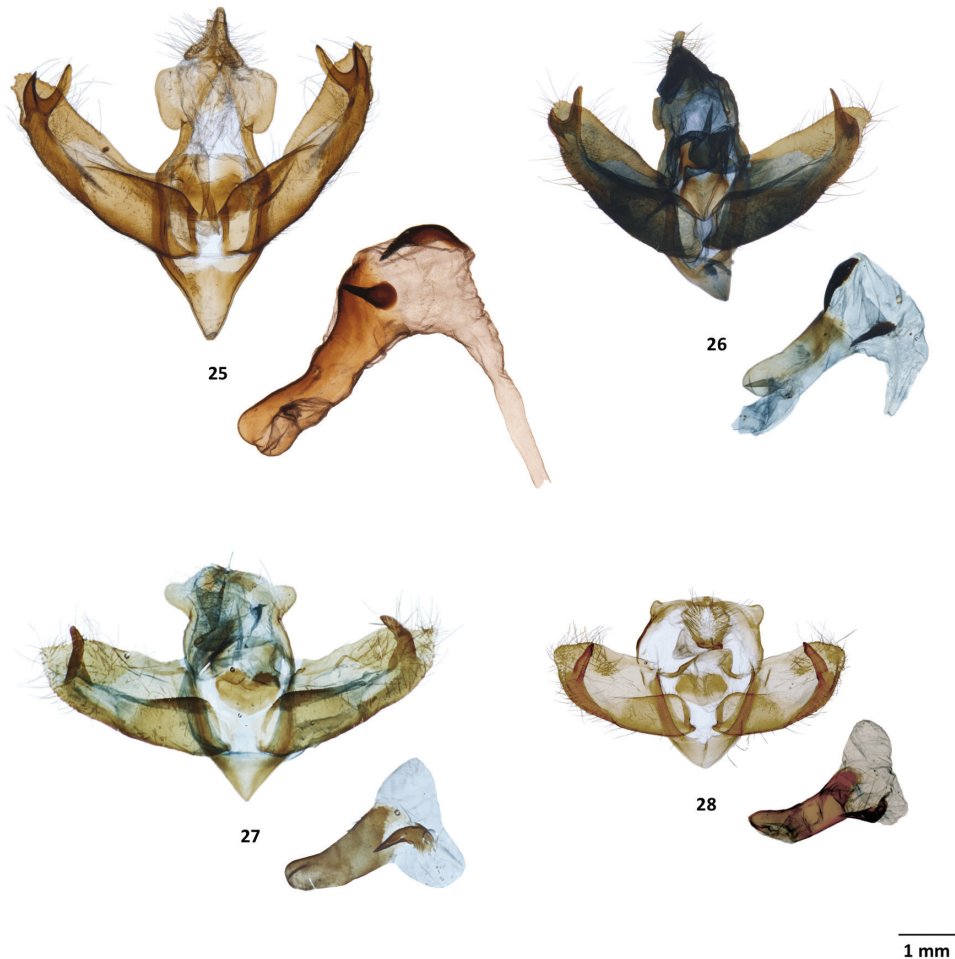
***Panthea hondurensis* Martinez, sp. nov.**

<http://zoobank.org/74B23D0F-684C-422A-9BB9-E832C7C224B2>

Figures 18, 26

Type material. *Holotype*: ♂, HONDURAS: Fco. Morazán, Reserva Biología Monte Uyuca, 1,600 m, 14.034858°, -87.075035°, 16 vii. 2015, coll. D. Matthews & J. Y. Miller / Honduras Biodiversity Survey MGCL Accession, #2015-56 / Barcode MGCL 270947, McGuire Center for Lepidoptera & Biodiversity, UF. [DNA voucher LEP-75397] deposited in MGCL. *Paratypes* (1 ♂ MGCL): Same collecting data as holotype.

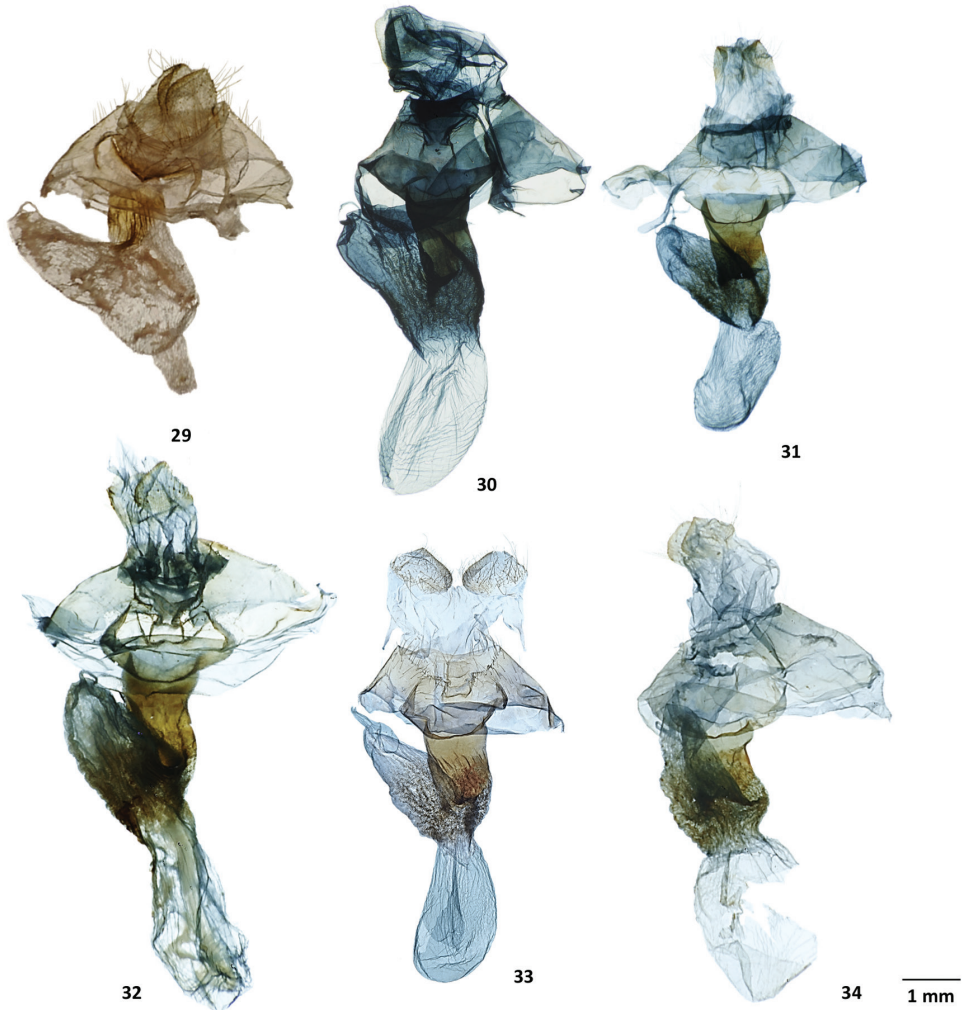
Etymology. This species is named after the only country in which it is known to occur.



Figures 25–28. Male genitalia of *Lafontaineana* and *Panthea* **25** *Panthea guatemala*, CNC, Oaxaca, Mexico **26** *P. hondurensis*, MGCL, holotype, Francisco Morazán, Honduras **27** *P. taina*, MGCL, holotype, La Vega, Dominican Republic **28** *P. reducta*, ♂, CNC, Pedernales, Dominican Republic.

Diagnosis. *Panthea hondurensis* is morphologically similar to *P. guatemala*. Externally, *P. hondurensis* is slightly smaller and darker with the lunate markings on the reniform spots longer than those of *P. guatemala*. In the male genitalia, *P. hondurensis* has wider valves without protuberances at the apex and shorter subuncal lobes. The aedeagus is noticeably shorter.

Description. Only known from two male specimens. **Head.** Male antenna brown and bipectinate; palpus black and dark brown; frons marbled with brown, white, and gray scales. **Thorax.** Marbled with brown and gray scales forming polygons outlined by black scales. **Wing.** Forewing length in male 21–23 mm; forewing with the basal, antemedial, and medial lines all in black, while the postmedial line is brown highlighted with gray scales; orbicular spot not present; reniform spot formed by long lunate mark-



Figures 29–34. Female genitalia of *Lichnoptera* and *Lafontaineana* **29** *Lichnoptera gulo*, MGCL, Cundinamarca, Colombia **30** *Lafontaineana alexandrae*, FSU, holotype, Zamora-Chinchi, Ecuador **31** *L. imama*, MGCL, paratype, Tolima, Colombia **32** *L. marmorifera*, MGCL, Cundinamarca, Colombia **33** *L. puma*, CNC, paratype, La Alegria, Ecuador **34** *L. thuta*, MGCL, paratype, Sucumbios, Ecuador.

ing; hindwing whitish brown with dark brown veins; wide well-developed pale-brown discal line, while the medial line is inconspicuous; fringe alternating with black and whitish brown scales; legs black with some dark brown and gray spots. **Abdomen.** Darker brown than thorax; dorsal and ventral sides black, tergite ends brown; last abdominal segment with long brownish gray scales. **Male genitalia.** Tegumen narrow; simple valva with narrow cucullar region and flattened apex; saccular region $1\frac{1}{2}\times$ wider than the cucullar region; saccular process ending in a Y-shaped clasper; juxta shield-shaped with the upper side concave; uncus tip flattened; subuncal lobes short; aedeagus short, $3\times$ longer than width; vesica with a small basal diverticulum and a long

sclerotized cornutus, second cornutus similar in size located laterally on the central region of the vesica.

Genetic characterization. DNA barcodes of *Panthea guatemala* and *P. hondurensis* differ by 1%, comparable to differences between other closely related species of the genus (Schmidt and Anweiler 2020) (Fig. 2).

Distribution. The only two known specimens were found in the cloud forest of south-central Honduras (Fig. 36).

Remarks. The holotype (Fig. 18) and paratype are in perfect condition.

***Panthea taina* Martinez, sp. nov.**

<http://zoobank.org/FF47C181-75E8-49D6-96FB-4C77EB1A1B68>

Figures 20, 27

Type material. Holotype: ♂, DOMINICAN REPUBLIC, Prov. La Vega 5 km W. of Manabao, 19–23-IV-2000, Blacklight, 3050 ft elev., coll. R. E. Woodruff & T. J. Henry / Finca Eladio Fernandez “Paso la Perra”, along Rio Yaque del Norte 3050 ft elev. / UF, FLMNH, MGCL 1034189. [DNA voucher LEP-75402] deposited in MGCL. **Paratypes** (1 ♂ MGCL): Same collecting data as holotype.

Etymology. The word *taina* comes from the Taínos, a group of indigenous people of the Caribbean islands.

Diagnosis. *Panthea taina* is most similar to *P. reducta* (Fig. 21), but they can be easily separated: *Panthea taina* is larger with darker wing markings, the transverse lines of the forewings are well developed, whereas in *P. reducta* they are inconspicuous. In *P. taina* the medial line is separated from the reniform spot, whereas in *P. reducta* the medial line is fused with the reniform spot, forming a square. The orbicular spot is present as a small line in *P. taina*, but is absent in *P. reducta*. The hindwing of *P. taina* has well-developed lines, which are absent in *P. reducta*. In the male genitalia, *P. taina* has longer valves and a pointed apex, while in *P. reducta* the valves are short and the apex rounded. The tegumen is wider in *P. reducta* and its subuncal lobes reduced, compared to the large and prominent lobes in *P. reducta*.

Description. Only known from two male specimens. **Head.** Male antenna is bipectinate and dark orange in color; dark brown palpus; dark grayish brown frons. **Thorax.** Marbled with brown and gray scales, with some patches of black scales. **Wing.** Forewing length of male 22–24 mm; forewing with all lines well-developed; orbicular spot formed by a small black line; reniform spot with a narrow lunate marking; hindwing paler color than forewing with black veins; discal spot V-shaped; medial and postmedial lines well developed; fringe black with white scales at the end of each vein. **Legs.** foreleg black with some dark gray spots, while the midleg and hindleg are marbled in gray, brown, and black. **Abdomen.** Marbled with brown and black scales, end of each tergite with gray scales; last abdominal segment with whitish gray hair-like scales. **Male genitalia.** Tegumen narrow; simple valva with cucullar and saccular regions similar in size; apex pointed; saccular process ending in a long clasper with a rounded tip; juxta heart-shaped; uncus long with rounded tip; subuncal lobes wide



Figure 35. Distribution of examined specimens of *Lafontaineana*.

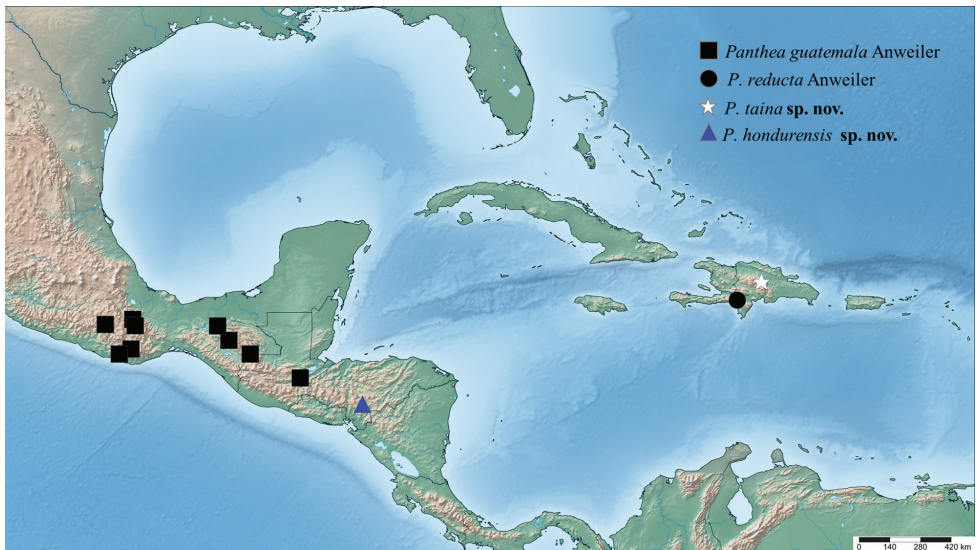


Figure 36. Distribution of examined specimens of *Panthea*.

and rounded; aedeagus short, $2\times$ longer than width; vesica wide, bean-like, with a large sclerotized cornutus.

Genetic characterization. Unknown.

Distribution. This species is endemic to the Dominican Republic and it was found in high elevations of the Cordillera Central (Fig. 36). *Panthea taina* and *P. reducta* may be endemic to two different mountain chains, *P. reducta* occurring in the Sierra de Bahoruco, 130 km far from the Cordillera Central.

Remarks. The holotype (Fig. 20) as well as the paratype are in perfect condition.

Discussion

The only previously known species of the new Neotropical genus *Lafontaineana* was included in the genus *Lichnoptera* for more than a century (Hampson 1913). However, we found that *Lafontaineana* is the sister clade to the *Gaujonia* genus group (Martinez 2020). Another important result of the phylogenetic analysis is that the paraphyly of the genus *Lichnoptera* is corroborated. Unfortunately, only seven of the eleven species are included in the COI gene analysis, and thus the generic placements of *Lichnoptera moesta* Herrich-Schäffer, 1858, *L. primulina* Dognin, 1912, *L. rufitincta* Hampson, 1913, and *L. pollux* (Edwards, 1887) are still not settled.

In regard to the life history and host plants, nothing is known about *Lafontaineana*, but following the sister group, it is possible that some species in this genus also feed on Rosaceae, Betulaceae, Fagaceae, or even Podocarpaceae (Anweiler 2009; Schmidt and Anweiler 2010; Martinez 2020; Schmidt and Anweiler 2020). *Lafontaineana* is endemic to the South American Andes Mountains with a distribution restricted to the cloud forests of Colombia and Ecuador. This genus may prove to be a reasonable flagship taxon for cloud forest conservation.

Acknowledgements

We thank Andy Warren and the MGCL at the Florida Museum of Natural History (University of Florida) for providing facilities. Special thanks are due to Alberto Zilli at the NHMUK who provided the photographs of the type species. We thank Christi Jaeger (CNC), David Plotkin (MGCL), and Ryan St Laurent (MGCL) for their help and support with the molecular analyses, and also to Charles V. Covell Jr. (MGCL) for his helpful comments. Many thanks to Gunnar Brehm (FSU) and Victor Sinyaev who provided additional specimens, and Tyler Shaw who helped prepare specimens for identification. We also thank Donald Lafontaine and Jocelyn Gill (CNC) for their support. We gratefully acknowledge the financial support of the National Geographic Society (EC-51416R-18).

References

- Anweiler GG (2009) Revision of the New World *Panthea* Hübner (Lepidoptera, Noctuidae) with descriptions of 5 new species and 2 new subspecies. *ZooKeys* 9: 97–134. <https://doi.org/10.3897/zookeys.9.157>
- Behounek G, Han HL, Kononenko VS (2013) Revision of the Old World genera *Panthea* Hübner, [1820] 1816 and *Pantheana* Hreblay, 1998 with description two new species from China (Lepidoptera, Noctuidae: Pantheinae). Revision of Pantheinae, contribution IX. *Zootaxa* 3746(3): 422–438. <https://doi.org/10.11646/zootaxa.3746.3.2>

- Hampson GF (1913) Catalogue Noctuidae Collection British Museum. In Catalogue of Lepidoptera Phalaenae in the British Museum, London, UK, 13: 609 pp.
- Ratnasingham S, Hebert PD (2013) A DNA-based registry for all animal species: the Barcode Index Number (BIN) system. PLoS ONE 8(7): e66213. <https://doi.org/10.1371/journal.pone.0066213>
- Herrich-Schäffer GAW (1856) Sammlung neuer oder wenig bekannter aussereuropäischer Schmetterlinge. Manz, G.J., Regensburg, Germany, 84 pp.
- Hoang DT, Chernomor O, Von Haeseler A, Minh BQ, Vinh LS (2018) UFBoot2: improving the ultrafast bootstrap approximation. Molecular biology and evolution 35(2): 518–522. <https://doi.org/10.1093/molbev/msx281>
- Kirby WF (1892) A synonymic catalogue of Lepidoptera Heterocera (Moths) (Vol. 1), *Sphinges* and *Bombyce*. Taylor and Francis, Oxford, 951 pp. <https://doi.org/10.5962/bhl.title.9152>
- Lafontaine JD (1987) Noctuoidea: Noctuidae (part): Noctuinae (Part – *Euxoa*). In: Dominick RB et al. (Eds) The Moths of North America. Fascicle 27.2. The Wedge Entomological Research Foundation, Washington, 237 pp.
- Lafontaine JD (2004) Noctuoidea: Noctuidae (part) – Agrotini. In: Hodges RW (Ed.) The Moths of North America. Fascicle 27.1. The Wedge Entomological Research Foundation, Washington, 394 pp.
- Martinez JI (2020) Revision of the South American genus *Gaujonia* Dognin (Noctuidae, Pantheinae) with descriptions of five new genera and twenty-one new species. ZooKeys 985: 71–126. <https://doi.org/10.3897/zookeys.985.51622>
- Minh BQ, Schmidt HA, Chernomor O, Schrempf D, Woodhams MD, Von Haeseler A, Lanfear R (2020) IQ-TREE 2: New models and efficient methods for phylogenetic inference in the genomic era. Molecular Biology and Evolution 37(5): 1530–1534. <https://doi.org/10.1093/molbev/msaa015>
- Nguyen LT, Schmidt HA, von Haeseler A, Minh BQ (2015) IQ-TREE: A fast and effective stochastic algorithm for estimating maximum-likelihood phylogenies. Molecular Biology and Evolution 32: 268–274. <https://doi.org/10.1093/molbev/msu300>
- Nye IWB (1975) The generic names of moths of the world, Volume 1 Noctuoidea (part): Noctuidae, Agaristidae, and Nolidae. London: British Museum (Natural History), London, 568 pp. <https://doi.org/10.5962/bhl.title.119777>
- Poole RW (1989) Lepidopterorum Catalogus (new series). Fascicle 118. Noctuidae. Part 1. E.J. Brill, Leiden/New York, 500 pp.
- Prittwitz O (1871) Lepidopterogisches. Entomologische Zeitung herausgegeben von dem Entomologischen Verein zu Stettin 7(32): 237–253.
- Schmidt BC, Anweiler GG (2010) The North American species of *Charadra* Walker, with a revision of the *Charadra pata* (Druce) group (Noctuidae, Pantheinae) In: Schmidt BC, Lafontaine JD (Eds) Contributions to the systematics of New World macro-moths II. ZooKeys 39: 161–181. <https://doi.org/10.3897/zookeys.39.432>
- Schmidt BC, Anweiler GG (2020) Noctuoidea: Noctuidae (Part) – Pantheinae, Raphiinae, Balsinae, Acronictinae. In: Lafontaine JD (Ed.) The Moths of North America. Fascicle 25.4. The Wedge Entomological Foundation, Washington, 479 pp.

- Seitz A (1919) Die Gross-Schmetterlinge der Erde. Abteilung II. Amerikanischen Faunengebieten. Band 7. Eulenartige Nachtfalter, Alfred Kernen, Stuttgart, 508 pp.
- Walker F (1862) Characters of undescribed Lepidoptera in the collection of W.W. Saunders, Esq. Transactions of the Entomological Society of London, series 3(1): 70–228.
- Walker F (1865) List of the Specimens of Lepidopterous Insects in the Collection of the British Museum London, UK. Order of Trustees (2): 324–706.

Supplementary material 1

Figure S1

Authors: Jose I. Martinez, B. Christian Schmidt, Jacqueline Y. Miller

Data type: phylogenetic tree

Explanation note: Gene tree of *Lafontaineana* inferred employing Maximum Likelihood in IQ-TREE based on the mitochondrial cytochrome oxidase (COI) marker.

Copyright notice: This dataset is made available under the Open Database License (<http://opendatacommons.org/licenses/odbl/1.0/>). The Open Database License (ODbL) is a license agreement intended to allow users to freely share, modify, and use this Dataset while maintaining this same freedom for others, provided that the original source and author(s) are credited.

Link: <https://doi.org/10.3897/zookeys.1028.56784.suppl1>

Supplementary material 2

Figure S2

Authors: Jose I. Martinez, B. Christian Schmidt, Jacqueline Y. Miller

Data type: phylogenetic tree

Explanation note: Gene tree of *Panthea* inferred employing Maximum Likelihood in IQ-TREE based on the mitochondrial cytochrome oxidase (COI) marker.

Copyright notice: This dataset is made available under the Open Database License (<http://opendatacommons.org/licenses/odbl/1.0/>). The Open Database License (ODbL) is a license agreement intended to allow users to freely share, modify, and use this Dataset while maintaining this same freedom for others, provided that the original source and author(s) are credited.

Link: <https://doi.org/10.3897/zookeys.1028.56784.suppl2>

Supplementary material 3

Table S1

Authors: Jose I. Martinez, B. Christian Schmidt, Jacqueline Y. Miller

Data type: molecular data

Explanation note: Sequence information utilized in this study obtained from GenBank (<http://www.ncbi.nlm.nih.gov/Genbank>) and the BARCODE OF LIFE DATA SYSTEM v4 (<http://barcodinglife.com>).

Copyright notice: This dataset is made available under the Open Database License (<http://opendatacommons.org/licenses/odbl/1.0/>). The Open Database License (ODbL) is a license agreement intended to allow users to freely share, modify, and use this Dataset while maintaining this same freedom for others, provided that the original source and author(s) are credited.

Link: <https://doi.org/10.3897/zookeys.1028.56784.suppl3>

Supplementary material 4

File S1

Authors: Jose I. Martinez, B. Christian Schmidt, Jacqueline Y. Miller

Data type: FASTA file

Explanation note: FASTA file containing the alignment of all COI sequences of the taxa included in Figure 1.

Copyright notice: This dataset is made available under the Open Database License (<http://opendatacommons.org/licenses/odbl/1.0/>). The Open Database License (ODbL) is a license agreement intended to allow users to freely share, modify, and use this Dataset while maintaining this same freedom for others, provided that the original source and author(s) are credited.

Link: <https://doi.org/10.3897/zookeys.1028.56784.suppl4>

Supplementary material 5

File S2

Authors: Jose I. Martinez, B. Christian Schmidt, Jacqueline Y. Miller

Data type: FASTA file

Explanation note: FASTA file containing the alignment of all COI sequences of the taxa included in Figure 2.

Copyright notice: This dataset is made available under the Open Database License (<http://opendatacommons.org/licenses/odbl/1.0/>). The Open Database License (ODbL) is a license agreement intended to allow users to freely share, modify, and use this Dataset while maintaining this same freedom for others, provided that the original source and author(s) are credited.

Link: <https://doi.org/10.3897/zookeys.1028.56784.suppl5>

Supplementary material 6

File S3

Authors: Jose I. Martinez, B. Christian Schmidt, Jacqueline Y. Miller

Data type: Tre file

Explanation note: Tree file in NEWICK format associated with the phylogenetic tree in Figure 1 and Figure S1.

Copyright notice: This dataset is made available under the Open Database License (<http://opendatacommons.org/licenses/odbl/1.0/>). The Open Database License (ODbL) is a license agreement intended to allow users to freely share, modify, and use this Dataset while maintaining this same freedom for others, provided that the original source and author(s) are credited.

Link: <https://doi.org/10.3897/zookeys.1028.56784.suppl6>

Supplementary material 7

File S4

Authors: Jose I. Martinez, B. Christian Schmidt, Jacqueline Y. Miller

Data type: Tre file

Explanation note: Tree file in NEWICK format associated with the phylogenetic tree in Figure 2 and Figure S2.

Copyright notice: This dataset is made available under the Open Database License (<http://opendatacommons.org/licenses/odbl/1.0/>). The Open Database License (ODbL) is a license agreement intended to allow users to freely share, modify, and use this Dataset while maintaining this same freedom for others, provided that the original source and author(s) are credited.

Link: <https://doi.org/10.3897/zookeys.1028.56784.suppl7>

Beginning the quest: phylogenetic hypothesis and identification of evolutionary lineages in bats of the genus *Micronycteris* (Chiroptera, Phyllostomidae)

Darwin M. Morales-Martínez^{1,2}, Hugo F. López-Arévalo², Mario Vargas-Ramírez^{1,3}

1 Grupo de Biodiversidad y Conservación Genética, Instituto de Genética, Universidad Nacional de Colombia, Universidad Nacional de Colombia, Carrera 45 No 26-85, Bogotá, Colombia **2** Grupo en Conservación y Manejo de Vida Silvestre, Instituto de Ciencias Naturales, Universidad Nacional de Colombia, Carrera 45 No 26-85, Bogotá, Colombia **3** Estación de Biología Tropical Roberto Franco, Universidad Nacional de Colombia, Carrera 33 #33-76, Barrio El Porvenir, Villavicencio, Meta, Colombia

Corresponding author: Darwin M. Morales-Martínez (dmmoralesmar@gmail.com)

Academic editor: DeeAnn Reeder | Received 20 November 2020 | Accepted 4 March 2021 | Published 6 April 2021

<http://zoobank.org/A2E56F35-FAC4-4925-9F53-F58725894589>

Citation: Morales-Martínez DM, López-Arévalo HF, Vargas-Ramírez M (2021) Beginning the quest: phylogenetic hypothesis and identification of evolutionary lineages in bats of the genus *Micronycteris* (Chiroptera, Phyllostomidae). ZooKeys 1028: 135–159. <https://doi.org/10.3897/zookeys.1028.60955>

Abstract

Thirteen species of Neotropical bats of the genus *Micronycteris* are currently recognized and are allocated to four subgenera *Leuconycteris*, *Micronycteris*, *Schizonycteris*, and *Xenonectes*. Despite that, the presence of polyphyletic clades in molecular phylogenies suggests that its diversity is underestimated. Additionally, the incorrect identification of some genetic sequences, the incorrect assignation of available valid names, and restricted geographic sampling have biased the identification of independently evolutionary lineages within *Micronycteris*. In this study, several unknown genealogical lineages in the genus are identified and an updated phylogenetic hypothesis is proposed using mitochondrial and nuclear DNA fragments. The phylogenetic analyses congruently showed all individuals in four well-supported subgenera, but *M. schmidtorum* was revealed as the sister taxon of *M. brosetti* in the subgenus *Leuconycteris*. Twenty-seven different genealogical lineages were identified. These included eight confirmed species: *M. brosetti*, *M. buriri*, *M. giovanniae*, *M. matses*, *M. schmidtorum*, *M. simmonsae*, *M. tresamici*, and *M. yatesi*. Nineteen either allopatric or parapatric candidate species were also confirmed, two within the *M. hirsuta* complex, nine within the *M. megalotis* complex, seven within the *M. minuta* complex, and one corresponding to “*M. sp.*”. These results revealed an extensive undescribed diversity within each subgenus of *Micronycteris*. Nevertheless, the evolutionary processes associated with the specific radiations are poorly understood. This is just the beginning of the assessment of the taxonomy and systematics of *Micronycteris*, which requires additional integrative taxonomical approaches for its advance.

Keywords

Distribution, neotropical bats, species delimitation, systematics, taxonomy

Introduction

Scientists describe between 200 and 300 mammal species per decade, mainly small species like rodents and bats (Patterson 2000; Reeder et al. 2007). Recent increases in species descriptions are due to discoveries based on fieldwork (Reeder et al. 2007), and the application of the genetic and phylogenetic species concepts (Solari and Martínez-Arias 2014). This is especially true for Neotropics, where a larger number of undiscovered mammal species remain undescribed (Patterson 2000; Reeder et al. 2007).

In particular, bats (Chiroptera) represent a highly diverse mammal group in the Neotropics, comprising 21% (1386 species) of the mammal diversity (6495 species) and with an elevated number of species described in the last 10 years (Burgin et al. 2018). Among the vast diversity of neotropical bats, phyllostomids represent the largest recent radiation with ca. 223 species currently recognized (Simmons and Cirranello 2020) and 59 species described or split since 2005 (Burgin et al. 2018).

Within Phyllostomidae, bats of the genus *Micronycteris* are gleaning insectivores that are common in Neotropical bat assemblages. This genus currently comprises 13 recognized species allocated to four subgenera (i.e., *Leuconycteris*, *Micronycteris*, *Schizonycteris*, and *Xenonectes*; Porter et al. 2007), and several studies using genetic data have suggested that the diversity of this group has been underestimated (Porter et al. 2007; Larsen et al. 2011; Siles et al. 2013; Siles and Baker 2020). At least, two widely distributed species, *M. megalotis* and *M. minuta* may have possible cryptic lineages because phylogenetic assessments for both species recovered strongly supported polyphyletic clades (Porter et al. 2007). Furthermore, some inconsistencies in the identity of the species assigned to the different clades have been identified: (1) some GenBank sequences lack voucher specimens and/or the confirmation of the sequence identification (e.g., Porter et al. 2007), (2) some names have been changed among phylogenetic hypotheses without robust arguments (e.g., Porter et al. 2007; Larsen et al. 2011; Siles et al. 2013), (3) some clades names were based on sequences from specimens collected far from the type locality without justification (e.g., *M. microtis* in Siles et al. 2013) and (4) the geographic coverage of the sequences has been extremely limited, with sequences from the central distribution of the genus from countries with a high diversity of the genus such as Colombia being practically nonexistent (see. Porter et al. 2007). Therefore, the correct interpretation of the diversity within *Micronycteris* depends on analyses including the assessment of genetic variation within the genus, incorporating vouchers from poorly surveyed portions of its distribution range.

Despite the evidence of cryptic diversity within *Micronycteris* (Porter et al. 2007; Larsen et al. 2011; Siles et al. 2013; Siles and Baker 2020), the identification of cryptic lineages has lacked a logical framework for their accurate delimitation. Such accurate

lineage delimitation is critical for the assessment of priority areas for conservation (Vieites et al. 2009; Burgin et al. 2018), the monitoring of biodiversity loss (Vieites et al. 2009), the identification of potential vectors of zoonotic diseases (Bickford et al. 2007), the evaluation of biological interactions, and the formulation and assessment of evolutionary or biogeographic hypotheses (Burgin et al. 2018).

In this study we aimed at assessing the diversity and evolutionary relationships of the lineages making up the genus *Micronycteris* by identifying a yet-undescribed portion of its genetic diversity and at proposing an updated phylogenetic hypothesis. For this, we analyzed a combination of molecular data including fragments of the cytochrome-b gene (Cytb) mitochondrial DNA (mtDNA) and the intron 7 of the nuclear fibrinogen, B beta polypeptide gene (Fgb-I7) nuclear DNA (nDNA). Furthermore, we included new sequences from individuals of several species of *Micronycteris* from wider geographical distribution.

Methods

Revision of specimens

To confirm the correct identification of the sequences in our analyses, we examined at least one voucher specimen from most of the clades reported in previous studies (Porter et al. 2007; Larsen et al. 2011; Siles et al. 2013; Siles and Baker 2020). The examined specimens (Suppl. material 1: Table S1) are housed in the following collections: The American Museum of Natural History (**AMNH**), USA; the Instituto de Ciencias Naturales of Universidad Nacional de Colombia (**ICN**), Colombia and the Pontificia Universidad Católica del Ecuador (**PUCE**), Ecuador.

Laboratory procedures

We extracted genomic DNA using the phenol-chloroform method (Sambrook et al. 1989) from fresh samples of liver or muscle tissues preserved in ethanol, and for museum specimens, we extracted punches of tissue from the plagiopatagium. We obtained DNA from individuals of five species, *M. hirsuta*, *M. megalotis*, *M. microtis*, *M. minuta*, and *M. schmidtorum* from several localities in Colombia (Suppl. material 2: Fig. S1). We amplified 32 sequences between 700 and 1100 base pairs (bp) of the cytochrome-b gene (Cytb) mitochondrial DNA (mtDNA) and 19 sequences between 500 and 700 bp of the fibrinogen beta chain (Fgb-I7) gene nuclear DNA (nDNA) from the newly obtained specimens. We used the same primers and followed the same laboratory protocols and methods of Porter et al. (2007) for both genes, albeit increasing the annealing temperature from 45–48 °C to 50.5 °C for the Cytb amplification. Additionally, we gathered 101 sequences of Cytb and Fgb-I7 of *Micronycteris* species from the GenBank and Bold Systems databases and 64 sequences provided in Siles and Baker (2020) and included in the analyses (Suppl. material 1: Table S1).

Phylogenetic analyses

For the phylogenetic analyses, we included 198 sequences of Cytb (mtDNA) comprising all currently recognizes species of *Micronycteris*, 150 sequences of Fgb-I7 (nDNA), and 146 individuals with complete data set (Cytb + Fgb-I7) of most of the *Micronycteris* species except by *M. sanborni* (list of specimens and sequence numbers in Suppl. material 1: Table S1), covering a wide portion of the geographic distribution of the genus (see Suppl. material 1: Table S1). We performed multiple sequence alignment for both genes using the Clustal W algorithm in BioEdit 7.2.6 software (Hall 1999). We analyzed the Cytb mtDNA, the Fgb-I7 nDNA, and the complete evidence (Cytb + Fgb-I7) data sets, using the following partition scheme: (i) unpartitioned, (ii) partitioned by gene (i.e., each gene fragment treated as a distinct partition) and (iii) maximum partitioning (i.e., each codon of the protein-coding gene Cytb and the Fgb-I7 gene fragment treated as distinct partitions). We assessed the optimal partitioning scheme and best-fit evolutionary models using PartitionFinder v2 and the Bayesian Information Criterion (Lanfear et al. 2016) and selected the maximum partitioning scheme. We applied the following resulting models in a Bayesian analysis (BA) with MrBayes v 3.2.1 (Ronquist et al. 2012): Cytb 1st codon – K80+G, Cytb 2nd codon – K81uf+I+G, Cytb 3rd codon – K80+G and Fgb-I7– HKY+I+G. Those models were incorporated into a single tree search (mixed model partition approach; Nylander et al. 2004), and two parallel runs were carried out using four Markov chains, run for 50 million generations, sampling every 100 generations. We discarded 25% of the resulting trees as burn-in, and 85% of the trees were used for generating a 50% majority-rule consensus. We assessed an acceptable level of the MCMC chains and estimated the effective sample sizes for all parameters using the software Tracer 1.5.4 (Rambaut et al. 2018). Additionally, we performed phylogenetic analyses of the same data sets using the Maximum Likelihood algorithm implemented in RAxML 1.5 beta software (Stamatakis 2014). The default GTR+G model was set across all partitions. Five independent Maximum Likelihood searches were performed with different starting conditions and the rapid bootstrap algorithm to explore the robustness of the branching patterns by comparing the best trees. Afterwards, 1000 non-parametric thorough bootstrap values were computed and plotted against the best tree. For all phylogenetic analyses, we used homologous sequences of other bat species including *Desmodus rotundus*, *Glossophaga soricina*, *Hsunnycteris cadenai*, *Hsunnycteris thomasi*, *Lampronycteris brachyotis*, *Lionycteris spurrelli*, and *Lonchophylla robusta* as outgroups (Suppl. material 1: Table S1). We based the description of the resulting phylogenetic hypothesis for the genus *Micronycteris* on the complete evidence data set analyses.

Lineage delimitation analyses

We evaluated whether populations within the genus *Micronycteris* corresponded to different independently evolving evolutionary lineages (the General Lineage Species Concept of de Queiroz 1999; 2007) when two or more independent lines of evidence supported their distinctiveness. For that, we used the following different lines of evidence: (1) identification of monophyletic lineages in the mtDNA and mtDNA +

nDNA phylogenies, (2) assessment of genetic distances using the mitochondrial gene, (3) identification of mitochondrial monophyletic clades matching unique nDNA haplotypes, and (4) the use of single locus species delimitation methods. Based on the concordance of those lines of evidence we identified whether those lineages corresponded to Confirmed Species or Confirmed Candidate Species (CCS); the later sensu Vieites et al. (2009) defined as: generally deep *Cytb* lineages (> 3% sequence divergence), differing clearly by morphology or with exclusively nDNA private haplotypes and recognized by at least one species delimitation method.

We started the lineage delimitation by determining the monophyletic clades through the phylogenetic analyses and afterward we searched for mitochondrial lineages with genetic divergences > 3%, using the Species Identifier 'Cluster' algorithm in Taxon DNA 1.7 (Meier et al. 2006). We used 3% because it was the percentage of the degree of genetic divergence that often corresponds to species-level units in several phyllostomid bats (see Genetic Species Concept in Bradley and Baker 2001 and Baker and Bradley 2006). We assessed the genetic distances between clades using uncorrected *p*-distances, implemented in the software Mega v.10.0.5 (Kumar et al. 2018).

Then, we searched for genealogical concordance between mitochondrial and nuclear lineages because such concordance has been considered an essential criterion for species recognition (Avice and Ball 1990). For that, we searched for unique haplotypes in the *Fgb-I7* gene corresponding to the mtDNA lineages revealed by the phylogenetic trees and showing genetic distances of > 3%. We trimmed all sequences of *Fgb-I7* to equal length and removed the sequences containing ambiguities that could not be interpreted as heterozygotes. We resolved nuclear DNA sequences to haplotypes with the PHASE algorithm (Stephens et al. 2001) implemented in the software DNAsp 6 (Rozas et al. 2017). The phased sequences were then used to construct a haplotype network in the software Haplotype Viewer (<http://www.cibiv.at/~greg/haploviewer/>), based on a Neighbour-joining tree from uncorrected *p*-distances computed with MEGA v.10.0.5 (Kumar et al. 2018).

In addition, we performed the following three different single-locus species delimitations models: (i) The Bayesian implementation of Poisson tree processes (bPTP), (ii) The single-threshold method of the generalized mixed Yule coalescent model (GMYC), and (iii) The multi-rate Poisson tree processes for single locus (mPTP). All analyses were performed using the Exelixis Lab's web server (bPTP – <http://species.h-its.org/ptp/>; mPTP – <https://mptp.h-its.org/#/tree>; GMYC – <http://species.h-its.org/gmyc/>). For the delimitation analyses, we used unique haplotypes of *Cytb* across the aligned region to avoid the influence of duplicate haplotypes in the analyses (147 terminals; Suppl. material 1: Table S1). We constructed an ultrametric tree with BEAST v1.7.2 (Drummond et al. 2012) using a lognormal relaxed-clock model, a coalescent constant-size tree prior, and a relative time set with a prior on the ingroup age of one (normal distribution: mean = 1, SD = 0.01). We ran two independent MCMC analyses for 50 million generations, sampling every 1000 generations. We assessed convergence, discarded a fraction of trees as burn-in, and summarized the trees as in MrBayes phylogenetic analyses above. The resulting tree was used for the delimitation analyses. The bPTP delimitation search was performed for 500,000 Markov chain Monte Carlo (MCMC) generations, with

thinning set to 100 and a burn-in of 25% of initial samples. The convergence of bPTP analysis was visually checked in the trace plot. Finally, we considered both, the Maximum likelihood and Bayesian solutions for the bPTP delimitation.

Data resources

The data underpinning the analysis reported in this paper are deposited in the Mendeley Repository at: <http://dx.doi.org/10.17632/vyp75f243x.1>

Results

Phylogenetic analyses

For the Cytb gene dataset and the complete evidence, both tree building methods placed all individuals into four well-supported major clades that corresponded to four subgenera of *Micronycteris* namely: *Leuconycteris*, *Micronycteris*, *Schizonycteris*, and *Xenonectes*, (Fig. 1). However, the phylogenetic position of *M. schmidtorum* was placed in the subgenus *Leuconycteris* (Figs 1, 2). *Leuconycteris* included the species *M. brosetti* and *M. schmidtorum*. *Micronycteris* included the species *M. buriri*, *M. giovanniae*, *M. matts*, an undescribed species “*M. sp.*”, and nine clades within *M. megalotis* complex (including *M. microtis*, see taxonomic comments in discussion). *Schizonycteris* included the species *M. tresamici*, *M. sanborni*, *M. yatesi*, *M. simmonsae*, and seven clades within the *M. minuta* complex. Finally, *Xenonectes* contain two clades of *M. hirsuta* complex (Figs 1, 2).

The first strongly supported major clade matched the subgenus *Schizonycteris* (Fig. 2). Within this major clade, the first strongly supported subclade corresponded to the species *M. tresamici* from Honduras. This subclade was recovered basal to the strongly supported species *M. yatesi* (BA: 1, ML: 90%) from Bolivia. The latter was recovered with robust support (BA: 1, ML: 98%) basal to the species *M. simmonsae* from Ecuador. These subclades were recovered by both phylogenetic analyses as successive sister taxa of seven subclades comprising the *M. minuta* complex (denoted with Mi abbreviation; Fig. 2). This complex is represented by two reciprocally monophyletic genetic groups; the first is robustly supported (BA: 1, ML: 99%) and included individuals from eastern Ecuador and Colombia (Mi A), the second showed lower support (not recovered in the ML analyses) included two genetic subgroups. The first subgroup contained an individual from eastern Colombia (Mi B), and its sister robustly supported subgroup (BA: 1, ML: 94%), included individuals from Colombia, Trinidad, and Venezuela (Mi C). The second weakly supported genetic group (BA: 0.9, ML: 38%) included a first strongly supported subgroup (BA: 1, ML: 100%) including individuals from French Guiana and Suriname (Mi E), and a second low supported subgroup made up of three strongly supported subclades including individuals from Bolivia (Mi D; BA: 1, ML: 92%), Guyana and Suriname (Mi G; BA: 1, ML: 100%), and Suriname (Mi F; BA: 1, ML: 100%; Fig. 2).

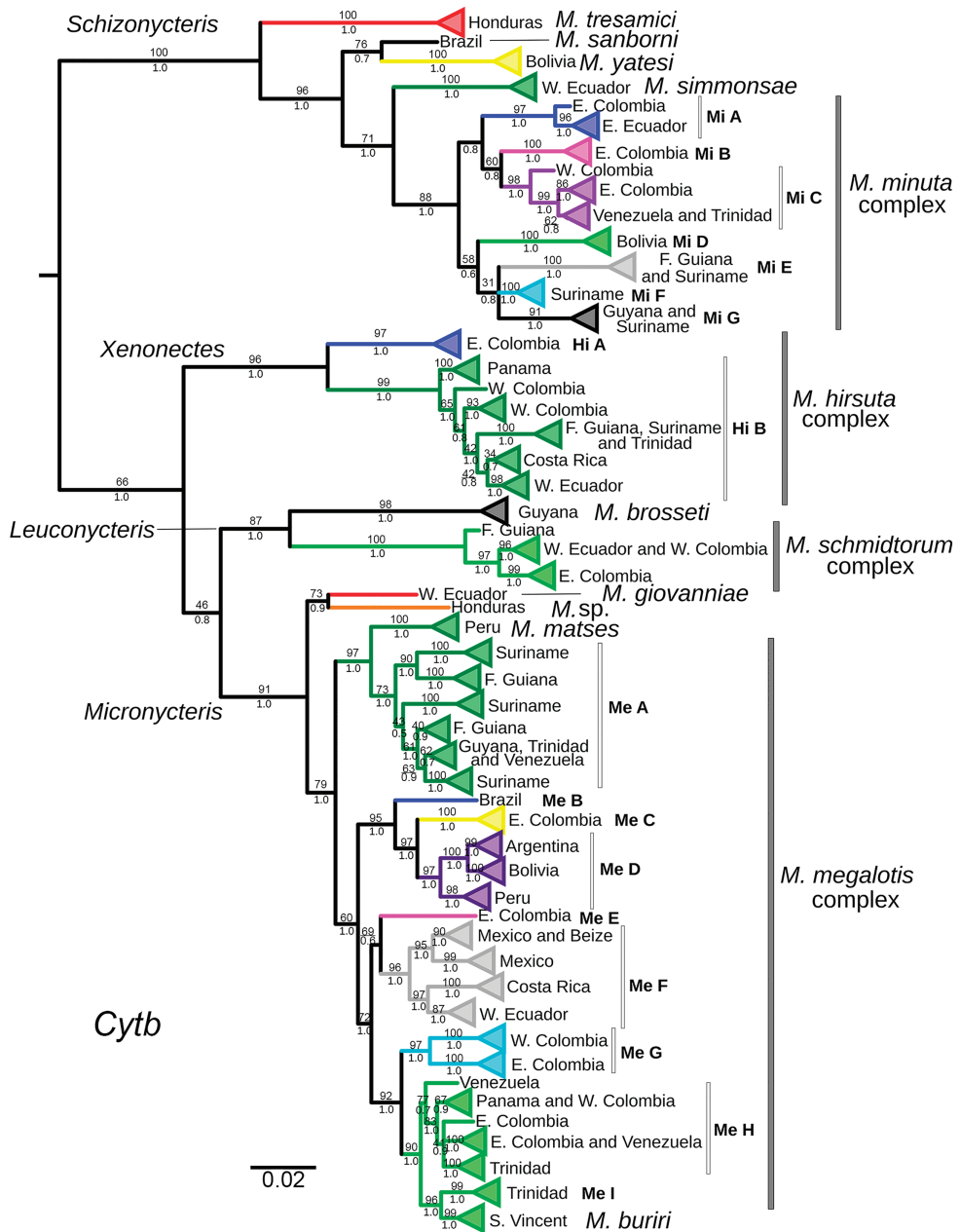


Figure 1. Bayesian phylogram of the genus *Micronycteris* from the phylogenetic analysis of the *Cytb* gene, mtDNA. Numbers below the nodes correspond to Bayesian posterior probabilities, and those above correspond to bootstrap support values (percentages). Colors indicate the clades with > 3% of genetic differentiation. Sequences within groups are listed in Suppl. material 1: Table S1 and depicted in Fig. 5. Bootstrap support values are missing in clades not recovered by ML analyses. *Micronycteris sanborni* was not included in mitochondrial genetic differentiation analyses because it is a chimeric sequence of two individuals.

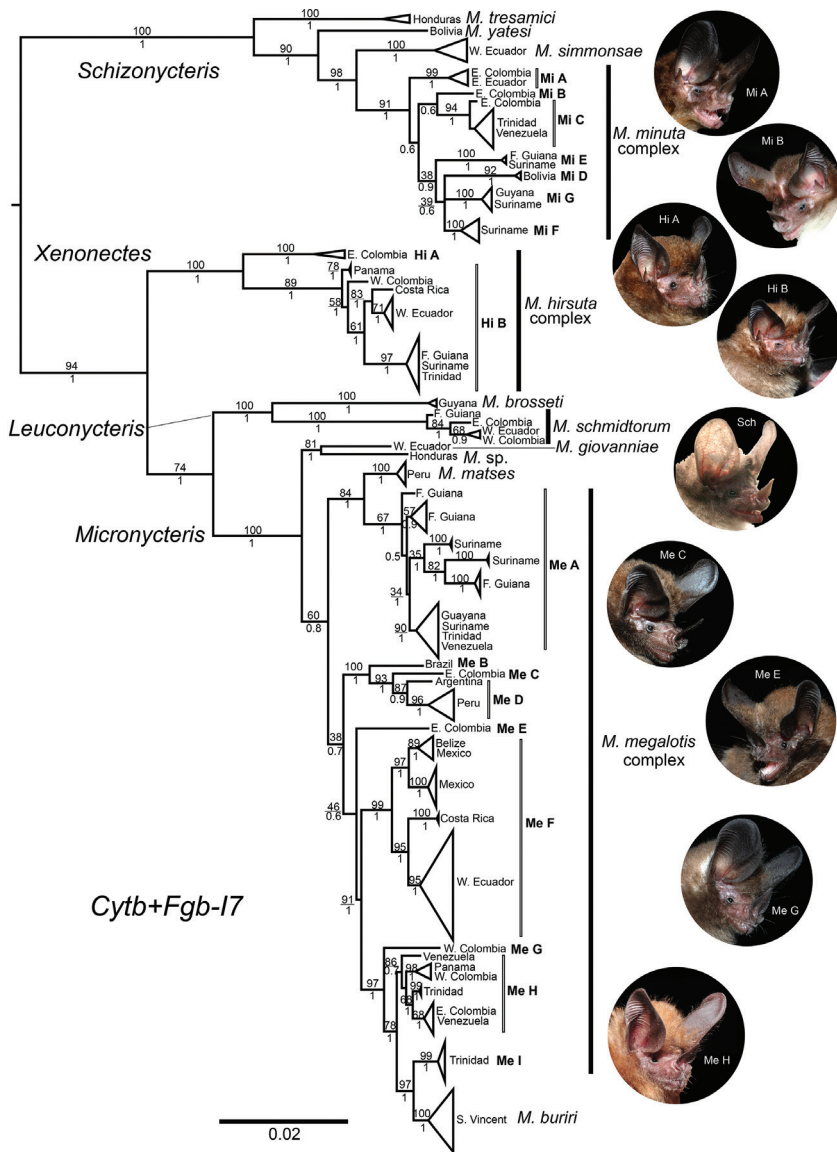


Figure 2. Bayesian phylogram of the genus *Micronycteris* from the phylogenetic analysis of combined evidence (mtDNA + nDNA). Numbers below the nodes correspond to Bayesian posterior probabilities, and those above correspond to bootstrap support values (percentages). The acronyms Mi, Hi, and Me represent the candidate species for *M. minuta*, *M. hirsuta* and *M. megalotis*, respectively. Sequences per group are listed in Table S1. Inset photos: (Mi A) ICN-24465♀: Colombia, Caquetá, Florencia, Vereda el Venado, Macagual; (Mi B) ICN 23912♂: Colombia, Vichada, Cumaribo, Matavén River; (Hi A) ICN-23867♀: Colombia, Guaviare, San José del Guaviare, Vereda Los Alpes, El Provenir farm; (Hi B) ICN Temporal D3M541♂, Colombia, Santander, Puerto Parra, Bocas del Carare; (Sch) ICN-24479♂: Colombia, Magdalena, Santa Marta, Tayrona National Natural Park; (Me C) ICN-23869♂: Colombia, Guaviare, San José del Guaviare, Vereda Los Alpes, El Provenir farm; (Me E) ICN-23839♂: Colombia, Guaviare, San José del Guaviare, Vereda El Raudal, Angosturas II; (Me G) ICN-24495♀: Colombia, Huila, Gigante, Vereda Matambo, La Ensillada farm; (Me H) ICN-23203♂. Colombia, Meta, La Macarena, Vereda Caño Canoas, High plain of Caño Canoas.

The second strongly supported major clade, matching the subgenus *Xenonectes*, corresponded to the *M. hirsuta* complex. This major clade was formed by two strongly supported monophyletic subclades (denoted with Hi abbreviation; Fig. 2). The first corresponded to a strongly supported subclade from eastern Colombia (Hi A; Fig. 2). The second is a strongly supported subclade (BA: 1, ML: 89%) included individuals from Panama, western Colombia, Costa Rica, French Guiana, Suriname, Trinidad, and western Ecuador (Hi B; Fig. 2).

The third major clade corresponded to the subgenus *Leuconycteris* and included two strongly supported reciprocally monophyletic subclades. The first subclade constituted by *M. brosetti* from Guyana; and the second subclade by *M. schmidtorum*, including individuals from French Guiana, western Ecuador, and both western and eastern Colombia (Fig. 2).

Finally, the fourth major clade represented by the subgenus *Micronycteris* included three inclusive reciprocally monophyletic subclades (Fig. 2). The first robustly supported subclade (BA: 1, ML: 81%) comprised the species *M. giovanniae*, formed by an individual from western Ecuador, and as the sister taxon to an undescribed species "*M. sp.*", from Honduras (Fig. 2). The second moderately supported monophyletic subclade (BA: 1, ML: 84%), comprised a strongly supported lineage corresponding to the species *M. matts*. This lineage represented by individuals from eastern Peru, and appeared as sister of a weakly supported genetic group (BA: 1, ML: 67%) composed of individuals from French Guyana, Surinam, Guyana, Trinidad, and southern Venezuela (Me A; Fig. 2). Finally, the third weakly supported monophyletic subclade (BA: 0.7, ML: 38%) comprised two genetic groups. The first group was a robustly supported lineage formed by an individual from Brazil (Me B), as the sister taxon of a robustly supported genetic group (BA: 1, ML: 93%) formed by an individual from eastern Colombia (Me C) and a robustly supported lineage (BA: 0.9, ML: 87%) composed by individuals from Argentina and Peru (Me D; Fig. 2). The second genetic group was recovered with weak support (BA: 0.6, ML: 46%), including an individual from eastern Colombia (Me E), as the sister of a lineage composed by two genetic subgroups. The first one corresponded to a strongly supported subgroup (BA: 1, ML: 99%), comprising individuals from Belize, Mexico, Costa Rica, and western Ecuador (Me F; Fig. 2). This genetic subgroup was shown to be the sister of a robustly supported subgroup (BA: 1, ML: 97%) formed by an individual from western Colombia (Me G), as the sister of a robustly supported genetic subgroup comprising a medium supported lineage (BA: 0.7, ML: 86%) including individuals from western Colombia, Panama, eastern Colombia, southern Venezuela (Me H; Fig. 2). The later genetic subgroup was revealed as the sister of a strongly supported subgroup that comprised a supported lineage (BA: 1, ML: 99%) from Trinidad and Tobago (Me I; Fig. 2), being sister of a strongly supported clade of *M. buriri* from Saint Vincent Island.

Lineage delimitation

The "Cluster" algorithm of TaxonDNA revealed 24 reciprocally monophyletic clades with genetic divergence of more than 3% (Fig. 1, colored clades). Within the subgenus *Schizonycteris* we found ten lineages, representing to *M. yatesi*, *M. tresamici*,

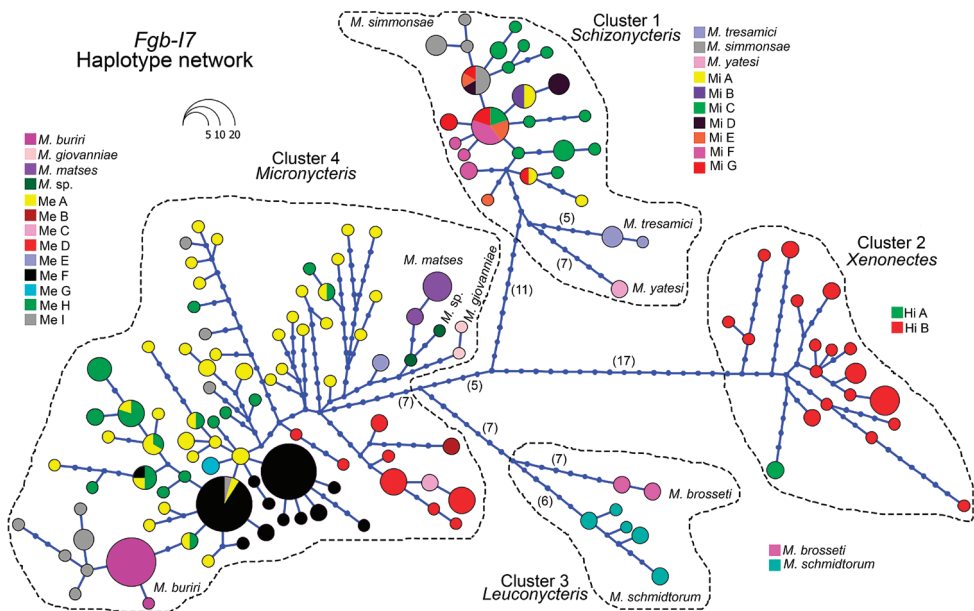


Figure 3. Haplotype network of the genus *Micronycteris* for the *Fgb-17* gene nDNA haplotypes based on an alignment of 686 bp. Circle size reflects haplotype frequency and missing haplotypes are represented by small circles. Each line connecting haplotypes corresponds to one mutational step. Colors within each nominal species haplogroup represent the candidate species and Mi, Hi, and Me correspond to their acronyms in *M. minuta*, *M. hirsuta*, and *M. megalotis* respectively.

M. simmonsae, and seven clades belonging to the *M. minuta* complex (Fig. 1; Suppl. material 3: Table S2). Within the subgenus *Xenonectes*, we found two subclades with > 3% of genetic distance (Fig. 1; Suppl. material 3: Table S2). Within the subgenus *Leuconycteris*, we found two subclades with > 3% of genetic distance, one corresponding to the recognized species *M. brosetti*, and the second by the species *M. schmidtorum* (Fig. 1; Suppl. material 3: Table S2). Lastly, within the subgenus *Micronycteris* we found ten subclades with > 3% genetic distance between them, including (i) *M. giovanniae*, (ii) an undescribed species (“*M. sp.*”), and (iii) eight clades forming the *M. megalotis* complex (Fig. 1; Suppl. material 3: Table S2). The nominal species *M. matses* and *M. buriri* failed to have a > 3% of the genetic distance with any other subclade (Suppl. material 3: Table S2; Fig. 1).

Our *Fgb-17* gene TCS haplotype network contained four genetic clusters separated by a minimum of 23 mutational steps (Fig. 3). These clusters corresponded to 130 haplotypes that matched the 24 mitochondrial lineages identified by the TaxonDNA analyses (> 3% genetically of divergence), and *M. matses* and *M. buriri* (that have < 3% of genetic distance; Fig. 1), all recovered by the complete evidence phylogeny too (Figs 2, 4). The subgenus *Schizonycteris* (Cluster 1) was formed by 27 haplotypes, matching the three recognized species (*M. tresamici*, *M. yatesi*, and *M. simmonsae*) and the seven mitochondrial lineages within the *M. minuta* complex (Mi A–Mi G) separated

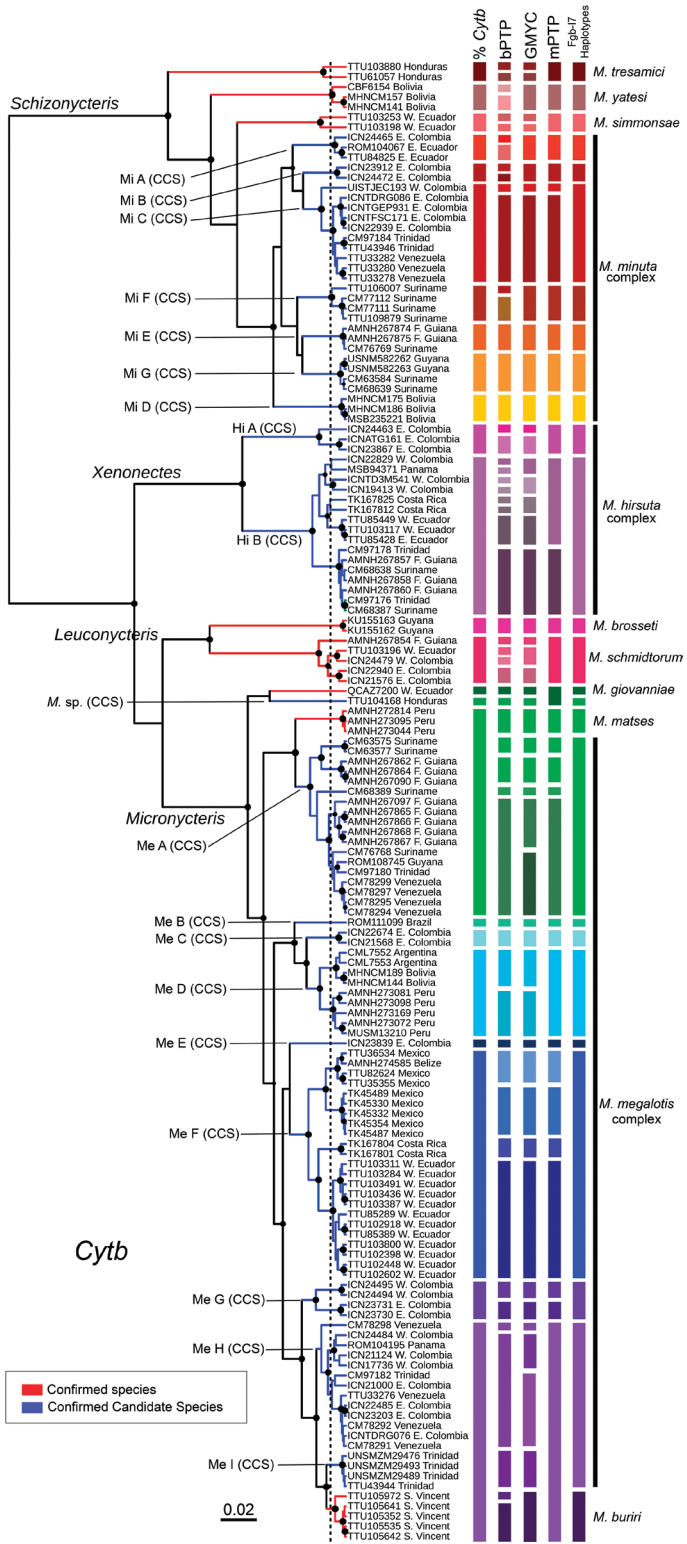
between one and 12 mutational steps. The subgenus *Xenonectes* (*M. hirsuta* complex, Cluster 2) was formed by 19 haplotypes that corresponded to the two mtDNA lineages Hi A and Hi B, separated by a minimum of seven mutational steps. The subgenus *Leuconycteris* (Cluster 3) included *M. schmidtorum* with five haplotypes and *M. brosetti* with two haplotypes, separated by a minimum of 13 mutational steps from the haplotypes of *M. schmidtorum* (Fig. 3). Finally, the most extensive haplotype cluster matched the subgenus *Micronycteris* (Cluster 4), formed by haplotypes that diverged between one to 27 mutational steps from each other. Unique haplotypes in this haplogroup matched three species (i.e., *M. matses*, *M. giovanniae*, and “*M. sp.*”) and nine lineages forming the *M. megalotis* complex (Fig. 3).

The single locus species delimitation analyses revealed contrasting results. The bPTP model delimited 55 entities. Nevertheless, only 15 of those clades showed posterior probabilities above 0.95 (Suppl. material 4). The other clades showed between 0.49 and 0.95, which suggests that caution should be considered when interpreting these clades as independently evolving lineages (Suppl. material 4). The single-threshold method of the GMYC model delimited 48 entities. The model was significantly better than the null hypothesis with the likelihood ratio test (LR = 5040.823, LRT results = 0***, threshold time = -0.008590693; Suppl. material 4). Finally, the mPTP model was somewhat more conservative, identifying 33 species (Fig. 4) that matched several lineages delimited by the bPTP and GMYC methods (Suppl. material 4).

Considering the different lines of evidence, we revealed 27 different genealogical lineages forming the genus (Fig. 4). They belong to eight confirmed species (CS): *M. brosetti*, *M. buriri*, *M. giovanniae*, *M. matses*, *M. schmidtorum*, *M. simmonsae*, *M. tresamici*, and *M. yatesi*, and 19 confirmed candidate species (CCS) with either allopatric or parapatric distribution within three species complexes. We present in Fig. 4 the position of each revealed evolutionary lineage in the Cytb tree and in Fig. 5 their hypothesized geographic distribution.

Confirmed candidate species (CCS)

We found seven CCS within the subgenus *Schizonycteris*, in the *M. minuta* complex: (1) lineage Mi A formed by individuals from the Amazon of Ecuador and Colombia; (2) lineage Mi B formed by individuals from the north Amazon of Colombia; (3) lineage Mi C formed by individuals from dry-forest of western Colombia, the Orinoco Llanos of Colombia and Venezuela, and the Trinidad Island; (4) lineage Mi D formed by individuals from Bolivia; (5) lineage Mi E formed by individuals from north French Guiana and Suriname; (6) lineage Mi F formed by individuals from south Suriname and (7) lineage Mi G formed by individuals from north Guyana and Suriname. Two more CCS were confirmed within the subgenus *Xenonectes* in the *M. hirsuta* group: (1) lineage Hi A, including individuals from eastern Colombia and (2) lineage Hi B, including individuals from Costa Rica, Trinidad, French Guyana, Panama, Suriname, western Colombia, and western Ecuador. Finally, ten CCS within the subgenus *Micronycteris*: (1) lineage “*M. sp.*” from Honduras; (2) lineage Me A including individ-



uals from Suriname, French Guyana, easternmost Venezuela, Guyana, and Trinidad; (3) lineage Me B including an individual from Brazil (this lineage could represent the nominal *M. megalotis* due to its type locality “unknown locality in Brazil”); (4) lineage Me C including individuals from north Amazon of Colombia; (5) lineage Me D comprising individuals from Argentina, Bolivia, and Peru; (6) lineage Me E including an individual from north Amazon of Colombia; (7) lineage Me F including individuals from Belize, Costa Rica, Mexico, and western Ecuador; (8) lineage Me G including individuals from the Magdalena valley and the eastern versant of the Andean Cordillera of Colombia; (9) lineage Me H formed by individuals from Panama, the dry forest of western Colombia and the Orinoco Llanos of Colombia and Venezuela and (10) lineage Me I formed by individuals from Trinidad. Due to the distribution of the Me F and Me H, two available names, *Micronycteris mexicana* and *Micronycteris microtis* might be applied to these lineages. Nonetheless, the applications of these names depend on a posterior taxonomic revision. We make no conclusions about the status of *M. sanborni* because we did not have enough information to include it in the applied framework.

Discussion

Our results showed contrasting evolutionary patterns between the different subgenera of *Micronycteris*. At the specific level, the evolutionary histories of widely distributed species such as *M. megalotis*, *M. hirsuta*, and *M. minuta* are more complex than previously known (Porter et al. 2007; Larsen et al. 2011; Siles et al. 2013), with several unknown genealogical lineages with allopatric and/or parapatric distributions. The different specific factors that may have influenced lineage differentiation within the genus *Micronycteris* are still unknown, however, distinctive ecological and ethological characteristics such as the size of familiar groups, home range, and movement behavior may have played a prominent role, because it is known that small social groups, rigid social structures, and low dispersal capacity induce high genetic variation (Bradley and Baker 2001). Generally, *Micronycteris* contains widely distributed species that use various types of refuges in small social groups (i.e., familiar groups with fewer than 12 individuals. Emmons 1997); and they tend to have high refuge fidelity (Kalka and Kalko 2006; Albrecht et al. 2007). In addition, due to its foraging strategy, the species of *Micronycteris* do not frequent open areas (Albrecht et al. 2007). Bats of the genus *Micronycteris* have small home ranges (ca. 3.8 ha; Albrecht et al. 2007) compared to

Figure 4. Bayesian phylogram of the genus *Micronycteris* from the analysis of Cytb gene mtDNA (BEAST), showing colored bars that represent the different delimitation schemes obtained with > 3% of genetic differentiation, bPTP, GMYC, mPTP, and Fgb-I7 haplotype network. CS: Confirmed species (Red), CCS: Confirmed Candidate Species (Blue). The dashed vertical line indicates the threshold between the Yule and the coalescent process estimated by the likelihood implementation of the GMYC model. Filled circles at internal nodes indicated strong support for Bayesian (BEAST: PP > 0.95), and the size is proportional between 0.95 to 1 PP. The acronyms Mi, Hi, and Me represent the candidate species in *M. minuta*, *M. hirsuta*, and *M. megalotis*, respectively. Sequences within groups are listed in Suppl. material 1: Table S1 and depicted in Fig. 5.

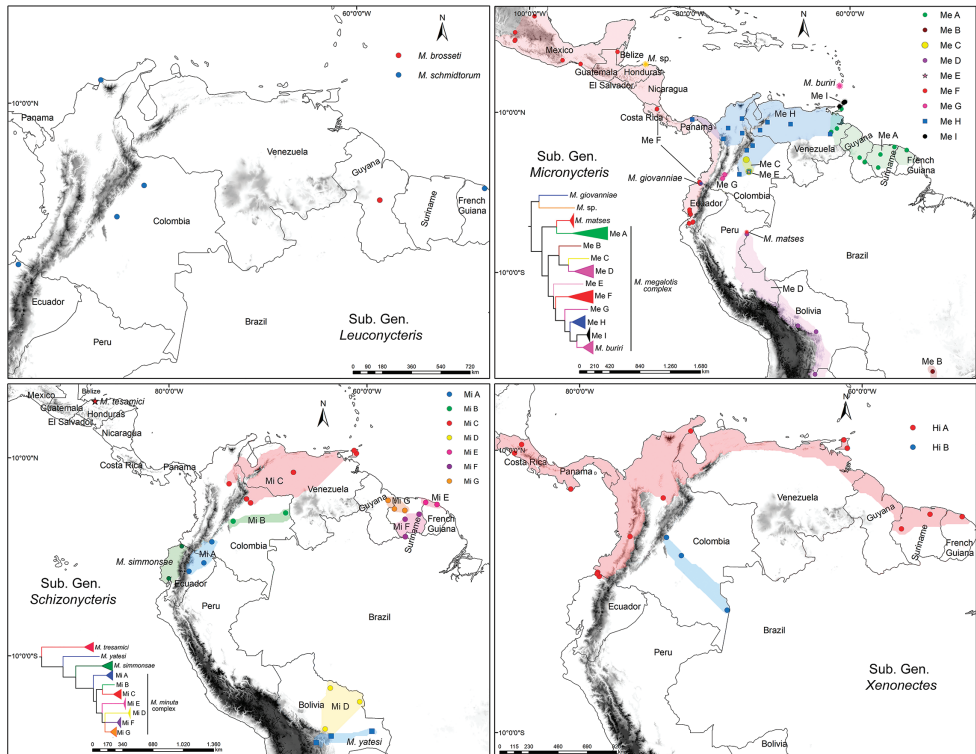


Figure 5. Geographic location of the individuals from which the sequences were obtained and included in the phylogenetic analyses. Shades represent a hypothetical estimation of the distribution of each clade based on the locality of the included individuals. The acronyms Mi, Hi, and Me represent the candidate species in *M. minuta*, *M. hirsuta*, and *M. megalotis*, respectively. Sequences within groups are listed in Suppl. material 1: Table S1.

other phyllostomid bats such as the insectivores *Macrophyllum macrophyllum* (24 ha ranging from 7–151 ha; Meyer et al. 2005), *Lophostoma silvicolium* (11–31 ha; Kalko et al. 1999), *Lampronnycteris brachyotis* (22–27 ha; Weinbeer and Kalko 2004), *Trachops cirrhosus* (46 ha ranging from 8–100 ha; Kalko et al. 1999). A similar situation occurs when compared with other frugivorous phyllostomid bats such as *Carollia perspicillata* (155 ha; Bernard and Fenton 2003), *Sturnira lilium* (36–90.7 ha; Loayza and Loiselle 2008), *Artibeus watsoni* (1.8–17.9 ha; Albrecht et al. 2007), and nectarivores bats like *Lonchophylla dekeyseri* (640 ha ranging from 230–1453 ha; Aguiar et al. 2014), and *Glossophaga soricina* (660 ha ranging from 427–893 ha; Aguiar et al. 2014). Therefore, considering these behavioral characteristics and diversification patterns, the genus *Micronycteris* represents an excellent biological model to study how the natural history of lineages influences evolutionary patterns.

An additional factor that could have influenced the lineage differentiation within the genus *Micronycteris* is the Andean Cordillera. In general, the Andes have impacted the diversification of lowland mammal fauna, inducing basal splits into trans-Andean

and cis-Andean components (Patterson et al. 2012) as is seen in *M. hirsuta*, *M. minuta*, and *M. schmidtorum* complexes. Furthermore, the altitudinal ranges of the Andes have been associated with the diversification of several lineages of other genera of Phyllostomid bats such as *Platyrrhinus* (Velazco and Patterson 2008) and *Sturnira* (Velazco and Patterson 2013). Only one clade within *M. megalotis* complex in our complete dataset represented an Andean population (2000 m a.s.l.) corresponding to a confirmed candidate species (Me G; Fig. 2), suggesting that a lineage diversification in the altitudinal ranges of *Micronycteris* is plausible. Notwithstanding, more information is needed to test this hypothesis.

Unknown evolutionary lineages

The assessment of species diversity within *Micronycteris* is a complex task due to the large morphological variation and a lack of precision in the assignment of genetic sequences to specific lineages. Our analyses identified several independently evolving evolutionary lineages that correspond to different species and could be described under an integrative taxonomic approach. Currently, 13 species are accepted (Siles and Baker 2020); but considering the high number of confirmed candidate species (CCS) discussed here, we estimate that the genus comprises at least 27 species. Nevertheless, despite our comprehensive data set there are still geographic gaps that need to be filled in the future, including Central America, Central Amazonia, and the Andean Cordillera.

Several authors have suggested that the genus *Micronycteris* includes high cryptic diversity (e.g., Porter et al. 2007). However, the assessment of cryptic diversity has been limited by: (1) the incongruence between mitochondrial and nuclear genetic data, (2) the use of the genetic species concept (Bradley and Baker 2001) as the principal line of evidence, and (3) the variability of morphological data. For example, Clare (2011) in a search for cryptic species revealed incongruence between the mitochondrial gene (COI) and a region of paternally inherited Y-chromosome (Dby^{7th} intron) in *M. megalotis*. The incongruence between markers was due to the slower divergence of the Y-chromosome region that could reflect incomplete lineage sorting in that gene (Clare 2011). However, our analyses revealed unique haplotypes in the Fgb-I7, matching most of the clades revealed by the mtDNA data analyses.

In another context, the use of genetic distance for species delimitation within *Micronycteris* (the genetic species concept) has not been homogeneously employed in the literature. For example, Clare (2011) proposes that *M. megalotis* is a species with a high intraspecific genetic variation that is the highest reported between recognized bats (COI: mean = 4.2%, range 0–7.7% using Kimura 2 parameter). Nevertheless, some authors have used smaller genetic values (near 2% in the Cytb) to identify and describe new species (e.g., *M. buriri* by Larsen et al. 2011). The genetic distance as the only criterion for defining species must be used with caution because such a measure is generally based on single mitochondrial genes with relatively high mutational rates like the Cytb (Bradley and Baker 2001). In our study, we used a conservative approach where the genetic distance between our identified genealogical lineages that correspond to

undescribed species ranged above 3.0%, except for *M. buriri* and *M. matses* that differed between 1.90% and 2.90% respectively from its most closely related lineage.

Finally, *Micronycteris* has had a complex morphological taxonomy for multiple reasons. Several of the recognized species were described based on morphological characters that, after being described, were re-evaluated or redefined posterior to the revision to a higher number of specimens. That was the case of *M. homezorum* and *M. minuta* (Ochoa and Sánchez 2005), *M. minuta* and *M. sanborni* (Feijó et al. 2015), and *M. microtis* and *M. megalotis* (Martins et al. 2014). Furthermore, the description of several species was based on the morphological revision of a few specimens from a few localities. This was the case of *M. matses* (eight specimens from only one locality; Simmons et al. 2002), *M. giovanniae* (one specimen from only one locality; Fonseca et al. 2009), *M. yatesi* (three specimens from only three localities; Siles et al. 2013) and *M. buriri* (19 specimens for San Vicente Island; Larsen et al. 2011). This problematic taxonomic scenario weakens the validity of several species of the genus due to the lack of discrete morphological characters, limited knowledge on morphological variation, and the use of the phylogenetic species concept based on a single locus and the small interspecific genetic distances of differentiation (see Bradley and Baker 2001; Zachos et al. 2013). Taking those problems into account and based on our results, in the following section we clarify some aspects concerning essential issues needed for taxonomic stability in the genus *Micronycteris*, and we propose some lines of research that should be considered for future exploration.

Taxonomic considerations

Subgenus *Schizonycteris*

A previous phylogenetic hypothesis showed *M. minuta* as paraphyletic (Siles et al. 2013). In our analyses, *M. minuta* was shown to be monophyletic, maintaining a high genetic divergence between its seven independently evolving evolutionary lineages (Suppl. material 3: Table S2). Consequently, by using integrative taxonomic methods combining molecular and robust morphological data, the identified evolutionary lineages within *M. minuta* should be described as new species. Furthermore, it is crucial to perform a broad geographic sampling throughout the distributional range of this species complex to reveal its real diversity. An additional critical issue is the assignment of the available names for each clade within the *M. minuta* complex. Nominal species has type locality in Bahia, eastern Brazil, but not sequences are included in our analyses near to that locality. Another two junior synonyms are *M. hypoleuca* from Santa Marta, Colombia (Northern Colombia; Allen 1900), and *M. homezorum* from Zulia, Venezuela (Pirlot 1967). Considering our hypothesized distributions, the lineage Mi C is distributed near these two type localities. Therefore, additional genetic information from museums or type localities is required to resolve the validity of these synonyms.

Micronycteris yatesi, *M. tresamici*, and *M. simmonsae* were supported in all our analyses performed with the Cytb gene and nuclear data confirming as valid species. Contrarily, it was not possible to include *M. sanborni* in our analyses because the only

sequence available corresponded to a partial sequence and a chimera of individuals from Brazil (see Siles et al. 2013); and no other sequences from Brazil are available for comparisons. Recently, the morphological characters that differentiated *M. minuta* and *M. sanborni* were revalidated based on comparisons of multiple sets of specimens assignable to both taxa (Feijó et al. 2015). Because of these problems, we cannot conclude that *M. sanborni* is valid. However, the validity of *M. sanborni* should be assessed by analyzing molecular and robust morphological data, including the complete cryptic diversity of *M. minuta*, morphologically most similar species.

Micronycteris schmidtorum (Sanborn, 1935). In this study, *M. schmidtorum* was recovered within the subgenus *Leuconycteris* and as a sister species of *M. brosetti*. This result contrasts other phylogenetic hypotheses that placed the species into the *M. minuta* clades within the *Schizonycteris* subgenus (Porter et al. 2007; Siles et al. 2013) but agrees with the most recent phylogenetic assessments of *Micronycteris* (Baker and Siles 2020). The position of *M. schmidtorum* of the subgenus *Leuconycteris* was recently reported by Siles and Baker (2020) providing a morphological redescription of both subgenus *Schizonycteris* and *Leuconycteris*. The previous inclusion of *M. schmidtorum* in the subgenus *Schizonycteris* was due to sequences misidentification. Previous sequences used in molecular phylogenetics were: (1) a specimen from Peru housed in the American Museum of Natural History (AMNH 273172) and preserved in ethanol. After a careful morphological revision made by DMMM, this specimen was confirmed as corresponding to *M. mattsiesi*. (2) one specimen reported by Porter et al. (2007) from Bolivia, Santa Cruz, National Park Noel Kempff Mercado (without an associated voucher specimen) was recently excluded from the most recent Bolivian mammal checklist (Aguirre et al. 2019), and (3) three specimens mentioned in the phylogenetic hypothesis of Larsen et al. (2011) as *M. cf. schmidtorum* were genetically indistinguishable from *M. minuta* for both the Cytb and Fgb-I7 genes, a situation also observed by Siles and Baker (2020).

The individuals of *M. schmidtorum* are commonly misidentified as *M. megalotis* and *M. minuta* (Morales-Martínez et al. 2018). However, all individuals of *M. schmidtorum* included in this research and morphologically identified by DMMM were genetically distinct from *M. megalotis* and *M. minuta*. *Micronycteris schmidtorum* has the following set of morphological characters that are similar to *M. brosetti* and are completely distinguishable from species of the subgenus *Schizonycteris* (*M. minuta*, *M. tresamici*, *M. sanborni*, *M. simmonsae*, and *M. yatesi*): (1) the second phalange of the IV digit is shorter than the first (similar in length in *Schizonycteris* species), (2) the calcar is longer than the foot (is shorter or similar in length in *Schizonycteris* species), the mastoid width is shorter than the zygomatic width (the mastoid width is greater than zygomatic width in *Schizonycteris* species) and (3) p3 is slightly shorter than p2 and p4 (p3 much shorter than p2 and p4 in *Schizonycteris* species).

Our phylogenetic analyses and the presence of unique nuclear haplotypes matching mtDNA haplotypes showed that *M. schmidtorum* was comprised of three lineages from both sides of the eastern Andean Cordillera and French Guiana. However, considering the geographical gaps of our assessment (Central America and Amazon) the genetic diversity could be greater. On the other hand, the genetic divergence for the three lineages

for the *Cytb* gene was low, between 1.8% and 2.0%, being smaller than the Genetic Species Concept values (ca. 4%; Baker and Bradley 2006) suggesting that no cryptic diversity is expected in *M. schmidtorum*. Nevertheless, Morales-Martínez et al. (2018) found morphometric differences between individuals of several countries and hypothesized that the Andes Cordillera and a possible cryptic diversity could explain that variation. Therefore, we suggest an assessment of those hypotheses using an integrative taxonomic approach including more individuals from different localities on both sides of the Andes.

Micronycteris hirsuta (Peters, 1869) was recovered as a species that exhibited a considerable high genetic variation; with 7.8% differentiation in the *Cytb* gene between its two forming clades (Suppl. material 3: Table S2). This value is higher than the values of interspecific variation reported for mammals in Bradley and Baker (2001). Additionally, these two clades were recognized by all species delimitation procedures, and they probably agreed with cytogenetic information. Ribas et al. (2013) reported that *M. hirsuta* has different karyotypic arrangements that do not represent a monotypic taxon, principally between the karyotypes of individuals from the Amazon in Brazil and western Ecuador. The analyzed data of Ribas et al. (2013) for the Amazon in Brazil were taken from individuals that came from localities far away from the Amazonian localities of the individuals included in this study. Although there is a direct correlation between the karyotypic differentiation and our molecular systematics results for *M. hirsuta*, we should be cautious because we cannot corroborate that the Amazonian individuals correspond to the lineage Hi A recovered by us.

Micronycteris matses Simmons, Voss & Fleck, 2002. *Micronycteris matses* is a species described based on eight specimens for one locality in the Peruvian Amazon (Simmons et al. 2002). The main differences that separate this species are based on the body size of the type series. This species was not shown to be a different evolutionary lineage using genetic distances because it showed less than 3% of divergence in the *Cytb* gene compared to *M. megalotis* (Me 1), but its distinction was recovered in all applied delimitation methods. We consider *M. matses* to be a valid species because it is validated by delimitation analyses, it presents unique nDNA haplotypes matching mtDNA haplotypes, and morphologically the cranium is more robust than in other clades of the *M. megalotis* species group (see Simmons et al. 2002).

Micronycteris microtis Miller, 1898. Simmons and Voss (1998) proposed a set of characters that differentiate *M. microtis* from *M. megalotis*, including the size of the ears and the length of the hairs in the anterior surface of the pinna. In contrast, Martins et al. (2014) described the variation of *M. microtis* and *M. megalotis* from Brazil and showed a superposition of the ear length with the length of the hairs of the pinna as the unique diagnostic character for distinguishing these two species. Porter et al. (2007) included specimens of the two species from Paracou (French Guiana) as determined by Simmons and Voss (1998) in their phylogenetic study, revealing those individuals as part of the same clade (clade D in Porter et al. 2007). Identifications of specimens from Colombia based on hair characters as *M. microtis* and *M. megalotis* sequenced by us, also appeared in the same clade (*M. megalotis* Me H in this study). This situation proved that such morphometric characters cannot distinguish between both species and suggested that both species may be part of the intraspecific variation within several

lineages of the *M. megalotis* complex. Posteriorly to Porter et al. (2007) hypothesis, *M. microtis* was included in Larsen et al. (2011) and Siles et al. (2013) as a clade in the middle of *M. megalotis* complex apparently due to the identification of the specimen ROM 111099 gathered from GenBank from Brazil (AY380755; Me B in this work). We do not recommend considering *M. microtis* and *M. megalotis* as distinct species and suggest including them both as *M. megalotis sensu lato* until a careful assessment of the diversity within the *M. megalotis* species complex is accomplished. If after a careful taxonomic revision of the *M. megalotis* complex *M. microtis* proven to be valid, that lineage should correspond to Me F or Me H clades of this study, based on the type locality in Central America (Greytown [= San Juan del Norte], Nicaragua; Miller 1898).

Micronycteris buriri Larsen, Siles, Pedersen & Kwiecinski, 2011. This species fails the genetic divergence limits for the Cytb gene but is recovered in two species delimitation models and has unique nDNA haplotypes. Additionally, its body size is distinguishable from other species of *Micronycteris* confirming as a valid species despite its low genetic divergence (< 2%) with other clades within the *M. megalotis* complex lineages. Other morphological characters of this species must be taken cautiously. For example, the interpretation of the lower hypsodont incisors in *M. buriri* is incorrect. This character is defined as: “the heights of crowns are roughly three times their widths” in *M. hirsuta* (Simmons 2002: fig. 3, p 9). This condition is not present in *M. buriri*, according to the images presented by Larsen et al. (2011, plate 3, p 699). Additionally, those comparisons were based on few specimens, omitting the wide morphological variation within all clades of *M. megalotis* complex.

Micronycteris megalotis species group. This species group (including *M. microtis*) varied extensively in the delimitation analyses. However, our research revealed at least nine genealogical lineages that are supported by most of the analyses. Several of those lineages are allopatric, parapatric, and sympatric, with two or three polyphyletic clades co-occurring in the same locality. For example, some individuals of the lineages Me C, Me E and Me H were collected at the same locality in San José del Guaviare, Guaviare Department, Colombia, and these individuals showed differences in size (see Morales-Martínez 2017). Clare (2011) proposed that the presence of polyphyletic clades with sympatric ranges is evidence that speciation is occurring in *Micronycteris*. For a posterior assessment of cryptic diversity and a description of the different evolutionary lineages representing different species, we recommend using integrative taxonomy including multiple genes mtDNA and nDNA molecular data, as well as other lines of evidence like morphology, bioacoustics, and cytogenetics.

Acknowledgements

We are especially thankful to the collection curators for permitting us to study the specimens under their care. Financial and logistic support for the development of this research project was provided by the grant: “Convocatoria nacional de proyectos para el fortalecimiento de la investigación, creación e innovación de la Universidad Nacional de Colombia 2016–2018” by the División de Investigación Sede Bogotá (DIB)

of Universidad Nacional de Colombia and the Grupo Biodiversidad y Conservación Genética of the Instituto de Genética, Universidad Nacional de Colombia. We thank Miguel E. Rodríguez-Posada, Camilo Fernández, Catalina Cardenas, Catherine Mora, and Javier Colmenares for sharing tissues samples. DMM thanks MRP and CCG for scientific discussions. We thank the research groups Biodiversidad y Conservación Genética of the Instituto de Genética, Conservación y Manejo de Vida Silvestre for the Universidad Nacional de Colombia, and Servicio de Secuenciación SIGMOL for their invaluable support. We thank Thomas Defler and Hector Ramírez-Chaves for his assistance with the English proofing of the manuscript. We thank the reviewers and the editor for their careful reading of our manuscript and their comments and suggestions to improve the final version.

References

- Aguiar LMS, Bernard E, Machado RB (2014) Habitat use and movements of *Glossophaga soricina* and *Lonchophylla dekeyseri* (Chiroptera: Phyllostomidae) in a Neotropical savannah. *Zoologia* 31: 223–229. <https://doi.org/10.1590/S1984-46702014000300003>
- Aguirre LF, Tarifa T, Wallace RB, Bernal HN, Siles L, Aliaga-Rossel E, Salazar-Bravo J (2019) Lista actualizada y comentada de los mamíferos de Bolivia. *Ecología en Bolivia* 54: 109–149.
- Albrecht L, Meyer CFJ, Kalko EV (2007) Differential mobility in two small phyllostomid bats, *Artibeus watsoni* and *Micronycteris microtis*, in a fragmented neotropical landscape. *Acta Theriologica* 52: 141–149. <https://doi.org/10.1007/BF03194209>
- Allen JA (1900) List of bats collected by Mr. H. H. Smith in the Santa Marta region of Colombia, with descriptions of new species. *Bulletin American Museum of Natural History* 13: 87–94.
- Avise JC, Ball RM (1990) Principles of genealogical concordance in species concepts and biological taxonomy. In: Futuyma D, Antonovics J (Eds) *Surveys in Evolutionary Biology*. Oxford University Press, New York, 45–67.
- Baker RJ, Bradley RD (2006) Speciation in mammals and the genetic species concept. *Journal of Mammalogy* 87: 643–662. <https://doi.org/10.1644/06-MAMM-F-038R2.1>
- Bickford D, Lohman DJ, Sodhi NS, Ng PKL, Meier R, Winker K, Ingram KK, Das I (2007) Cryptic species as a window on diversity and conservation. *Trends in Ecology and Evolution* 22: 148–155. <https://doi.org/10.1016/j.tree.2006.11.004>
- Bradley RD, Baker RJ (2001) A test of the Genetic Species Concept: cytochrome-b sequences and mammals. *Journal of Mammalogy* 82: 960–973. [https://doi.org/10.1644/1545-1542\(2001\)082%3C0960:ATOTGS%3E2.0.CO;2](https://doi.org/10.1644/1545-1542(2001)082%3C0960:ATOTGS%3E2.0.CO;2)
- Bernard E, Fenton MB (2003) Bat mobility and roosts in a fragmented landscape in Central Amazonia, Brazil. *Biotropica* 35: 262–277. <https://doi.org/10.1646/02156>
- Burgin CJ, Colella JP, Kahn PL, Upham NS (2018) How many species of mammals are there? *Journal of Mammalogy* 99: 1–11. <https://doi.org/10.1093/jmammal/gyx147>
- Clare EL (2011) Cryptic Species? Patterns of Maternal and Paternal Gene Flow in Eight Neotropical Bats. *PLoS ONE* 6: 1–13. <https://doi.org/10.1371/journal.pone.0021460>

- de Queiroz K (1999) The General Lineage Concept of species and the defining properties of the species category. In: Wilson RA (Ed.) Species: New Interdisciplinary Essays. MIT Press, Cambridge, 57–75.
- de Queiroz K (2007) Species concepts and species delimitation. *Systematic Biology* 56: 879–886. <https://doi.org/10.1080/10635150701701083>
- Drummond AJ, Suchard MA, Xie D, Rambaut A (2012) Bayesian phylogenetics with BEAUti and the BEAST 1.7. *Molecular Biology and Evolution* 29: 1969–1973. <https://doi.org/10.1093/molbev/mss075>
- Feijó A, Da Rocha PA, Ferrari SF (2015) How do we identify *Micronycteris* (*Schizonycteris*) *sanborni* Simmons 1996 (Chiroptera, Phyllostomidae) reliably and where we can find this species in Brazil? *Papéis Avulsos de Zoologia* 55: 269–280. <https://doi.org/10.1590/0031-1049.2015.55.20>
- Fonseca RM, Hofer SR, Porter CA, Cline CA, Parish DA, Hoffmann FG, Baker RJ (2007) Morphological and molecular variation within little Big-eared bats of the genus *Micronycteris* (Phyllostomidae: Micronycterinae) from San Lorenzo, Ecuador. In: Kelt DA, Lessa EP, Salazar-Bravo J, Patton JL (Eds) *The Quintessential Naturalist: Honoring the Life and Legacy of Oliver P. Pearson*. University of California publications in zoology, Berkeley, 721–746. <https://doi.org/10.1525/california/9780520098596.003.0020>
- Hall TA (1999) BioEdit: a user-friendly biological sequence alignment editor and analysis program for Windows 95/97/NT. *Nucleic Acids Symposium Series* 41: 95–98.
- Kalka M, Kalko EKV (2006) Gleaning bats as underestimated predators of herbivorous insects: diet of *Micronycteris microtis* (Phyllostomidae) in Panama. *Journal of Tropical Ecology* 22: 1–10. <https://doi.org/10.1017/S0266467405002920>
- Kalko EKV, Friemel D, Handley CO, Schnitzler HU (1999) Roosting and foraging behavior of two neotropical gleaners, *Tonatia silvicola* and *Trachops cirrhosus* (Phyllostomidae). *Biotropica* 31: 344–353. <https://doi.org/10.1111/j.1744-7429.1999.tb00146.x>
- Kumar S, Stecher G, Li M, Knyaz C, Tamura K (2018) MEGA X: Molecular Evolutionary Genetics Analysis across computing platforms. *Molecular Biology and Evolution* 35: 1547–1549. <https://doi.org/10.1093/molbev/msy096>
- Lanfear R, Frandsen PB, Wright AM, Senfeld T, Calcott B (2016) PartitionFinder 2: new methods for selecting partitioned models of evolution for molecular and morphological phylogenetic analyses. *Molecular Biology and Evolution* 34: 772–773. <https://doi.org/10.1093/molbev/msw260>
- Larsen PA, Siles L, Pedersen SC, Kwiecinski GG (2011) A new species of *Micronycteris* (Chiroptera: Phyllostomidae) from Saint Vincent, Lesser Antilles. *Mammalian Biology* 76: 687–700. <https://doi.org/10.1016/j.mambio.2011.01.006>
- Loayza AP, Loiselle BA (2008) Preliminary information on the home range and movement patterns of *Sturnira lilium* (Phyllostomidae) in a naturally fragmented landscape in Bolivia. 2008. *Biotropica* 40: 630–635. <https://doi.org/10.1111/j.1744-7429.2008.00422.x>
- Martins L, Milagres A, Tavares V (2014) Distribution and taxonomy of the common big-eared bat *Micronycteris microtis* (Chiroptera: Phyllostomidae) in South America. *Mammalia* 79: 439–447. <https://doi.org/10.1515/mammalia-2014-0057>
- Meier R, Kwong S, Vaidya G, Ng PKL (2006) DNA barcoding and taxonomy in Diptera: a tale of high intraspecific variability and low identification success. *Systematic Biology* 55: 715–728. <https://doi.org/10.1080/10635150600969864>

- Meyer CFJ, Weinbeer M, Kalko EKV (2005) Home-range size and spacing patterns of *Macrophyllum macrophyllum* (Phyllostomidae) foraging over water. *Journal of Mammalogy* 86: 587–598. [https://doi.org/10.1644/1545-1542\(2005\)86\[587:HSASPO\]2.0.CO;2](https://doi.org/10.1644/1545-1542(2005)86[587:HSASPO]2.0.CO;2)
- Miller GS (1898) Descriptions of five new Phyllostomine bats. *Proceedings of the Academy of Natural Science Philadelphia* 50: 326–337.
- Morales-Martínez DM (2017) Taxonomía y sistemática de los murciélagos del género *Micronycteris* Gray, 1982 (Chiroptera: Phyllostomidae) en Colombia. MSc thesis, Bogotá, Colombia: Universidad Nacional de Colombia. <http://bdigital.unal.edu.co/64661/>
- Morales-Martínez DM, Camacho MA, Burneo SF (2018) Distribution and morphometric variation of *Micronycteris schmidtorum* (Sanborn, 1935) (Chiroptera: Phyllostomidae) in north South America with the first record from Ecuador. *Mastozoología Neotropical* 25: 391–398. <https://doi.org/10.31687/saremMN.18.25.2.0.14>
- Nylander JA, Ronquist F, Huelsenbeck JP, Nieves-Aldrey JL (2004) Bayesian phylogenetic analysis of combined data. *Systematic Biology* 53: 47–67. <https://doi.org/10.1080/10635150490264699>
- Ochoa JG, Sánchez JH (2005) Taxonomic status of *Micronycteris homezi* (Chiroptera, Phyllostomidae). *Mammalia* 69: 323–335. <https://doi.org/10.1515/mamm.2005.026>
- Patterson BD (2000) Patterns and trends in the discovery of new neotropical mammals. *Diversity and Distributions* 6: 145–151. <https://doi.org/10.1046/j.1472-4642.2000.00080.x>
- Patterson BD, Solari S, Velazco PM (2012) The role of the Andes in the diversification and biogeography of neotropical mammals. In: Patterson BD, Costa LP (Eds) *Bones, Clones and Biomes. The history and geography of recent neotropical mammals*. The University of Chicago Press, Chicago, 351–378. <https://doi.org/10.7208/chicago/9780226649214.003.0015>
- Pirlot P (1967) Nouvelle récolte de chiroptères dans l'ouest du Venezuela. *Mammalia* 31: 260–274. <https://doi.org/10.1515/mamm.1967.31.2.260>
- Porter CA, Hooper SR, Cline CA, Hoffmann FG, Baker RJ (2007) Molecular phylogenetics of the phyllostomid bat genus *Micronycteris* with descriptions of two new subgenera. *Journal of Mammalogy* 88: 1205–1215. <https://doi.org/10.1644/06-MAMM-A-292R.1>
- Rambaut A, Drummond AJ, Xie D, Baele G, Suchard MA (2018) Posterior summarisation in Bayesian phylogenetics using Tracer 1.7. *Systematic Biology* 67: 901–904. <https://doi.org/10.1093/sysbio/syy032>
- Reeder DM, Helgen KH, Wilson DE (2007) Global trends and biases in new mammal species discoveries. *Occasional papers, Museum of Texas Tech University* 269: 1–35. <https://doi.org/10.5962/bhl.title.156951>
- Ribas TFA, Rodrigues LRR, Nagamachi CY, Gomes AJB, Benathar TCM, O'Brien PCM, Yang F, Ferguson-Smith MA, Pieczarka JC (2013) Two new cytotypes reinforce that *Micronycteris hirsuta* Peters, 1869 does not represent a monotypic taxon. *BMC Genetics* 14(119): 1–10. <https://doi.org/10.1186/1471-2156-14-119>
- Ronquist F, Teslenko M, van der Mark P, Ayres DL, Darling A, Höhna S, Larget B, Liu L, Suchard MA, Huelsenbeck JP (2012) MRBAYES 3.2: Efficient Bayesian phylogenetic inference and model selection across a large model space. *Systematic Biology* 61: 539–542. <https://doi.org/10.1093/sysbio/sys029>
- Rozas J, Ferrer-Mata A, Sánchez-DelBarrio JC, Guirao-Rico S, Librado P, Ramos-Onsins SE, Sánchez-Gracia A (2017) DnaSP 6: DNA Sequence Polymorphism Analysis of Large

- Datasets. *Molecular Biology and Evolution* 34: 3299–3302. <https://doi.org/10.1093/molbev/msx248>
- Sambrook J, Fritsch EF, Maniatis T (1989) *Molecular cloning: a laboratory manual* (2nd edn.) Cold Spring Harbor Laboratory Press, 1885 pp.
- Siles L, Baker RJ (2020) Revision of the pale-bellied *Micronycteris* Gray, 1866 (Chiroptera, Phyllostomidae) with descriptions of two new species. *Journal of Zoological Systematics and Evolutionary Research* 00: 1–21. <https://doi.org/10.1111/jzs.12388>
- Siles L, Brooks DM, Aranibar H, Tarifa T, Vargas MRJ, Rojas JM, Baker RJ (2013) A new species of *Micronycteris* (Chiroptera: Phyllostomidae) from Bolivia. *Journal of Mammalogy* 94: 881–896. <https://doi.org/10.1644/12-MAMM-A-259.1>
- Simmons NB, Cirranello AL (2020) Bat Species of the World: A taxonomic and geographic database. <https://batnames.org/>
- Simmons NB, Voss RS (1998) The mammals of Paracou, French Guiana, a Neotropical lowland rainforest fauna. Part 1, Bats. *Bulletin of the American Museum of Natural History* 237: 1–219.
- Simmons NB, Voss RS, Fleck DW (2002) A New Amazonian Species of *Micronycteris* (Chiroptera: Phyllostomidae) with Notes on the Roosting Behavior of Sympatric Congeners. *American Museum Novitates* 3358: 1–14. [https://doi.org/10.1206/0003-0082\(2002\)358%3C0001:ANASOM%3E2.0.CO;2](https://doi.org/10.1206/0003-0082(2002)358%3C0001:ANASOM%3E2.0.CO;2)
- Solari S, Martínez-Arias V (2014) Cambios recientes en la sistemática y taxonomía de murciélagos Neotropicales (Mammalia: Chiroptera). *Therya* 5: 167–196. <https://doi.org/10.12933/therya-14-180>
- Stamatakis A (2011) RAxML Version 8: A tool for Phylogenetic Analysis and Post-Analysis of Large Phylogenies. *Bioinformatics* 30: 1312–1313. <https://doi.org/10.1093/bioinformatics/btu033>
- Stephens M, Smith NJ, Donnelly P (2001) A new statistical method for haplotype reconstruction from population data. *American Journal of human Genetics* 68: 978–989. <https://doi.org/10.1086/319501>
- Velazco PM, Patterson BD (2008) Phylogenetics and biogeography of the broad-nosed bats, genus *Platyrrhinus* (Chiroptera: Phyllostomidae). *Molecular Phylogenetics and Evolution* 49: 749–759. <https://doi.org/10.1016/j.ympev.2008.09.015>
- Velazco PM, Patterson BD (2013) Diversification of the Yellow-shouldered bats, Genus *Sturnira* (Chiroptera, Phyllostomidae), in the New World tropics. *Molecular Phylogenetics and Evolution* 68: 683–698. <https://doi.org/10.1016/j.ympev.2013.04.016>
- Vieites DR, Wollenberg KC, Andreone F, Köhlerd J, Glawe F, Vences M (2009) Vast underestimation of Madagascar's biodiversity evidenced by an integrative amphibian inventory. *PNAS* 106: 8267–8272. <https://doi.org/10.1073/pnas.0810821106>
- Weinbeer M, Kalko EKV (2004) Morphological characteristics predict alternate foraging strategy and microhabitat selection in the orange-bellied bat, *Lampronnycteris brachyotis*. *Journal of Mammalogy* 85: 1116–1123. <https://doi.org/10.1644/BWG-206.1>
- Zachos FE, Apollonio M, Bärman EV, Festa-Bianchet M, Göhlich U, Habel JC, Haring E, Kruckenhauser L, Lovari A, McDevitt AD, Pertoldi C, Rössner GE, Sánchez-Villagra MR, Scandura M, Suchentrunk F (2013) Species inflation and taxonomic artefacts – A critical comment on recent trends in mammalian classification. *Mammalian Biology* 78: 1–6. <https://doi.org/10.1016/j.mambio.2012.07.083>

Supplementary material 1

Table S1. GenBank accession numbers of sequences included and specimens examined, its specimen number, and source of the sequences

Authors: Darwin M. Morales-Martínez, Hugo F. López-Arévalo, Mario Vargas-Ramírez

Data type: molecular data

Explanation note: Specimen with an asterisk represent specimens revised by authors to confirm identifications. List of collections acronym that appear in table: American Museum of Natural History (AMNH); Carnegie Museum of Natural History (CMNH); Colección Boliviana de Fauna (CBF); Museo de Historia Natural Alcide d'Orbigny (MHNC–M); Museum of Southwestern Biology (MSB–catalog number, NK–tissue number); Museum of Texas Tech University (TTU–voucher number, TK–tissue number); Pontificia Universidad Católica del Ecuador (QCAZ); Royal Ontario Museum (ROM); United States National Museum of Natural History (NMNH); Instituto de Ciencias Naturales-Universidad Nacional de Colombia (ICN); EAFIT University, Colombia (EAFIT); Universidad Industrial de Santander (UIS). Temp: Specimens deposited in collection but uncatalogued. Boldface identifies sequences used in the delimitation analyses. Acronyms of countries: Arg: Argentina, Bel: Belize, Bol: Bolivia, Bra: Brazil, Col: Colombia, CRic: Costa Rica, Ecu: Ecuador, FGui: French Guiana, Gua: Guatemala, Guy: Guyana, Hon: Honduras, Mex: Mexico, Nic: Nicaragua, Pan: Panama, Per: Peru, Sur: Suriname, SVin: Saint Vincent and the Grenadines, Tri: Trinidad and Tobago, Ven: Venezuela..

Copyright notice: This dataset is made available under the Open Database License (<http://opendatacommons.org/licenses/odbl/1.0/>). The Open Database License (ODbL) is a license agreement intended to allow users to freely share, modify, and use this Dataset while maintaining this same freedom for others, provided that the original source and author(s) are credited.

Link: <https://doi.org/10.3897/zookeys.1028.60955.suppl1>

Supplementary material 2

Figure S1. Geographic location of sequences used in molecular analyses

Authors: Darwin M. Morales-Martínez, Hugo F. López-Arévalo, Mario Vargas-Ramírez

Data type: occurrences

Copyright notice: This dataset is made available under the Open Database License (<http://opendatacommons.org/licenses/odbl/1.0/>). The Open Database License (ODbL) is a license agreement intended to allow users to freely share, modify, and use this Dataset while maintaining this same freedom for others, provided that the original source and author(s) are credited.

Link: <https://doi.org/10.3897/zookeys.1028.60955.suppl2>

Supplementary material 3

Tables S2–S2.4

Authors: Darwin M. Morales-Martínez, Hugo F. López-Arévalo, Mario Vargas-Ramírez
Data type: molecular data

Explanation note: **Table S2.** Average p -genetic distances within (diagonal) and between (below the diagonal) species and clades per subgenus of *Micronycteris* based on the Cytb gene. Acronyms represent the lineages of *M. megalotis*, *M. hirsuta* and *M. minuta* species complex. **Table S2.1.** Subgenus *Micronycteris*. **Table S2.2.** Subgenus *Xenonectes*. **Table S2.3.** Subgenus *Leuconycteris*. **Table S2.4.** Subgenus *Schizonycteris*.

Copyright notice: This dataset is made available under the Open Database License (<http://opendatacommons.org/licenses/odbl/1.0/>). The Open Database License (ODbL) is a license agreement intended to allow users to freely share, modify, and use this Dataset while maintaining this same freedom for others, provided that the original source and author(s) are credited.

Link: <https://doi.org/10.3897/zookeys.1028.60955.suppl3>

Supplementary material 4

Results of the delimitation analyses

Authors: Darwin M. Morales-Martínez, Hugo F. López-Arévalo, Mario Vargas-Ramírez
Data type: Species delimitation analyses

Copyright notice: This dataset is made available under the Open Database License (<http://opendatacommons.org/licenses/odbl/1.0/>). The Open Database License (ODbL) is a license agreement intended to allow users to freely share, modify, and use this Dataset while maintaining this same freedom for others, provided that the original source and author(s) are credited.

Link: <https://doi.org/10.3897/zookeys.1028.60955.suppl4>

**Corrigenda: Three new and one little-known species
of Hypogastruridae (Collembola)
from Russia’s northeast. ZooKeys 1005: 1–20.
<https://doi.org/10.3897/zookeys.1005.54882>**

Anatoly Babenko¹, Boris Efeykin^{1,2}, Mikhail Bizin¹

1 Severtsov Institute of Ecology & Evolution, Russian Academy of Sciences, Leninski pr. 33, 119071, Moscow, Russia **2** Kharkevich Institute for Information Transmission Problems, Russian Academy of Sciences, Bol’shoi Karetnyi per. 19, 127051, Moscow, Russia

Corresponding author: Anatoly Babenko (lsdc@mail.ru)

Academic editor: L. Deharveng | Received 26 February 2021 | Accepted 18 March 2021 | Published 6 April 2021

<http://zoobank.org/213CDBF7-870A-4338-B911-6B61EC36DFB1>

Citation: Babenko A, Efeykin B, Bizin M (2021) Corrigenda: Three new and one little-known species of Hypogastruridae (Collembola) from Russia’s northeast. ZooKeys 1005: 1–20. <https://doi.org/10.3897/zookeys.1005.54882>. ZooKeys 1028: 161–162. <https://doi.org/10.3897/zookeys.1028.65169>

After our recent publication (Babenko et al. 2020), Dr. Cyrille A. D’Haese, of the Muséum national d’Histoire naturelle, Paris, France, called our attention to the errors contained in Table 1 (column: COI sequence number). We would like to take this opportunity to sincerely thank him and correct the following errors:

Table 1. Species used for molecular study, primers, and GenBank accession numbers of the sequences.

Species	Forward primer	Reverse primer	COI sequence number	Sequence size
<i>Hypogastrura variata</i> sp. nov.	colfol-for: ttccaacaatcataargayatygg	colfol-rev: taaacttcnggrtgnccaaaaaatca	MW518020 MW518021 MW518022	647 bp
<i>Hypogastrura yosii</i> Stach, 1964	colfol-for: ttccaacaatcataargayatygg	colfol-rev: taaacttcnggrtgnccaaaaaatca	MW507473 MW507474 MW507475	647 bp
<i>Xenylla arnei</i> sp. nov.	LCO1490_t1: tgtaaaacgacggccagrtgg tccaacaatcataagatatattgg	HCO2198_t1: caggaaacagctatgactaaacttc agggrtgaccaaaaaatca	MW517749 MW549335 MW549336	658 bp

Other corrections:

Page 3, Additional material to *Hypogastrura variata* sp. nov., lines 3–4: Their partial COI genes were... deposited in the GenBank under the sample ID: **MW518020–MW518022**.

Page 8, Material to *Hypogastrura yosii* Stach, 1964, lines 3–4: Their partial COI genes were... deposited in the GenBank under the sample ID: **MW507473–MW507475**.

Page 13, Additional material to *Xenylla arnei* sp. nov., lines 2–4: Their partial COI genes were...deposited in the GenBank under the sample ID: **MW517749, MW549335–MW549336**.

Reference

Babenko A, Efeykin B, Bizin M (2020) Three new and one little-known species of Hypogastruridae (Collembola) from Russia's northeast. ZooKeys 1005: 1–20. <https://doi.org/10.3897/zookeys.1005.54882>